



PROFILES OF DRUG
SUBSTANCES, EXCIPIENTS,
AND RELATED
METHODOLOGY

Volume 30

Harry G. Brittain

EDITORIAL BOARD

Abdullah A. Al-Badr

Gunawan Indrayanto

Alekha K. Dash

Leroy Shervington

Klaus Florey

Profiles of Drug Substances, Excipients, and Related Methodology

Volume 30

edited by

Harry G. Brittain

*Center for Pharmaceutical Physics
10 Charles Road
Milford, New Jersey 08848, USA*

Founding Editor

Klaus Florey



ELSEVIER
ACADEMIC
PRESS

Amsterdam • Boston • Heidelberg • London • New York • Oxford
Paris • San Diego • San Francisco • Singapore • Sydney • Tokyo

ELSEVIER Inc.
360 Park Avenue South
New York, NY 10010-1710, USA

© 2003 Elsevier Inc. All rights reserved.

This work is protected under copyright by Elsevier, and the following terms and conditions apply to its use:

Photocopying

Single photocopies of single chapters may be made for personal use as allowed by national copyright laws. Permission of the Publisher and payment of a fee is required for all other photocopying, including multiple or systematic copying, copying for advertising or promotional purposes, resale, and all forms of document delivery. Special rates are available for educational institutions that wish to make photocopies for non-profit educational classroom use.

Permissions may be sought directly from Elsevier's Science & Technology Rights Department in Oxford, UK: phone: (+44) 1865 843830, fax: (+44) 1865 853333, e-mail: permissions@elsevier.com. You may also complete your request on-line via the Elsevier homepage (<http://www.elsevier.com>), by selecting 'Customer Support' and then 'Obtaining Permissions'.

In the USA, users may clear permissions and make payments through the Copyright Clearance Center, Inc., 222 Rosewood Drive, Danvers, MA 01923, USA; phone: (978) 7508400, fax: (978) 7504744, and in the UK through the Copyright Licensing Agency Rapid Clearance Service (CLARCS), 90 Tottenham Court Road, London W1P 0LP, UK; phone: (+44) 207 631 5555; fax: (+44) 207 631 5500. Other countries may have a local reprographic rights agency for payments.

Derivative Works

Tables of contents may be reproduced for internal circulation, but permission of Elsevier is required for external resale or distribution of such material.

Permission of the Publisher is required for all other derivative works, including compilations and translations.

Electronic Storage or Usage

Permission of the Publisher is required to store or use electronically any material contained in this work, including any chapter or part of a chapter.

Except as outlined above, no part of this work may be reproduced, stored in a retrieval system or transmitted in any form or by any means, electronic, mechanical, photocopying, recording or otherwise, without prior written permission of the Publisher.

Address permissions requests to: Elsevier Health's Science & Technology Rights Department, at the phone, fax and e-mail addresses noted above.

Notice

No responsibility is assumed by the Publisher for any injury and/or damage to persons or property as a matter of products liability, negligence or otherwise, or from any use or operation of any methods, products, instructions or ideas contained in the material herein. Because of rapid advances in the medical sciences, in particular, independent verification of diagnoses and drug dosages should be made.

First edition 2003

Library of Congress Cataloging in Publication Data

A catalog record from the Library of Congress has been applied for.

British Library Cataloguing in Publication Data

A catalogue record from the British Library has been applied for.

Academic Press

An Imprint of Elsevier

525 B Street, Suite 1900, San Diego, California 92101-4495, USA

<http://www.academicpress.com>

ISBN: 0 12 260830 5 (this volume)

ISSN: 0099 5428 (series)

Typeset by Keyword Publishing Services, Barking

Printed in Great Britain by MPG Books Ltd, Bodmin, Cornwall

 The paper used in this publication meets the requirements of ANSI/NISO Z39.48-1992 (Permanence of Paper).

**Profiles of Drug Substances,
Excipients, and
Related Methodology**

CONTENTS

<i>Affiliations of Editor and Contributors</i>	vii
--	-----

Profiles of Drug Substances

1. Acyclovir: Comprehensive Profile	3
<i>Mochammad Yuwono and Gunawan Indrayanto</i>	
2. Ceftriaxone Sodium: Comprehensive Profile	21
<i>Heather M. Owens and Alekha K. Dash</i>	
3. Ipratropium Bromide:	
3.1 Physical Properties	59
3.2 Methods of Chemical and Biochemical Synthesis	85
3.3 Analytical Methods	101
3.4 Drug Metabolism and Pharmacokinetics	117
<i>Heba H. Abdine, F. Belal and Abdullah A. Al-Badr</i>	
4. Ornidazole: Comprehensive Profile	123
<i>Paramjeet Singh, Rohit Mittal, G.C. Sharma, Sukhjeet Singh and Amarjit Singh</i>	
5. Sertraline (L)-Lactate: Comprehensive Profile	185
<i>Michael D. Likar, Jon Bordner, Diane M. Rescek and Thomas R. Sharp</i>	

Profiles of Excipients

6. Propylparaben: Physical Characteristics	237
<i>Marcellino Rudyanto, Masataka Ihara, Kiyosei Takasu, Masahiro Yoshida, Hadi Poerwono, I Ketut Sudiana, Gunawan Indrayanto and Harry G. Brittain</i>	

Related Methodology Review Articles

7. X-Ray Diffraction of Pharmaceutical Materials	273
<i>Harry G. Brittain</i>	

Cumulative Index	321
-------------------------	-----

AFFILIATIONS OF EDITOR AND CONTRIBUTORS

Heba H. Abdine: Department of Pharmaceutical Chemistry, College of Pharmacy, King Saud University, P.O. Box 2457, Riyadh – 11451, Kingdom of Saudi Arabia

Abdullah A. Al-Badr: Department of Pharmaceutical Chemistry, College of Pharmacy, King Saud University, P.O. Box 2457, Riyadh – 11451, Kingdom of Saudi Arabia

F. Belal: Department of Pharmaceutical Chemistry, College of Pharmacy, King Saud University, P.O. Box 2457, Riyadh – 11451, Kingdom of Saudi Arabia

Jon Bordner: Chemical Research and Development, Pfizer Inc., Pfizer Global Research and Development, Groton, CT 06340, USA

Harry G. Brittain: Center for Pharmaceutical Physics; 10 Charles Road, Milford, NJ 08848, USA

Alekha K. Dash: Department of Pharmacy Sciences, School of Pharmacy and Health Professions, Creighton University, Omaha, NE 68178, USA

Masataka Ihara: Graduate School of Pharmaceutical Sciences, Tohoku University, Aobayama, Sendai 980-8578, Japan

Gunawan Indrayanto: Faculty of Pharmacy, Airlangga University, Jalan Dharmawangsa Dalam, Surabaya 60286, Indonesia

Michael D. Likar: Analytical Research and Development, Pfizer Inc., Pfizer Global Research and Development, Groton, CT 06340, USA

Rohit Mittal: Research & Development Centre, Panacea Biotech Ltd., P.O. Lalru 140 501, Punjab, India

Heather M. Owens: Department of Pharmacy Sciences, School of Pharmacy and Health Professions, Creighton University, Omaha, NE 68178, USA

Hadi Poerwono: Faculty of Pharmacy, Airlangga University, Jalan Dharmawangsa Dalam, Surabaya 60286, Indonesia

Diane M. Rescek: Exploratory Medicinal Sciences, Pfizer Inc., Pfizer Global Research and Development, Groton, CT 06340, USA

Marcellino Rudyanto: Faculty of Pharmacy, Airlangga University, Jalan Dharmawangsa Dalam, Surabaya 60286, Indonesia

G.C. Sharma: Research & Development Centre, Panacea Biotec Ltd., P.O. Lalru 140 501, Punjab, India

Thomas R. Sharp: Analytical Research and Development, Pfizer Inc., Pfizer Global Research and Development, Groton, CT 06340, USA

Amarjit Singh: Research & Development Centre, Panacea Biotec Ltd., P.O. Lalru 140 501, Punjab, India

Paramjeet Singh: Research & Development Centre, Panacea Biotec Ltd., P.O. Lalru 140 501, Punjab, India

Sukhjeet Singh: Research & Development Centre, Panacea Biotec Ltd., P.O. Lalru 140 501, Punjab, India

I Ketut Sudiana: Faculty of Medicine, Airlangga University, Jalan Prof. Dr. Moestopo 47, Surabaya 60131, Indonesia

Kiyosei Takasu: Graduate School of Pharmaceutical Sciences, Tohoku University, Aobayama, Sendai 980-8578, Japan

Masahiro Yoshida: Graduate School of Pharmaceutical Sciences, Tohoku University, Aobayama, Sendai 980-8578, Japan

Mochammad Yuwono: Faculty of Pharmacy, Airlangga State University, Dharmawangsa Dalam, Surabaya 60286, Indonesia

Profiles of Drug Substances

Acyclovir: Comprehensive Profile

Mochammad Yuwono and Gunawan Indrayanto*

*Faculty of Pharmacy
Airlangga State University
Dharmawangsa Dalam
Surabaya 60286
Indonesia*

*Author for correspondence

CONTENTS

1.	Compendial Methods of Analysis.	4
1.1	Identification	4
1.1.1	Bulk drug substance.	4
1.1.2	Acyclovir in pharmaceutical preparations.	5
1.2	Water content	5
1.3	Impurity analyses.	6
1.3.1	Ordinary impurities	6
1.3.2	Sulfate	6
1.3.3	Organic volatile impurities	6
1.3.4	Limit of guanine	6
1.4	Assay methods.	7
1.4.1	Acyclovir bulk drug substance	7
1.4.2	Acyclovir in pharmaceutical preparations.	7
2.	Potentiometric Titration.	8
3.	Spectroscopic Methods of Analysis	8
3.1	Spectrophotometry.	8
3.2	Colorimetry.	9
3.3	Fluorimetry.	9
3.4	Vibrational spectroscopy.	9
3.5	Mass spectrometry	10
4.	Chromatographic Methods of Analysis.	10
4.1	Thin-layer chromatography.	10
4.2	High-performance liquid chromatography	15
4.3	Capillary electrophoresis.	16
5.	Determination in Body Fluids and Tissues	17
5.1	Radio-immunoassay methods	17
5.2	Enzyme-immunoassay methods	17
5.3	Chromatographic methods	17
6.	Acknowledgments	18
7.	References	18

1. COMPENDIAL METHODS OF ANALYSIS

1.1 Identification

1.1.1 Bulk drug substance

According to the United States Pharmacopoeia 25 [1], the identification of acyclovir is verified on the basis of characteristic infrared

absorption, following the directive general test <197K> (method A). In addition, identification is effected using a liquid chromatography procedure (described under 'Assay and Limit for Guanine').

Other compendia also use the infrared absorption method for identification purposes. The particular methods are as follows:

British Pharmacopoeia 2000: method <2.2.24> [2]

Deutsche Arzneibuch 10: method <V.6.18> [3]

Indonesian Pharmacopoeia 1995 [4]

1.1.2 Acyclovir in pharmaceutical preparations

United States Pharmacopeia 25 describes a liquid chromatography method for identification of acyclovir in the pharmaceutical preparations [1]. The method uses a L1 type column (octadecyl silane chemically bonded to porous silica or ceramic microparticles, 3–10 μm in diameter). The mobile phase is a solution containing degassed glacial acetic acid in water (1 in 10,000).

British Pharmacopeia 2000 Volume II uses characteristic light absorption (230–350 nm) as the identification method (A) [5]. The spectrum should have a maximum at 255 nm and a broad shoulder about 274 nm. For method (B), British Pharmacopeia 2000 Volume II describes a thin-layer chromatography (TLC) method using cellulose F₂₅₄ as the stationary phase. The first mobile phase is ethyl acetate, and the second mobile phase is a mixture of 1-propanol/13.5 M ammonia/5% solution of ammonium sulfate in a 10/30/60 v/v/v ratio. The spots of guanine and acyclovir are detected using 254 nm ultraviolet light. The guanine spot should not be more intense than that of the guanine standard (prepared to be 6.0 mg in 100 mL of 0.1 M NaOH).

1.2 Water content

In the various compendia, the water content of acyclovir is determined by titration methods:

United States Pharmacopeia 25: general test <921>, method I [1]

British Pharmacopoeia 2000: semimicro method <2.2.24> [2]

Deutsche Arzneibuch 10: Karl-Fischer method [3]

Indonesian Pharmacopoeia 1995: method <1031> [4]

In all four the compendia, the specification is not more than 6.0%.

1.3 Impurity analyses

1.3.1 Ordinary impurities

Thin-layer chromatography methodology is used to detect the ordinary impurities of acyclovir:

United States Pharmacopoeia 25: method <466> [1]

British Pharmacopoeia 2000: method <2.2.27> [2]

Deutsche Arzneibuch 10: method <V.6.20.2> [3]

Indonesian Pharmacopoeia 1995: method <481> [4]

In these methods, either silica gel GF₂₅₄ [2, 3] or silica gel [1, 4] is used as the stationary phase. The respective mobile phases are 80/20/2 v/v/v methylene chloride/methanol/ammonium hydroxide [2, 3], and 80/20/2 v/v/v chloroform/methanol/ammonium hydroxide [1, 4]. In all procedures, visualization of the plates is performed using 254 nm UV light.

1.3.2 Sulfate

In British Pharmacopoeia 2000, the sulfate content is determined using general test <2.4.14> [2], while in Deutsche Arzneibuch 10 method <V.3.2.14> is used [3]. Both compendial specifications are not more than 0.1%.

1.3.3 Organic volatile impurities

The United States Pharmacopoeia 25 requires a measurement of the organic volatile impurities by gas chromatography, specifically through the use of general test <467>, method V [1].

1.3.4 Limit of guanine

For assaying the level of guanine impurity, a liquid chromatography method is used by all compendia [1–4].

The British Pharmacopoeia 2000 [2] and Deutsche Arzneibuch 10 [3] use octadecylsilyl silica gel for chromatography R(3 µm) as the stationary phase. The mobile phase is prepared as a mixture of an aqueous solution (6.0 g sodium dihydrogen phosphate and 1.0 g of sodium decanesulfate in 900 mL water, pH 3 ± 0.1, with phosphoric acid), 40 mL acetonitrile, and finally diluted with water to 1 L.

The United States Pharmacopoeia 25 [1] and Indonesian Pharmacopoeia [4] use stationary phase type L1 (octadecyl silane chemically bonded to

porous silica or ceramic microparticles, 3–10 μm in diameter). The mobile phase in this method is a 1 in 10,000 solution of degassed glacial acetic acid in water.

The specification for guanine content in bulk drug substance is not more than 0.7%.

1.4 Assay methods

1.4.1 *Acyclovir bulk drug substance*

The United States Pharmacopeia 25 [1] and Indonesian Pharmacopoeia [4] both use the liquid chromatography method as described above as 'Limit of Guanine' for the assay of acyclovir.

The British Pharmacopeia 2000 [2] and Deutsche Arzneibuch 10 [3] use a potentiometric titration method, based on the use of perchloric acid as the titrant, for the determination of acyclovir. This methodology will be described in more detail in a later section.

The assay specifications for bulk acyclovir differ with the compendia:

United States Pharmacopeia 25; Indonesian Pharmacopoeia 1995: not less than 98.0 and not more than 101.0%, acyclovir, calculated on the anhydrous basis [1, 4]

British Pharmacopoeia 2000; Deutsche Arzneibuch 10: not less than 98.5 and not more than 101.0%, acyclovir, calculated on the anhydrous basis [2, 3]

1.4.2 *Acyclovir in pharmaceutical preparations*

For assaying acyclovir content in capsules, ointment, tablets, and oral suspensions, the United States Pharmacopeia 25 [1] described a liquid chromatography method using a L1 type column (octadecyl silane chemically bonded to porous silica or ceramic microparticles, 3–10 μm in diameter), a solution of 0.02 M acetic acid as the mobile phase, and detection on the basis of UV absorbance at 254 nm.

For analyzing acyclovir in injection preparations, the United States Pharmacopeia 25 [1] uses a variable mixture of two solutions as the mobile phase. Solution A consists of a 125/8 mixture of 0.17 M acetic acid/methanol, and solution B is methanol.

British Pharmacopeia 2000 Volume II [5] describes a spectrophotometric method for analyzing acyclovir in pharmaceutical preparations (creams,

intravenous infusion solutions, and tablets). After extraction of the analyte, the acyclovir content was measured on the basis of UV absorbance at 255 nm.

A fluorimetric method was described in British Pharmacopeia 2000 Volume II [5] for the determination of acyclovir in oral suspensions. After extraction of the oral suspension with sulfuric acid and water, a mixture of 0.01% cetrimide in 0.05 H_2SO_4 is added. The analyte is then determined using the fluorimetric procedure that will be described in a subsequent section.

2. POTENTIOMETRIC TITRATION

The British Pharmacopeia 2000 (method (2.5.12)) [2] and Deutsche Arzneibuch 10 (method (V.6.14)) [3] describe an official method for the assay of acyclovir that is based on the use of potentiometric titration.

In this method, 0.150 g of acyclovir is dissolved in 60 mL anhydrous acetic acid, and then titrated with 0.1 M perchloric acid. The end point is determined potentiometrically, and a blank titration should be performed. 1.0 mL of 0.1 M HClO_4 acid is equivalent to 22.52 mg of anhydrous acyclovir.

3. SPECTROSCOPIC METHODS OF ANALYSIS

3.1 Spectrophotometry

The British Pharmacopeia 2000 Volume II [5] describes various spectrophotometric methods for the assay of acyclovir in its pharmaceutical preparations. These may be summarized as follows:

Cream Formulations: After the cream formulation is extracted with a combination solvent of 0.5 M sulfuric acid and ethyl acetate, the absorbance of the analyte is measured at 255 nm. The acyclovir content is calculated by taking 562 as the value for the $A(1\%, 1\text{ cm})$ parameter.

Eye Ointment Formulations: The ointment is extracted with a combination solvent of hexane, 0.1 M NaOH, and 2M HCl, and after that the absorbance of the analyte is measured at 255 nm. The content of acyclovir is calculated by taking 560 as the value for the $A(1\%, 1\text{ cm})$ parameter.

Intravenous Infusion Formulations: After dissolving the preparation with 0.1 M HCl, the absorbance of the analyte is then measured at 255 nm.

The content of acyclovir is calculated by taking 560 as the value for the $A(1\%, 1\text{ cm})$ parameter.

Tablets: Tablets were extracted using a combination solvent of 0.1 M NaOH and 0.1 M HCl, and then the absorbance of the analyte is measured at 255 nm. The content of acyclovir is calculated by taking 562 as the value for the $A(1\%, 1\text{ cm})$ parameter.

3.2 Colorimetry

Basavalah and Prameela reported the determination of acyclovir in bulk drug substance and in its formulations by reacting the compound with the Folin–Ciocalteu reagent in an alkaline medium [6]. The blue colored product was quantitated on the basis of its absorption at 760 nm.

The method was found to be linear over the range of 50–450 $\mu\text{g/mL}$ ($r = 0.9998$, $n = 9$). The detection limit and quantitation limit were reported to be 5.68 and 18.95 $\mu\text{g/mL}$, respectively. The relative standard deviation associated with the accuracy and precision of the method was less than 2%.

3.3 Fluorimetry

The British Pharmacopeia Volume II [5] described a fluorimetric method for the assay of acyclovir in oral suspension preparations. An equivalent preparation containing 0.4 g acyclovir was extracted (using ultrasonification) with 400 mL water and 25 mL of 1 M sulfuric acid. The mixture is then filtered, and after discarding the first filtrate, 5 mL of the filtrate is mixed with 200 mL of 0.05 M sulfuric acid. 10 mL of the resulting solution is then mixed with 5 mL of 0.01% w/v of cetrимide in 0.05 M sulfuric acid, and diluted to 100 mL with 0.05 M sulfuric acid. Acyclovir was then determined by measuring the fluorescence of the reaction product at 415 nm (excitation wavelength of 388 nm).

3.4 Vibrational spectroscopy

Georgiou reported a method for the direct determination of acyclovir tablets within their PVC-blister package (without extraction) through the use of FT-Raman spectroscopy [7]. A stepwise multiple linear regression at the Raman bands 1690 and 1482 cm^{-1} was found to be linear ($r = 0.997$) over the range of 0–100% w/w ($n = 8$).

The limit of detection of the method was reported to be in the range of 2.8–11.1% and 3.7–8.8% w/w for band intensity and band area measurements, respectively. The RSD ($n=3$) associated with the precision determination was in the range of 0.7–5.6% and 0.4–4.5% w/w for band intensity and band area measurements, respectively.

3.5 Mass spectrometry

Xu *et al.* [8] and Brown *et al.* [9] described the application of selected reaction monitoring/mass spectrometry for the determination of acyclovir and ganciclovir in plasma and tissue. After extraction and separation, the analyte was determined using high-performance liquid chromatography (HPLC) (the experimental parameters are summarized in Table 1). The fragments having $m/z=226$ and $m/z=152$ (for acyclovir), and $m/z=256$ and $m/z=152$ (for ganciclovir), were monitored to quantitate the analyte.

The method of Xu *et al.* was reported to be reproducible and linear over the range of 10–10,000 ng/mL, with the accuracy and precision being in the range of 89–109% and 2.0–6.9%, respectively [8].

4. CHROMATOGRAPHIC METHODS OF ANALYSIS

4.1 Thin-layer chromatography

For identification and determination of ordinary impurities in acyclovir bulk drug substance, the United States Pharmacopeia 25 [1], British Pharmacopeia 2000 [2], Deutsche Arzneibuch 10 [3], and Indonesian Pharmacopeia [4] describe official TLC methods. These were described in previous sections (for instance, see Section 1.3.1).

Boryski *et al.* reported TLC methods for the qualitative identification of acyclovir and its N-substituted derivatives [10]. The methods use silica as the stationary phase, and mixtures of isopropanol/ammonia/water (7/1/2), 1-butanol/acetic acid/water (5/3/2), or chloroform/methanol (4/1) as various mobile phases.

Dubhashi and Vavia described a high-performance TLC (HPTLC) method for analyzing acyclovir in its topical formulation, and for *in vitro* skin permeation studies [11]. Silica gel 60 F₂₅₄ HPTLC plates (10 × 10 cm) were used as the stationary phase, the mobile phase was 15/9/4 v/v/v

Table 1

HPLC Methods for Acyclovir

Column	Mobile phase	Detection	Sample	Reference
XDB C-8	10 mM acetate-citrate buffer/ 3.7 mM octanesulfonic acid (87.5/12.5 v/v)	UV 254 nm	Plasma and amniotic fluids	Brown <i>et al.</i> 2002 [14]
XDB C-8	30 mM acetate-citrate buffer- 5 mM octanesulfonic acid/ acetonitrile (91/1 v/v)	UV 254 nm	Placental tissue	Brown <i>et al.</i> 2002 [14]
Silica	Acetonitrile/formate buffer (8/2 v/v)	ESI-MS/MS	Rat plasma and tissues	Brown <i>et al.</i> 2002 [9]
Guanine adducts	50 mM sodium acetate, 2% methanol, pH 5.2 with 50 μ L acetic acid	Coul Array (300, 400, 475, 620, 675, 775, 850 mV vs Pd reference)	Human plasma	Esa's application note [15]
Develosil RP aqueous	Acetonitrile/1 mM phosphate buffer (18/82 v/v)	Fluorescence after derivitization using phenyglyoxal	Human serum	Tsuchie <i>et al.</i> 2001 [16]

(continued)

Table 1 (continued)

Column	Mobile phase	Detection	Sample	Reference
ODS-AQ	Gradient. Solvent A: 5 mM NH ₄ OAc/methanol (95/5); Solvent B: 5 mM NH ₄ OAc in pure methanol. 90–55% A in 4 min; than to 20% A 2 min, and back to 90% A.	SIM-MS	Plasma, Acyclovir as Internal standard for determination of ganciclovir	Xu <i>et al.</i> [8]
Novaflex C 18	Octanesulfonic acid buffer pH 2.5/methanol (92/8, v/v)	UV 254 nm	Human plasma	Bangaru <i>et al.</i> 2000 [17]
Spherisorb ODA	Phosphate buffer pH 3/methanol (95/5, v/v)	UV 254 nm	Liposomal formulation	Caamano <i>et al.</i> 1999 [18]
Symmetry Shield RP-8	Acetonitrile/ammonium phosphate buffer (2/98, v/v)	UV 254 nm	Human biological fluids	Pham <i>et al.</i> 1999 [19]
C-18	18% acetonitrile, 5 mM duodecyl sulfate, and 30 mM phosphate buffer pH 2.1	Fluorescence, excitation 285 nm, emission 380 nm	Serum and urine	Svensson <i>et al.</i> 1997 [20]
Lichrosorb RP-18	1% acetonitrile in 0.02 M disodium hydrogen orthophosphate pH 2.5	Fluorescence, excitation 270 nm, emission 380 nm	Human plasma	Peh and Yuen 1997 [21]

Hypersil ODS 3	Potassium dihydrogen phosphate solution pH 3.5	UV 254 nm	Human plasma	Boulieu <i>et al.</i> 1997 [22]
Nucleosil C-18	Gradient, acetonitrile to 20 mM perchloric acid (0–100%, for 3 min); 45–55% for 3 min	Fluorescence excitation 260 nm, emission 375 nm	Blood and urine	Vergin <i>et al.</i> 1995 [23]
NovaPak C-18	Methanol/10 mM Na ₂ HPO ₄ + 10 mM sodium octanesulfonate (7/93, v/v) final pH 2.80 with H ₃ PO ₄	UV 250 nm	Blood	Swart <i>et al.</i> 1994 [24]
Pecosphere 5C-C 18	Acetonitrile/0.1% acetic acid (2/98)	UV 254 nm	Perfusate	Volpato <i>et al.</i> 1995 [25]
μBondapak C-18	Acetonitrile/50 mM ammonium acetate (2/98)	UV 254 nm	Blood	Lim <i>et al.</i> (1994) [26]
RP-8	Methanol/100 mM phosphate buffer pH 3 containing 50 mM octanesulfonic acid (5/95)	UV 254 nm	Blood	Nebinger and Koel (1993) [27]
Nucleosil 120 C 18	Gradient. Solution A: 20 mM perchloric acid; B: Acetonitrile/20 mM perchloric acid (45/55). A/B (100/3 for 3 min, 0/100) for 3 min, step gradient	Fluorescence excitation 260 nm, emission 375 nm	Blood	Mascher <i>et al.</i> (1992) [28]

(continued)

Table 1 (continued)

Column	Mobile phase	Detection	Sample	Reference
YWGC18 H37	Methanol/water (50/50)	UV 254 nm	Human plasma	Zhang and Dong (1993) [29]
μ Bondapak C-18	Acetonitrile/50 mM ammonium acetate (2/98)	UV 254 nm	Blood, urine	Kelloway <i>et al.</i> (1991) [30]
μ Bondapak C-18	Acetonitrile/50 mM ammonium acetate (2/98)	UV 262 nm (plasma); UV 254 nm (urine)	Blood, urine	Kearns <i>et al.</i> (1991) [31]
NovaPak C 18	Gradient. Solution A 50 mM Na ₂ HPO ₄ ; B: methanol/water containing 5 mM Na ₂ HPO ₄ . A/B (99/1) for 1.5 min, to (5/95) over 18.5 min, reequilibrate at initial condition for 10 min	UV 254 nm	Blood	Boyd <i>et al.</i> (1988) [32]
Spheron Micro 300	Buffer containing 100 mM phosphoric acid and 100 mM sodium sulfate, pH 1.8	Fluorescence excitation 285 nm, emission 370 nm	Blood	Salamoun <i>et al.</i> (1987) [33]

chloroform/methanol/ammonia, and detection is effected using 255 nm UV light. The method was found to be linear over the range of 10–20 $\mu\text{g/mL}$, and the detection limit and quantitation limit were reported as 30 and 50 ng, respectively. Average recoveries of the method were 101.8 and 100.1%.

Sia *et al.* reported a TLC method for the assay of acyclovir in pharmaceutical preparations (tablets and creams) [12]. TLC plates pre-coated with silica gel 60 F₂₅₄ were used as the stationary phase, a 15/9/6 v/v/v mixture of 1-butanol/glacial acetic acid/water was used as the mobile phase, and detection was effected at 277 nm. The method was shown to be linear over the range of 100–900 ng/spot ($n=9$, $r=0.9985$, $V_{\text{xo}}=3.2\%$), and the detection limit was reported as 36 ng/spot. The mean recoveries were in the range of 100.2–101.5%, and all RSD values for the intermediate precision were less than 2%.

4.2 High-performance liquid chromatography

As described in Section 1.3.4, the United States Pharmacopeia 25 described a HPLC method for determination of acyclovir in bulk drug substance and in its pharmaceutical preparations [1].

An excellent review of separation of acyclovir, and some related antiviral compounds, through the use of HPLC and capillary electrophoresis (CE) methodology was recently published by Loregian *et al.* [13].

A number of HPLC bio-analysis methods for the determination of acyclovir have been reported [8, 9, 14–33], and a summary of these methods is given in Table 1.

The stability of acyclovir in 5% dextrose and 0.9% sodium chloride injection solutions was studied by Zhang *et al.* [34] and Gupta *et al.* [35]. In their work, Zhang *et al.* used a $\mu\text{Bondapak C-18}$ column as the stationary phase, and a mobile phase of 5 mM sodium acetate in water (pH 3.0) [34]. Gupta *et al.* used the same stationary phase, but a mobile phase consisting of 3% v/v acetonitrile in 0.1 M monosodium phosphate buffer [35]. Both methods used UV detection at 254 nm, and the method of Gupta *et al.* used a 0.2% solution of salicylic acid as an internal standard [35]. Linearity of the calibration plot was observed over the range of 0.025–0.150 mg/mL ($r > 0.9999$), when using an injection volume of 20 μL [34]. It was reported that degradation product peaks did not interfere the intact acyclovir peak.

Ashton *et al.* reported a significant correlation of the chromatography hydrophobicity index of acyclovir and its 18 esters to the calculated octanol–water partition coefficient ($\log P$) ($r > 0.96$) [36]. In this work, they used a Zorbax C8 column, a mobile phase containing various amounts of methanol (5–95%), and detection at 254 nm. By using an immobilized human serum albumin column and a mixture of 1% isopropanol and 10 mM phosphate buffer (pH 3) as the mobile phase, the binding properties of acyclovir and its 18 esters were determined.

Lipka-Belloli *et al.* described a HPLC method using a chiral column, cellulose tris-3,5-dimethylphenylcarbamate (Chiralcel OD-H), for the determination of the enantiomeric purity of nucleoside analogs related to acyclovir [37].

4.3 Capillary electrophoresis

Vo *et al.* reported a sensitive assay for acyclovir in plasma based on high-performance capillary electrophoresis (HPCE) [38]. The method uses uncoated capillaries with internal diameter of 75 μm , external diameter of 360 μm , and length of 60.2 cm (50 cm to detector). Separation was achieved with no plasma interference using micellar electrokinetic chromatography (175 mM SDS and 100 mM hydroxypropyl- β -cyclodextrin) in 90 mM borate buffer (pH 8.8, containing 0.2% NaCl). All separations were carried out at 22°C using 20 kV throughout the experiments, and detection at 254 nm was used. Using this method, linearity was achieved from 20 to 10,000 ng/mL ($R^2 > 0.999$), the recovery was $102.9 \pm 14.2\%$, and the limit of quantification was 20 ng/mL.

Zhang *et al.* described a HPCE method with on-column amperometric detection [39]. The method used α -amino-5-mercapto-3,4-dithiazole as the internal standard for analysis of acyclovir in pharmaceuticals and urine. Analysis was performed using capillaries with a high voltage electric isolating joint (50 μm id., 40.5 cm length for separation, and 1.7 cm for detecting capillaries). The HPCE systems was operated with anode injection by applying 20 ± 0.1 kV for 5 s and maintained at $20 \pm 0.2^\circ\text{C}$. The separation voltage was 20 ± 0.1 kV, and separation was performed using 40 mM borax buffer. Linearity was achieved from 0.5 to 20 mg/L, recoveries were in the range of 98–101%, and the detection limit was 0.15 mg/L.

Zhang *et al.* [40] reported that the HPCE and HPLC methods for assaying acyclovir in pharmaceuticals and urine yielded comparable

results in terms of linearity, range, recovery, and reproducibility. Loregian *et al.* [13] stated that CE is more economical and environment-friendly than conventional HPLC, although the sensitivity of CE was limited compared to that of HPLC. By increasing the quantity of injected sample, the sensitivity of CE could be made comparable to that of HPLC.

5. DETERMINATION IN BODY FLUIDS AND TISSUES

5.1 Radio-immunoassay methods

Tadepalli and Quinn described a homogenous, single tube scintillation radio-immunoassay method to determine acyclovir in human plasma [41]. The reagents used in this method were anti-acyclovir monoclonal antibody, tritiated acyclovir, and goat antimouse immunoglobulin G coupled to fluoromicrospheres. The standard curve covered the range of 0.7–90 ng/mL, the 50% inhibitory concentration was 5.0 ng/mL, and the limit of quantitation was 7 ng/mL. Analyte recovery was found to be in the range between 90 and 110%. Before analysis, plasma samples (containing EDTA as an anticoagulant) were frozen at -20°C .

5.2 Enzyme-immunoassay methods

A simple and sensitive-linked immunosorbant assay for detection and quantitation of acyclovir in human plasma and urine was reported [42]. Acyclovir immobilized on a solid phase and free acyclovir in the sample solution were allowed to compete for a limited amount of anti-acyclovir monoclonal antibody, and detected by use of alkaline phosphatase-conjugated antimouse immunoglobulin. The Hill plot for acyclovir was found to be linear over a hundredfold concentration range, with a lower concentration limit of 0.2 nM. This method showed significant cross reaction with BW B759U {9-(2-hydroxy-1-hydroxymethylethoxy)-methylguanine}.

5.3 Chromatographic methods

Most publications that have appeared in the last 15 years on the chromatographic methods for assaying acyclovir in biological fluids have used HPLC technology (see Table 1). Some HPTLC and CE methods have also been published, and these were discussed in previous sections.

Before analysis, biological samples should be deproteinized using perchloric acid and then extracted using solid-phase extraction. Such

methodology is covered in the review by Loregian *et al.* [13]. Acyclovir was shown to be stable over a period of four weeks when stored at -20°C , while blood samples should be collected and centrifuged without delay at 4°C [13]. Xu *et al.* recommended storage of plasma samples at -80°C before analysis [8].

6. ACKNOWLEDGMENTS

We thank DAAD, Bonn, Germany, for scholarships during 2002 supporting work at the Universities of Wuerzburg (MY) and Duesseldorf (GI), Germany, and Junaedi Khotib (Hoshi University, Tokyo, Japan) for his kind technical assistance.

7. REFERENCES

1. The United States Pharmacopoeia, 25th edn., United States Pharmacopoeial Convention, Rockville, MD 20852, pp. 47–50 (2001).
2. British Pharmacopoeia 2000, Volume I, The Stationary Office, London, pp. 43–45 (2000).
3. Deutsche Arzneibuch 10, Band 2 A-L, Deutscher Apotheker Verlag Stuttgart, Govi-Verlag GmbH, Frankfurt (1996).
4. Farmakope Indonesia (Indonesian Pharmacopoeia), Edisi IV, Departemen Kesehatan Republik Indonesia, Jakarta, p. 57 (1995).
5. British Pharmacopoeia 2000, Volume II, The Stationary Office, London, pp. 1706–1709 (2000).
6. K. Basavalah and H.C. Pramaela, *Farmaco*, **57**, 443–449 (2002).
7. C.A. Georgiou, <http://www.aua.gr/georgiou/index.htm> (1/2/2003)
8. K. Xu, M. Lanuti, E.S. Lambright, S.D. Force, S.M. Albelda, and A.I. Blair, *Biomed. Chromatogr.*, **14**, 93–98 (2000).
9. S.D. Brown, C.A. White, and M.G. Bartlett, *Rapid Commun. Mass Spectrom.*, **16**, 1871–1876 (2002).
10. J. Boryski, B. Golankiewicz, and D.D. Clerq, *J. Medical Chem.*, **31**, 1351–1355 (1988).
11. S.S. Dubhashi and P.R. Vavia, *J. Pharm. Biomed. Anal.*, **23**, 1017–1022 (2000).
12. T.K. Sia, L. Wualandari, and G. Indrayanto, *J. Planar. Chromatogr.*, **15**, 42–45 (2002).

13. A. Loregian, R. Gatti, G. Palu, and E.F. De Palo, *J. Chromatogr. B.*, **764**, 289–311 (2001).
14. S.D. Brown, CA. White, C.K. Chun, and M.G. Bartlett, *J. Chromatogr. B.*, **772**, 327–334 (2002).
15. Esa Application Note, <http://www.norlab.fi/esa/esa10311sov0047/pdf> (3/1/2003).
16. M. Tssuchie, S. Hara, M. Kimura, M. Fuji, N. Ono, and M. Kai, *Anal. Sci.*, **17**, 811–814 (2001).
17. R.A. Bungaru, Y.K. Bansai, A.R. Rao, and T.P. Gandhi, *J. Chromatogr. B.*, **739**, 231–237 (2000).
18. M.M. Camaano, L.V. Garcia, B. Elorza, and J.R. Chantres, *J. Pharm. Biomed. Anal.*, **21**, 619–624 (1999).
19. C. Pham-Huy, F. Stathouloupoulou, P. Sandouk, J.M. Scherrman, J.M. Palombo, C. Girre, *J. Chromatogr. B.*, **732**, 47–53 (1999).
20. J.O. Svensson, L. Barkholt, J. Sawe, *J. Chromatogr. B.*, **690**, 363–366 (1997).
21. K.K. Peh and K.H. Yuen, *J. Chromatogr. B.*, **693**, 241–244 (1997).
22. R. Boulieu, C. Gallant, and N. Silberstain, *J. Chromatogr. B.*, **693**, 233–236 (1997).
23. H. Vergin, C. Kikuta, H. Mascher, and R. Metz, *Arzneimittelforschung*, **45**, 508–515 (1995).
24. K.J. Swart, H.K.L. Hundt, and A.M. Groenewald, *J. Chromatogr. B.*, **663**, 65–69 (1994).
25. N.M. Volpato, P. Santi, and P. Colombo, *Pharm. Res.*, **12**, 1623–1625 (1995).
26. J.M. Lim, A. Marco, P. Mojaverian, and P. Lin, *J. Pharm. Biomed. Anal.*, **12**, 699–703 (1994).
27. P. Nebinger and M. Koel, *J. Chromatogr.*, **619**, 342–344 (1993).
28. H. Mascher, C. Kikuta, R. Metz, and H. Vergin, *J. Chromatogr.*, **583**, 122–127 (1992).
29. C. Zhang and S.N. Dong, *Yao Xue Xue Bao*, **28**, 629–633 (1993).
30. J.S. Kelloway, W.M. Awni, C.C. Lin, J. Lim, M.B. Affrime, W.F. Keane, G.R. Matzke, and C.E. Halstenson, *Antimicrob. Agents Chemother.*, **35**, 2267–2274 (1991).
31. G.I. Kearns, M.D. Reed, R.F. Jacobs, M. Ardite, R.D. Yogeve, and J.L. Blumer, *Antimicrob. Agents Chemother.*, **35**, 2078–2084 (1991).
32. M.R. Boyd, T.H. Bacon, and D. Sutton, *Antimicrob. Agents Chemother.*, **32**, 358–363 (1988).

33. J. Salamoun, V. Sprta, T. Sladek, and M. Smrz, *J. Chromatogr.*, **420**, 197–222 (1987).
34. Y. Zhang, L.A. Trissel, and J.F. Martinez, *Am. J. Health Syst. Pharm.*, **55**, 574–577 (1998).
35. D.V. Gupta, Y. Pramar, and C. Bethea, *J. Clin. Pharm. Ther.*, **14**, 451–456 (1989).
36. D.S. Ashton, C. Beddel, A.D. Ray, and K. Valko, *J. Chromatogr. A.*, **707**, 367–372 (1995).
37. E. Lipka-Belloli, V. Glacon, G. Mackenzie, D. Ewing, C. Len, C. Vaccher, and J.P. Bonte, *J. Chromatogr. A.*, **972**, 211–239 (2002).
38. H.C. Vo, P.A. Henning, D.T. Leung, and S.L. Sacks, *J. Chromatogr. B.*, **772**, 291–297 (2002).
39. S.S. Zhang, Z.B. Yuan, H.X. Liu, H. Zou, H. Ziong, and Y.J. Wu, *Electrophoresis*, **21**, 2995–2998 (2000).
40. S.S. Zhang, H.X. Liu, and Z.B. Yuan, *Biomed. Chromatogr.*, **10**, 256–257 (1996).
41. S.M. Tadepalli and R. P. Quinn, *J. Pharm. Biomed. Anal.*, **15**, 157–163 (1996).
42. S.M. Tadepalli, R.P. Quinn, and D.R. Averett, *Antimicrob. Agents Chemother.*, **29**, 93–98 (1986).

Ceftriaxone Sodium: Comprehensive Profile

Heather M. Owens and Alekha K. Dash

*Department of Pharmacy Sciences
School of Pharmacy and Health Professions
Creighton University
Omaha, NE 68178, USA*

CONTENTS

1.	Description	23
1.1	Nomenclature	23
1.1.1	Systematic chemical name.	23
1.1.2	Nonproprietary name.	23
1.1.3	Proprietary names	23
1.2	Formulae.	24
1.2.1	Empirical formula, molecular weight, CAS number	24
1.2.2	Structural formula	24
1.3	Elemental analysis	24
1.4	Appearance	24
1.5	Uses and applications.	24
1.5.1	History	24
1.5.2	Therapeutic aspects	25
2.	Method of Preparation	26
3.	Physical Properties	27
3.1	Ionization constants	27
3.2	Partition coefficient.	27
3.3	Solubility characteristics	28
3.4	Optical activity	28
3.5	X-Ray powder diffraction	30
3.6	Thermal methods of analysis.	31
3.6.1	Melting behavior	31
3.6.2	Differential scanning calorimetry.	31
3.6.3	Thermogravimetric analysis	34
3.7	Spectroscopy	35
3.7.1	UV–VIS spectroscopy	35
3.7.2	Vibrational spectroscopy	35
3.7.3	Nuclear magnetic resonance spectrometry	35
3.7.3.1	¹ H-NMR spectrum	35
3.7.3.2	¹³ C-NMR spectrum.	35
3.8	Mass spectrometry	36
4.	Methods of Analysis	42
4.1	Identification	42
4.2	Spectrophotometric analysis	42
4.3	Chromatographic methods of analysis	42
4.3.1	Thin-layer chromatography	42
4.3.2	High-performance liquid chromatography	44
4.4	Biological methods.	46

5.	Stability	46
6.	Pharmaceutical Dosage Forms	48
7.	Drug Metabolism and Pharmacokinetics	48
7.1	Pharmacokinetics	48
7.1.1	Absorption and plasma concentrations	50
7.1.2	Volume of distribution	51
7.1.3	Protein binding	51
7.1.4	Fluid and tissue penetration	51
7.1.5	Elimination	52
7.1.6	Half-life	52
7.1.7	Influence of age on pharmacokinetic parameters	52
7.1.8	Influence of disease on the pharmacokinetic parameters	53
7.2	Metabolism	53
8.	Toxicity	53
9.	Acknowledgments	54
10.	References	54

1. DESCRIPTION

1.1 Nomenclature

1.1.1 Systematic chemical name [1]

[6*R*-[6 α ,7 β , (Z)]]-5-thia-1-azabicyclo-[4.2.0]-oct-2-ene-2-carboxylic acid, 7-[[[(2-amino-4-thiazolyl)(methoxyimino)-acetyl]amino]-8-oxo-3-[[[(1,2,5,6-tetrahydro-2-methyl-5,6-dioxo-1-2,4-triazin-3-yl)-thio]methyl]]-, disodium salt

1.1.2 Nonproprietary name [1]

Ceftriaxone Sodium

1.1.3 Proprietary names [2]

Rocephin[®], Roche
 Rocephin ADD-Vantage[®], Roche
 Rocephin[®] Piggyback, Roche
 Rocephin[®] in iso-osmotic dextrose injection (Galaxy[®]), Roche, Baxter
 Rocefacin[®], Roche
 Rocefin[®], Roche
 Rocephine[®], Roche

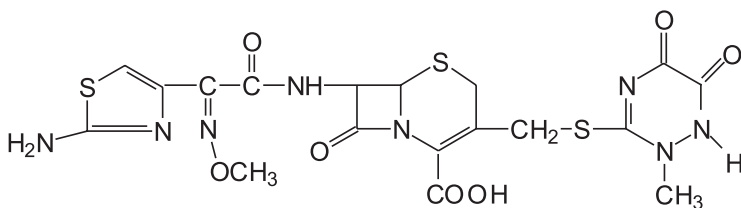
1.2 Formulae

1.2.1 Empirical formula, molecular weight, CAS number

$C_{18}H_{18}N_8O_7S_3$ [MW = 554.53 g/mol]

CAS number = 74578-69-1

1.2.2 Structural formula



1.3 Elemental analysis

The calculated elemental composition is as follows:

carbon:	38.98%
hydrogen:	3.27%
oxygen:	20.20%
nitrogen:	20.21%
sulfur:	17.34%

1.4 Appearance [2]

Commercially available ceftriaxone sodium is a white to yellowish-orange odorless crystalline powder, which is obtained as the hemiheptahydrate. Its color in solution varies from light yellow to amber, depending on the concentration and length of storage.

1.5 Uses and applications

1.5.1 History

Ceftriaxone belongs to a group of antibiotics known as the cephalosporins, which are closely related to penicillin [3]. The discovery of the first cephalosporin was made serendipitously by Giuseppe Brotzu, a professor of hygiene in Sardinia. His mistaken idea that the production of antibiotics by fungi was responsible for the self-purification of sewage led to the production of a new class of antibiotics that became known as the

cephalosporins. Using the *Penicillium* fungus model, which produced penicillin antibiotics, he cultured the Cagliari sewage run-off for fungi. In 1945, he isolated an antibiotic-producing fungus, *Cephalosporium acremonium*, which produced three different antibiotics that were active against both gram-negative and gram-positive bacteria. Dr. Brotzu injected these crude extracts, either intramuscularly or intravenously, into both animals and patients with a variety of infections, including those of the soft-tissue, brucellosis, and typhoid fever [3].

The results of Dr. Brotzu's research interested British scientists, and they later discovered that the antibacterial activity of cephalosporins was not found in the major antibiotic substances that the fungus synthesized, but instead in the small amounts of cephalosporin C it produced. At this time, Sir Howard Florey (one of the scientists who discovered penicillin) became interested in cephalosporin C as a result of the increasing problem of penicillin-resistant infections due to penicillinase-producing staphylococci [3].

In 1960, the British government closed the Antibiotics Research Station which had been studying cephalosporin C. Pharmaceutical companies then became interested in producing cephalosporins, however, the discovery of methicillin (an antibiotic highly active against penicillin-resistant staphylococci) in 1961 decreased the urgency for further development of the cephalosporin antibiotics. In 1964, the first cephalosporin, cephalothin, was introduced. Cephalosporins are classified as first, second, or third generation on the basis of their spectrum of activity against gram-negative rods [3–5]. In 1979, the first second-generation drugs, cefamandole and cefoxitin, were placed on the market. In 1981, the first third-generation drug, cefotaxime, was introduced. Ceftriaxone is considered a third-generation antibiotic [3].

1.5.2 Therapeutic aspects

The cephalosporanic acid moiety possesses a β -lactam ring constituent in conjunction with a dihydro-metathiazine ring. The mechanism of action associated with cephalosporins is similar to that of penicillin, since they inhibit the cross-linking of the peptidoglycan units in the bacterial cell wall by occupying the (D)-alanyl-(D)-alanine substrate site of transpeptidase [4–6].

Ceftriaxone has obtained high status among the cephalosporin drugs. Like other third generation cephalosporins, it is considerably less active

than first generation drugs against gram-positive bacteria, but has a much broader spectrum of activity against gram-negative organisms. It is also effective against gram-negative anaerobes and *Enterobacteriaceae* (*E. coli*, *Enterobacter*, *Klebsiella pneumoniae*) [6]. Ceftriaxone exhibits high stability to beta-lactamases excluding those produced by *B. fragilis* and various strains of *Klebsiella*, *Proteus vulgaris*, and *Pseudomonas cepacia* [6].

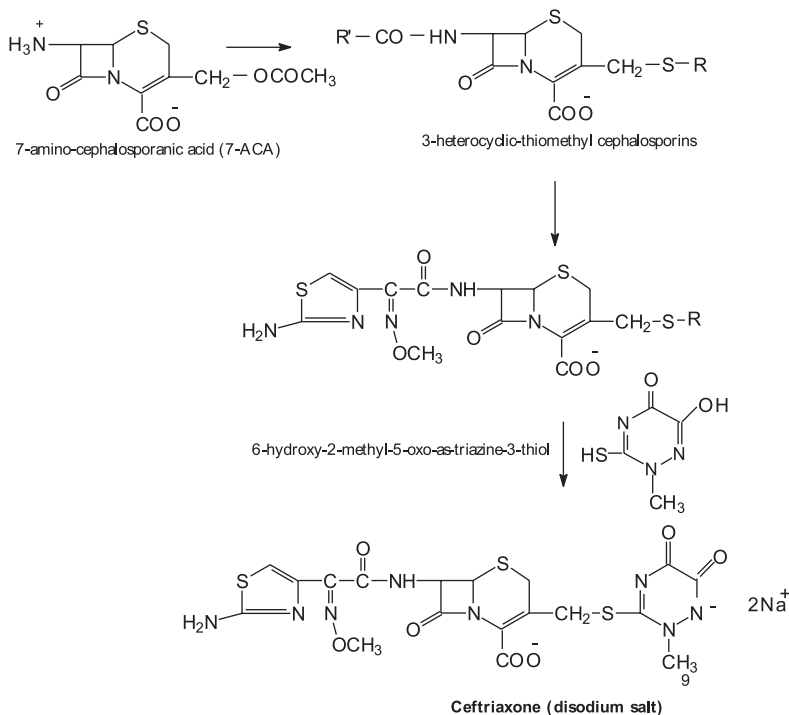
Ceftriaxone is effective in the treatment of various infections caused by susceptible organisms including those of the bone and joint, abdomen, lower respiratory tract, meninges, pelvic area, skin and soft tissue, and the urinary tract. It is also effective in the treatment of septic arthritis, bacteremia, and gonorrhea, caused by organisms susceptible to the antibiotic. It is also useful in the prevention of postoperative infections, but is no more effective than first or second generation cephalosporins [3, 7].

The main therapeutic advantages of Ceftriaxone include its once-daily dosing schedule, its usefulness in the treatment of bacterial meningitis and gonorrhea caused by susceptible organisms, and its use in the outpatient setting. Indeed, patients can be given Ceftriaxone at home with once-daily intravenous dosing of the antibiotic [3, 6].

The cerebrospinal fluid concentrations of Ceftriaxone in the treatment of acute bacterial meningitis in children (following twice-daily dosing) are much higher than its minimum inhibitory concentration (MIC) for *H. influenzae*. However, it lacks activity against *Listeria*. Thus, it is ineffective in the newborn population with meningitis caused by this organism [8].

2. METHOD OF PREPARATION

Ceftriaxone is synthesized by using 7-amino-cephalosporanic acid (7-ACA) as the starting material [9]. The compound was synthesized by the addition of an acyl moiety at the 7-amino position, and displacement of the acetoxy group by heterocyclic-thio substituent at the 3-methyl position. Subsequently, replacement of the *R*-alkyl side group was achieved by the addition of 6-hydroxy-2-methyl-5-oxas-triazine-3-thiol, while the *R'*-alkyl group was replaced with the 2-(2-amino-4-thiazolyl)-2-[(*Z*)-methoxyamino]-acetyl group to complete the synthesis of Ceftriaxone. The synthetic method is illustrated in Scheme 1.



Scheme 1. Synthesis of Ceftriaxone sodium.

3. PHYSICAL PROPERTIES

3.1 Ionization constants

Three pK_a values have been reported for Ceftriaxone [13]:

$$\begin{aligned} \text{pK}_{\text{a}1} &= 3.0 \text{ (COOH)} \\ \text{pK}_{\text{a}2} &= 3.2 \text{ (NH}_3^+) \\ \text{pK}_{\text{a}3} &= 4.1 \text{ (enolic OH)} \end{aligned}$$

The pH of a 10-mg/mL Ceftriaxone sodium solution in normal saline was found to be 5.7. However, a solution at a similar concentration in 5% (w/v) dextrose exhibited a pH of 5.79 [13].

3.2 Partition coefficient

The partitioning of Ceftriaxone sodium in aqueous 0.9% w/v sodium chloride and aqueous 5% w/v of dextrose against octanol and hexane

has been investigated [13]. The $\log P_{O/W}$ (octanol–water partition coefficient) and $\log P_{H/W}$ (hexane–water partition coefficient) could not be measured since its partition coefficient was found to be less than or equal to the minimum detectable $\log(P)$ value of the methodology used [13].

An investigation into the partitioning characteristics of Ceftriaxone was carried out using the ACD PhysChem (Version 6.0) computational program. Two tautomeric forms were identified, but the $\log(P)$ values calculated for each were found to be very similar. The calculations indicate that the compound should be fairly hydrophilic in nature. The structures of the tautomeric forms, and their computed $\log(P)$ values are found in Figure 1.

Additional insight into the partitioning characteristics of Ceftriaxone was obtained by using the ACD PhysChem computational program to deduce the pH dependence of the distribution coefficient associated with the major tautomeric form. The results of these calculations are shown in Figure 2, where one may note that the compound is predicted to be very hydrophilic at pH values above neutral.

3.3 Solubility characteristics

The solubility of Ceftriaxone at room temperature has been reported [2]. The compound is readily soluble in water (40 g/100 mL at 25°C), sparingly soluble in methanol, slightly soluble in ethanol (1 g/mL at 25°C) [1].

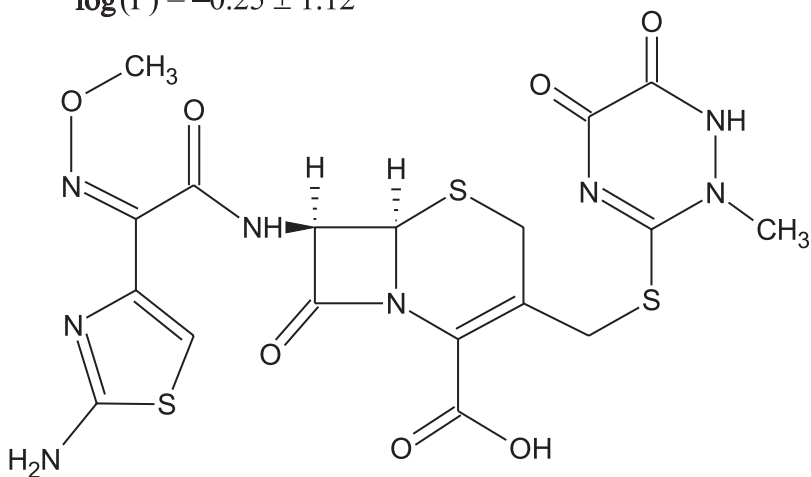
Additional insight into the solubility characteristics of Ceftriaxone was obtained by using the ACD PhysChem computational program to deduce the pH dependence of the aqueous solubility associated with the major tautomeric form. The results of these calculations are shown in Figure 3, where one may note that Ceftriaxone is predicted to be extremely soluble in aqueous media above neutral pH values. This finding provides a basis for the high degree of water solubility noted in the empirical studies [2].

3.4 Optical activity

The specific rotation of Ceftriaxone sodium at the sodium-D line (589 nm) and at 25°C has been reported to be -165° ($c = 1$ in water), when calculated on the anhydrous basis [1].

Major tautomeric form

$$\log(P) = -0.25 \pm 1.12$$



Minor tautomeric form

$$\log(P) = -0.24 \pm 1.11$$

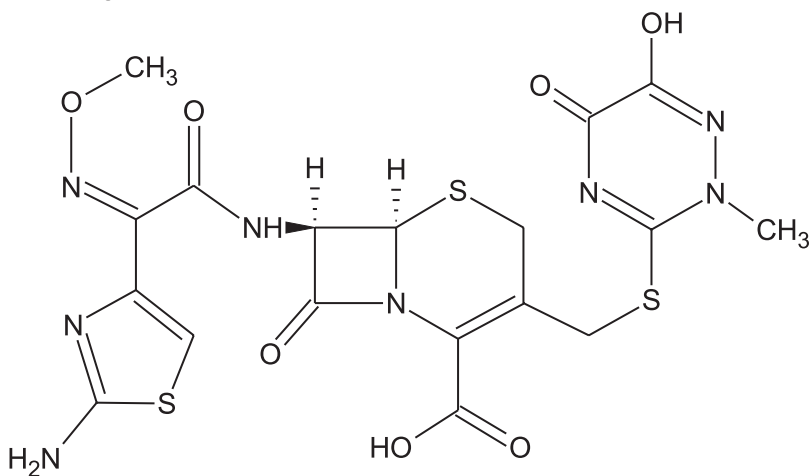


Figure 1. Octanol–water partition coefficients calculated for two tautomeric forms of Ceftriaxone.

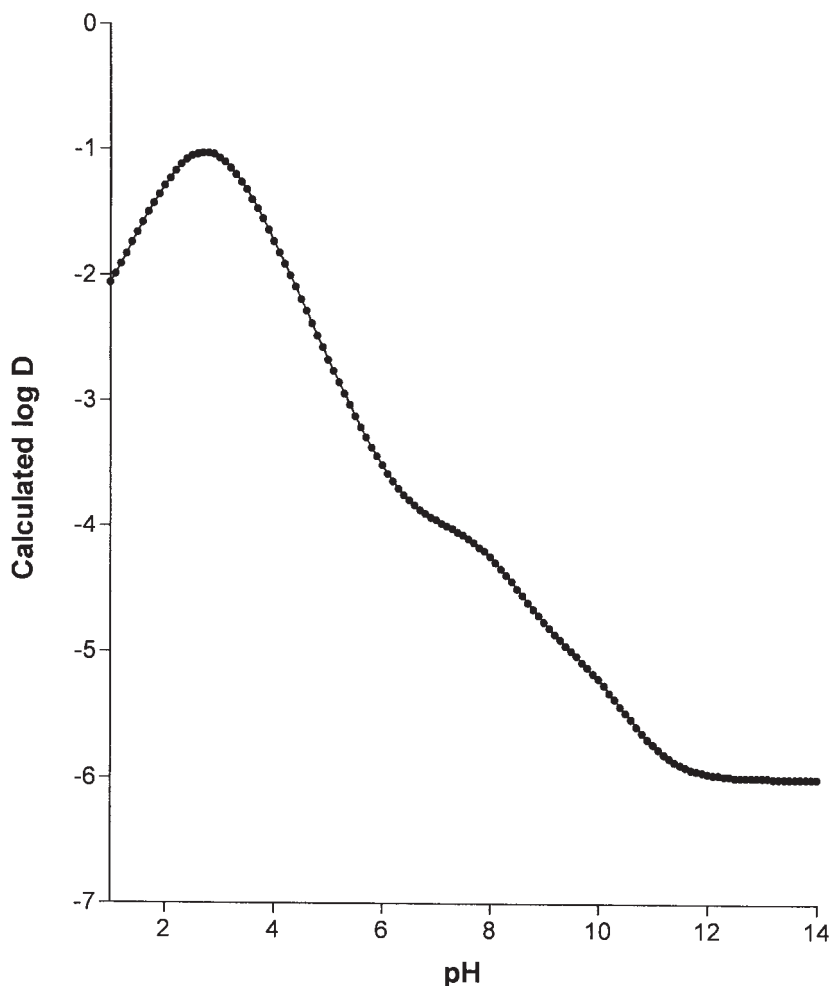


Figure 2. pH dependence of the distribution coefficient calculated (using ACD PhysChem, Version 6.0) for the major tautomeric form of Ceftriaxone.

3.5 X-Ray powder diffraction

The X-ray powder pattern of Ceftriaxone sodium was obtained using a wide angle X-ray diffractometer (model D 500, Siemens), with the sample being contained in a zero-background holder [10]. The powder pattern is shown in Figure 4, and the calculated d -spacings and relative intensities associated with the diffraction are given in Table 1.

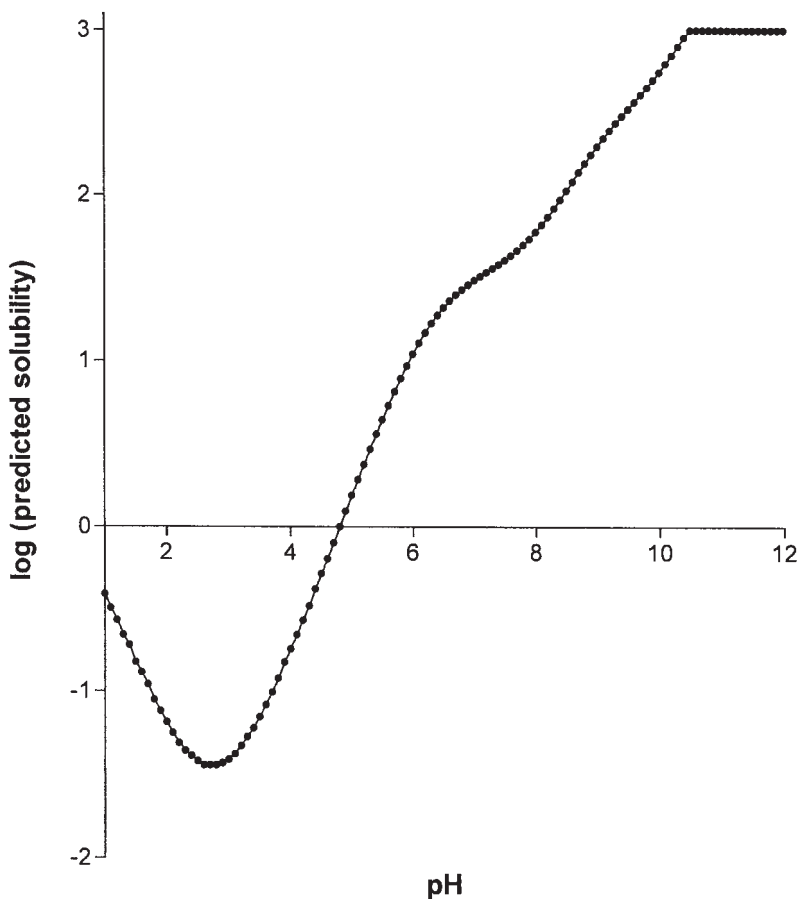


Figure 3. pH dependence of the aqueous solubility calculated (using ACD PhysChem, Version 6.0) for the major tautomeric form of Ceftriaxone. For ease in visualization, the logarithm of the predicted solubility has been plotted.

3.6 Thermal methods of analysis

3.6.1 Melting behavior

When heated beyond 155°C, Ceftriaxone melts with decomposition [1].

3.6.2 Differential scanning calorimetry

The DSC thermogram of Ceftriaxone sodium is shown in [Figure 5\(a\)](#) and was obtained using a Shimadzu model DSC-50 thermoanalytical

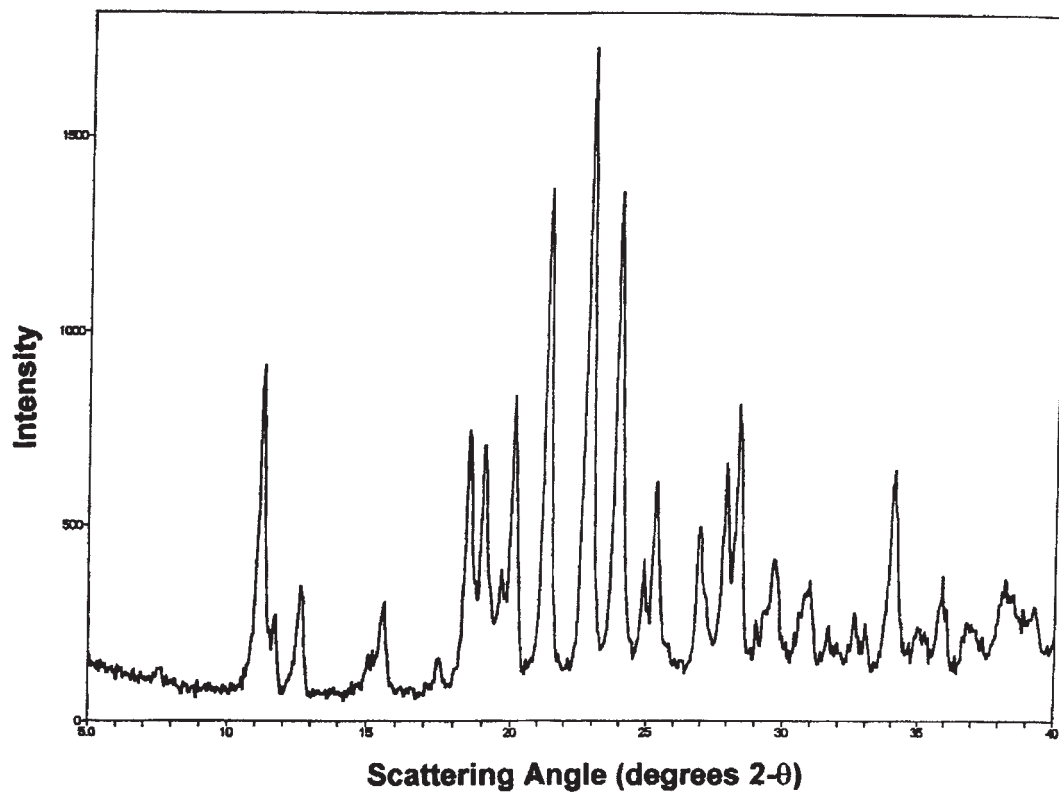


Figure 4. X-ray powder diffraction pattern of Ceftriaxone sodium.

Table 1

Crystallographic Results Derived from the X-Ray Powder Diffraction Pattern of Ceftriaxone Sodium

Scattering angle (°2 θ)	<i>d</i> -Spacing (Å)	Relative intensity I/I ₀ (%)
11.236	7.8684	53.9
12.608	7.0151	17.2
15.583	5.6819	13.9
18.507	4.7902	42.0
19.044	4.6564	23.3
20.097	4.4147	41.8
21.343	4.1597	79.9
22.892	3.8815	100.0
23.947	3.7129	75.4
25.342	3.5115	28.8
26.944	3.3064	20.6
27.907	3.1944	29.2
28.363	3.1441	40.0
29.657	3.0098	14.7
30.940	2.8879	12.1
34.049	2.6309	30.9
35.894	2.4998	13.3

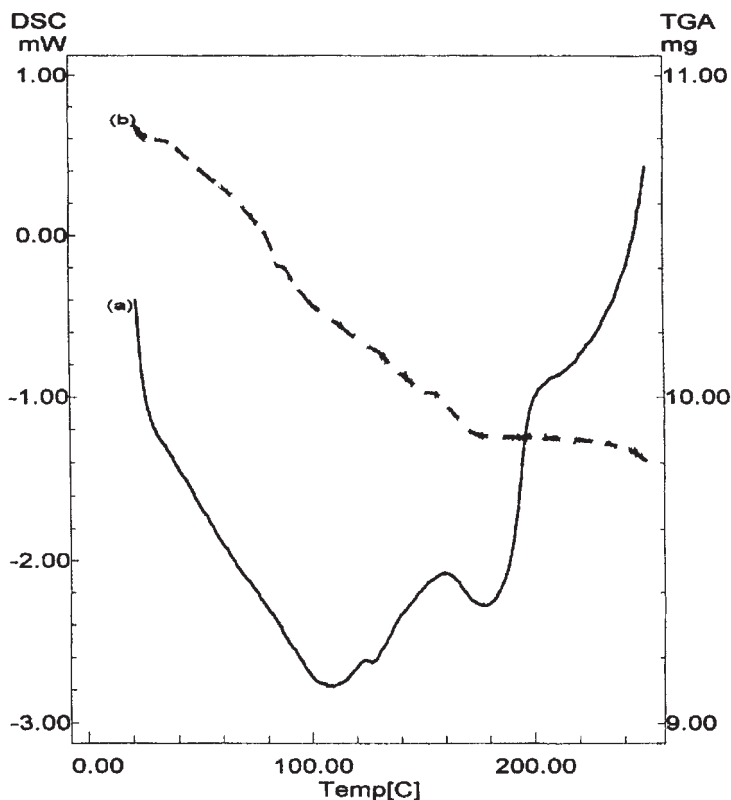


Figure 5. (a) Differential scanning calorimetry thermogram and (b) thermogravimetric analysis obtained for Ceftriaxone sodium.

system [10]. The sample was heated in a nonhermetically crimped aluminum pan at a rate of $10^{\circ}\text{C}/\text{min}$, over the range of $30\text{--}300^{\circ}\text{C}$.

Three endothermic peaks were observed in the DSC thermogram. The first and second endothermic peaks (at 108 and 127°C , respectively) were attributed to dehydration processes. The last endothermic peak (at 178°C) was assigned to the melting/decomposition transition.

3.6.3 Thermogravimetric analysis

The TGA thermogram shown in Figure 5(b) was obtained using a Shimadzu model TGA-50 thermogravimetric analyzer programmed to heat the sample at the same rate used for the DSC analysis.

The first two endothermic peaks in the DSC curve corresponded exactly with the same temperature range associated with two different weight losses in the TGA thermogram, enabling the deduction that the first two DSC endothermic features were due to compound dehydration. The weight loss that takes place at temperatures exceeding 200°C is most likely due to further decomposition.

3.7 Spectroscopy

3.7.1 UV-VIS spectroscopy

The UV absorption spectrum of Ceftriaxone sodium was recorded on a UV-VIS spectrophotometer (Shimadzu, model UV-1601 PC) over the spectral range of 300–400 nm at a nominal concentration of 50 µg/mL [10]. The absorption spectra obtained in water and in methanol are shown in Figure 6(a) and (b), respectively. The absorption maximum of Ceftriaxone in methanol was found to be 227 nm and the absorption maximum in water was found to be 330 nm.

It has also been reported that in water, Ceftriaxone sodium exhibits absorption maxima at 242 nm (molar absorptivity = 32,300) and at 272 nm (molar absorptivity = 29,530).

3.7.2 Vibrational spectroscopy

The infrared spectrum of Ceftriaxone was obtained in a KBr pellet (0.5% w/w), using a Perkin–Elmer model 1600 FTIR spectrometer [10]. The resulting spectrum is shown in Figure 7, and assignments for the observed absorption bands are provided in Table 2.

3.7.3 Nuclear magnetic resonance spectrometry

3.7.3.1 ¹H-NMR spectrum

The ¹H-NMR spectrum of Ceftriaxone sodium in deuterated water was obtained using a Varian XL-400 NMR spectrophotometer [10]. The resulting NMR spectrum is shown in Figure 8, and the assignments for the observed resonance bands are provided in Table 4. Both the NH₂ and NH protons do not show up completely in the spectral analysis due to the full exchange of these protons with deuterium from the solvent.

3.7.3.2 ¹³C-NMR spectrum

The ¹³C-NMR spectrum (Figure 9) of Ceftriaxone sodium in deuterated water was obtained using a Varian XL-400 NMR spectrophotometer.

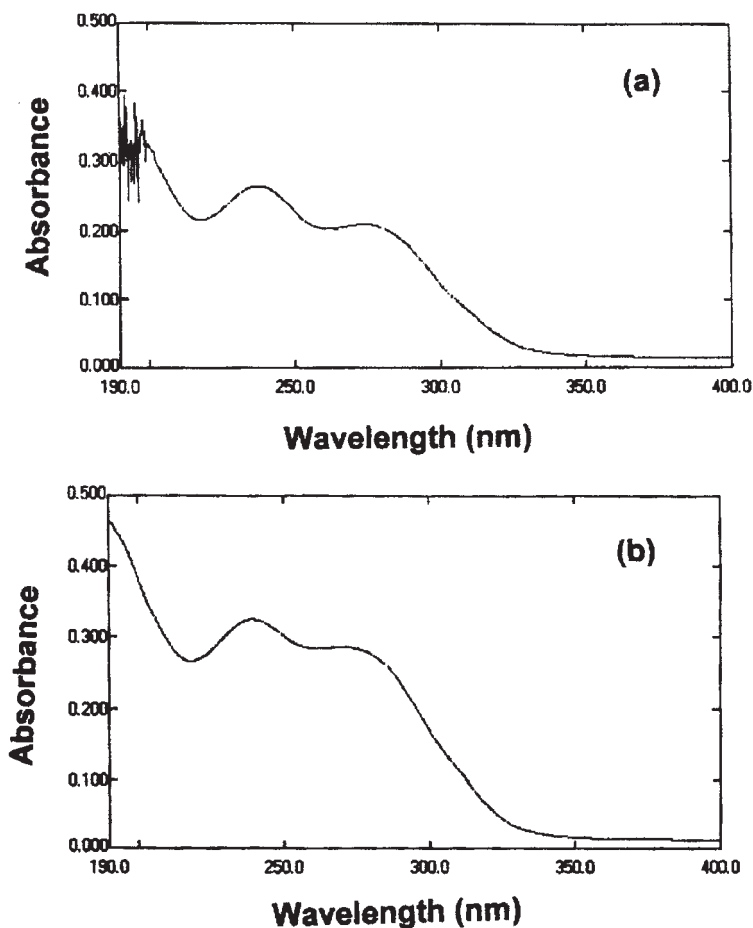


Figure 6. Ultraviolet absorption spectrum of Ceftriaxone sodium dissolved in (a) methanol, 55 µg/mL, and (b) water, 50 µg/mL.

Due to the complexity of the molecule, it was not possible to provide unambiguous carbon atom assignments for each of the resonance bands. [Table 3](#) contains these general assignments.

3.8 Mass spectrometry

The mass spectrum of Ceftriaxone sodium was obtained using a mass spectrometer operated in the electron impact mode [11]. A general

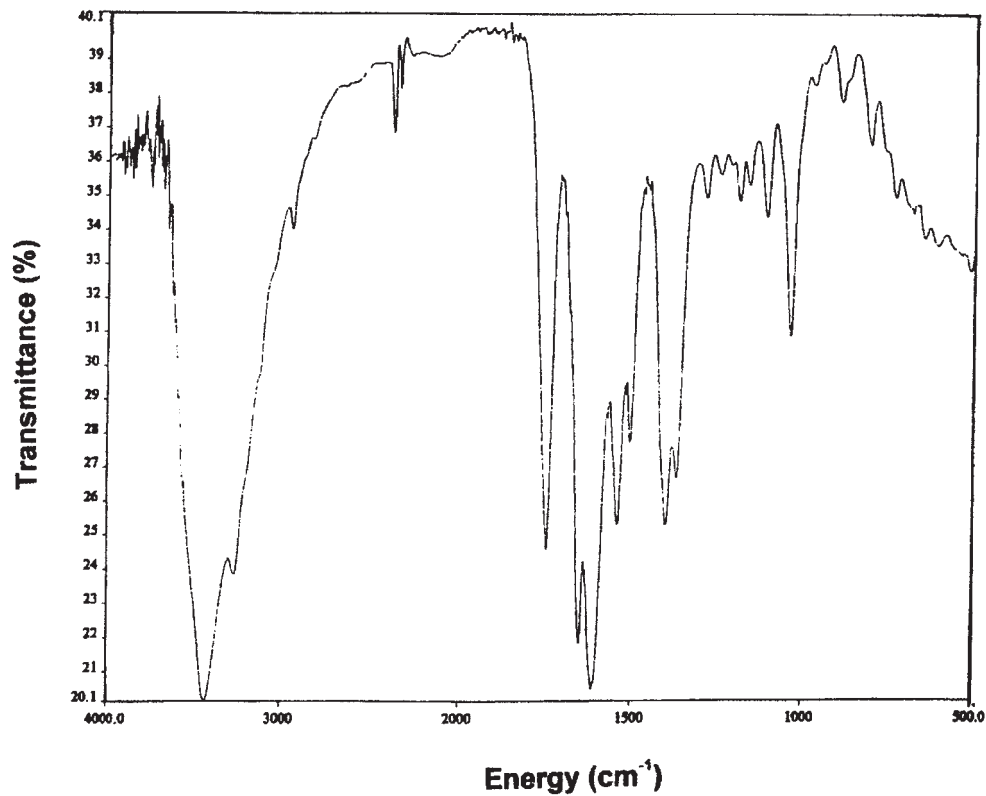


Figure 7. Infrared absorption spectrum of Ceftriaxone sodium, obtained in a KBr pellet.

Table 2

Assignments for the Major Infrared Absorption
Transitions of Ceftriaxone Sodium

Energy (cm ⁻¹)	Assignment
3530–3570	N–H stretching mode of the hydrogen-bonded amide group
2948	6-H, 7-H stretching vibrations in the β -lactam ring
2948	CH ₃ asymmetric stretching mode
1772	β -lactam C=O stretching mode
1670	Amide C=O stretching mode
1650–1550	Asymmetric carboxylate stretching mode
1592	Oxime C=N stretching mode
1570–1515	Acyclic amide stretching mode
1460	CH ₃ deformation in the CH ₃ O group
1096	C–O stretching mode in the CH ₃ O group
1060, 1025	C–O and N–O stretching modes of the carbamate and oxime moieties in the CH ₃ O groups

scheme for the fragmentation is provided in [Figure 10](#), and assignments for the major fragment ions are given in [Table 4](#).

Mass spectra, obtained by the fast atom bombardment of Ceftriaxone in serum samples are shown in [Figure 11](#).

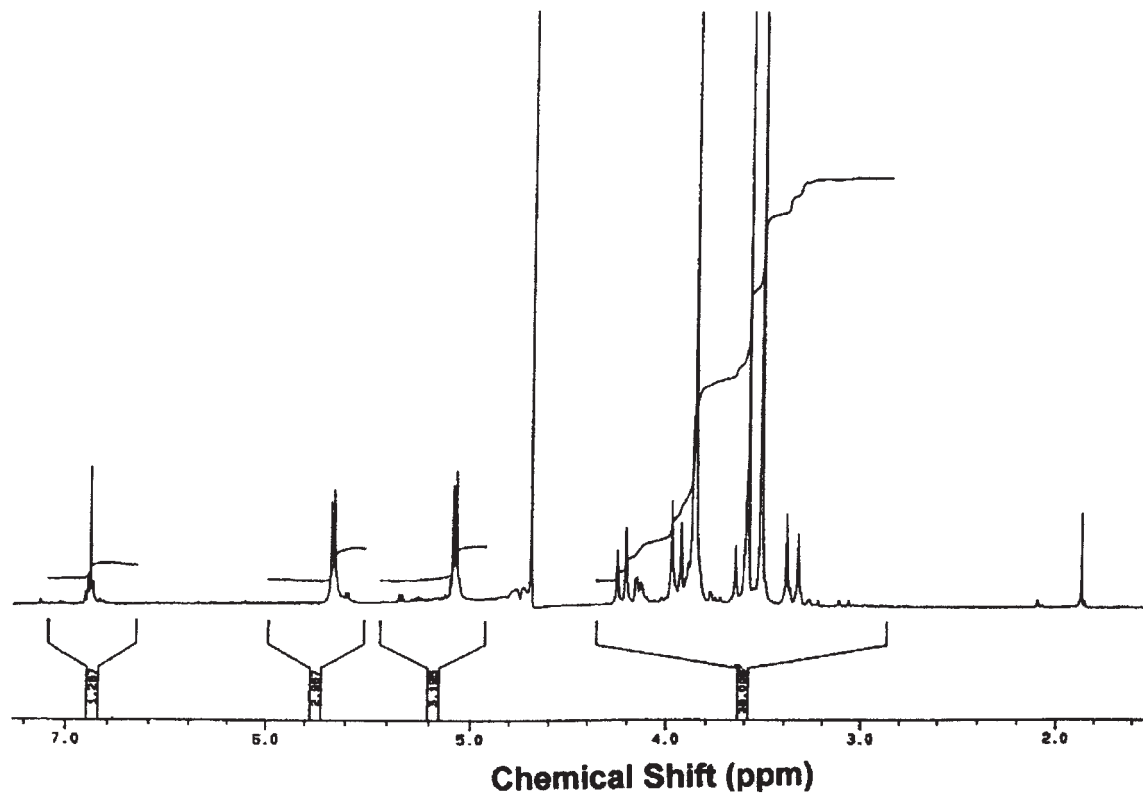


Figure 8. ^1H -nuclear magnetic resonance spectrum of Ceftriaxone sodium.

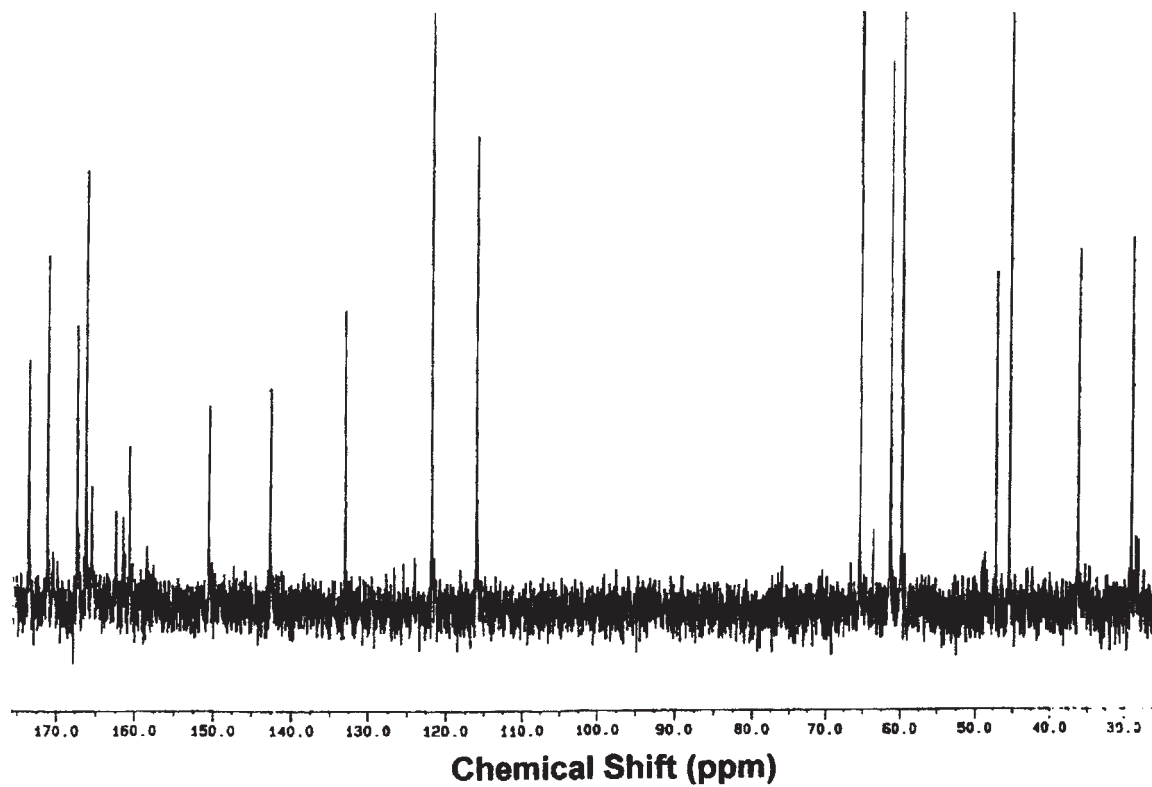
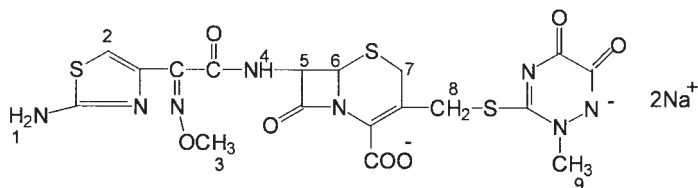


Figure 9. ^{13}C -nuclear magnetic resonance spectrum of Ceftriaxone sodium.

Table 3

Assignments for the Resonance Bands in the Nuclear Magnetic Resonance Spectra of Ceftriaxone Sodium



¹H-NMR Resonance Band Assignments

Chemical shift (ppm)	Number of protons	Assignments
6.89–6.88	1	(s) aromatic C–H at position 2
5.67–5.65	1	(d) proton at position 5
5.09–5.05	1	(d) proton at position 6
4.68	3	(s) proton at position 3
3.86	1	(s) proton at position 7
3.85	2	(s) proton at position 8
3.58	3	(s) proton at position 9
		(s) = singlet
		(d) = doublet

(continued)

Table 3 (continued)

¹³C-NMR Resonance Band Assignments

Chemical shift (ppm)	Assignment
173.58, 171.19, 167.42, 166.58, 162.49, 160.70, 150.50, 142.68, 133.06, 121.76, 115.97	Carbonyl carbons; olefinic carbons, carbons in double-bonded carbon–nitrogen bonds
65.37, 61.36, 59.84, 47.20, 45.46, 36.35, 29.20	Aliphatic and alicyclic carbons

4. METHODS OF ANALYSIS

4.1 Identification

The infrared absorption spectra of a potassium iodide dispersion of Ceftriaxone should show absorption maxima at the same wavelengths as that of an authentic Reference Standard [14]. In the chromatographic analysis of Ceftriaxone, the retention time of the major peak in the chromatogram obtained during performance of the assay method is observed at the same retention time as the major peak in the chromatogram of the standard preparation [14].

4.2 Spectrophotometric analysis

A spectrophotometric method has been developed for the determination of Ceftriaxone in pharmaceutical formulations [15]. This method is based on the formation of a colored complex formed by the reaction of palladium chloride and Ceftriaxone. The absorption maximum of the reaction product was reported to be 344 nm.

4.3 Chromatographic methods of analysis

4.3.1 Thin-layer chromatography

High-performance TLC for the analysis of Ceftriaxone was performed using precoated silica gel HPTLC plates, with a concentrating zone of 2.5×10 cm [16]. The mobile phase consisted of 5 : 2.5 : 5 : 1.5 v/v/v/v ethyl

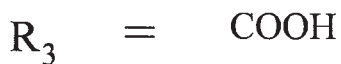
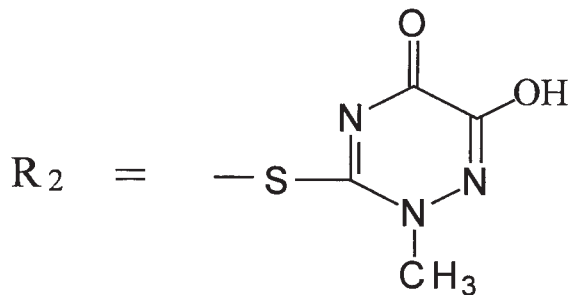
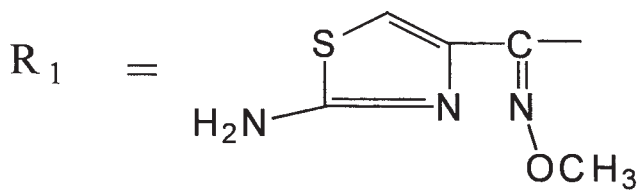
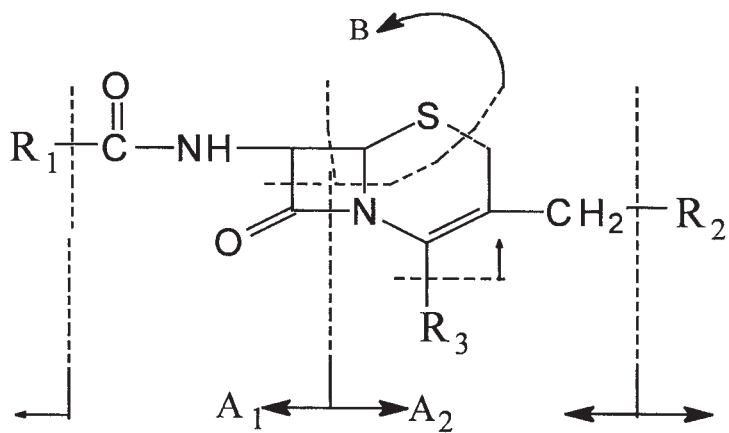


Figure 10. Electron impact mass spectrum fragmentation of Ceftriaxone sodium.

Table 4

Electron Impact Mass Spectra Fragmentation Ions of Ceftriaxone Sodium

Method	m/z	(% I)	Fragments
Positive ion FAB (with glycine)	555	5	M + H
	241	8	A + H
	156	50	R ₁
	160	23	R ₂ + 2H
	396	8	M - R ₂
	126	100	R ₁ -OCH ₃
	141	25	Other
	211	15	Other
Negative ion FAB (with glycine)	553	Not detected	M - H
	239	5	A ₁ + H
	158	100	R ₂
	58	18	Other
	144	17	Other
Negative ion FAB (with diethanol-amine)	239	5	A ₁ -H
	158	100	R ₂
	58	40	Other
	82	22	Other
	124	17	R ₁ -OCH ₃ -H
	144	17	Other

acetate/acetone/methanol/water, and the TLC scanner was set at 270 nm in the reflectance/absorbance mode. Calibration curves were developed that related the peak height and peak area in the range of 125–500 ng Ceftriaxone.

4.3.2 High-performance liquid chromatography

The USP assay method for the analysis of Ceftriaxone sodium bulk drug substance is described in the United States Pharmacopeia XXIII [14]. The mobile phase consisted of pH 7.0 buffer (4.4% v/v), pH 5.0 buffer (0.4% v/v), 3.2 g tetraheptylammonium bromide (THAB) dissolved in 400 mL acetonitrile (40% v/v), and water (55.2 v/v). In this assay,

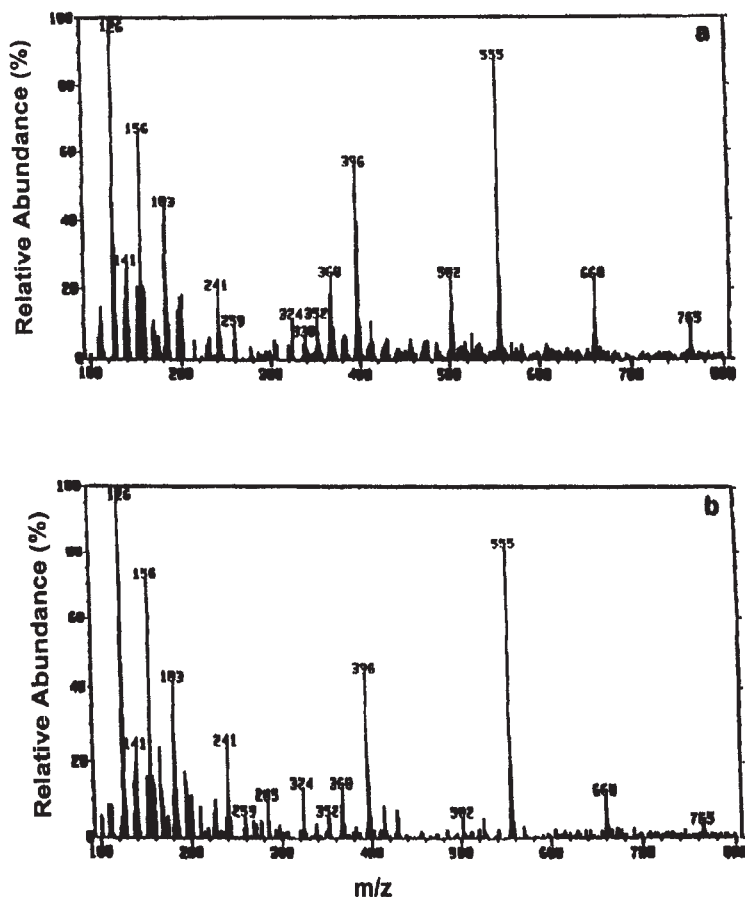


Figure 11. Fast atom bombardment mass spectrum fragmentation of a: Ceftriaxone sodium in serum, and b: using the positive mode with diethanolamine.

standard solutions were prepared by dissolving Ceftriaxone in mobile phase to obtain a concentration of approximately 0.2 mg/mL. In the first method of sample preparation, 40 mg of sterile Ceftriaxone was dissolved in 200 mL of mobile phase. In the second and third methods of sample preparation, Ceftriaxone was dissolved in mobile phase to obtain a concentration of 180 µg/mL. The chromatographic system consisted of a 270-nm detector and a 4.0-mm × 15-cm column that contained 5-µm packing L1 (octadecyl silane chemically bonded to porous silica or ceramic microparticles, 3–10 µm in diameter). In the assay, the flow rate was maintained at approximately 2 mL/min. Freshly prepared solutions

(20 μL) were injected into the HPLC system for subsequent chromatographic analysis.

Several HPLC methods have been reported for the analysis of Ceftriaxone in aqueous and biological samples at a high concentration [17–20].

A simple LC method was also developed and validated for the analysis of Ceftriaxone in aqueous and biological samples. The chromatographic separation was achieved using a reversed phase C-18 microbore column (Hypersil, 5 mM–2 mm), with UV detection at 270 nm. This isocratic system was operated at ambient temperature and required less than 10 min of chromatographic time. The flow rate was maintained at 0.5 mL/min. Cetyltrimethylammonium bromide (0.01 M) was utilized as the ion-pairing agent. For the aqueous system, the mobile phase consisted of 20:20:60 v/v/v methanol/acetonitrile/phosphate buffer pH 7.4. The plasma and CSF system used the same mobile phase constituents in a slightly different ratio (30:40:30 v/v/v). Lidocaine was used as the internal standard, and peak height ratios of the drug to the internal standard were linear over the concentration range of 0.0–16 $\mu\text{g/mL}$. Within-day and day-to-day relative standard deviations ranged from 0.3 to 2.2% and 1.1 to 5.9%, respectively [21].

4.4 Biological methods

Ceftriaxone susceptibility studies have been reported using a disk diffusion method, with the disks usually containing 30 μg of the drug substance [22].

The *in vitro* activity of Ceftriaxone-incorporated acrylic bone cement has been evaluated using a microbiological assay. *Staphylococcus aureus* ATCC 25923 was used as the test organism in this study [23].

5. STABILITY

Ceftriaxone in its sterile bulk powder form should be stored at room temperature (25°C or 77°F) or below, and protected from light [2].

The color of Ceftriaxone solutions ranges from light yellow to amber, depending upon the length of storage, concentration, and diluent used [2].

Ceftriaxone formulated as a solution preparation for intramuscular use remains stable (*i.e.*, loss of potency less than 10%) for the time periods shown in Table 5 [8].

Table 5

Ceftriaxone Sodium Intramuscular Solution Stability Data

		Storage condition	
Diluent used	Concentration (mg/mL)	Room temperature*	Refrigerated**
Sterile water for injection	100	3 days	10 days
0.9 % NaCl	250	24 h	3 days
5 % dextrose solution	100	3 days	10 days
5 % dextrose solution	250	24 h	3 days
Bacteriostatic water + 0.9% benzyl alcohol	100	24 h	10 days
Bacteriostatic water + 0.9% benzyl alcohol	250	24 h	3 days
1% Lidocaine solution (without epinephrine)	100	24 h	10 days
1% Lidocaine solution (without epinephrine)	250	24 h	3 days

*Room temperature as 25°C.

**Refrigerated temperature as 4°C.

Table 6
Ceftriaxone Sodium Intravenous Solution Stability in Glass
or PVC Containers

	Storage condition	
Diluent used	Room temperature*	Refrigerated**
Sterile water	3 days	10 days
0.9% sodium chloride solution	3 days	10 days
5% dextrose solution	3 days	10 days
10% dextrose solution	3 days	10 days
5% dextrose + 0.9% sodium chloride solution	3 days***	Incompatible
5% dextrose + 0.45% sodium chloride solution	3 days	Incompatible

*Room temperature at 25°C.

**Refrigerated temperature as 4°C.

***Data were available only for 10–40 mg/mL concentrations in this diluent in PVC containers.

When stored in glass or PVC containers, Ceftriaxone formulated as intravenous solutions (10, 20, and 40 mg/mL) remained stable (*i.e.*, loss of potency less than 10%) for the time periods shown in [Table 6](#) [8].

6. PHARMACEUTICAL DOSAGE FORMS

A number of parenteral formulations of Ceftriaxone sodium are available, and the defining properties of these are summarized in [Table 7](#).

7. DRUG METABOLISM AND PHARMACOKINETICS

7.1 Pharmacokinetics

The pharmacokinetics of Ceftriaxone dosing has been extensively characterized following intravenous, intramuscular, intraperitoneal,

Table 7

Parenteral Formulations of Ceftriaxone Sodium [9]

Ceftriaxone sodium preparations		
Dosage form	Strength	Manufacturer
Sterile solution for parenteral use	250 mg (Ceftriaxone)	Rocephin [®] , Roche
	500 mg (Ceftriaxone)	Rocephin [®] , Roche
	1 g (Ceftriaxone)	Rocephin [®] , Roche
	2 g (Ceftriaxone)	Rocephin [®] , Roche
	10 g (Ceftriaxone) pharmacy bulk package	Rocephin [®] , Roche
Sterile solution, for IV infusion	1 g (Ceftriaxone)	Rocephin ADD-Vantage [®] , Roche; Rocephin [®] Piggyback, Roche
	2 g (Ceftriaxone)	Rocephin ADD-Vantage [®] , Roche; Rocephin [®] Piggyback, Roche

Ceftriaxone sodium in dextrose preparations		
Dosage form	Strength	Manufacturer
Parenteral	20 mg (of Ceftriaxone) per mL (1 g) in 3.8% Dextrose	Rocephin in iso-osmotic Dextrose Injection (Galaxy [®]), Roche, (Baxter)
Injection (frozen, for IV infusion)	40 mg (Ceftriaxone) per mL (2 g) in 2.4% Dextrose	Rocephin in iso-osmotic Dextrose Injection (Galaxy [®]), Roche, (Baxter)

and subcutaneous administration of single and multiple daily doses in both healthy patients and those with bacterial disease. Pharmacokinetic parameters have also been studied in children with various bacterial infections, and in patients with impaired renal or hepatic function.

7.1.1 Absorption and plasma concentrations

Following intravenous bolus administration of 0.5 and 1.5 g, the mean peak plasma concentrations of Ceftriaxone were 151 and 286 mg/L, respectively. After 30-min infusions of 0.5, 1, and 2 g, mean peak plasma concentrations were 82, 151, and 257 mg/L, respectively [24–26]. Since Ceftriaxone experiences saturable plasma protein binding, the plasma and area-under-time curve (AUC) of total Ceftriaxone (bound + unbound) did not increase in a dose-proportional manner. Thus, total plasma concentrations following intravenous administration of doses greater than 1 g were less than those exhibiting linear dose-relationships [27–28].

In contrast, the plasma concentrations and AUC of free (unbound) Ceftriaxone were linear and independent of the dose administered. Upon increasing the dose, the peak plasma concentration of free (unbound) Ceftriaxone increased in a disproportionate manner. Thus, once-daily administration of Ceftriaxone in one large dose is supported over dividing an equivalent daily dose into smaller ones [29].

The bioavailability of Ceftriaxone following intramuscular injection of the drug was similar to that found upon intravenous administration of an equivalent dose [30]. In contrast, mean peak plasma concentrations of Ceftriaxone following intramuscular injection are approximately half of those following intravenous administration of the drug. After 2 h, mean plasma Ceftriaxone concentrations were similar for both administration routes [31].

Mean maximum plasma concentrations of Ceftriaxone (following repeated intravenous administration of 0.5 or 1 g at 12 h intervals) after the final dose were 32–40% greater than after the initial dose. Plasma trough levels were 34 to 50% higher than after the first dose [32]. In contrast, repeated intravenous administration of the antibiotic caused an increase of 8% in the maximum mean plasma concentration, but caused a greater amount of tissue penetration when compared to the twice-daily dosing regimen [33]. Thus, the accumulation of Ceftriaxone in plasma, following either 12 or 24-h intravenous administration, was approximately 40 or 8%, respectively [32–34].

7.1.2 Volume of distribution

In various studies which examined the kinetics of both the total and free concentrations of Ceftriaxone, the apparent volume of distribution of total (bound + unbound) Ceftriaxone during the terminal elimination phase of the drug increased with increasing doses of the drug. However, the volume of distribution of free drug (unbound) remained fairly constant [27].

7.1.3 Protein binding

Drugs which are highly protein-bound, such as Ceftriaxone, will only have a small fraction of free drug circulating in the blood at any given time. Despite this fact, protein binding is a dynamic process, and equilibrium occurs between bound and unbound drug. In addition, more than 50% of albumin is located in the interstitial space, and may act as a reserve to replenish active (unbound) drug stores. Thus, for the antibiotic Ceftriaxone, the albumin-binding sites become saturated, and thus available levels of Ceftriaxone during dosing may greatly exceed average concentrations of unbound drug [35].

Ceftriaxone exhibits nonlinear concentration-dependent protein binding. In several studies using equilibrium dialysis, the free fraction of Ceftriaxone was approximately 5% (95% bound) at plasma concentrations less than 70 mg/L. The free fraction increased to 16% at 300 mg/L, 26.5% at 500 mg/L, and approximately 42% at 600 mg/L [25, 27, 36].

7.1.4 Fluid and tissue penetration

Several studies have concluded that mean inhibitory concentrations (MIC) of Ceftriaxone for gram-negative bacteria (2 mg/L) are present in most body fluids and tissues [37]. This includes both the cerebrospinal fluid and meninges (inflamed or noninflamed) following a 24-h intravenous administration of 1–2 g of Ceftriaxone [37, 38].

Ceftriaxone is commonly given once daily for the treatment of a variety of infectious disease states. Drug concentrations in various body tissues and fluids have exceeded the MIC₉₀ of Ceftriaxone for most *Haemophilus*, *Neisseria*, and *Salmonella* species, *Enterobacteriaceae*, and *C. diversus* after a 24-h time period following single doses or repeated once-daily intravenous Ceftriaxone administration of 1 or 2 g.

Ceftriaxone entered the cerebrospinal fluid of neonates, infants, and children [31, 37, 39]. The specimen to plasma concentration ratios were higher in patients with inflamed meninges relative to those without

inflamed meninges. They were also higher in patients with bacterial relative to aseptic meningitis [37, 40].

7.1.5 *Elimination*

Ceftriaxone is eliminated in an unchanged form by the kidney and the liver. Indeed, 45–60% of an intravenous dose of 0.5–3.0 g will be excreted in the urine of healthy individuals within a 48-h time period [31].

Renal clearance of total (bound + unbound) Ceftriaxone varied with both the dose given and time [26, 41]. However, renal clearance of the free drug did not vary with the dose and time. Renal clearance of the drug, estimated using unbound plasma concentrations, is approximately 9.6 L/h (only somewhat higher than the glomerular filtration rate). Thus, the glomerular filtration is primarily responsible for the renal elimination of Ceftriaxone [27].

7.1.6 *Half-life*

The mean elimination half-life of Ceftriaxone is approximately 6–9 h in healthy adult subjects following single or multiple intravenous, intramuscular, or subcutaneous injection [30, 31, 42]. Thus, Ceftriaxone has a much longer elimination half-life than any of the currently available cephalosporins or cephamycins [43]. The half-life does not vary significantly with the route of administration, dose size, or use of single or multiple doses. It is only slightly affected in patients with decreased renal function and somewhat normal nonrenal elimination. However, it is increased in neonates and patients over 75 years of age [44–46].

7.1.7 *Influence of age on pharmacokinetic parameters*

Age-associated changes in Ceftriaxone pharmacokinetics have been studied in neonate, infants, and child patients, in healthy young adults, and in the elderly [31, 45]. The plasma elimination half-life did not vary significantly between most of the patient-age groups, with the exception of the elderly and newborn neonates in which the half-life was much longer [45].

The total volume of distribution (expressed per unit of body area) did not appear to vary with age [45]. Mean systemic clearance of free Ceftriaxone concentrations was greater in young adults than in newborns or in the elderly [44]. In neonates, approximately 70% of a dose was eliminated in the urine. On the other hand, in adults, 40–50% of a dose is eliminated in the urine. Plasma protein binding was reduced in neonates, infants, and young children when compared to that of adults [44]. There was a

significant increase in the unbound fraction of Ceftriaxone in elderly patients (mean age 70.5 years) when compared to young adults (mean age 29 years old) [47].

In neonates, there was a considerable decrease in the clearance of unbound Ceftriaxone (0.96 L/h/m^2) when compared to young adults (10.32 L/h/m^2) and middle-aged adults (7.5 L/h/m^2). This was thought to be due to the immature clearance mechanism for Ceftriaxone in the neonates [44].

7.1.8 Influence of disease on the pharmacokinetic parameters

The pharmacokinetics of Ceftriaxone has been studied in patients with different degrees of renal or hepatic dysfunction.

In patients with mild to moderate renal dysfunction, the elimination half-life of 10–15 h has been reported [31]. This observation is most likely due to the decrease in protein binding which causes an increase in the nonrenal clearance of the total concentration of Ceftriaxone. In severe renal dysfunction, the elimination half-life may increase to 50 h [48, 49]. Therefore, these patients will require dose adjustments to avoid drug accumulation in their systems. Hemodialysis does not increase the clearance of Ceftriaxone [26, 50].

In patients with varying degrees of liver failure (alcoholic fatty liver cirrhosis with or without ascites), there was only a slight alteration in the pharmacokinetic properties of Ceftriaxone [29]. The elimination half-life was not increased. The increased unbound fraction of Ceftriaxone contributed to an increase in the volume of distribution, total clearance of the antibiotic, and normal elimination half-life [29].

7.2 Metabolism

Ceftriaxone is eliminated unchanged in the urine by glomerular filtration (60%) and bile (40%) [51].

8. TOXICITY

The toxic effects of Ceftriaxone are similar to other cephalosporins. Hypersensitivity reactions including rash, drug fever, serum sickness, and anaphylaxis may occur on a rare basis (less than 2% of the patient population). Thus, cross-reactivity with penicillin antibiotics can occur and Ceftriaxone should not be used in patients who have a history of

Table 8

LD₅₀ of Ceftriaxone in Mice and Rats [1]

Animal species	Route of administration	LD ₅₀ (mg/kg)
Mouse		
Male	I.V.	≥ 3000
Female	I.V.	≥ 2800
Rat		
Male	I.V.	≥ 2175
Female	I.V.	≥ 2175

anaphylaxis due to penicillin, other severe immediate reactions, or in patients with a reactive skin test to penicillin antibiotics [52].

Ceftriaxone does not contain the 3-tetraolylthiomethyl substituent found in the structure of moxalactam, cefoperazone, and cefamandole. Thus, it is unlikely to elicit the clotting abnormalities reported for these antibiotics. For similar reasons, the disulfiram-like reaction associated with cefoperazone and moxalactam is unlikely with Ceftriaxone [51]. The LD₅₀ of Ceftriaxone in mice and rats is shown in Table 8 [1].

9. ACKNOWLEDGMENTS

The authors wish to thank Dr. R. Suryanarayanan (University of Minnesota) and Mr. William Ihm (Eastern Nebraska Forensic Lab, Omaha), for the powder X-ray diffraction and mass spectrum studies, respectively.

10. REFERENCES

1. *The Merck Index*, 11th edn., S. Budavari, ed., Merck and Co., Inc., Rahway, N.J., U.S.A., p. 300 (1989).
2. *AHFS Drug Information*, G.K. McEvoy, ed., American Society of Hospital Pharmacists, Maryland, pp. 92–98 (1993).

3. G.L. Mandell and M.A. Sande. "Antimicrobial agents: penicillins, cephalosporins, and other beta-lactam antibiotics", in: ***Goodman and Gilman's Pharmacological Basis of Therapeutics***, 8th edn, A.G. Gilman, ed., Pergamon Press, New York, pp. 1065–1097 (1990).
4. H.C. New, *Annals of Internal Medicine*, **97**, 408–419 (1982).
5. P. Garzone, J. Lyon, and V.L. Yu, *Drug Int. Clin. Pharm.*, **17**, 507–515 (1983).
6. L. Balant, P. Dayer, and R. Auckenthaler, *Clin. Pharmacokinetics*, **10**, 101–143 (1985).
7. ***Martindale The Extra Pharmacopoeia***, J. E. Reynolds, K. Parfitt, A. V. Parsons, S. C., and Sweetman, eds., The Pharmaceutical Press, London, p. 167 (1989).
8. ***Drug Evaluation Monographs***, Ceftriaxone, Micromedex Inc., p. 89 (1974–1996).
9. R. Reiner, *Drugs Exp. Clin. Res.*, **12**, 299–302 (1986).
10. H.M. Owens and A. K. Dash, unpublished results.
11. K. Kobayashi, K. Sato, Y. Mizuno, and Y. Katsumata *J. Chromatogr. B*, **677**, 275–290 (1996).
12. G.R. Donowitz and G.L. Mandell, *New Eng. J. Med.*, **18**, 419–426 (1988).
13. D.R. Jenke, *Pharm. Res.*, **11**, 984–989 (1994).
14. ***United States Pharmacopeia 23***, Ceftriaxone Sodium, United States Pharmacopoeial Convention, Inc., Rockville, MD, pp. 314 (1995).
15. A.F. El-Walily, A.A. Gazy, S.F. Belal, and E.F. Khamis, *J. Pharm. Biomed. Anal.*, **22**, 385–392 (2000).
16. S. Eric-Jovanovic, D. Agbaba, D. Zivanov-Stakic, S. Vladimirov, *J. Pharm. Biomed. Anal.*, **18**, 893–898 (1998).
17. L.J. Strausbaugh and M.J. Sande, *J. Infect. Dis.*, **137**, 251–260 (1978).
18. J. Rockowitz and A.R. Tunkel, *Drugs*, **50**, 838–853 (1995).
19. V.A. Levin, *J. Med. Chem.*, **23**, 682–684 (1980).
20. M.J. Hall, D. Westmacott, and P. Wong-Kai-In, *J. Antimicrob. Chemother.*, **8**, 193–203 (1981).
21. H.M. Owens, C.J. Destache, and A.K. Dash, *J. Chromatogr. B*, **728**, 97–105 (1999).
22. M.J. Bittner, D.L. Dworzack, L.C. Preheim, R.W. Tofte, and K.B. Crossley, *Ant. Microb. Chemother.*, **23**, 261–266 (1986).
23. N.J. Beeching, M.J. Thomas, S. Roberts, and S.D.R. Land, *J. Antimicrob. Chemother.*, **17**, 173–184 (1986).

24. R. Delsignore, C.M. Baroni, G. Crotti, F. Mineo, and U. Butturini, *Chemotherapy*, **29**, 157–162 (1983).
25. J. Le Van Thoi, B. Koumare, F. Lhoste, C.J. Soussy, and J. Duval, *Pathologic Biologie.*, **30**, 345–347 (1982).
26. I.H. Patel, S. Chen, M. Parsonnet, M.R. Hackman, and M.A. Brooks, *Antimicrobial Agents and Chemotherapy*, **20**, 634–641 (1982).
27. K. Stoeckel, P.J. McNamara, R. Brandt, H. Plozza-Nottebrock, and W.H. Ziegler, *Clin. Pharm. Therap.*, **29**, 650–656 (1981).
28. K. Stoeckel, P.J. McNamara, R. Brandt, and W.H. Ziegler, in: *Current Chemotherapy and Immunotherapy*, A. Periti, ed., Proceedings of the 12th International Congress of Chemotherapy, Florence., 1981, pp. 454–455, American Society for Microbiology, Washington, D.C. (1982).
29. K. Stoeckel, H. Tuerk, V. Trueb, and P.J. McNamara, *Clin. Pharma. Therap.*, **36**, 500–509 (1984).
30. K. Borner, H. Lode, B. Hampel, M. Pfeuffer, and P. Koeppe, *Chemotherapy*, **31**, 237–245 (1985).
31. D.M. Richards, R.C. Heel, R.N. Brogden, T.M. Speight, and G.S. Avery, *Drugs*, **27**, 469–527 (1984).
32. A.A. Holazo, I.H. Patel, R.E. Weinfeld, J.J. Konikoff, and M. Parsomet, *Eur. J. Clin. Pharm.*, **30**, 109–112 (1986).
33. M. Le Bel, S. Greogoire, M. Caron, and M.G. Bergeron, *Antimicrob. Agents Chemo.*, **28**, 123–127 (1985).
34. F. Frashini, P.C. Braga, G. Scarpazza, F. Scaglione, and O. Pignataro, *Chemotherapy*, **32**, 192–199 (1986).
35. J. L. Blumer, *Ceftriaxone: Data on File*, Roche Inc. (1987).
36. C. Fiset, F. Vallee, M. LeBel, and M.G. Bergeron, *Therap. Drug Monit.*, **8**, 483–489 (1986).
37. E. Martin, J.R. Koup, U. Pravichini, and K. Stoeckel, *J. Pediatrics*, **105**, 475–481 (1984).
38. V. Vlahov, P. Dobrev, N. Alexiev, N. Bacracheva, and P. Chervenakov, *Clin. Trial J.*, **24**, 137–142 (1987).
39. M.C. Nahata, D.E. Durrell, and W.J. Barson, *Chemotherapy*, **32**, 89–94 (1986).
40. E. Martin, *Eur. J. Micro.*, **2**, 509–515 (1983).
41. A.A. Pollock, P.E. Tee, I.H. Patel, J. Spicehandler, and M.S. Simberkoff, *Antimicrob. Agents Chemo.*, **22**, 816–823 (1982).
42. B.E. Scully, K.P. Fu, and H.C. New, *Am. J. Med.*, **77**, 112–116 (1984).
43. T. Bergan, *Drugs*, **34(Supp 2)**, 89–104 (1987).

44. W.L. Hayton and K. Stoeckel, *Eur J. Clin. Pharm.*, **31**, 123–124 (1986).
45. W.L. Hayton and K. Stoeckel, *Clin. Pharmacokinetics*, **11**, 76–86 (1986).
46. A. Mulhall, J. de Louvois, J. James, *Eur. J. Pediatrics*, **144**, 379–382 (1985).
47. J.R. Luderer, I.H. Patel, J. Durkin, and D.W. Schneck, *Clin. Pharmacol. Therap.*, **35**, 19–25 (1984).
48. K. Stoeckel, P.J. McNamara, G. Hoppe-Seyler, A. Blumberg, and E. Keller, *Clin. Pharmacol. Therap.*, **33**, 633–641 (1983).
49. R. Wise and N. Wright, *Infection*, **13(Suppl. 1)**, 145–150 (1985).
50. T. Teow-Yee, L. Fortin, J.A. Kreeft, D.S. East, and R.I. Ogilvie, *Antimicrob. Agents Chemo.*, **25**, 83–87 (1984).
51. T.N. Riley, R.G. Fischer, U.S. Pharmacist. September, 38–56 (1985).
52. G.R. Donwitz, G.L. Mandell, *New Eng. J. Med.*, **18**, 490–500 (1988).

Ipratropium Bromide: Physical Properties

Heba H. Abdine, F. Belal and Abdullah A. Al-Badr

Department of Pharmaceutical Chemistry

College of Pharmacy

King Saud University

P.O. Box 2457

Riyadh – 11451

Kingdom of Saudi Arabia

CONTENTS

1.	General Information	60
1.1	Nomenclature	60
1.1.1	Systematic chemical names	60
1.1.2	Nonproprietary names	61
1.1.3	Proprietary names	61
1.1.4	Synonyms	61
1.2	Formulae	61
1.2.1	Empirical formula, molecular weight, CAS number	61
1.2.2	Structural formula	61
1.3	Elemental analysis	62
1.4	Appearance	62
2.	Physical characteristics	62
2.1	Solution pH	62
2.2	Solubility characteristics	62
2.3	Optical activity	62
2.4	X-Ray powder diffraction pattern	62
2.5	Thermal methods of analysis	62
2.5.1	Melting behavior	62
2.5.2	Differential scanning calorimetry	65
2.6	Spectroscopy	65
2.6.1	Ultraviolet spectroscopy	65
2.6.2	Vibrational spectroscopy	65
2.6.3	Nuclear magnetic resonance spectrometry	65
2.6.3.1	^1H -NMR spectrum	65
2.6.3.2	^{13}C -NMR spectrum	67
2.7	Mass spectrometry	69
3.	Stability and storage	69
4.	References	83

1. GENERAL INFORMATION

1.1 Nomenclature

1.1.1 Systematic chemical names [1, 2]

(\pm)-(endo,syn)-8-Azoniabicyclo[3.2.1]octane,3-(3-hydroxy-1-oxo-2-phenylpropoxy)-8-methyl-8-(1-methylethyl)-,bromide monohydrate
 (endo-syn)-(\pm)-3-(3-Hydroxy-1-oxo-2-phenylpropoxy)-8-methyl-8-(1-methyl-ethyl)-8-azaniabicyclo[3.2.1]octane bromide

(±)-(endo, syn)-8-Azabicyclo[3,2,1]octane, 3-(3-hydroxy-1-oxo-2-phenylpropoxy)-8-methyl-8-(isopropyl)-, bromide
 (8r)-3α-Hydroxy-8-isopropyl-1αH,5αH-tropanium bromide (±)-tropate monohydrate
 (1R, 3r, 5S, 8r)-8-isopropyl-3-[(±)-tropoyloxy]tropanium bromide monohydrate
 3α-hydroxy-8-isopropyl-1αH, 5αH-tropanium bromide (±)-tropate
 8-Isopropyl noratropine methanebromide
 Isopropyl noratropinium bromomethylate
 8-Isopropylatropine bromide

1.1.2 *Nonproprietary names*
 Ipratropium bromide

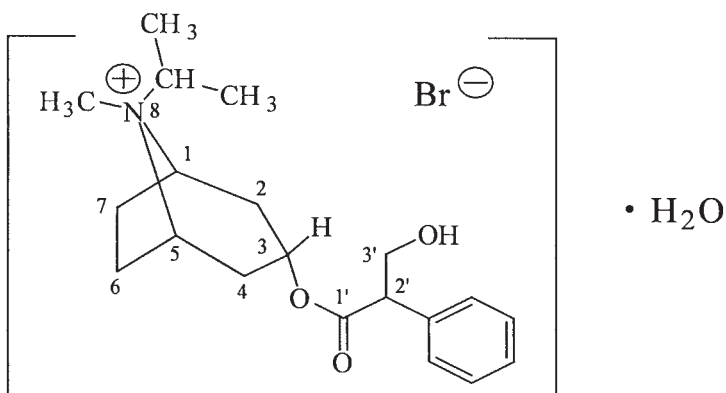
1.1.3 *Proprietary names [2, 3]*
 Atrovent, Bitrop, Itrop, Narilet, Rinatec, Atem, Disne-Asmol

1.1.4 *Synonyms [3]*
 Sch-1000, Sch-1000-Br-mono-hydrate

1.2 Formulae

1.2.1 *Empirical formula, molecular weight, CAS number [1]*
 Anhydrate: $C_{20}H_{30}BrNO_3$ 412.37 [22254-24-6]
 Monohydrate: $C_{20}H_{30}BrNO_3 \cdot H_2O$ 430.38 [66985-17-9]

1.2.2 *Structural formula*



1.3 Elemental analysis

Anhydrate

C 58.25%, H 7.33, Br 19.38, N 3.40, O 11.64

Monohydrate

C 55.82, H 7.49, Br 18.57, N 3.25, O 14.87

1.4 Appearance

Ipratropium bromide is a white or almost white, odorless, and tasteless crystalline powder [2].

2. PHYSICAL CHARACTERISTICS

2.1 Solution pH

The pH of a 1% (w/v) solution in water is 5–7.5 [3].

2.2 Solubility characteristics

Ipratropium bromide is freely soluble in water and lower alcohols. The substance is also insoluble in ether, chloroform, and fluorohydrocarbons [1].

2.3 Optical activity

For a 1% w/v solution, the observed angle of rotation is -0.01° – $+0.10^{\circ}$ [4].

2.4 X-Ray powder diffraction pattern

The X-ray powder diffraction pattern of ipratropium bromide was performed using a Simons XRD-5000 diffractometer. Figure 1 shows the X-ray powder diffraction pattern of ipratropium bromide, which was acquired on a pure sample of the drug substance. Table 1 shows values for the scattering angles ($^{\circ}2\theta$), the interplanar d -spacings (Å), and the relative intensities (%) observed for the major diffraction peaks of ipratropium bromide.

2.5 Thermal methods of analysis

2.5.1 Melting behavior

Ipratropium bromide melts at about 230°C with decomposition [1].

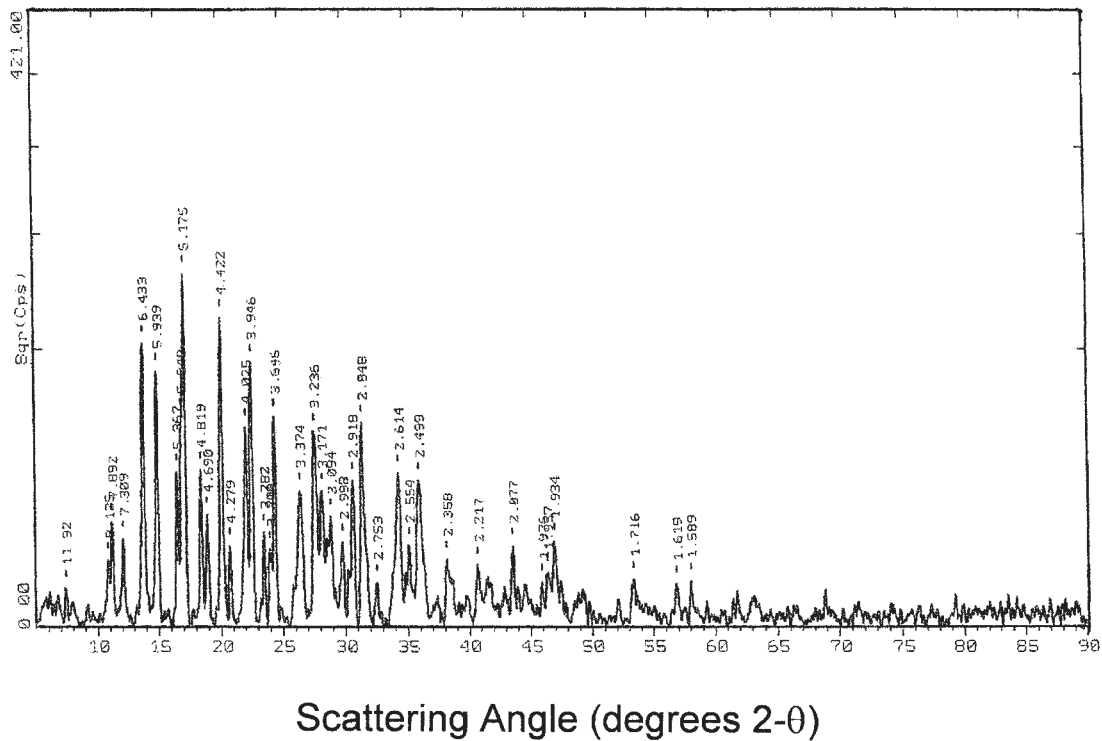


Figure 1. X-ray powder diffraction pattern of ipratropium bromide.

Table 1

Crystallographic Data from the X-Ray Powder
Diffraction Pattern of Ipratropium Bromide

Scattering angle (°2 θ)	<i>d</i> -spacing (Å)	Relative intensity (%)	Scattering angle (°2 θ)	<i>d</i> -spacing (Å)	Relative intensity (%)
7.412	11.9177	1.18	10.880	8.1248	3.43
11.202	7.8924	8.77	12.099	7.3091	6.15
13.753	6.4334	64.47	14.903	5.9393	52.42
16.504	5.3666	19.24	16.880	5.2481	35.61
17.119	5.1755	100.00	18.396	4.8188	19.73
18.908	4.6896	9.95	20.065	4.4217	76.76
20.740	4.2792	5.13	22.066	4.0250	32.22
22.516	3.9455	55.99	23.503	3.7820	7.07
23.982	3.7077	4.74	24.392	3.6462	35.41
26.393	3.3741	14.86	27.540	3.2361	30.79
28.115	3.1713	14.79	28.829	3.0943	9.63
29.775	2.9981	5.70	30.616	2.9176	17.16
31.385	2.8479	33.42	32.499	2.7527	1.49
34.277	2.6139	18.86	35.107	2.5540	5.25
35.910	2.4987	17.26	38.139	2.3576	3.57
40.668	2.2167	3.01	43.533	2.0772	5.14
45.894	1.9757	1.56	46.353	1.9572	2.28
49.935	1.9343	5.74	53.360	1.7155	1.73
56.814	1.6192	1.43	57.973	1.5895	1.61

2.5.2 Differential scanning calorimetry

The differential scanning calorimetry (DSC) thermogram of ipratropium bromide was obtained using a DuPont TA-9900 thermal analyzer system. The thermogram shown in Figure 2 was obtained at a heating rate of 10°C/min, and was run over the range of 40–400°C. In this study, the compound was found to melt at 239.6°C.

2.6 Spectroscopy

2.6.1 Ultraviolet spectroscopy

The ultraviolet absorption spectrum of ipratropium bromide in water, shown in Figure 3, was recorded using a Shimadzu UV–Visible Spectrophotometer 1601 PC. The compound was found to only weakly absorb light in the UV region, and exhibited three maxima and a shoulder:

λ_{\max} (nm)	A [1%, 1 cm]	Molar absorptivity
263.3	3.06	126
257.3	4.11	170
251.6	3.35	148
241.1	—	—
(shoulder)		

2.6.2 Vibrational spectroscopy

The infrared absorption spectrum of ipratropium bromide was obtained in a KBr pellet using a Perkin–Elmer infrared spectrophotometer. The IR spectrum is shown in Figure 4, where the principal peaks were observed at 3490, 3410, 3360, 2960, 2860, 1696, 1625, 1480, 1440, 1238, 1218, 995, 960, 730 and 690, cm^{-1} . Assignments for the major infrared absorption bands are provided in Table 2.

2.6.3 Nuclear magnetic resonance spectrometry

2.6.3.1 ^1H -NMR spectrum

The proton NMR spectrum of ipratropium bromide was obtained using a Bruker Avance Instrument operating at 300, 400, or 500 MHz. Standard Bruker Software was used to obtain DEPT, COSY, and HETCOR spectra. The sample was dissolved in D_2O , and tetramethylsilane (TMS) was added to function as the internal standard. The proton NMR spectra are shown in Figures 5 and 6, while the COSY ^1H -NMR spectra are shown in Figures 7 and 8, and the gradient HMQC-NMR

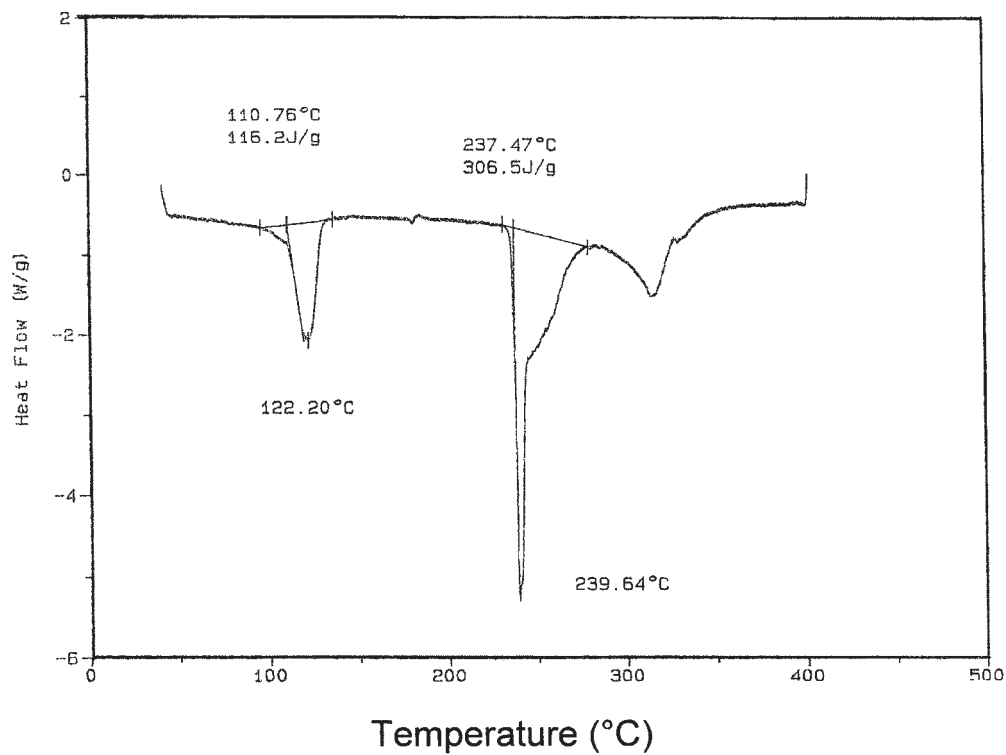


Figure 2. Differential scanning calorimetry thermogram of ipratropium bromide.

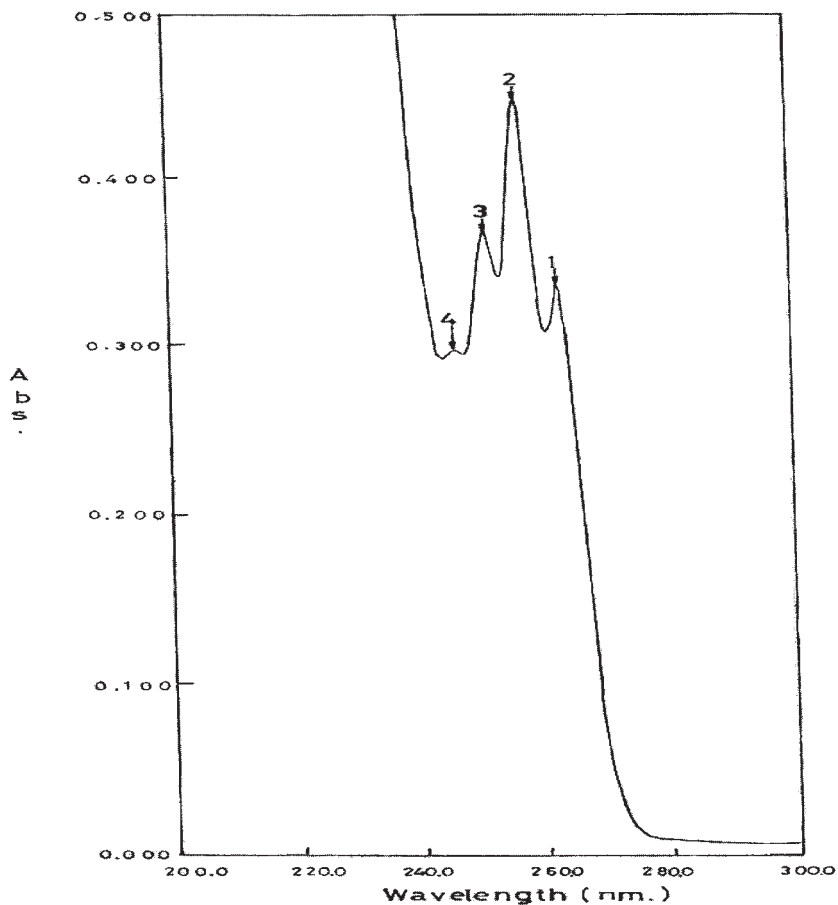


Figure 3. The ultraviolet absorption spectrum of ipratropium bromide in water.

spectrum is shown in [Figure 9](#). The ^1H -NMR spectral assignments for ipratropium bromide are provided in [Table 3](#).

2.6.3.2 ^{13}C -NMR spectrum

The carbon-13 NMR spectrum of ipratropium bromide was obtained using a Bruker Avance Instrument operating at 75, 100, or 125 MHz. The sample was dissolved in D_2O and tetramethylsilane (TMS) was added to function as the internal standard. The ^{13}C -NMR spectrum of ipratropium bromide is shown in [Figure 10](#), and the DEPT-NMR

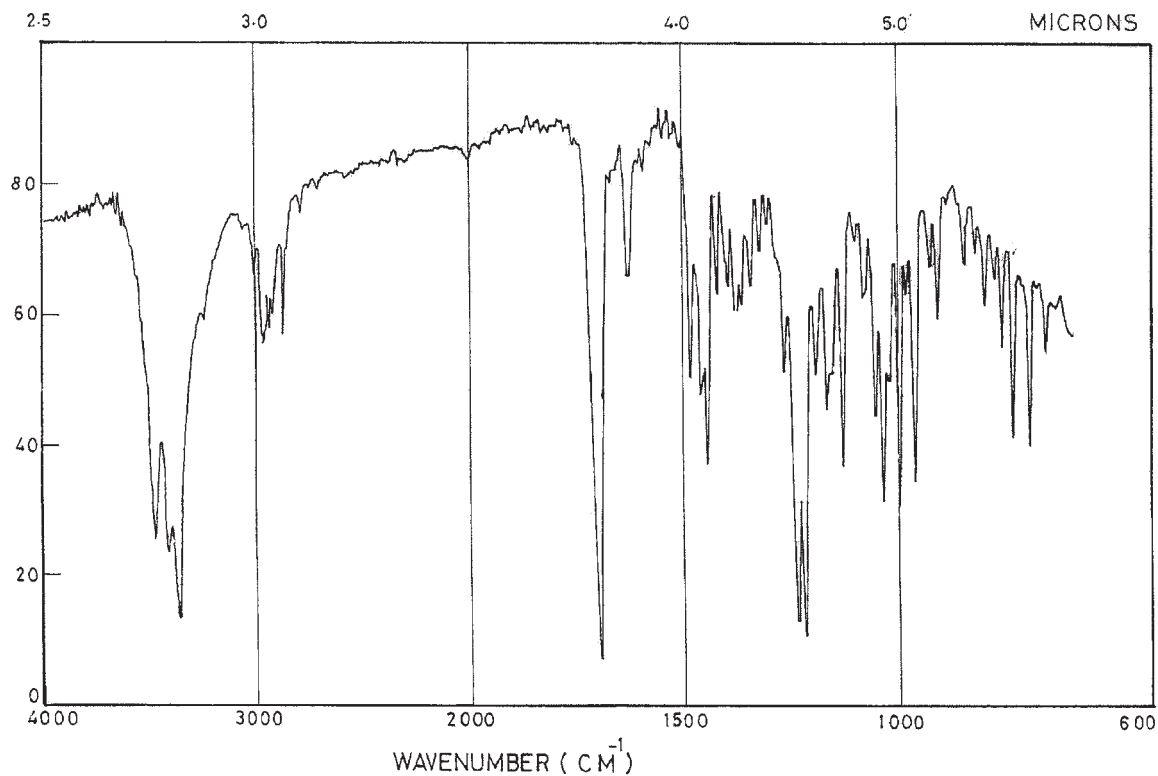


Figure 4. The infrared absorption spectrum of ipratropium bromide obtained in a KBr pellet.

Table 2

Assignments for the Infrared Absorption Bands of Ipratropium Bromide

Frequency (cm^{-1})	Assignments
3490, 3410, 3360	OH stretch
2960	Aliphatic C–H stretch
2860	N–C stretch
1696	C=O stretch
1625	Aromatic C=C stretch
1480, 1440	C–O and C–N stretch
1238, 1218	C–O–C ether stretch
995, 960, 730, 690	Monosubstituted benzene

spectra are shown in [Figures 11 and 12](#). Assignments for the observed resonance bands associated with the various carbons are provided in [Table 4](#).

2.7 Mass spectrometry

The mass spectrum of ipratropium bromide was obtained utilizing a Shimadzu PQ5000 mass spectrometer, with the parent ion being collided with helium as the carrier gas. [Figure 13](#) shows the detailed mass fragmentation pattern, and [Table 5](#) provides the proposed mass fragmentation pattern of the substance.

3. STABILITY AND STORAGE

Ipratropium bromide is fairly stable in neutral and acidic solutions, but is rapidly hydrolyzed in alkaline solution [2]. Ipratropium bromide aerosol

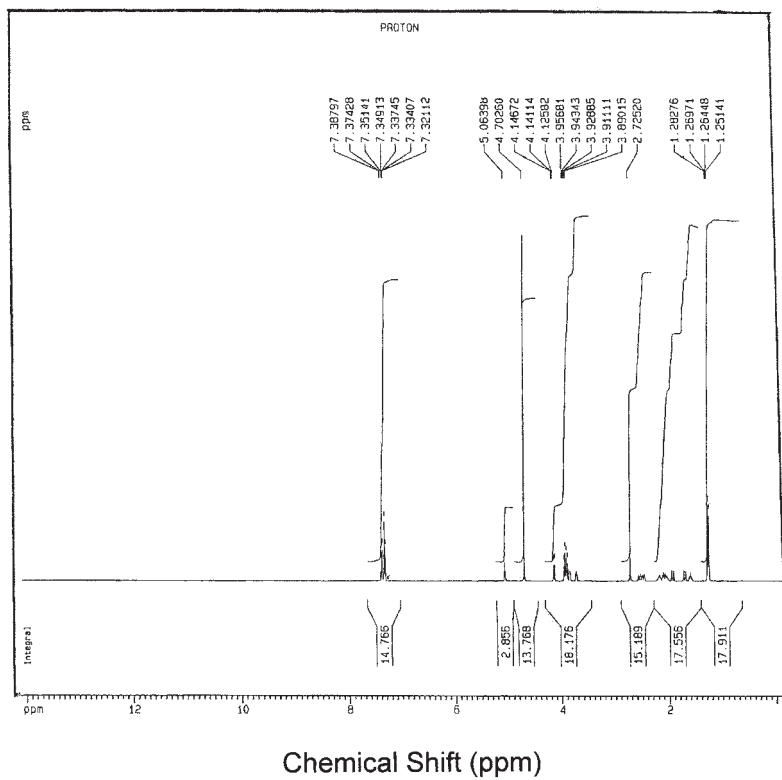
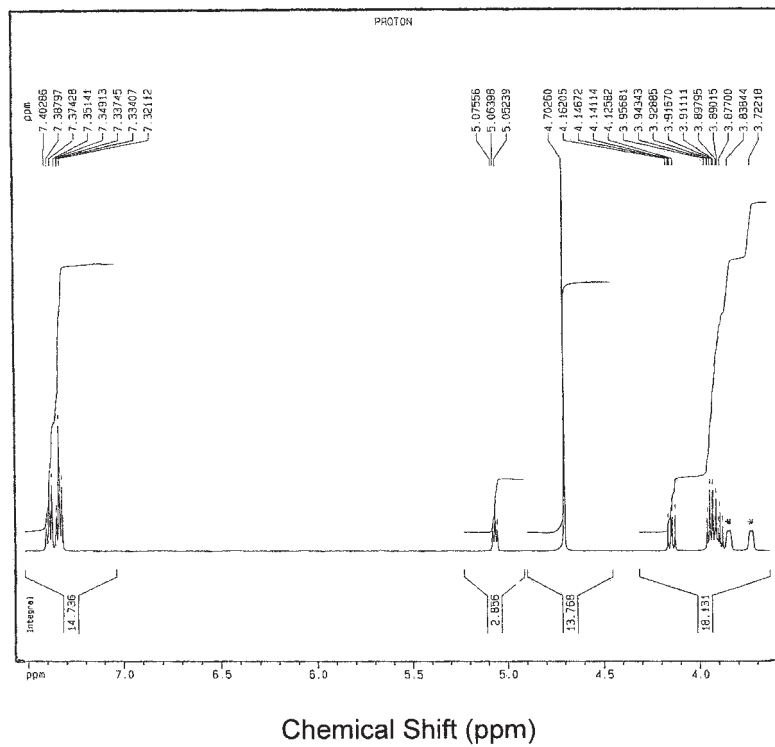
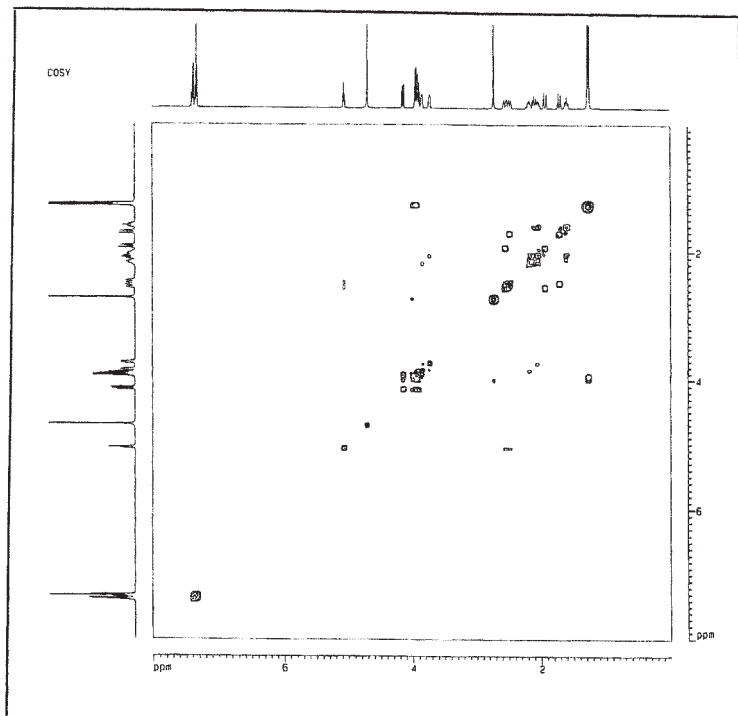


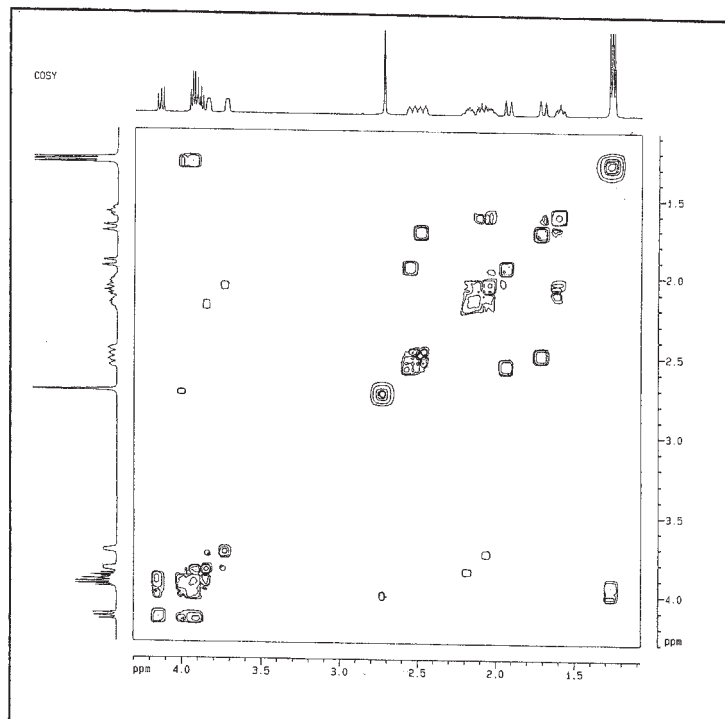
Figure 5. The ^1H -NMR spectrum of ipratropium bromide in D_2O .





Chemical Shift (ppm)

Figure 7. COSY ^1H -NMR spectrum of ipratropium bromide in D_2O .



Chemical Shift (ppm)

Figure 8. COSY ^1H -NMR spectrum of ipratropium bromide in D_2O .

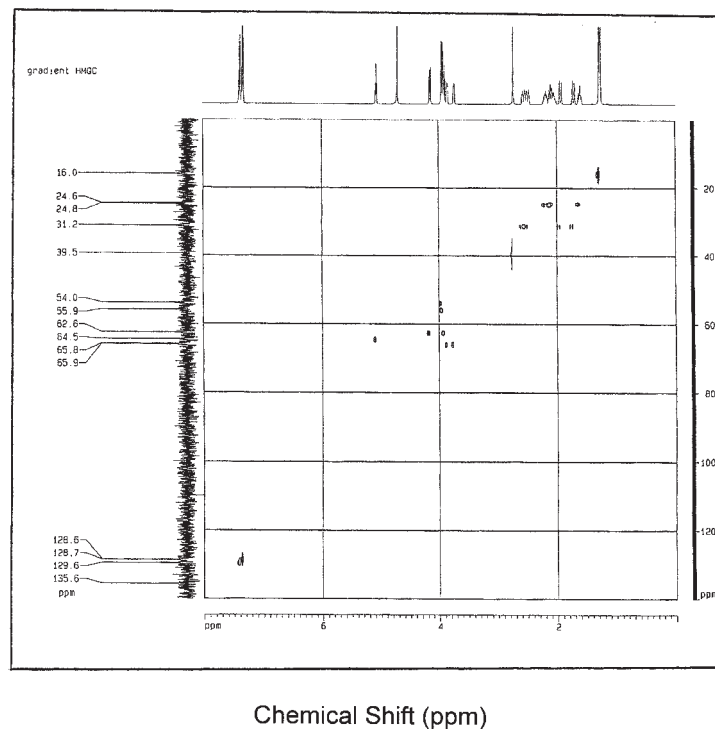
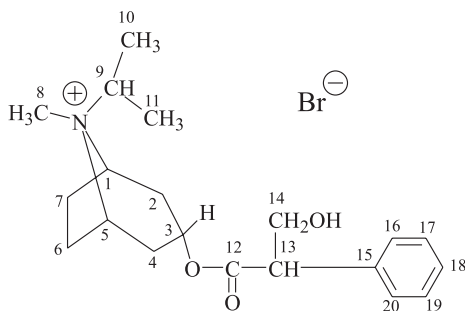


Figure 9. Gradient HMQC NMR spectrum of ipratropium bromide in D_2O .

Table 3

Proton Nuclear Magnetic Resonance Assignments for Spectrum of Ipratropium Bromide



Chemical shift, (ppm relative to TMS)	Number of protons	Multiplicity s: singlet, t: triplet, q: quartet, m: multiplet	Assignment (proton at carbon #)
1.25	6	q	(10 and 11)
1.26–1.28	8	m	(2, 4, 6, 7)
2.73	3	s	(8)
3.89–3.96	4	m	(1, 5, 9, 13)
4.13–4.15	2	m	(14)
5.06	1	t	(3)
7.23–7.39	5	m	(16–20)

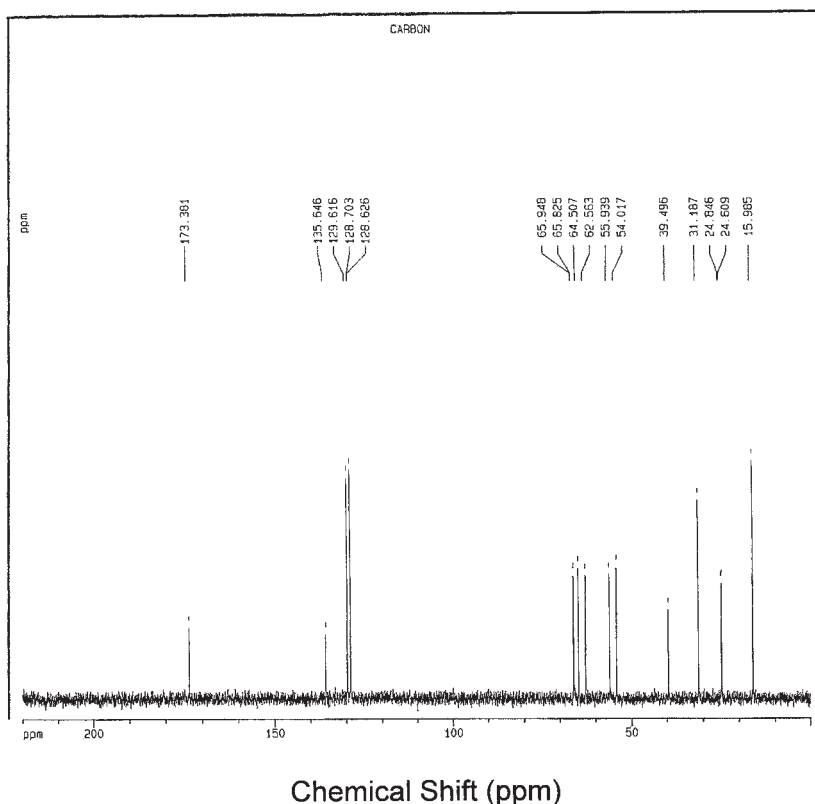


Figure 10. ^{13}C -NMR spectrum of ipratropium bromide in D_2O .

formulations should not be stored at temperatures above 30°C (86°F), or in the presence of excessive humidity.

Inhalation solutions should be stored at room temperature between 58 and 86°F (15 and 30°C), and unused vials should be kept in the foil pouch, protected from light. The nasal spray formulation of the drug should be stored between 59 and 86°F (15 and 30°C), and should not be allowed to freeze [7].

A nebulizer solution consisting of an admixture of ipratropium and salbutamol in equal ratios was found to retain more than 90% of its initial concentrations after storage for 5 days at 4°C or 22°C in the dark, or at 22°C under continuous fluorescent lighting [3, 5, 6].

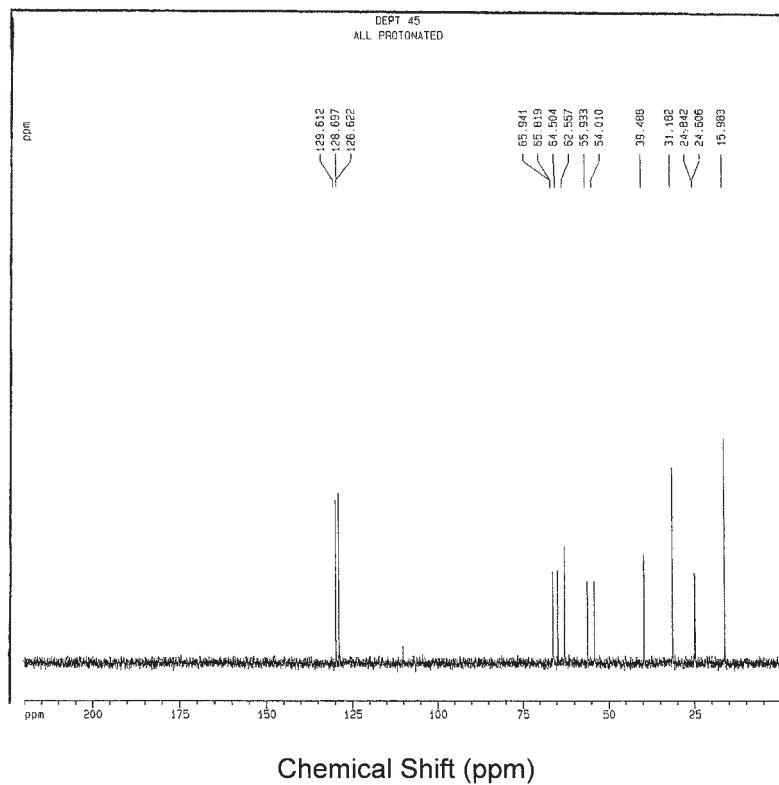


Figure 11. DEPT 45 ^1H -NMR spectrum of ipratropium bromide in D_2O .

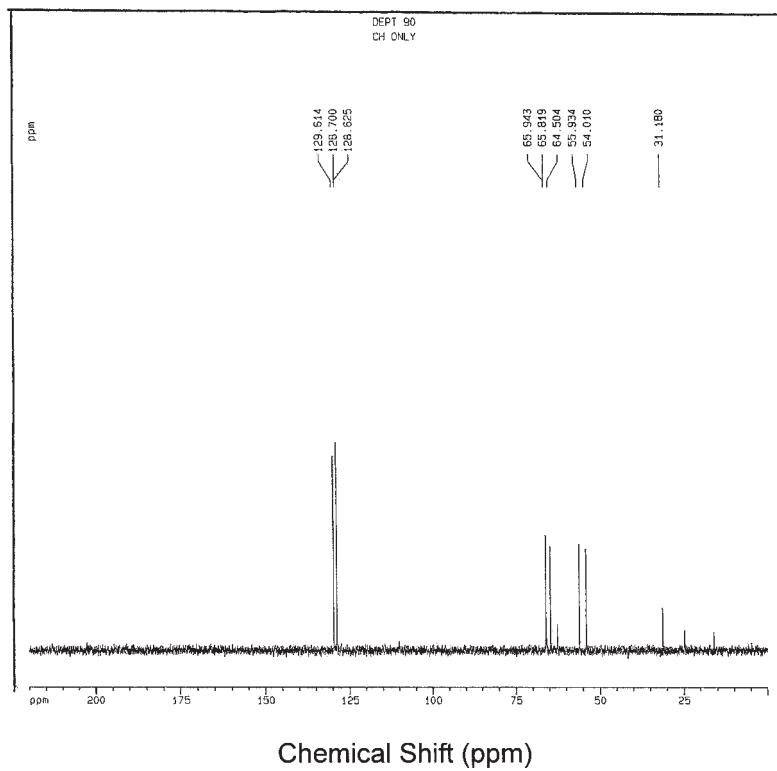
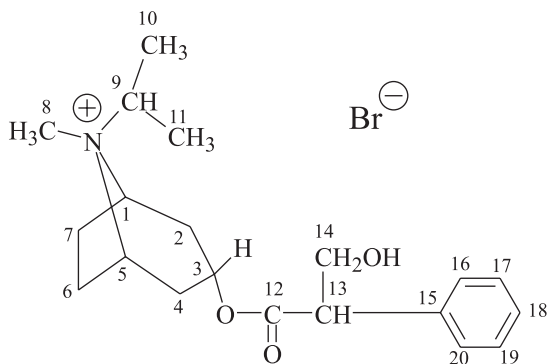


Figure 12. DEPT 90 ^1H -NMR spectrum of ipratropium bromide in D_2O .

Table 4

Carbon-13 Nuclear Magnetic Resonance Assignments
for Spectrum of Ipratropium Bromide

Chemical shift, (ppm relative to TMS)	Assignments at carbon number	Chemical shift, (ppm relative to TMS)	Assignment at carbon number
173.381	12	55.939	13
135.646	15	54.017	9
129.616	16 + 20	39.496	8
128.703	17 + 19	31.187, 31.173	2 + 4
128.626	18	24.846	6 or 7
65.948	1 or 5	24.605	6 or 7
65.825	1 or 5	15.985	10 + 11
64.507	3	62.563	14

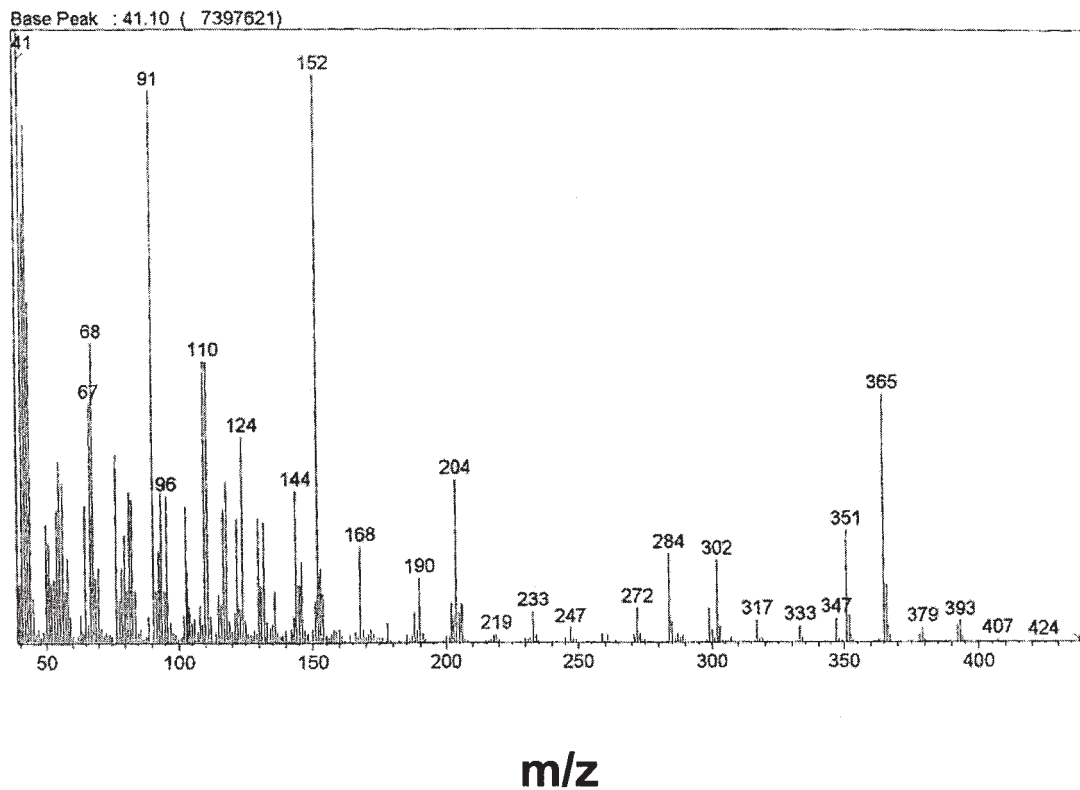


Figure 13. Mass spectrum of ipratropium bromide.

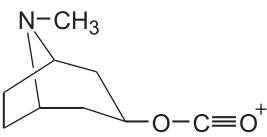
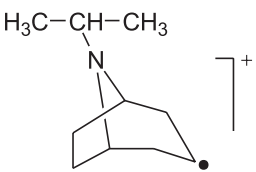
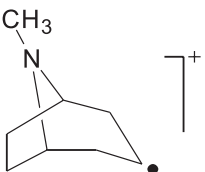
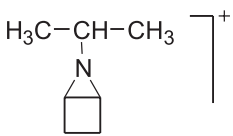
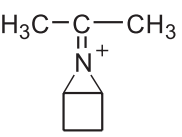
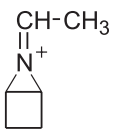
Table 5

Assignments for the Fragmentation Pattern Observed in the Mass Spectrum of Ipratropium Bromide

m/z	Relative intensity	Fragment
317	3.5%	$\text{H}_3\text{C}-\text{CH}-\text{CH}_3$
302	12.5%	$\text{H}_3\text{C}-\text{CH}=\text{N}^+$
284	13.0%	$\text{CHCH}_3=\text{N}^+$
272	4.5%	$\text{CHCH}_3=\text{N}^+$
204	24.0%	

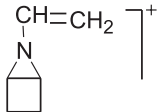
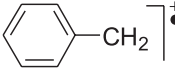
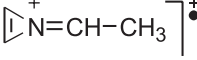
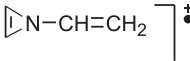
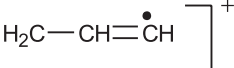
(continued)

Table 5 (continued)

m/z	Relative intensity	Fragment
168	13.5%	
152	85.0%	
124	30.0%	
111	41.0%	
110	41.0%	
96	21.5%	

(continued)

Table 5 (continued)

m/z	Relative intensity	Fragment
95	22.0%	
91	83.0%	
68	44.5%	
67	36.0%	
41	100.0%	

4. REFERENCES

1. *Remington's: The Science and Practice of Pharmacy*, 19th edn., Volume II, A.R. Gennaro, ed., Mack Publishing Co., Pennsylvania, p 1024 (1995).
2. *The Merck Index*, 12th edn., S. Budavari, ed., Merck and Co., NJ, p 870 (1996).
3. *Martindale, The Extra Pharmacopoeia*, 29th edn., K. Parfitt, ed., The Pharmaceutical Press, Massachusetts, p 537 (1999).
4. *British Pharmacopoeia 1998*, Volume II, His Majesty's Stationary Office, London, p. 740, 1761 (1998).
5. G.A. Jacobson and G.M. Peterson, *Inst. J. Pharm. Pract.*, **3**, 169 (1995).
6. G.A. Jacobson and G.M. Peterson, *J. Pharm. Biomed. Anal.*, **12**, 825 (1994).
7. Drugdex Drug Evaluations, Micromedex, Healthcare Series, Volume 116 Expires 6/2003.

Ipratropium Bromide: Methods of Chemical and Biochemical Synthesis

Heba H. Abdine, F. Belal and Abdullah A. Al-Badr

Department of Pharmaceutical Chemistry

College of Pharmacy

King Saud University

P.O. Box 2457

Riyadh – 11451

Kingdom of Saudi Arabia

CONTENTS

1.	Introduction	87
2.	Chemical Methods of Synthesis	87
2.1	Partial synthesis	87
2.2	Total synthesis of atropine and ipratropium bromide.	87
2.2.1	Total synthesis of tropine	87
2.2.1.1	Willstätter's total synthesis of tropine	87
2.2.1.2	Robinson's total synthesis of tropine	89
2.2.1.3	Willstätter's second synthesis of tropine	89
2.2.1.4	Elming synthesis of tropine	90
2.2.2	Total synthesis of tropic acid	91
2.2.2.1	Landenburg's synthesis of tropic acid	91
2.2.2.2	McKenzie and Wood's synthesis of tropic acid	91
2.2.2.3	Muller's synthesis of tropic acid	92
2.2.2.4	Chambon's synthesis of tropic acid	92
2.2.2.5	Blicke's synthesis of tropic acid	92
2.3	Synthesis of atropine and ipratropium bromide.	93
2.4	Synthesis of labeled atropine and labeled ipratropium bromide	93
2.4.1	Synthesis of labeled tropic acid	93
2.4.2	Synthesis of labeled tropine	94
2.4.2.1	Labeled at carbons 6 and 7.	94
2.4.2.1.1	Method one	94
2.4.2.1.2	Method two	94
2.4.2.2	Labeled at N-methyl carbon	94
2.4.2.3	Labeled at carbon 1 or 5.	95
3.	Biosynthesis of Atropine	95
3.1	Biosynthesis of tropine	95
3.2	Biosynthesis of tropic acid	97
4.	References	97

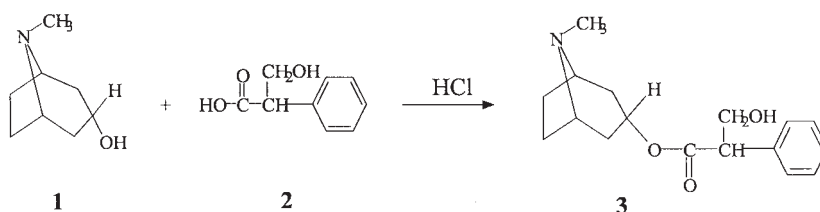
1. INTRODUCTION

Ipratropium bromide is the quaternary ammonium compound obtained by treating atropine with isopropyl bromide. The synthesis of atropine, which is an ester prepared from tropic acid and tropine, was reported earlier in the profile of atropine [1]. It is therefore appropriate to report all of the methods of chemical and biochemical synthesis, as these are also the synthetic routes used for the preparation of ipratropium bromide.

2. CHEMICAL METHODS OF SYNTHESIS

2.1 Partial synthesis

Atropine (**3**) was synthesized by Landenburg [2] by heating tropine **1** and tropic acid **2** in the presence of hydrogen chloride.



2.2 Total synthesis of atropine and ipratropium bromide

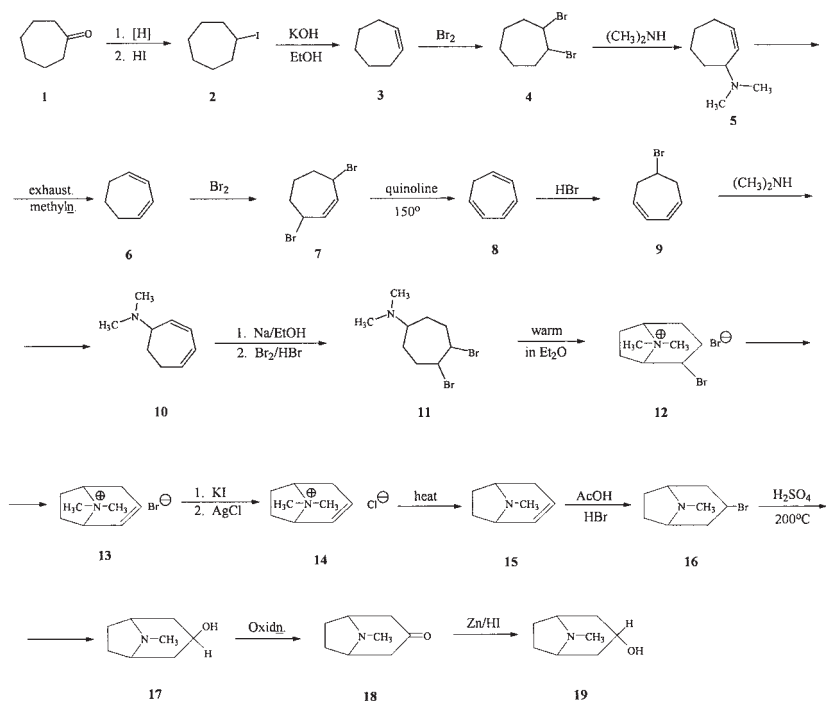
The total synthesis of tropine and tropic acid, from which both atropine and ipratropium bromide are obtained by esterification (atropine), and subsequent quaternization with isopropyl bromide (ipratropium bromide) are described in the following sections.

2.2.1 Total synthesis of tropine

2.2.1.1 Willstatter's total synthesis of tropine [3]

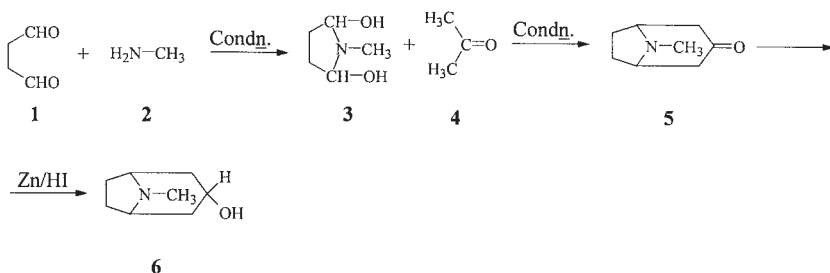
Cycloheptanone (suberone, **1**) was reduced to cycloheptanol (suberol), which was treated with hydrogen iodide to give suberyl iodide (**2**). The treatment of suberyl iodide with potassium hydroxide in ethanol gave the cycloheptene (**3**). The latter compound was brominated to give 1,2-dibromocycloheptane (**4**), which was treated with dimethylamine to yield dimethylaminocyclohept-2-ene (**5**). This compound was then converted to cyclohepta-1,3-diene (**6**) by exhaustive methylation. Compound (**6**) was

brominated at the 1,4-positions to give 1,4-dibromocyclohept-2-ene (7). Elimination of two moles of hydrogen bromide from compound (7) was effected by quinoline to give cycloheptatriene (8). Compound (8) was treated with hydrogen bromide to give bromocyclohepta-3,5-diene (9), which was reacted with dimethylamine to give dimethylaminocyclohepta-2,4-diene (10). The latter compound was treated with sodium in ethanol, followed by bromination, to give 1,2-dibromo-5-dimethylaminocycloheptane (11). This compound was warmed in ether, causing intramolecular alkylation to occur and yielding 2-bromotropane methobromide (12). Hydrogen bromide was eliminated from compound (12) by the action of an alkali to yield tropidine methobromide (13). This compound was transformed to tropidine methochloride (14) by the action of potassium iodide, followed by the action of silver chloride. Compound (14) was then pyrolyzed to give tropidine (15). To an acetic acid solution of tropidine, hydrogen bromide was added to yield 3-bromotropane (16), which was hydrolyzed with 10% sulfuric acid at 200–210°C to give pseudotropine (17). This compound was then oxidized with chromium trioxide to give tropinone (18). This ketone was finally reduced with zinc and hydroiodic acid to tropine (19).

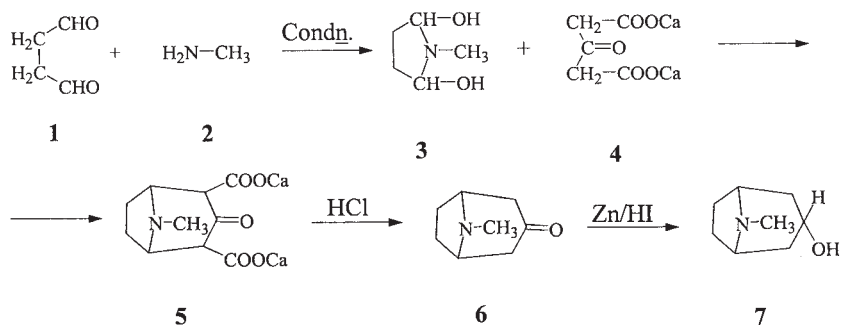


2.2.1.2 Robinson's total synthesis of tropine [4]

Succinic dialdehyde (**1**) was condensed with methylamine (**2**) to give the condensate biscarbinolamine (**3**). This was in turn condensed with acetone (**4**) to give tropinone (**5**). Tropinone (**5**) was reduced with zinc and hydroiodic acid to yield tropine (**6**).



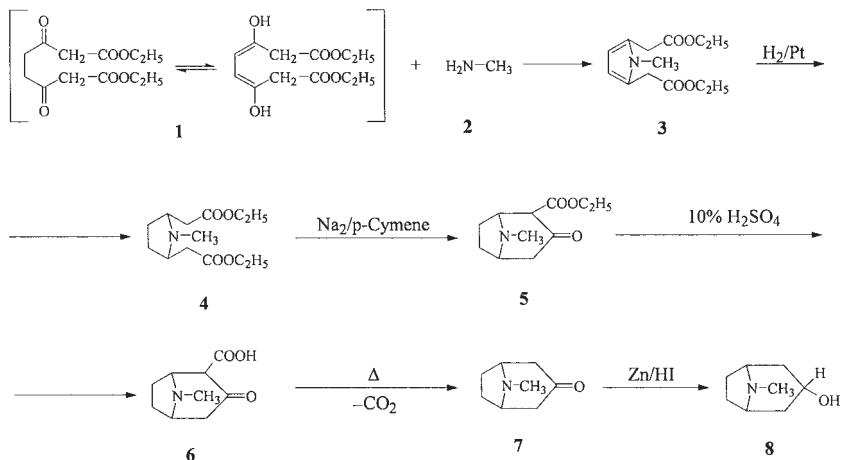
The use of acetone dicarboxylate, or its ester, instead of acetone alone was found to improve the yield of tropine. Therefore, the condensation of succinodialdehyde (**1**) with methylamine (**2**) gives biscarbinolamine (**3**), which was then condensed with calcium acetonedicarboxylate (**4**) to afford the condensate (**5**). Compound (**5**) was warmed with hydrochloric acid to give tropinone (**6**) which was then reduced with zinc and hydroiodic acid to tropine (**7**).



2.2.1.3 Willstätter's second synthesis of tropine [5]

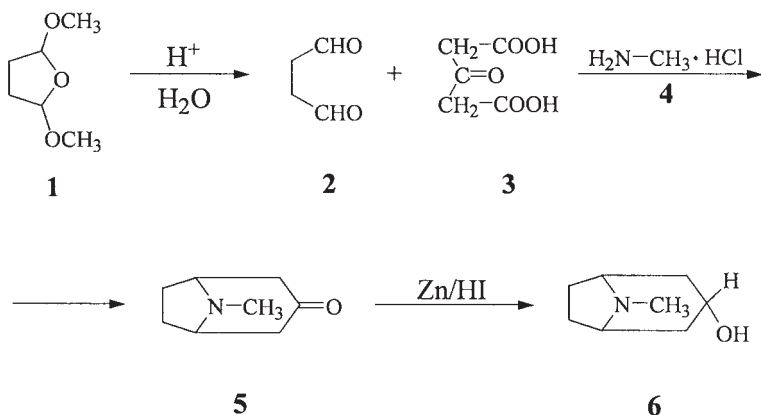
Succinyldiacetic ethyl ester (**1**) was condensed with methylamine (**2**) to give diethyl-*N*-methyl-pyrrolediacetate (**3**). This compound was reduced to afford diethyl-*N*-methylpyrrolidine diacetate (**4**). The *cis* form of compound (**4**) was cyclized in the presence of sodium and *p*-cymene to give ethyltropinone-2-carboxylate (**5**). Hydrolysis of compound (**5**) with

10% sulfuric acid gave tropinone-2-carboxylic acid (6). The latter compound was then heated to yield tropinone (7), which was reduced with zinc and hydroiodic acid to tropine (8).



2.2.1.4 Elming synthesis of tropine [6]

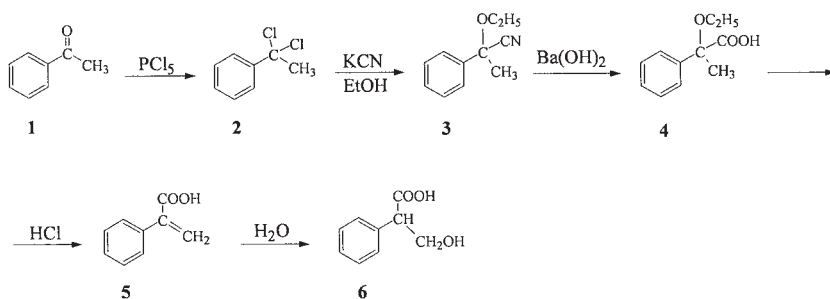
Tropinone (**5**) and tropine (**6**) were synthesized using methylamine hydrochloride (**4**) and acetone dicarboxylic acid (**3**). Succindialdehyde (**2**) was generated *in situ* by action of the acid on 2,5-dimethoxytetrahydrofuran (**1**), and finally reduction with zinc and hydroiodic acid yielded tropinone (**6**):



2.2.2 Total synthesis of tropic acid

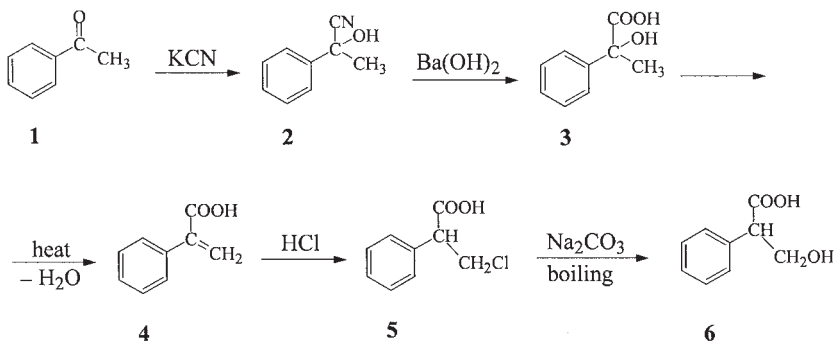
2.2.2.1 Landenburg's synthesis of tropic acid [7]

Acetophenone (**1**) was converted to α,α -dichloroethylbenzene (**2**) by the action of phosphorous pentachloride. Compound (**2**) was reacted with potassium cyanide and ethanol to give α -ethoxy- α -cyanoethylbenzene (**3**). This compound was then hydrolyzed with barium hydroxide solution to give atrolactic ethylether (**4**). The latter compound was heated with hydrogen chloride to yield atropic acid (**5**), and then converted to tropic acid (**6**).



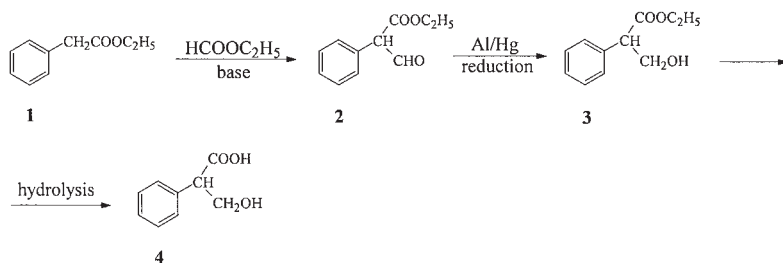
2.2.2.2 McKenzie and Wood's synthesis of tropic acid [8]

Acetophenone (**1**) was converted to acetophenone cyanohydrin (**2**) by the action of potassium cyanide. Compound (**2**) was hydrolyzed to give atrolactic acid (**3**), which was heated under pressure to yield atropic acid (**4**). Atropic acid (**4**) was then treated with hydrogen chloride in ethereal solution to form β -chlorohydroatropic acid (**5**). Compound (**5**) was boiled with aqueous sodium carbonate to give tropic acid (**6**).



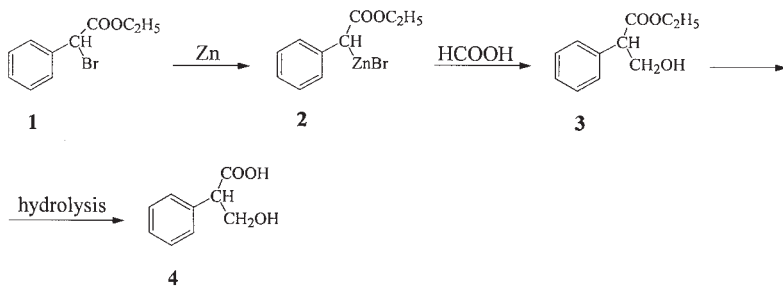
2.2.2.3 Muller's synthesis of tropic acid [9]

Ethylphenyl acetate (**1**) was condensed with ethylformate to give ethyl- α -formylphenyl acetate (**2**). Compound (**2**) was reduced with aluminum amalgam to yield (*DL*)-tropic ester (**3**), which was then hydrolyzed to give tropic acid (**4**).



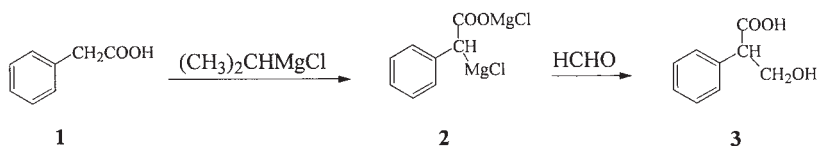
2.2.2.4 Chambon's synthesis of tropic acid [10]

Ethyl α -bromophenylacetate (**1**) was treated with zinc to give ethyl- α -zinc-bromophenylacetate (**2**). This compound was treated with formic acid to yield (*DL*)-tropic ethyl ester (**3**), and the hydrolysis of compound (**3**) yielded tropic acid (**4**).



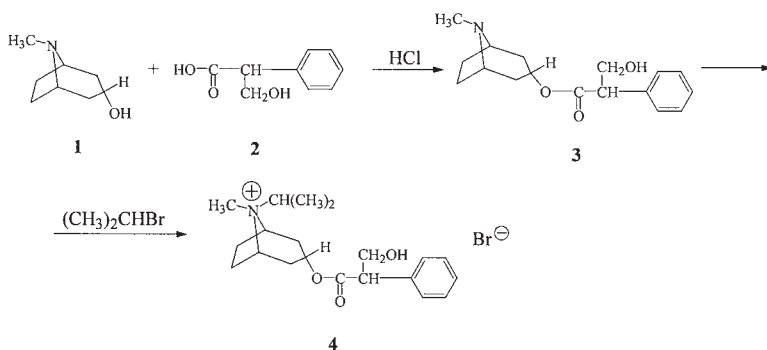
2.2.2.5 Blicke's synthesis of tropic acid [11]

Phenylacetic acid (**1**) was boiled with isopropylmagnesium chloride in an ethereal solution to give compound (**2**). Treatment of the latter Grignard reagent (**2**) with formaldehyde yielded tropic acid (**3**).



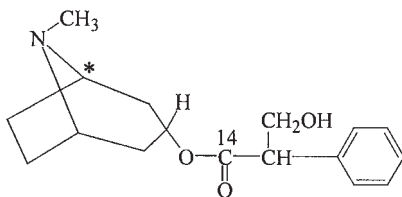
2.3 Synthesis of atropine and ipratropium bromide

Heating of tropine (**1**) with tropic acid (**2**) in the presence of hydrogen chloride (the Fischer–Speier esterification) gives atropine (**3**). Quaternization of atropine (**3**) with isopropyl bromide yields ipratropium bromide (**4**).



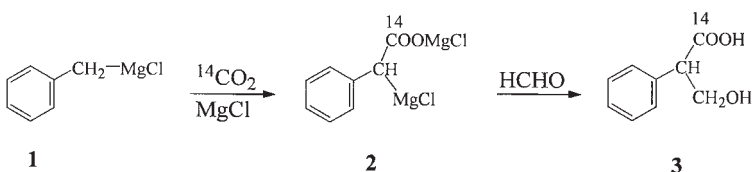
2.4 Synthesis of labeled atropine and labeled ipratropium bromide

Labeled atropine and labeled ipratropium bromide are synthesized from labeled tropine and/or labeled tropic acid to yield labeled or double labeled atropine. This compound is then quaternized with isopropyl bromide to give the labeled or double labeled ipratropium bromide.



2.4.1 Synthesis of labeled tropic acid

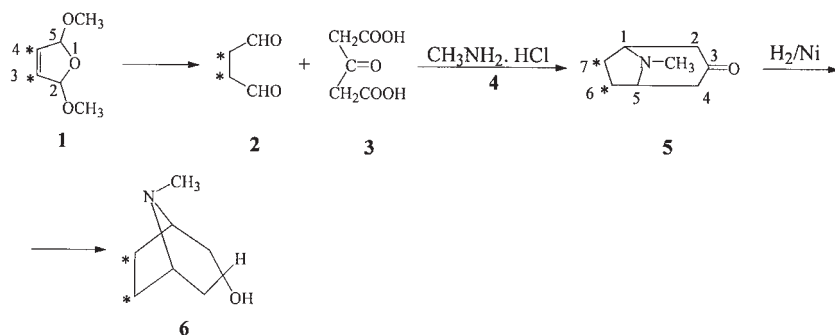
Benzylmagnesium chloride (**1**) was treated with $^{14}\text{CO}_2$, followed by magnesium chloride, to give the condensate (**2**). The addition of formaldehyde to condensate (**2**) gives the labeled tropic acid (**3**) [12].



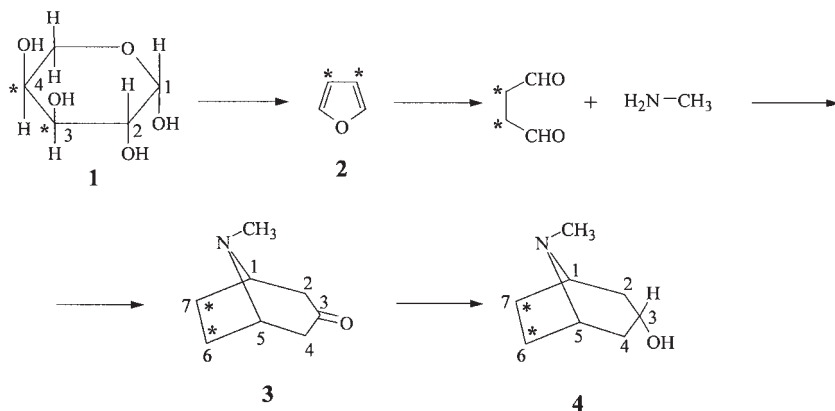
2.4.2 Synthesis of labeled tropine

2.4.2.1 Labeled at carbons 6 and 7

2.4.2.1.1 Method one The synthesis of tropine-6,7-T (**6**), was achieved by the catalytic tritium addition to 2,5-dimethoxy-2,5-dihydrofuran (**1**) and following Robinson's route to yield tropinone-6, 7T (**5**) by subsequent reduction with hydrogen over Raney nickel [13].



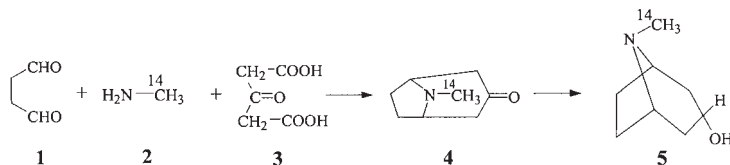
2.4.2.1.2 Method two The use of arabinose-3,4-¹⁴C serves to yield 6,7-¹⁴C tropinone (**3**), and then eventually 6,7-¹⁴C tropine (**4**) [14].



2.4.2.2 Labeled at N-methyl carbon

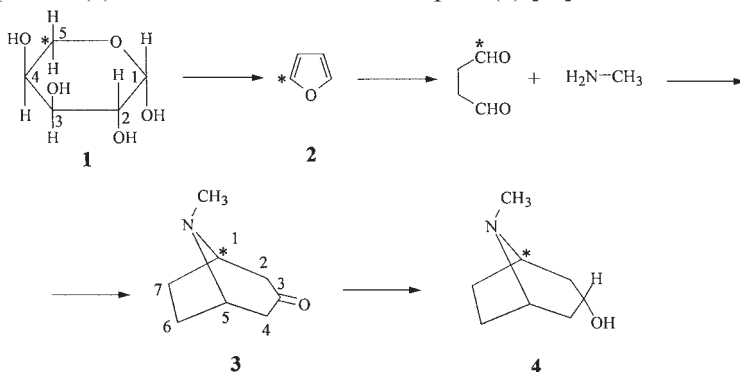
Synthesis of methyl-¹⁴C labeled tropine (**5**) was carried out from sodium cyanide (Na¹⁴CN) via methylamine-¹⁴C (**2**) and based on Robinson's route; methyl-¹⁴C tropinone (**4**) was obtained in 70% overall yield and

tropine ^{14}C (**5**) in 68% yield [15].



2.4.2.3 Labeled at carbon 1 or 5

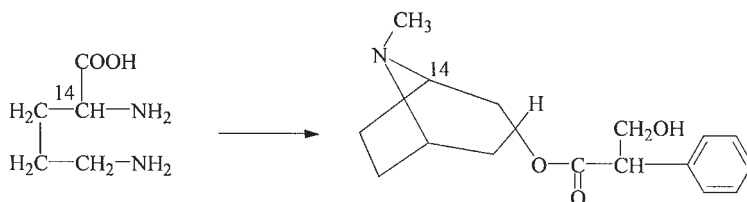
Synthesis of 1- ^{14}C tropine (**4**) can be obtained by starting with arabinose-5- ^{14}C (**1**), conversion into furan (**2**), and application of the Clauson-Kaas route to succinaldehyde. From here, one takes either 1- or 5- ^{14}C tropinone (**3**) on to either 1- or 5- ^{14}C tropine (**4**) [16].



3. BIOSYNTHESIS OF ATROPINE

3.1 Biosynthesis of tropine

Ornithine and related compounds (amino acids such as glutamic acid and proline) have been shown to be the precursors of the pyrrolidine ring system of tropine [17–22]. Feeding [2- ^{14}C]-ornithine to *Datura stramonium* results in formation of radioactive hyoscyamine labeled only at the C-1 bridgehead carbon atom of tropine [23]. Use of 5- ^{14}C proline resulted in radioactive hyoscyamine labeled only the C-5 position of tropine [21].

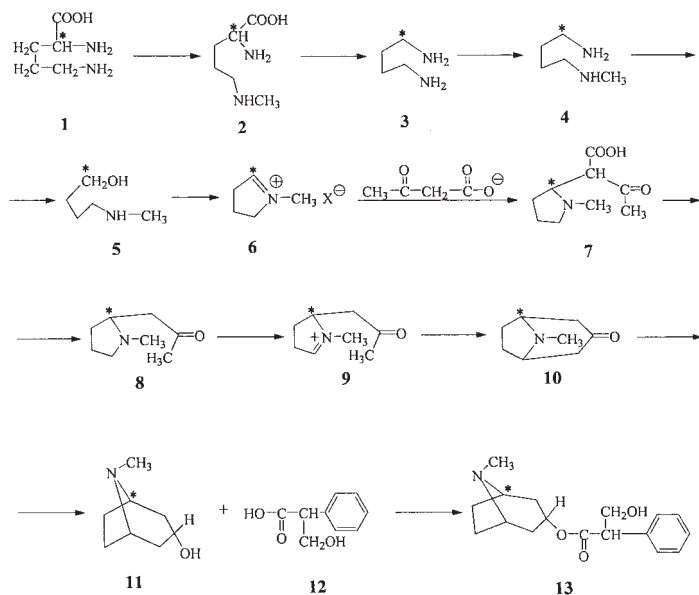


[2- ^{14}C , δ - ^{15}N]-ornithine has been reported to be incorporated into the tropine moiety of hyoscyamine, and the δ -amino group of ornithine is an

efficient precursor of the tropine nitrogen [21, 23]. The incorporation of glutamic acid and proline was considered to occur via ornithine [23].

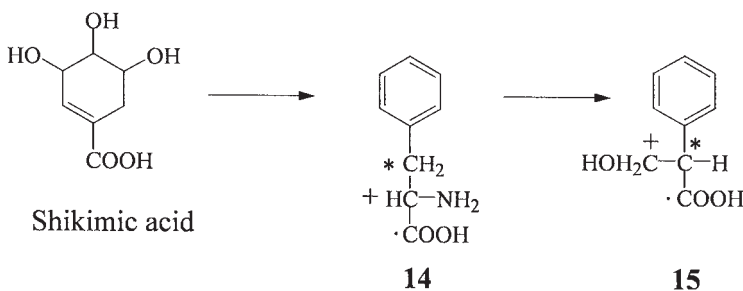
Ornithine (1) was incorporated into tropine via δ -*N*-methylornithine (2) [24–26], as [methyl- ^{14}C]- δ -*N*-methyl-[2- ^{14}C]-ornithine was incorporated into hyoscyamine labeling at C-1, and the *N*-methyl group. Compound (2) was decarboxylated to yield *N*-methylputrescine (4) [27, 28]. Putrescine (3) has been shown to be a precursor of the tropine alkaloids [20, 29–31]. It was suggested [23] that putrescine (3) is converted by some enzymes in *Datura* plants to *N*-methylputrescine (4). Oxidation of the primary alcohol of (4) affords 4-methylaminobutanol (5). This latter compound was cyclized to give *N*-methyl- Δ^1 -pyrrolinium salt (6).

Carbons 2, 3, and 4 of tropine are derived from acetate [32, 33], and it was assumed that the acetate is incorporated via acetoacetic acid or some suitable activated derivative such as coenzyme A ester [23]. Compound (6) was therefore condensed with acetoacetate to give hygrine- α -carboxylic acid (7). Decarboxylation of compound (7) afforded hygrine (8), which is an established precursor of tropine [33, 34]. Compound (8) was dehydrogenated to give dehydrohygrine (9). The latter compound was cyclized to yield tropinone (10). Stereospecific reduction of compound (10) yields tropine (11), and esterification of tropine (11) with tropic acid (12) gives atropine (14).

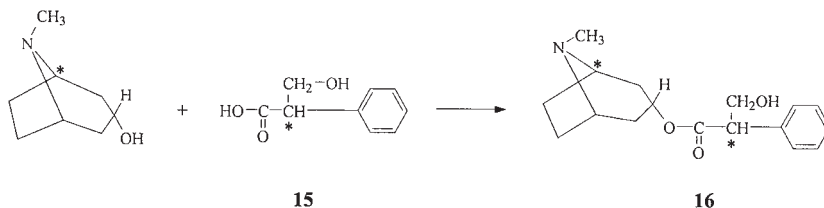


3.2 Biosynthesis of tropic acid

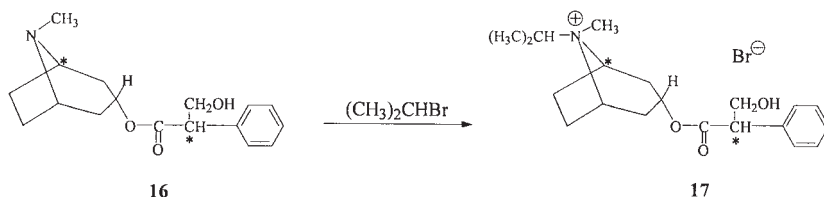
Tropic acid (**15**) is formed by the intramolecular rearrangement of phenylalanine (**14**) [35]. Compounds which are metabolically related to phenylalanine, such as phenylpyruvic acid, are also reported to be incorporated into tropic acid [36, 37].



Tropine (**11**) is then esterified with tropic acid (**15**) to give atropine (**16**).



And finally atropine (**16**) is quaternized with isopropyl bromide to give ipratropium bromide (**17**).



4. REFERENCES

1. A.A. Al-Badr and F.J. Muhtadi, "Atropine", in *Analytical Profiles of Drug Substances*, Volume 14, K. Florey, ed., pp. 325–389 (1985).

2. A. Landenburg, *Ber.*, **12**, 946 (1879); *Ann.*, **217**, 74 (1883).
3. R. Willstätter, *Ber.*, **29**, 936 (1896); *Ber.*, **31**, 1537 (1898); *Ber.*, **34**, 129, 3163 (1901); *Ann.*, **317**, 204, 267, 307 (1901); *Ann.*, **326**, 1, 23 (1903).
4. R. Robinson, *J. Chem. Soc.*, **111**, 762 (1917).
5. R. Willstätter and A. Pfannenstiel, *Ann.*, **422**, 1 (1921); R. Willstätter and M.B. Bommer, *Ann.*, **422**, 15 (1921).
6. Elming *et al.* (1958), through I.L. Finar *Organic Chemistry* Volume 2, 5th edn., Longmans, London, p. 726 (1975).
7. A. Landenburg and L. Rügheimer, *Ber.*, **13**, 2041 (1880); *Ber.*, **22**, 2590 (1889).
8. A. McKenzie and J.K. Wood, *J. Chem. Soc.*, **115**, 828 (1919).
9. E. Müller, *Ber.*, **51**, 252 (1918).
10. M.M. Chambon, *Compt. Rendu*, **186**, 1630 (1928).
11. Blicke *et al.* (1952), through I.L. Finar *Organic Chemistry* Volume 2, 5th edn., Longmans, London, p. 722 (1975).
12. G. Fodor, in *The Alkaloids, Chemistry and Physiology*, R.H.F. Manske, ed., Volume XIII, Academic Press, New York, p. 351 (1971).
13. W. Hespe, W.J.F. Klopper, and W.T. Nauta, *Rec. Trav. Chim.*, **84**, 476 (1965).
14. G.C. Schmidt, T.E. Eling, and J.M. McOwen *J. Pharm. Sci.*, **57**, 443 (1968).
15. G. Werner, H.L. Schmidt, and E. Kassner, *Ann.*, **644**, 109 (1961).
16. G.C. Schmidt, T.E. Eling, J.M. McOwen, and J.C. Drach, *J. Pharm. Sci.*, **56**, 1453 (1967).
17. E. Leete, *J. Am. Chem. Soc.*, **84**, 55 (1962).
18. E. Leete, *Tetrahedron Lett.*, 1619 (1964).
19. E. Leete, L. Marion, and I.D. Spenser, *Can. J. Chem.*, **32**, 1116 (1954).
20. H.W. Liebisch, H. Ramin, and J. Schoffinius, *Z. Naturforsch.*, **20b**, 1183 (1965).
21. H.W. Liebisch and H.R. Schutte, *Z. Pflanzenphysiol.*, **57**, 434 (1967).
22. N. Herbert, *Phytochem.*, **20**, 2064 (1981).
23. E. Leete, *Planta Medica*, **36**, 97 (1979).
24. A. Ahmad and E. Leete, *Phytochem.*, **9**, 2345 (1970).
25. F.E. Baralle and E.G. Gros, *Chem. Comm.*, **721**, (1969).
26. F.E. Baralle and E.G. Gros, *Anales Asoc. Quim. Argentina*, **58**, 299 (1970).
27. H.W. Liebisch, W. Maier, and H.R. Schutte, *Tetrahedron Lett.*, 4079 (1966).

28. H.W. Liebisch, A.S. Radwan, and H.R. Schutte, *Ann.*, **721**, 163 (1969).
29. J. Kaczkowski and L. Marion, *Can. J. Chem.*, **41**, 2651 (1963).
30. E. Leete and M.C.L. Loudon, *Chem. and Ind. (London)*, 1725 (1963).
31. H.W. Liebisch, H.R. Schutte, and K. Mothes, *Ann.*, **668**, 139 (1963).
32. J. Kaczkowski, H.R. Schutte, and K. Mothes, *Biochem. Biophys. Acta*, **46**, 588 (1961).
33. H.W. Liebisch, K. Peisker, A.S. Radwan, and H.R. Schutte, *Z. Pflanzepphysiol.*, **67**, 1 (1972).
34. D.G.O'Donovan and M.F. Keogh, *J. Chem. Soc. C*, 223 (1969).
35. E. Leete, N. Kowanko, and R.A. Newmark. *J. Am. Chem. Soc.* **97**, 6826 (1975).
36. W.C. Evans and J.G. Woolley, *Phytochem.* **15**, 287 (1976).
37. E. Leete and E.P. Kirven, *Phytochem.* **13**, 1501 (1974).

Ipratropium Bromide: Analytical Methods

Heba H. Abdine, F. Belal and Abdullah A. Al-Badr

Department of Pharmaceutical Chemistry

College of Pharmacy

King Saud University

P.O. Box 2457

Riyadh – 11451

Kingdom of Saudi Arabia

CONTENTS

1.	Compendial Methods of Analysis.	103
1.1	Identification methods for the drug substance.	103
1.1.1	Test A	103
1.1.2	Test B.	103
1.1.3	Test C	103
1.1.4	Test D	104
1.1.5	Test E.	104
1.2	Identification methods for formulated ipratropium bromide.	104
1.2.1	Test A	104
1.2.2	Test B.	105
1.3	Methods for impurities and related substances	106
1.3.1	8s Ipratropium	106
1.3.2	Apo-ipratropium	107
1.3.3	Thin-layer chromatography method.	107
1.4	Water	108
1.5	Sulfated ash.	108
1.6	Assay methods of analysis.	109
1.6.1	Potentiometry	109
1.6.2	Liquid chromatographic methods	109
1.6.2.1	Disposition of the emitted dose . . .	109
1.6.2.2	Pressurized inhalation formulations.	110
2.	Methods of Analysis Reported in the Literature	111
2.1	Titrimetric methods	111
2.1.1	Nonaqueous titration method.	111
2.1.2	Potentiometric method of analysis.	111
2.2	Spectrophotometric methods	111
2.3	Chromatographic methods of analysis	112
2.3.1	High-performance liquid chromatography . .	112
2.3.2	Capillary electrophoresis.	113
2.4	Radioreceptor assay methods	115
3.	References	115

1. COMPENDIAL METHODS OF ANALYSIS

1.1 Identification methods for the drug substance

The European Pharmacopoeia [1] recommends the following five tests for the identification of ipratropium bromide bulk drug substance.

1.1.1 Test A

Examine the test article by infrared absorption spectrophotometry, and compare with the spectrum obtained with an ipratropium bromide reference standard.

1.1.2 Test B

Examine by thin-layer chromatography, using a suitable silica gel as the coating substance on the TLC plate. The method requires preparation of the following solutions:

Test solution: Dissolve 5 mg of the test article in 1 mL of methanol.

Reference solution (a): Dissolve 10 mg of ipratropium bromide reference standard in 2 mL of methanol.

Reference solution (b): Dissolve 5 mg of methylatropine bromide reference standard in 1 mL of reference solution (a).

Apply separately to the plate 2 μ L of each solution, and develop over a bath of 10 cm using a mixture of 2.5 volumes of anhydrous formic acid, 7.5 volumes of water, 45 volumes of alcohol, and 45 volumes of methylene chloride. Allow the plate to dry in air, and spray with potassium iodobismuthate solution. The principal spot in the chromatogram obtained with the test solution is similar in position, color, and size to the principal spot in the chromatogram obtained with reference solution (a). The test is not valid unless the chromatogram obtained with reference solution (b) shows two clearly separated principal spots.

1.1.3 Test C

Dissolve 0.5 g of ipratropium bromide in carbon dioxide-free water, and dilute to 50 mL with the same solvent. To 5 mL of this solution, add 2 mL

of dilute sodium hydroxide solution. The test is positive if no precipitate is formed.

1.1.4 Test D

To about 1 mg of ipratropium bromide, add 0.2 mL of nitric acid and evaporate to dryness on a water bath. Dissolve the residue in 2 mL of acetone, and add 0.1 mL of a 30 g/L solution of potassium hydroxide in methanol. The test is positive if a violet color develops.

1.1.5 Test E

Ipratropium bromide gives the characteristic reaction of bromides.

1.2 Identification methods for formulated ipratropium bromide

The British Pharmacopoeia [2] describes the following two tests for the identification of ipratropium bromide in its pressurized inhalation formulations.

1.2.1 Test A

Identification is effected using a thin-layer chromatography method that uses high-performance silica gel precoated HPTLC plates (Merck Silica Gel 60), and a mobile phase consisting of a mixture of 5 volumes of water, 8 volumes of anhydrous formic acid, 28 volumes of methanol, and 70 volumes of dichloromethane. The method requires that one prepare the following solutions:

Solution-1: Punch a small hole in the ferrule of each three cooled containers, allow the propellant to evaporate for about 1 min, and transfer the content of the container (through the punched hole) to a beaker. Using a magnetic stirring device, stir for about 10 min, and then add 3.5 mL of 0.01 M hydrochloric acid. Continue stirring for about 1 h (until the propellant has completely evaporated), filter, and add 10 mL of chloroform to the filtrate. Shake vigorously for 1 min, and allow the phases to separate. Use the upper layer in preparation of Solution-2.

Solution 2: Dilute 1 volume of Solution-1 to 50 volumes with 0.01 M hydrochloric acid.

Solution 6: Contains 0.008% w/v of ipratropium bromide reference standard in 0.01 M hydrochloric acid.

The method requires that one apply separately to the plate 5 μ L of Solution-2 and Solution-6, and allow the system to develop so that the solvent front of the mobile phase ascends 6 cm above the line of application. The principal spot in the chromatogram obtained with Solution-2 corresponds to that in the chromatogram obtained with Solution-6.

1.2.2 Test B

Determine the content of ipratropium bromide delivered by the first ten successive combined actuations of the valve after priming. Remove the pressurized containers from the actuator, wash this with a mixture of equal volumes of 0.001 M hydrochloric acid and methanol, and dilute the combined solution and washings using 20 mL of the same solvent mixture in the vessel. Use the same solvent mixture to wash the pressurized container and to dilute the combined solution and washings obtained from the set of 10 combined actuations to 50 mL (this is solution-A). Determine the amount of ipratropium in the 10 combined actuations using the following liquid chromatography method of analysis, and the following two solutions:

Solution 1: Contains 0.00040% w/v of ipratropium bromide reference standard in a mixture of equal volumes of 0.001 M hydrochloric acid and methanol.

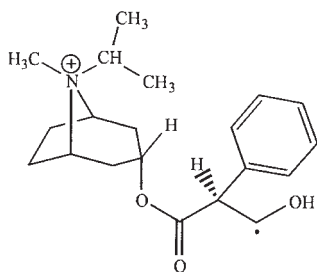
Solution 2: Use solution A.

The liquid chromatography system consists of a stainless steel column (12.5 cm \times 4 mm) packed with stationary phase B (Lichrosphere RP 8–B). The mobile phase consists of a mixture of 345 volumes of acetonitrile and 750 volumes of 0.012 M-sodium heptanesulfonate (previously adjusted to pH 3.2 with 0.05 M orthophosphoric acid), and is eluted at a flow rate of 2 mL/min. Detection is on the basis of the UV absorbance at 210 nm.

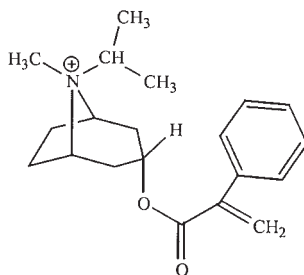
The chromatogram obtained with Solution-1 shows a peak with the same retention time as the peak due to authentic ipratropium bromide in the chromatogram obtained with Solution-2.

1.3 Methods for impurities and related substances

The European Pharmacopoeia [1] contains methods to determine the following two impurities in ipratropium bromide:



(8s) ipratropium



apo-ipratropium

1.3.1 *8s* Ipratropium

This related substance is determined by liquid chromatography, and the method requires preparation of the following three solutions:

Test Solution: Dissolve 25 mg of ipratropium bromide in the mobile phase (see below) and dilute to 100 mL with the mobile phase.

Reference Solution (a): Dissolve 25 mg of 8s-ipratropium bromide reference standard in 200 mL of the mobile phase (solution A). Dilute 1 mL of the solution to 100 mL with the mobile phase (see below).

Reference Solution (b): Mix 1 volume of the test solution and 2 volumes of solution A.

The chromatographic procedure is carried out using a stainless steel column (0.125 m in length, and 4 mm internal diameter) packed with octylsilyl silica gel for chromatography R (5 μ m particles). The mobile phase consists of 1 g of sodium methanesulfonate dissolved in a mixture of 120 mL of acetonitrile and 1000 mL of 0.05 M phosphoric acid, which is eluted at a flow rate of 2 mL/min. Detection is effected on the basis of the UV absorbance at 210 nm.

The procedure is to inject 20 μ L of each solution onto the chromatography system. Each chromatogram is run for twice the retention time of

the principal peak of the chromatogram obtained for the test solution. The test is not valid unless in the chromatogram obtained with Reference Solution (b), the resolution between the peaks corresponding to ipratropium and 8s-ipratropium is at least 1.5. Additionally, in the chromatogram obtained with the test solution, the symmetry factor of the principal peak is less than 2.2, and in the chromatogram obtained with Reference Solution (a) the signal-to-noise ratio of the principal peak is at least five.

In the chromatogram obtained with the test solution, the area of any peak corresponding to 8s-ipratropium is not greater than the area of the peak in the chromatogram obtained with Reference Solution (a) [*i.e.*, not more than 0.5%]. In addition, the area of any peak, apart from the principal peak and any peak corresponding to 8s-ipratropium, is not greater than half the area of the peak in the chromatogram obtained with Reference Solution (a) [*i.e.*, not more than 0.25%].

1.3.2 *Apo-ipratropium*

Dissolve 0.14 g of the test article in 0.01 M hydrochloric acid, and dilute to 100 mL with the same acid. Measure the absorbance of the resulting solution at 246 nm (A_{246}) and 263 nm (A_{263}). Calculate the percentage content of apo-ipratropium using the expression:

$$\left[\frac{A_{246}}{A_{263}} - 0.863 \right] \times 100$$

The test article may not contain more than 0.5% apo-ipratropium.

1.3.3 *Thin-layer chromatography method*

British Pharmacopoeia [2] recommends the following TLC procedure for the analysis of the related substances in the ipratropium bromide pressurized inhalation. Use high performance silica gel precoated plates, and a mixture of 5:8:28:70 water : anhydrous formic acid : methanol : dichloromethane as the mobile phase. Apply 5 μ L of each of the following six solutions separately to the plate.

Solution 1: Punch a small hole in the ferrule of each of the three cooled containers, allow the propellant to evaporate for about 1 min and transfer the content of the containers (through the punched hole) to a beaker. Using a magnetic stirrer, stir for about 10 min.

Then add 3.5 mL of 0.01 M hydrochloric acid and continue stirring for about 1 h (until the propellant has completely evaporated). After that, filter, add 10 mL of chloroform to the filtrate, and shake vigorously for 1 min. Allow the phases to separate, and use the upper layer in preparation of the following solutions:

Solution 2: Dilute 1 volume of Solution (1) to 50 volumes with 0.01 M hydrochloric acid.

Solution 3: Dilute 1 volume of Solution (2) to 4 volumes with 0.01 hydrochloric acid.

Solution 4: Dilute 2 volumes of Solution (3) to 5 volumes with 0.01 M hydrochloric acid.

Solution 5: Contains 0.008% w/v of 8s-isopropyl-3 β -hydroxytropanium bromide reference standard in 0.01 M hydrochloric acid.

Solution 6: Contains 0.008% w/v of ipratropium bromide reference standard in 0.01 M hydrochloric acid.

After removal of the plate, dry it in a current of warm air for about 30 min. Spray the plate with a mixture of 1 volume of potassium iodobismuthate solution, 2 volumes of glacial acetic acid, and 10 volumes of water. Allow to dry briefly, spray with a 5% w/v solution of sodium nitrite, and immediately examine the plate. In the chromatogram obtained with Solution (1), any spot corresponding to 8s-isopropyl-3 β -hydroxytropanium bromide is not more intense than the spot in the chromatogram obtained with Solution (2) [*i.e.*, not more than 2%]. Any other secondary spot is not more intense than the spot in the chromatogram obtained with Solution (3) [*i.e.*, not more than 0.5%], and not more than two such spots are more intense than the spot in the chromatogram obtained with Solution (4) [*i.e.*, not more than 0.2%].

1.4 Water

The permissible water content in a test article is 3.9–4.4%, when determined on a 0.5 g sample using the semimicro determination of water.

1.5 Sulfated ash

The permissible content is not more than 0.1%, when determined on a 1 g sample.

1.6 Assay methods of analysis

1.6.1 Potentiometry

The European Pharmacopoeia [1] recommends the following assay method. Dissolve 0.35 g of ipratropium bromide in 50 mL of water, and add 3 mL of dilute nitric acid. Titrate with 0.1 M silver nitrate, determining the end point potentiometrically. 1 mL of 0.1 M silver nitrate is equivalent to 41.24 mg of $C_{20}H_{30}BrNO_3$.

1.6.2 Liquid chromatographic methods

1.6.2.1 Disposition of the emitted dose

The British Pharmacopoeia [2] describes the following procedure for a liquid chromatographic method to be used in the analysis of the deposition of an emitted dose of ipratropium bromide in an ipratropium pressurized inhalation formulation. The method uses the described Apparatus A, with 7 mL of 0.001 M hydrochloric acid in the upper impingement chamber and 40 mL of a mixture of equal volumes of 0.001 M hydrochloric acid and methanol in the lower impingement chamber. Use of the following two solutions is also required:

Solution (1): Contains 0.00007% w/v of ipratropium bromide reference standard in a mixture of equal volumes of 0.001 M hydrochloric acid and methanol.

Solution (2): Use the diluted solution from the lower impingement chamber.

The liquid chromatography system consists of a stainless steel column (12.5 cm \times 4 mm) packed with stationary phase B (Lichrosphere RP8-B). The mobile phase consists of a 345 : 750 mixture of acetonitrile/0.012 M sodium heptanesulfonate (previously adjusted to pH 3.2 with 0.05 M orthophosphoric acid), and eluted at a flow rate of 2 mL/min. Detection is on the basis of the UV absorbance at 210 nm. The test is not valid unless in the chromatogram obtained with Solution (1), the symmetry factor of the peak due to ipratropium bromide is less than 3 and unless the signal-to-noise ratio of the peak is at least 3.

Calculate the amount of ipratropium bromide (as $C_{20}H_{30}BrNO_3 \cdot H_2O$), delivered to the lower impingement chamber per actuation of the valve using the declared content of $C_{20}H_{30}BrNO_3 \cdot H_2O$ in the ipratropium

bromide reference standard. Not less than 25% of the average amount of ipratropium bromide delivered per actuation of the valve, calculated as the average of the three results as determined in the Assay, is deposited in the lower impingement chamber.

1.6.2.2 Pressurized inhalation formulations

The British Pharmacopoeia [2] recommends a liquid chromatographic procedure for the analysis of ipratropium in ipratropium pressurized inhalation formulations. Determine the content of the active ingredient delivered by the first ten successive combined actuation of the valve after priming. Remove the pressurized container from the actuator, wash it using 20 mL of a mixture of equal volumes of 0.001 M-hydrochloric acid and methanol in the vessel. Use this mixture to wash the pressurized container, and to dilute the combined solution and washings obtained from the set of 10 combined actuations to 50 mL (Solution A). Determine the amount of the active ingredient in the 10 combined actuations using the following liquid chromatographic procedure of analysis. The method requires preparation of the following solutions:

Solution 1: Contains 0.00040% w/v of ipratropium bromide reference standard in a mixture of equal volumes of 0.001 M hydrochloric acid and methanol.

Solution 2: Solution A above.

The liquid chromatography system consists of a stainless steel column (12.5 cm \times 4 mm) packed with Lichrosphere RP8-B. The mobile phase is a mixture of 345 volumes of acetonitrile and 750 volumes of 0.012 M sodium heptanesulfonate (previously adjusted to pH 3.2 with 0.05 M orthophosphoric acid), eluted at a flow rate of 2 mL/min. Detection is effected at wavelength of 210 nm.

In the chromatogram obtained with Solution (1), long-eluting peaks due to excipients may appear. The test is not valid unless in the chromatogram obtained from Solution (1), the symmetry factor for the peak due to ipratropium bromide is less than 3. Calculate the average content of $C_{20}H_{30}BrNO_3 \cdot H_2O$ delivered by a single actuation of the valve using the declared content of $C_{20}H_{30}BrNO_3 \cdot H_2O$ in ipratropium bromide reference standard.

2. METHODS OF ANALYSIS REPORTED IN THE LITERATURE

2.1 Titrimetric methods

2.1.1 *Nonaqueous titration method*

Nakazawa and Tanaka reported the use of a nonaqueous titration method for determination of ipratropium bromide [5].

2.1.2 *Potentiometric method of analysis*

Ipratropium bromide has been determined by a potentiometric titration method against 0.01 M sodium tetraphenylborate, using NIO electrode as a working electrode and silver/silver chloride reference electrode [4].

2.2 Spectrophotometric methods

Hassan described three simple and sensitive spectrophotometric methods for the determination of ipratropium bromide in formulation liquids for nebulization [5]. The first method is based on the formation of a charge transfer complex with iodine. The reaction product was measured spectrophotometrically at 278 nm. The second method is based on the formation of an ion association complex between the drug and an acidic dye (bromocresol green), which is extractable into chloroform and has an absorption maximum at 418 nm. The third method uses derivative spectrophotometry for the determination of ipratropium bromide by measuring the D_2 value at 232 nm. Beer's law is obeyed over the concentration range 1–10, 2–16, and 5–30 $\mu\text{g/mL}$ for methods 1, 2, and 3 respectively. Mean percentage recoveries were found to be 99.67 ± 0.79 , 99.26 ± 1.06 , and 100.21 ± 0.85 for methods 1, 2, and 3 respectively.

Hassan also reported a sensitive and accurate method for the determination of ipratropium bromide in vials using a kinetic and first derivative spectrophotometric method [6]. The kinetic method is based on the alkaline oxidation of ipratropium bromide with potassium permanganate. After a fixed reaction time of 20 min, the formed manganate ion was measured at 608 nm, and the concentration of ipratropium bromide was calculated using a regression equation deduced for the fixed-time method. The determination of ipratropium bromide by first-concentration and rate constant methods is feasible through the use of regression equations, but the fixed-time method was found to be more applicable. The second method uses first-derivative

spectrophotometry for the determination of ipratropium bromide at 254–268 nm.

2.3 Chromatographic methods of analysis

2.3.1 High-performance liquid chromatography

Nayak *et al.* estimated ipratropium bromide in aerosols using an isocratic, reversed phase HPLC method [7]. An aerosol containing the bronchodilator was actuated 50 times in a vessel containing 50 mL of acetonitrile. The resulting solution was warmed at 50°C for 5 min, cooled, and diluted to 50 mL with acetonitrile. A 20 μ L portion of this solution was analyzed by isocratic reversed phase HPLC on a column (15 cm \times 4.6 mm) of Econosphere ODS (5 μ m), using a mobile phase of acetonitrile/sodium dihydrogen orthophosphate (0.05 M)/diethylamine (50:50:0.1, v/v) pH adjusted to 4.5 with phosphoric acid. The method used a flow rate of 1.0 mL/min, and the analytes were detected at 219 nm. Recoveries were in the range of 98–102% of ipratropium bromide from the aerosol, and fluoxetine hydrochloride (0.1 mg/mL) was used as an internal standard for quantification.

Jacobson and Peterson developed a reversed-phase ion-pair HPLC assay method for the simultaneous determination of ipratropium bromide combined with other bronchodilating drugs in nebulizer solutions [8]. Chromatographic separation was achieved with a Nova-Pak C₁₈ (4 μ m) (10 cm \times 8 mm i.d.), and a Radia-Pak cartridge inside a Waters RCM 8 \times 10 compression module, with detection being made at 220 nm. Ternary gradient elution (2 mL/min) was carried out starting with 50% of H₂O and 50% of aqueous 40% THF containing 2.5 mM-Pic B-8 reagent low UV (solvent A) up to 7.7 min, then changing linearly to 60% of A, 15% of H₂O and 25% of aqueous 50% methanol at 13 min. Linearity in the calibration curves was obtained over the range of 20.8–250 μ g/mL of ipratropium bromide.

Simms *et al.* described a HPLC method for the separation of ipratropium bromide and its related compounds [9]. An alltima C₁₈ column (25 cm \times 4.6 mm i.d., 5 μ m), operated at 35°C, was used in conjunction with an injection volume of 20 μ L. The mobile phase consisted of 100 mM KH₂PO₄/acetonitrile (4:1; mobile phase A) and (11:9; mobile phase B) and gradient elution. The method consisted of 100% A (held for 0–5 min) to 100% B (held for 8–13 min) in 5–8 min, and then to 100% A (held for 14–20 min) in 13–14 min. Flow rates of 1 mL/min were used for 0–14 min, and 2 mL/min for 14–20 min. Detection is made at 210 nm.

A linear response was obtained for 10–1000 $\mu\text{g/mL}$ of ipratropium bromide, with a detection limit of 60 ng/mL .

Hopfgartner *et al.* reported the use of a high flow ion-spray liquid chromatography–mass spectrometric method for the determination of ipratropium bromide [10]. A liquid shield device [11, 12] was used to protect the ion sampling orifice region, and was incorporated into an ion spray liquid chromatography–mass spectrometry system, coupled to a heated ion sampling capillary. The LC column effluent was passed at 2 mL/min through a fused silica capillary (4 in. \times 0.004 in. i.d), protruding from a stainless steel capillary housed in the ion-spray interface [13]. A voltage of 3–5 kV is applied to the effluent near the sprayer tip. Nitrogen was passed through the annular space between the inner and outer capillaries to afford pneumatic assistance. The system was applied for the LC–MS analysis of ipratropium bromide. The column (15 \times 4.6 mm) contained Zobrax SB-CN (5 μm particles), and used a mobile phase (1.2 mL/min) consisting of 4:1 acetonitrile/5 mM ammonium acetate. The detection limit was 250 pg for ipratropium bromide.

Greving *et al.* reported the use of a novel chromatographic method for monitoring ipratropium bromide and other quaternary ammonium compounds in biological fluids [14].

2.3.2 Capillary electrophoresis

Cherkaoui *et al.* described a validated capillary electrophoresis (CE) method for the determination of ipratropium bromide in pharmaceutical formulations [15]. The solubilized contents of tablets, suppositories, and aerosols in solution were injected for 10 s at 25 mbar into a fused-silica capillary (64.5 cm \times 50 μm i.d., 56 cm to detector), operated at an applied voltage of 30 kV. 80 mM-citrate buffer (pH 2.5) containing 2.5 mM-hydroxypropyl- β -cyclodextrin was used as the running buffer, and detection was effected at 191 nm. Calibration graphs were found to be linear from 50 to 150 $\mu\text{g/mL}$ for ipratropium bromide, with detection limit of 0.6 $\mu\text{g/mL}$.

Cherkaoui *et al.* also described a nonaqueous CE method for the separation and analysis of ipratropium and other tropine alkaloid in plant extracts [16]. The separation of alkaloids in the plant extracts was studied with the use of a nonaqueous capillary zone electrophoresis (CZE) and micellar electrokinetic capillary chromatography (MEKC), as previously described by Cherkaoui [17]. Synthetic mixed alkaloid

solutions in methanol were used, and a root extract was obtained by the method of Dupraz *et al.* [18]. The MEKC method was unable to separate ipratropium from atropine unless 20% methanol was added to the electrolyte, which increased the separation time to over 40 min. For the nonaqueous CZE method, a fused silica tube (64.5 cm \times 50 μ m i.d., 56 cm to detector) operated at an applied voltage of 25 kV was used with a buffer containing 1 M acetic acid and 25 mM ammonium acetate in acetonitrile–methanol. Electropherograms shown in the publication reveal partial separations with best results at 25% methanol content. Partial separation in 16 min of ipratropium and the other alkaloids was achieved with the use of a buffer consisting of 1 M-TFA and 25 mM ammonium acetate in acetonitrile.

Cherkaoui *et al.* also reported the use of a rapid method for the separation of ipratropium and other basic drugs by nonaqueous CE [19]. A high electric field was obtained by using short capillaries, and baseline separations of the basic drugs were achieved in 1 min by selection of the appropriate organic solvent and electrolyte composition. The method was therefore shown to be amenable toward high-throughput analysis. Peak efficiency up to 9154 theoretical plates/s was achieved in a separation performed at 923 V/cm. No discernible loss in resolution was observed when a conventional capillary of 64.5 cm was replaced by a short 32.5 cm capillary.

Koppenhoefer *et al.* reported the use of a CZE method for the enantioseparation of ipratropium and other 85 drugs using permethyl γ -cyclodextrin and a chiral solvating agent [20].

Tang *et al.* developed a capillary electrophoresis–mass spectrometry (CE–MS) method for the analysis of ipratropium bromide and other quaternary ammonium drugs in equine urine [21]. Drugs were first extracted from equine urine by ion-pair extraction, and then analyzed by CE–MS in the positive electrospray ionization (ESI) mode. Within 12 min, eight of the quaternary ammonium drugs (each at 1 ng/mL in horse urine) could be detected. The confirmation of the drug in urine samples was achieved by capillary electrophoresis tandem mass spectrometry (CE–MS/MS). A direct comparison of this method was made with the existing liquid chromatography–mass spectrometry (LC–MS) methods in the detection and confirmation of glycopyrrolate and ipratropium bromide in horse urine. The two drugs could be detected within the same CE–MS runs at 1 ng/mL in urine, but they could only be detected in separate LC–MS runs at 5 ng/mL in urine.

2.4 Radioreceptor assay methods

Ensinger *et al.* developed a radioreceptor assay method for the determination of ipratropium bromide in human plasma [22]. In this method, [^3H]-*N*-methylscopolamine was used as the radioligand to label the muscarinic cholinergic receptors in a membrane preparation of rat cerebral cortex. There was no interference with the parent compound due to cross-reactivity of three metabolites of ipratropium (5.2, 1.5, and 0.004%, respectively). The validity of the assay was verified between 20 pg/mL and 1000 pg/mL drug. In a pilot study, plasma levels following a single oral dose of 30 mg were determined to examine the applicability of the radioreceptor assay to clinical and pharmacokinetic studies, and for the measurement of plasma levels after therapeutic oral doses. The peak plasma concentration in three volunteers (322 pg/mL) occurred within 1–3 h.

Ensign *et al.* described a radioreceptor assay method for the analysis of ipratropium bromide in plasma and urine [23]. The method is based on competition between [^3H]-*N*-methylscopolamine chloride and ipratropium bromide for binding to lyophilized muscarinic receptors from calf brains. The assay has been optimized with respect to incubation conditions and extraction by ion-pair formation with sodium picrate. Detection limits for the drug were 5 ng/mL in urine and 500 pg/mL in plasma, after extraction of 2 mL of sample. The method is applicable to monitoring the drug in plasma and urine after therapeutic dosing.

3. REFERENCES

1. *European Pharmacopoeia*, 3rd edn. Supplement 13, Council of Europe, Strasbourg, p. 613 (2001).
2. *British Pharmacopoeia 1998*, Volume II, Her Majesty's Stationary Office, London, p. 740, 1761 (1998).
3. S. Nakazawa and K. Tanaka, *Bunseki Kagaku*, **27**, 100 (1978).
4. Anonymous, *Metrohm Application Bulletin*, **263**, 11 (2001).
5. E. Hassan, *Anal. Lett.*, **33**, 1531 (2000).
6. E. Hassan, *J. Pharm. Biomed. Anal.*, **21**, 1183 (2000).
7. V.G. Nayak, V.R. Bhate, S.N. Dhumal, V.R. Nerurkar, S.M. Purandare, P.M. Dikshit, and C.D. Gaitonde, *Drug Dev.-Ind. Pharm.*, **18**, 1681 (1992).
8. G.A. Jacobson and G.M. Peterson, *J. Pharm. Biomed. Anal.*, **12**, 825 (1994).

9. P.J. Simms, R.W. Towne, C.S. Gross, and R.E. Miller, *J. Pharm. Biomed. Anal.*, **17**, 841 (1998).
10. G. Hopfgartner, T. Wachs, K. Bean, and J. Henion, *Anal. Chem.*, **65**(4), 439 (1993).
11. K.L. Duffin, T. Wachs, and J.D. Henion, *Anal. Chem.*, **64**, 61 (1992).
12. V. Katta, S.K. Chowdhury, and B.T. Chait, *Anal. Chem.*, **63**, 174 (1991).
13. A.P. Bruins, T.R. Covey, and J.D. Henoin, *Anal. Chem.*, **59**, 2642 (1987).
14. J.E. Greving, J.H.G. Jonkman, H.G.M. Westenberg, and R.A. De-Zeeuw, *Pharm. Weekbl. Sci.*, **2**, 81 (1980).
15. S. Cherkaoui, L. Mateus, P. Christen, and J.L. Veuthey, *J. Pharm. Biomed. Anal.*, **17**, 1167 (1998).
16. S. Cherkaoui, L. Mateus, P. Christen, and J.L. Veuthey, *Chromatographia*, **49**, 54 (1999).
17. S. Cherkaoui, L. Mateus, P. Christen, and J.L. Veuthey, *Chromatographia*, **46**, 351 (1997).
18. Dupras *et al.*, *Planta Med.* **60**, 158 (1994).
19. S. Cherkaoui, L. Geiser, and J.L. Veuthey, *Chromatographia*, **53**, 401 (2000).
20. B. Koppenhoefer, A. Jakob, X.F. Zhu, and B.C. Lin, *J. High Resolut. Chromatogr.*, **23**, 413 (2000).
21. F.P. Tang, G.N. Leung, and T.S. Wan, *Electrophoresis*, **22**, 2201 (2001).
22. H.A. Ensinger, D. Wahl, and V. Brantl, *Eur. J. Clin. Pharmacol.*, **33**, 459 (1987).
23. K. Ensing, M. Pol, and R.A. De-Seeuw, *J. Pharm. Biomed. Anal.*, **6**, 433 (1988).

Ipratropium Bromide: Drug Metabolism and Pharmacokinetics

Heba H. Abdine, F. Belal and Abdullah A. Al-Badr

Department of Pharmaceutical Chemistry

College of Pharmacy

King Saud University

P.O. Box 2457

Riyadh – 11451

Kingdom of Saudi Arabia

CONTENTS

1. Uses, Applications, and Associated History. 118

2. Absorption and Bioavailability. 119

3. Metabolism. 119

4. Excretion 120

5. References 120

1. USES, APPLICATIONS, AND ASSOCIATED HISTORY

Ipratropium bromide is an *N*-isopropyl derivative of atropine which is used in the treatment of chronic obstructive lung diseases. The substance antagonizes the bronchi-constricting effect of acetylcholine released by stimulation of the vagus nerve. It can also antagonize vagal stimulation in other peripheral organs, which may cause considerable side effects, such as tachycardia and reduced salivation [1]. Ipratropium bromide is used by inhalation as a bronchodilator in the treatment of chronic reversible airway obstruction, and particularly in chronic bronchitis.

The drug has also been administered by inhalation as a nebulized solution. The usual dose is 20 or 40 µg (1 or 2 puffs of a metered-dose inhaler) three or four times daily by inhalation, although single doses of up to 80 µg have been required during the initial stages of the treatment. In children aged 6–12 years, the usual dose is 20 to 40 µg three times daily, and below 6 years the usual dose is 20 µg three times daily [1].

When inhaled, ipratropium bromide is an effective bronchodilating agent in patients with asthma, chronic bronchitis, or undifferentiated chronic obstructive airway disease [2–7]. The drug provides protection against both acetylcholine and methacholine-induced bronchoconstriction [2, 8–11], as well as adenosine [8] and water-induced bronchoconstriction [12]. Most likely, the drug produces bronchodilation by competitive inhibition of cholinergic receptors in bronchial smooth muscles by antagonizing the action of acetylcholine in its membrane-bound receptor site, thus blocking the bronchoconstrictor action of vagal efferent impulse [13]. The inhibition of the vagal tone results in dilation of the large central airways [2, 14–17] and small airways [2, 14, 18–21]. When the drug is applied directly to the nasal mucosa, it inhibits the secretions from the serous and seromucous gland [22]. Ipratropium has little or no effect on sputum viscosity, ciliary motility, or the rate of

mucociliary clearance [2, 23–27]. Long term use of ipratropium decreases sputum volume [28]. When the drug is combined with a β -adrenergic agonist or theophylline, the combination was found to enhance the bronchodilator effect. However, in clinical trials, this increased response has not always been statistically significant [2, 29–32].

2. ABSORPTION AND BIOAVAILABILITY

Ipratropium bromide is poorly absorbed from the gastrointestinal tract [1]. The bioavailability of the drug by inhalation is 0.03–6.9% [33, 34], and about 90% of the inhaled dose is swallowed [35]. Following the inhalation of 2 mg, the bioavailability was found to be 6.9% [33]. The bioavailability of the intranasal dose is less than 20% [22].

The bioavailability of the drug following oral administration was found to be 2% in one study involving healthy male volunteers [33]. The bioavailability was determined from the cumulative renal excretion (0–24 h) [2]. The drug does not cross into the cerebrospinal fluid [22], and very low or minimal amounts of drug was found in placenta [13].

3. METABOLISM

Ipratropium bromide, which is poorly absorbed from the gastrointestinal tract, has been reported to be partly metabolized following oral administration and to be excreted in the urine and feces as unchanged drug and metabolite. One of eight metabolites (out of six in very small amounts) was identified as *N*-isopropyl-methyl-nortropium bromide [1, 34]. None of the eight metabolites of ipratropium bromide have significant anticholinergic activity [13].

After administration of ipratropium bromide by mouth, intravenously, and by inhalation, the cumulative renal excretion was 9.3, 72.1, and 3.2%, respectively, and the fecal excretion was 88.5, 6.3, and 69.4%, respectively. The half-life of elimination from plasma was 3.2–3.8 h for all methods of administration. Comparison of results from oral administration and inhalation leads to the conclusion that the pharmacokinetics of inhaled ipratropium bromide is due to the swallowed portion of the dose [1, 34].

The metabolism of ipratropium bromide in the rat is shown in Figure 1 [36].

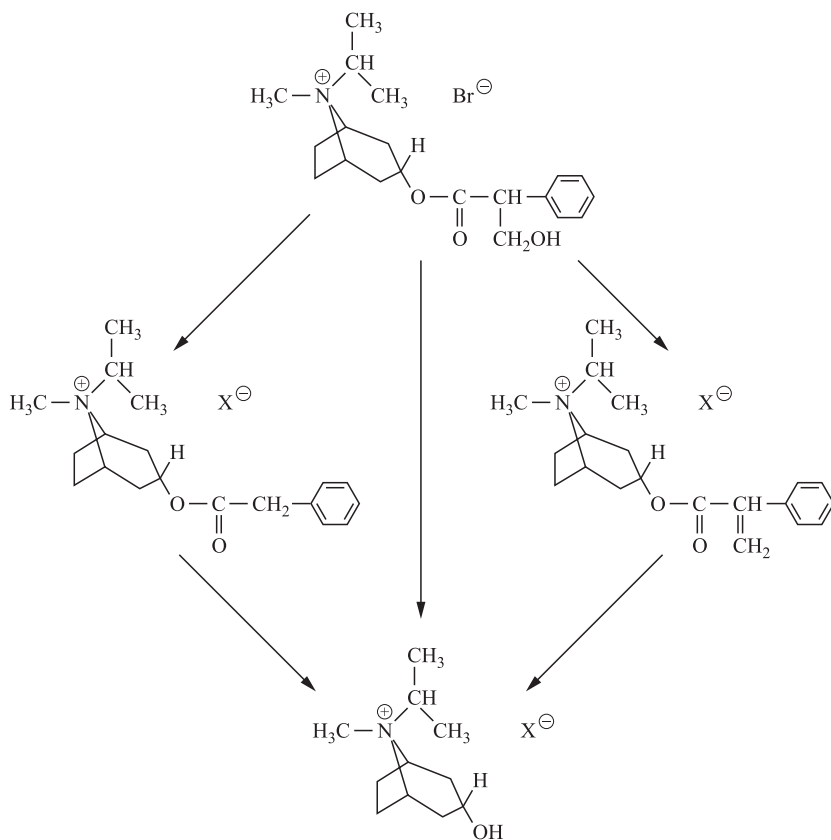


Figure 1. Metabolism of ipratropium bromide in the rat.

4. EXCRETION

Insignificant amounts of ipratropium are expected to be excreted into breast milk, since ipratropium is a lipid-insoluble quaternary base and is poorly absorbed following inhalation [13, 22]. 2.8% of the drug is excreted through the kidneys [34], and 48% was found to be excreted through the feces [22]. The elimination half-life of the drug was 2–3.8 h [22, 34].

5. REFERENCES

1. *Martindale, The Extra Pharmacopoeia*, 29th edn., K. Parfitt, ed., The Pharmaceutical Press, London (1999).

2. Drugdex Drug Evaluations, Micromedex, Healthcare Series, Volume 116, Expires 6/2003.
3. G. Kaik, *Wien Klin. Wochenschr*, **87**, 653 (1975).
4. H. Feldner, *Wien Med. Wochenschr*, **126**, 332 (1976).
5. W.T. Ulmer, J. Dorsch, J. Irvani, *et al.*, *Arzneimittelforschung*, **23**, 468 (1973).
6. T. Vlagopoulos, R.G. Townley, S. Ghazanshahi, *et al.*, *Ann. Allergy*, **36**, 223 (1976).
7. H. Yeager, R.M. Weinberg, L.V. Kaufman, *et al.*, *J. Clin. Pharmacol.*, **16**, 198 (1976).
8. N. Crimi, F. Palermo, R. Oliveri, *et al.*, *Eur. Respir. J.*, **5**, 560 (1992).
9. D. Nottle, *Postgrad. Med. J.*, **51** (suppl), 103 (1975).
10. B. Gamain, *Postgrad. Med. J.*, **51** (suppl), 102 (1975).
11. H.M. Beumer, *Postgrad. Med. J.*, **51** (suppl), 101 (1975).
12. C.M.E. Tranfa, *Eur. Respir. J.*, **8**, 600 (1995).
13. G.E. Pakes, R.N. Brogden, R.C. Heel, *et al.*, *Drugs*, **20**, 237 (1980).
14. N.J. Douglas, I. Davidson, and M.F. Sudlow, *Thorax*, **34**, 51 (1979).
15. R. Pistilli, F. Potalaro, S.M. Liberator, *et al.*, *Eur. J. Respir. Dis.*, **64**, 499 (1983).
16. W.W. Storms, G.A. DoPico, and C.E. Reed, *Am. Rev. Respir. Dis.*, **111**, 419 (1975).
17. E. Firstater, E. Mizrochi, and M. Topilsky, *Ann., Allergy*, **79**, 332 (1981).
18. N.J. Douglas, M.F. Sudlow, and D.C. Flenley, *J. Appl. Physiol.*, **46**, 256 (1979).
19. N.J. Gross, *Am. Rev. Respir. Dis.*, **112**, 823 (1975).
20. M.R. Partridge and K.B. Saunders, *Thorax*, **36**, 530 (1981).
21. B. Frith, P.D. Thomas and R.D. McEvoy, *Aust. N.Z.J. Med.*, **12**, 686 (1982).
22. Product Information: Atrovent[®], Ipratropium bromide. Boehringer Ingelheim, Ridgefield, C.T. 1996.
23. E. Krieger and U. Reitberger, *Postgrad. Med. J.*, **51**, 108 (1975).
24. D. Pavia, J. Roderich, and M. Bateman, *Thorax*, **34**, 501 (1979).
25. A. Monetti, *Postgrad. Med. J.*, **51**, 153 (1975).
26. J.A. Bell, B.M. Bluestein, I. Danta, *et al.*, *Mt Sinai J. Med.*, **51**, 215 (1984).
27. A. Wanner, *Am. J. Med.*, **81**, 23 (1986).
28. M.A. Ghafouri, K.D. Patil, and I. Kass, *Chest*, **86**, 387 (1984).

29. G.R. Petrie and K.N.V. Palmer, *Postgrad. Med. J.*, **51** (suppl), 117 (1975).
30. R.E. Ruffin, G.D. Fitzgerald, and A.S. Rebuck, *J. Allergy Clin. Immunol.*, **59**, 136 (1977).
31. M.J. Ward, P.H. Fentem, and W.H.R. Smith, *Br. Med.*, **282**, 598 (1981).
32. K.L. Massey and V.P. Gotz, *Drug Intell. Clin. Pharm.*, **19**, 5 (1985).
33. K. Ensing, M. Pol, and R.A. De-Zeeuw, *J. Pharm. Biomed. Anal.*, **6**, 433 (1988).
34. J. Adlung, K.D. Höhle, S. Zeren, and D. Wahl, *Arzneim. Forsch. (Drug Res.)*, **26**, 1005 (1976).
35. D.S. Davies, *Postgrad. Med. J.*, **51**, 69 (1975).
36. H.J. Förster, I. Kramer, K.H. Pook, and D. Wahi, *Arzneim.-Forsch. (Drug Res.)*, **26**, 992 (1976).

Ornidazole: Comprehensive Profile

Paramjeet Singh, Rohit Mittal, G.C. Sharma,
Sukhjeet Singh and Amarjit Singh*

*Research & Development Centre
Panacea Biotec Ltd.
P.O. Lalru 140 501
Punjab, India*

*Author for correspondence

PROFILES OF DRUG SUBSTANCES,
EXCIPIENTS, AND RELATED
METHODOLOGY – VOLUME 30
DOI: 10.1016/S0099-5428(03)30007-3

123

Copyright © 2003 Elsevier Inc.
All rights reserved

CONTENTS

1.	Description	125
1.1	Nomenclature	125
1.1.1	Systematic chemical names	125
1.1.2	Nonproprietary names	125
1.1.3	Proprietary names	125
1.2	Formulae.	126
1.2.1	Empirical formula, molecular weight, CAS number	126
1.2.2	Structural formula	126
1.3	Elemental analysis	126
1.4	Appearance	126
1.5	Uses and applications	126
2.	Methods of Preparation	127
3.	Physical Properties	128
3.1	Ionization constants	128
3.2	Partition coefficient.	128
3.3	Solubility characteristics	129
3.4	Hygroscopicity.	130
3.5	Optical activity	130
3.6	Particle morphology	131
3.7	Crystallographic properties	133
3.7.1	Single crystal structure	133
3.7.2	X-ray powder diffraction pattern.	133
3.8	Thermal methods of analysis.	135
3.8.1	Melting behavior	135
3.8.2	Differential scanning calorimetry.	136
3.8.3	Thermogravimetric analysis	139
3.9	Spectroscopy	140
3.9.1	UV–VIS spectroscopy	140
3.9.2	Vibrational spectroscopy	140
3.9.3	Nuclear magnetic resonance spectrometry	140
3.9.3.1	¹ H-NMR spectrum.	140
3.9.3.2	¹³ C-NMR spectrum	141
3.10	Mass spectrometry	142
4.	Methods of Analysis	143
4.1	Identification	143
4.1.1	Infrared spectrum	143
4.1.2	Ultraviolet absorption	143
4.1.3	High-performance liquid chromatography	143

4.2	Titrimetric analysis.	143
4.3	Electrochemical analysis	148
4.3.1	Polarography.	152
4.3.2	Voltammetry	153
4.4	Spectroscopic analysis.	154
4.4.1	Spectrophotometry.	154
4.4.2	Colorimetry.	155
4.4.3	Nuclear magnetic resonance	157
4.5	Chromatographic methods of analysis	157
4.5.1	Thin-layer chromatography	157
4.5.2	Gas chromatography	158
4.5.3	High-performance liquid chromatography	158
4.5.3.1	HPLC determination in pharmaceutical products	158
4.5.3.2	HPLC determination in biological matrices.	160
4.5.4	Capillary electrophoresis.	160
5.	Stability	160
5.1	Solution-phase stability.	160
5.2	Photolytic stability	164
6.	Drug Metabolism and Pharmacokinetics	165
6.1	Absorption, distribution, and excretion	165
6.2	Metabolism	167
7.	Toxicity	167
8.	Pharmacology	169
9.	Pharmaceutics	170
10.	References	173

1. DESCRIPTION

1.1 Nomenclature

1.1.1 Systematic chemical names

1-(3-chloro-2-hydroxypropyl)-2-methyl-5-nitroimidazole [1]

1-Chloro-3-(2-methyl-5-nitroimidazol-1-yl)propan-2-ol [2]

α -(Chloromethyl)-2-methyl-5-nitro-1*H*-imidazole-1-ethanol [1, 3]

1.1.2 Nonproprietary names [1–3]

Ornidazole

1.1.3 Proprietary names [1–3]

Avrozor, Betiral, Biteral, Danubial, Giro, Kolpicid, Madelen, Ornidal, Ro-7-0207, Tibal, Tiberol, Tinerol

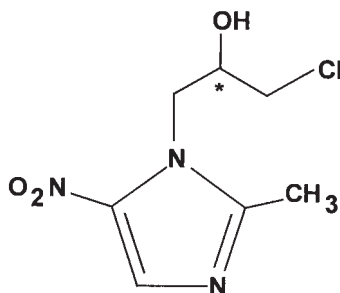
1.2 Formulae

1.2.1 Empirical formula, molecular weight, CAS number

$C_7H_{10}ClN_3O_3$ [MW = 219.625]

CAS number = 16773-42-5

1.2.2 Structural formula



1.3 Elemental analysis

The calculated elemental composition is as follows [1]:

carbon:	38.28%
hydrogen:	4.59%
chlorine:	16.14%
nitrogen:	19.13%
oxygen:	21.85%

1.4 Appearance

Ornidazole is a white to light yellow, practically odorless, crystalline powder.

1.5 Uses and applications

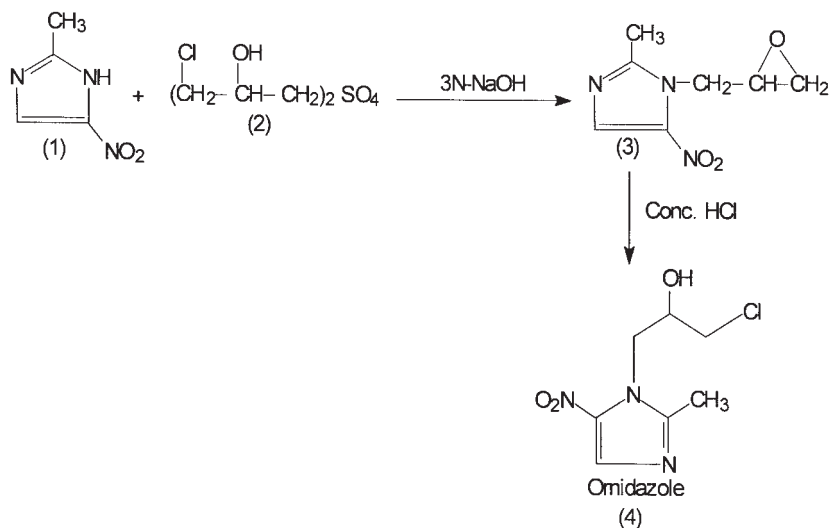
Ornidazole has antiprotozoal and antibacterial properties against anaerobic bacteria. The antimicrobial activity of this compound is due to reduction of the nitro group to a more reactive amine group that attacks microbial DNA, inhibiting further synthesis, and leading to degradation of existing DNA [4].

Ornidazole is also used in the treatment of severe hepatic and intestinal amoebiasis, giardiasis, and trichomoniasis of the uro-genital tract and

bacterial vaginosis. It is also used in the treatment and prophylaxis of susceptible anaerobic infections in dental and gastrointestinal surgery. In combination with other drugs, ornidazole is also advocated in the management of *Helicobacter pylori* duodenal ulcers.

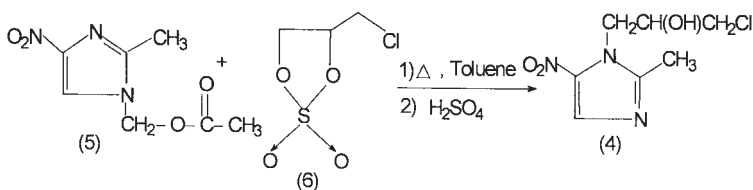
2. METHODS OF PREPARATION

Ornidazole was synthesized by Hoffmann-La-Roche in 1966 [5], and the general outline of their method is shown below. The synthesis involves heating of 2-methyl-4(or 5)-nitro-imidazole (1) with bis(3-chloro-2-hydroxypropyl)sulfate (2) for 3 h at 125–135°C, and subsequent extraction with dichloromethane in 3N NaOH to give 1-(2,3-epoxypropyl)-2-methyl-5-nitroimidazole (3). Further chlorination results when compound (3) reacts with hydrochloric acid, yielding ornidazole (4).

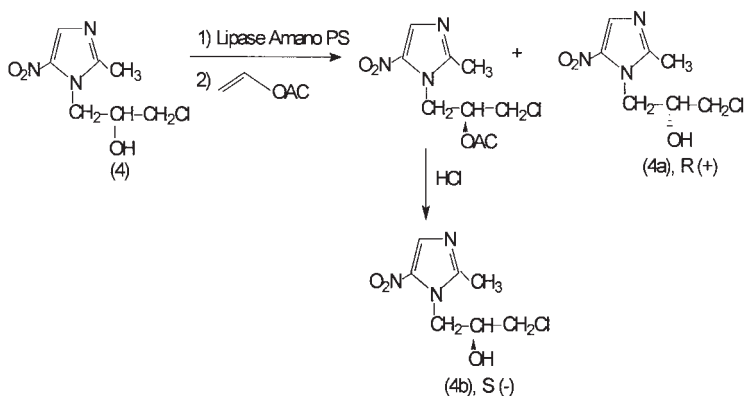


Alternate methods have been reported in the literature where treatment of 2-methyl-4(or 5)-nitroimidazole with epichlorohydrin in formic acid [6], H_2SO_4 [7, 8] or in presence of a Lewis acid [9–11] gives ornidazole in moderate yields.

The following scheme describes another method [12], where a mixture of 1-acetoxy-2-methyl-4-nitroimidazole (5) and sulfate of chloro-3-propanediol-1,2 (6) is heated, and then hydrolyzed to give ornidazole in 90% yield.



Ornidazole is a racemic chlorohydrin with the halogen in the terminal position. The resolution of its enantiomers [13] has been achieved by acetylation of the racemic compound with vinyl acetate in the presence of lipase amano PS, which on column chromatography provides the (*S*)-acetate and the (*R*)-alcohol (**4a**). Deacetylation of the (*S*)-acetate yields (*S*)-(-) ornidazole (**4b**):



3. PHYSICAL PROPERTIES

3.1 Ionization constants

Ornidazole is characterized by a single ionization constant, for which the pK_a is approximately 2.4 [1, 6, 7].

Using the ACD PhysChem predictive program (Version 6.0), a pK_a of 2.72 ± 0.35 was calculated for the hydroxy group of the chlorohydrin sidechain. The program further predicts the existence of charged species at pH values less than 3 and greater than 13.

3.2 Partition coefficient

The octanol–water partition coefficient of ornidazole is 4.8, corresponding to log P value of 0.618124 [14, 15]. This demonstrates the drug

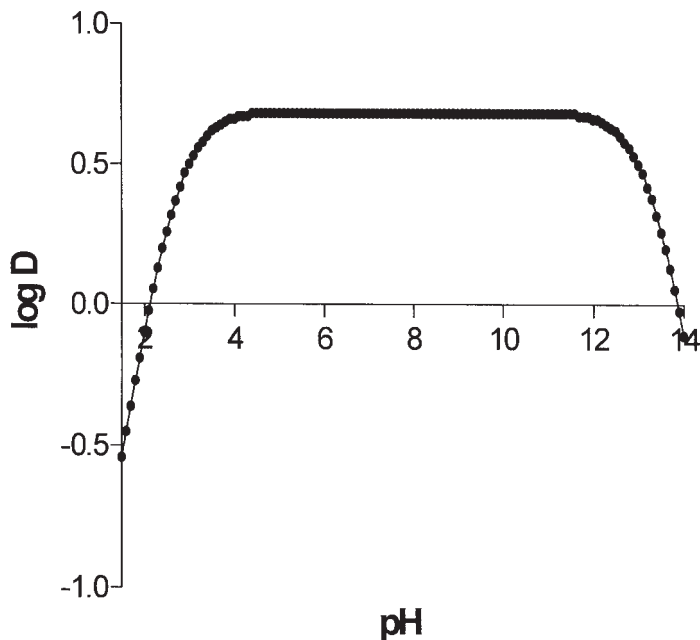


Figure 1. Calculated pH dependence of the distribution coefficient of ornidazole.

substance should exhibit some hydrophilic character at neutral pH values.

Using the ACD PhysChem predictive program (Version 6.0), the pH dependence of the distribution coefficient was calculated. As shown in [Figure 1](#), the compound is predicted to be very hydrophilic below pH 3 and above pH 13, and moderately hydrophilic over the pH range of 3–13.

3.3 Solubility characteristics

Ornidazole is practically insoluble in nonpolar solvents but its solubility is very high in moderately polar and highly polar solvents [14]. A selection of solubility data is provided in [Table 1](#).

Using the ACD PhysChem predictive program (Version 6.0), the pH dependence of the aqueous solubility was calculated. As shown in [Figure 2](#), the compound is predicted to be very soluble below pH 3 and above pH 13, and moderately soluble over the pH range of 3–13.

Table 1

Solubility Characteristics of Ornidazole

Solvent system	Solubility (mg/mL)
Hexane	0.0155
Toluene	9.85
Dichloromethane	431.99
Ethyl Acetate	296.14
Acetone	610.4
Ethanol (95%)	708.82
Methanol	627.58
Acetonitrile	662.5
Water	17.312

3.4 Hygroscopicity

When exposed to relative humidities ranging from 60 to 70% (at an equilibrium temperature ranging from 25 to 40°C), ornidazole did not exhibit any measurable moisture pick-up in over seven days. The compound is therefore determined to be nonhygroscopic [14].

3.5 Optical activity

Although ornidazole contains one center of dissymmetry, only the racemic form of the compound has been commercialized. The racemic nature of the commercial product was confirmed by measuring the specific rotation in dichloromethane (sodium D line at 589 nm, 100-mm cell) using a polarimeter manufactured by Advance Research Instruments Co., India. The measured optical rotation obtained was zero at a solute concentration of 1 g/100 mL.

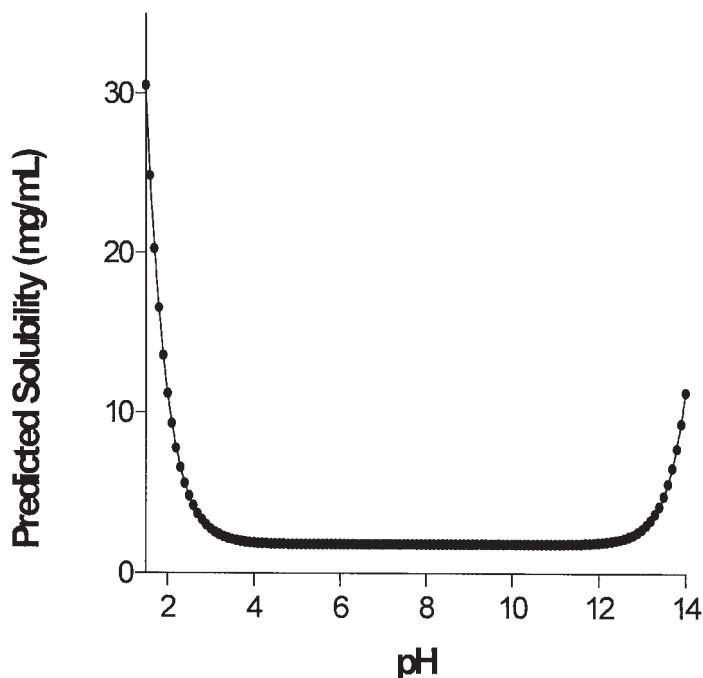


Figure 2. Calculated pH dependence of the aqueous solubility of ornidazole.

Resolution of both enantiomers of ornidazole using lipase catalysis has been used to determine the absolute configuration of two compounds by X-ray crystallography [13]. It was reported that the (*R*)-form exhibited a specific rotation of $[\alpha]_{\text{D}}^{20} = +65.5^\circ$ ($C = 1.0$, CH_2Cl_2), 98% ee ($^1\text{H-NMR}$), and that the (*S*)-form exhibited a specific rotation of $[\alpha]_{\text{D}}^{20} = -67.8^\circ$ ($C = 0.99$, CH_2Cl_2), greater than 98% ee ($^1\text{H-NMR}$).

3.6 Particle morphology

A commercial sample of ornidazole was recrystallized from toluene, which yielded light yellow crystals [14]. The sample was evaluated using electron microscopy, with the data being obtained on a JEOL JSM-6100 system [14]. As evident in the representative photomicrographs shown in Figure 3, the majority of the crystals exhibited a rectangular, thick plate-like morphology. Most of the crystals were found to be approximately 0.5–2.0 mm in length, and 0.08–0.6 mm in width.

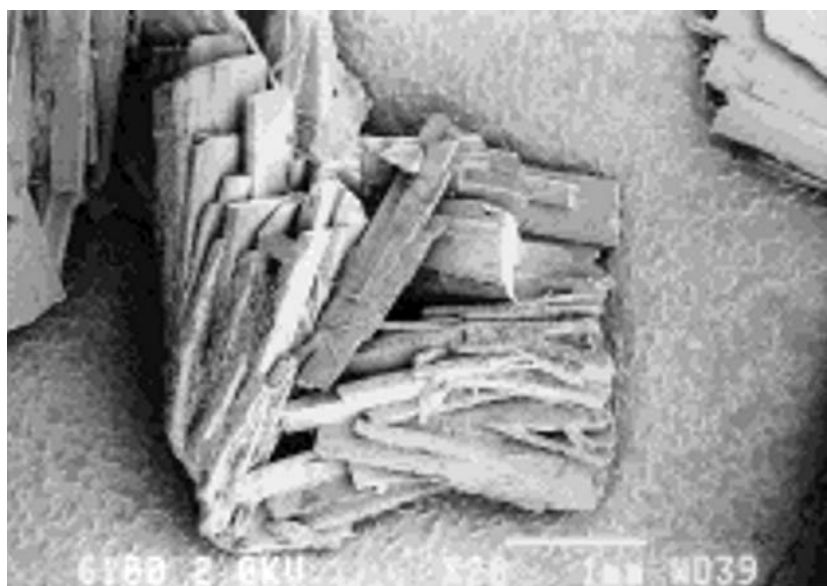
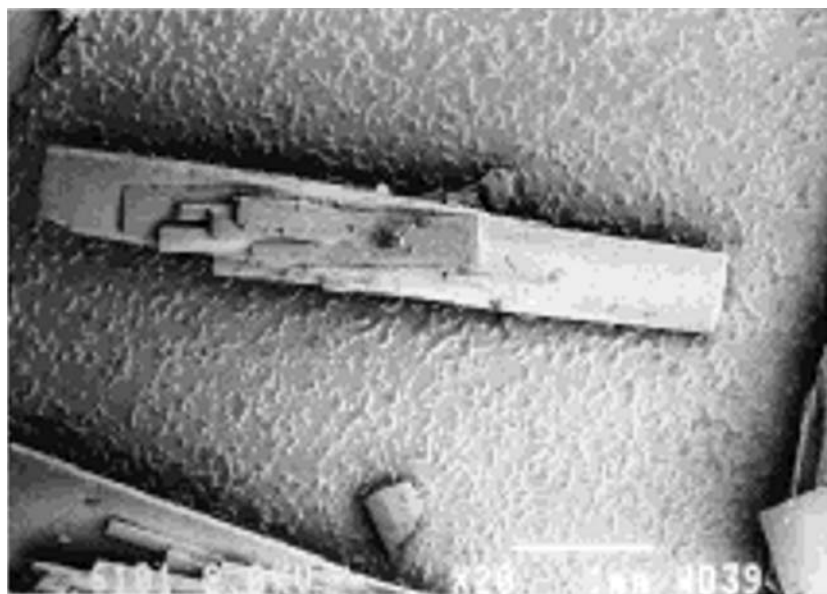


Figure 3. Photomicrographs obtained at a magnification of 20X of ornidazole recrystallized from a commercial sample.

3.7 Crystallographic properties

3.7.1 Single crystal structure

Crystallographic data for racemic ornidazole have been reported [16], with the compound crystallizing in the triclinic space group P1. The reported unit cell parameters were:

$$a = 13.605 \text{ (2)}$$

$$b = 14.054 \text{ (1)}$$

$$c = 8.913 \text{ (5)}$$

$$\alpha = 71.59 \text{ (2)}$$

$$\beta = 78.73 \text{ (2)}$$

$$\gamma = 64.86 \text{ (1)}$$

$$Z = 6$$

$$\text{Calculated density} = 1.499 \text{ g/mL}$$

$$\text{Measured density} = 1.497 \text{ g/mL}$$

The structure was solved by direct methods, and refined by block-diagonal least squares to a final R of 0.081 ($R_w = 0.047$) for 1952 reflection with $F_o > 3\sigma(F_o)$. The asymmetric unit contains three independent molecules of the title compound, and the bond lengths and bond angles are comparable with values found in other nitro-substitute compounds. The crystal structure is linked by two intermolecular hydrogen bonds (O–H \cdots N type) and one intermolecular hydrogen bond (O–H \cdots O type). The molecular structures (with an atomic numbering scheme), and the crystal packing diagram obtained for this structural form of ornidazole, are shown in Figures 4 and 5, respectively.

Crystallographic data for the (*R*)-(+)-enantiomer of ornidazole have also been reported in the literature [13]. The molecular confirmation of the compound in this structure is shown in Figure 6.

3.7.2 X-ray powder diffraction pattern

The X-ray powder diffraction pattern of ornidazole was obtained using a Shimadzu 6000 X-ray diffractometer system [14]. The radiation source was a copper ($\lambda = 1.54060 \text{ \AA}$) high intensity X-ray tube, operated at 40 kV and 30 mA.

Ornidazole was found to exhibit a strong and characteristic X-ray powder diffraction pattern, showing the crystalline nature of the powder. The powder pattern is given in Figure 7, and Table 2 provides a summary of scattering angles, d -spacings, and relative intensities. The observed

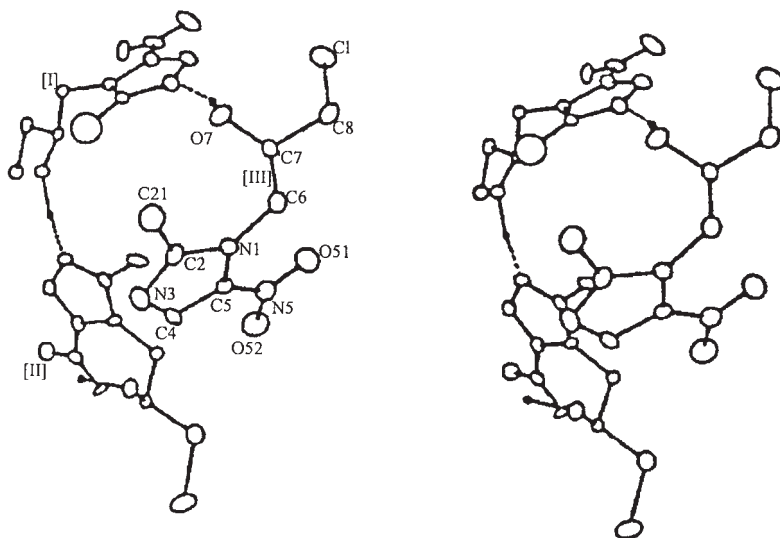


Figure 4. Stereoscopic drawing of the molecular structure of ornidazole. The hydrogen bonding is illustrated using dotted connection lines.

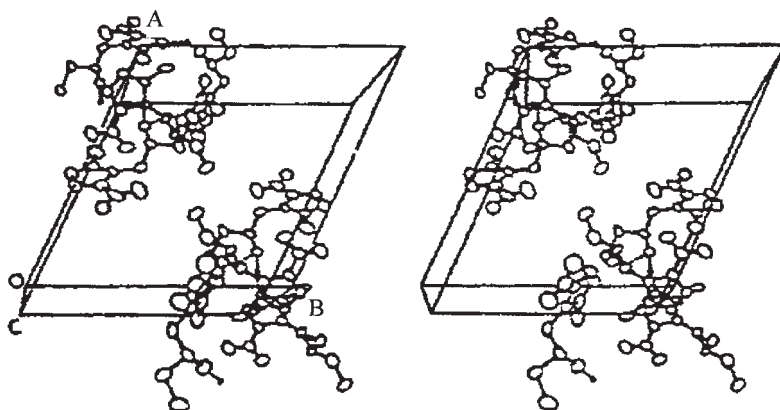


Figure 5. Stereoscopic drawing of the crystal packing of ornidazole, with dotted lines indicating the intermolecular hydrogen bonding.

scattering peaks were able to be indexed using the cell parameters of the published crystal structure [16], indicating that the crystal form of the powder pattern is the same as that of the published single crystal structure.

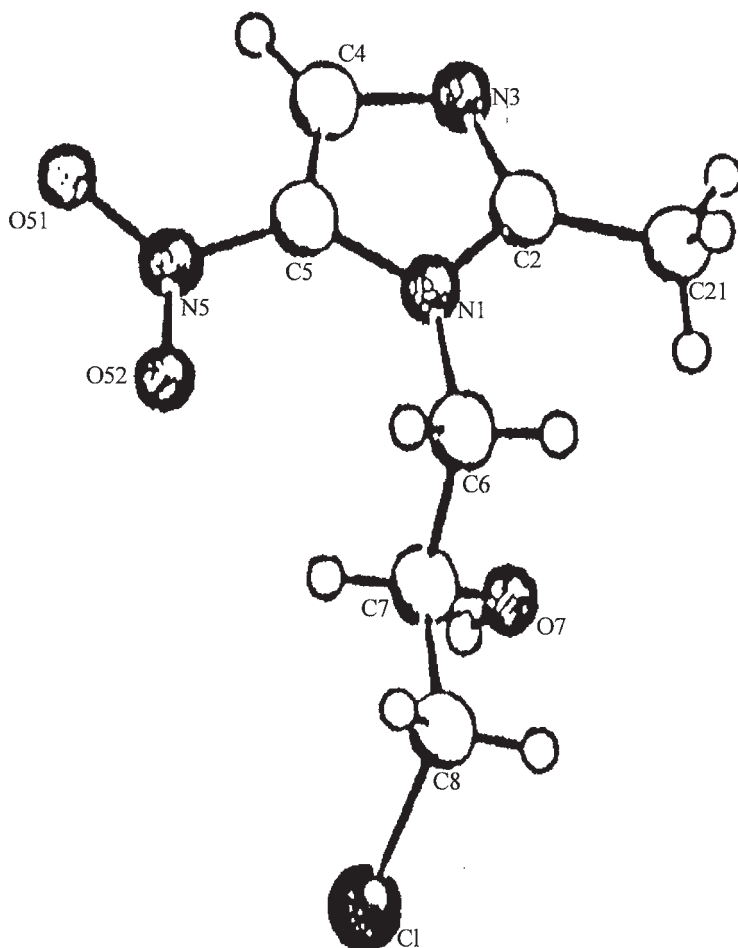


Figure 6. Molecular conformation of (*R*)-(+)-ornidazole.

Since the powder pattern is dominated by the intense scattering peaks located at 13.27 , 20.05 , and $20.88^{\circ}2\theta$, these would be considered as being characteristic for identification purposes.

3.8 Thermal methods of analysis

3.8.1 Melting behavior

The melting range of the ornidazole sample studied in the present work was found to be $89\text{--}91^{\circ}\text{C}$, and the substance appeared to melt without decomposition [14].

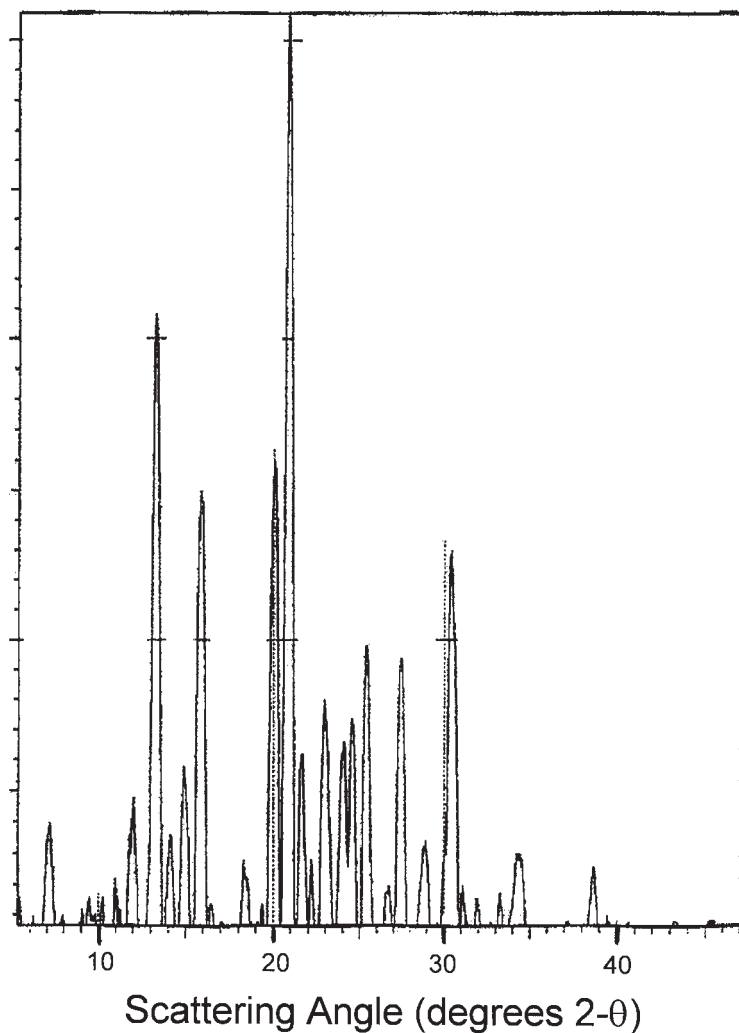


Figure 7. X-ray powder diffraction pattern of ornidazole.

Other reported values in the literature for the melting range are 77–78°C [1, 3, 5–7, 17] and 90–92°C [13, 18].

3.8.2 Differential scanning calorimetry

The DSC thermogram of ornidazole was obtained using a model DSC821 Mettler-Toledo system, which was calibrated using 99.999% indium [14].

Table 2

Crystallographic Parameters Derived from the X-Ray Powder Diffraction Pattern of Ornidazole, Indexed According to the Published Crystal Structure [16]

Scattering angle ($^{\circ}2\theta$)	<i>d</i> -Spacing (\AA)	Miller indices of the scattered peaks	Relative intensity, I/I_0 (%)
7.1375	12.37506	101; 010	13
11.0562	7.99615	011; 111	9
11.9600	7.39384	1–10; 101	16
13.2791	6.66218	210; 120	69
14.1425	6.25733	121; 0–11	12
14.9739	5.91173	–1–11; –111; 211	19
15.8720	5.57918	021; 220	49
18.4100	4.81536	–201; 2–10; 1–20	10
20.0507	4.42488	0–21; 310; 130; 231; 112	52
20.8800	4.25097	321; 320; 230; –211; 311; 122	100
21.6450	4.10242	031; –2–21; 300; 030; 2–11; 102	21
22.1975	4.00155	022; 222; 212	10

(continued)

Table 2 (continued)

Scattering angle ($^{\circ}2\theta$)	<i>d</i> -Spacing (\AA)	Miller indices of the scattered peaks	Relative intensity, I/I_0 (%)
22.9637	3.86974	1-21; -112; 331	27
24.0537	3.69679	330; 0-12; 2-20; 132; -3-11	22
24.5750	3.61954	-1-12; 202; -301	25
25.3903	3.50513	-1-31; 3-10; 1-30; 1-12; -131; -122; 241	33
27.4275	3.24923	2-12; -311; -212; 2-21; 411	30
28.8575	3.09139	142; 400; 040	11
30.4670	2.93165	-222; 113; 422; 4-11; 3-20; 1-22; 2-30	42
34.3400	2.60935	0-32; 4-11; -2-32; -411; 0-13	11
38.6225	2.32930	0-23; -421; -1-23; 3-22	10

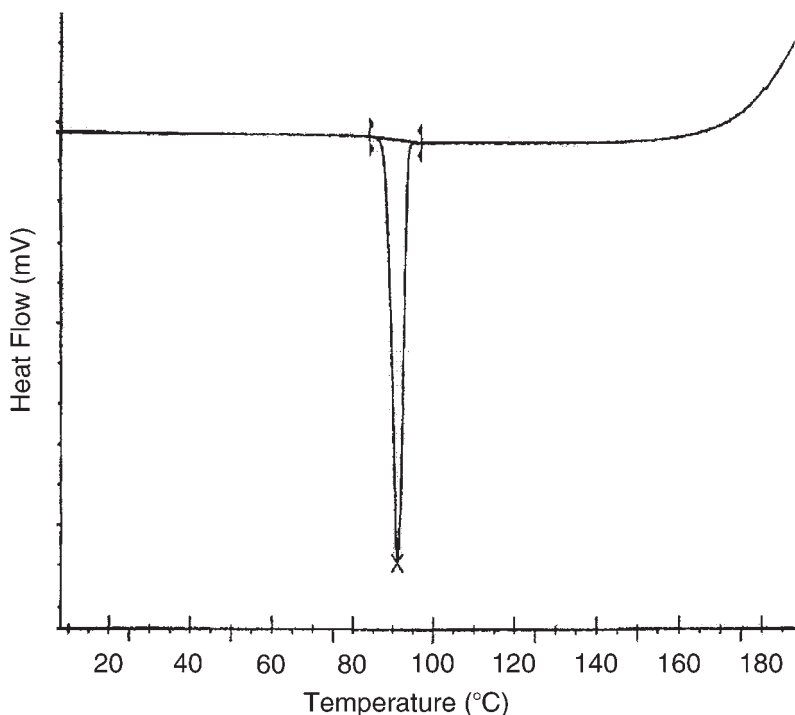


Figure 8. Differential scanning calorimetry thermogram of ornidazole.

The thermogram shown in Figure 8 was obtained using a heating rate at 5°C/min, under an atmosphere of nitrogen.

The DSC thermogram consisted of a single sharp endotherm, having an onset of 88.4°C, a maximum at 90.1°C, and a return to baseline at 93.7°C. The endotherm is assigned to the melting of the compound, and is characterized by an enthalpy of fusion equal to 835 J/g (183.3 kJ/mol). The quality of the thermogram indicates that DSC could be used as one of the techniques to determine the purity of ornidazole.

3.8.3 Thermogravimetric analysis

As an anhydrous material, ornidazole exhibit no loss in weight until heated beyond the temperature of its thermal decomposition (approximately 190°C). The thermogravimetric analysis thermogram is shown in Figure 9 [14].

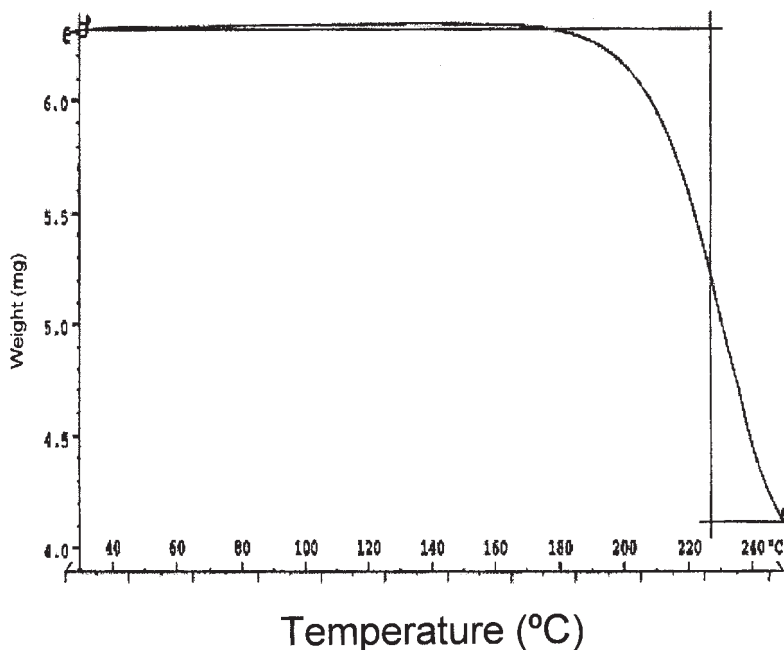


Figure 9. Thermogravimetric analysis of ornidazole.

3.9 Spectroscopy

3.9.1 UV-VIS spectroscopy

The ultraviolet spectrum of ornidazole was recorded using a Perkin-Elmer Lambda 20 spectrophotometer, at a solute concentration of 20 $\mu\text{g/mL}$ in isopropanol. The spectrum shown in Figure 10 exhibits maxima at 230 (molar absorptivity = 5292 $\text{L} \cdot \text{cm/mol}$) and 311 nm (molar absorptivity = 11447 $\text{L} \cdot \text{cm/mol}$) [14].

3.9.2 Vibrational spectroscopy

The infrared spectrum of ornidazole was obtained in a KBr pellet, and recorded on a Nicolet-Impact-400 FTIR spectrometer. The IR spectrum is shown in Figure 11, and the vibrational mode assignments for the major observed bands are provided in Table 3 [14].

3.9.3 Nuclear magnetic resonance spectrometry

3.9.3.1 ^1H -NMR spectrum

The ^1H -NMR spectrum of ornidazole was obtained in both deuteriochloroform and in deuterium oxide using a Bruker AC300F NMR

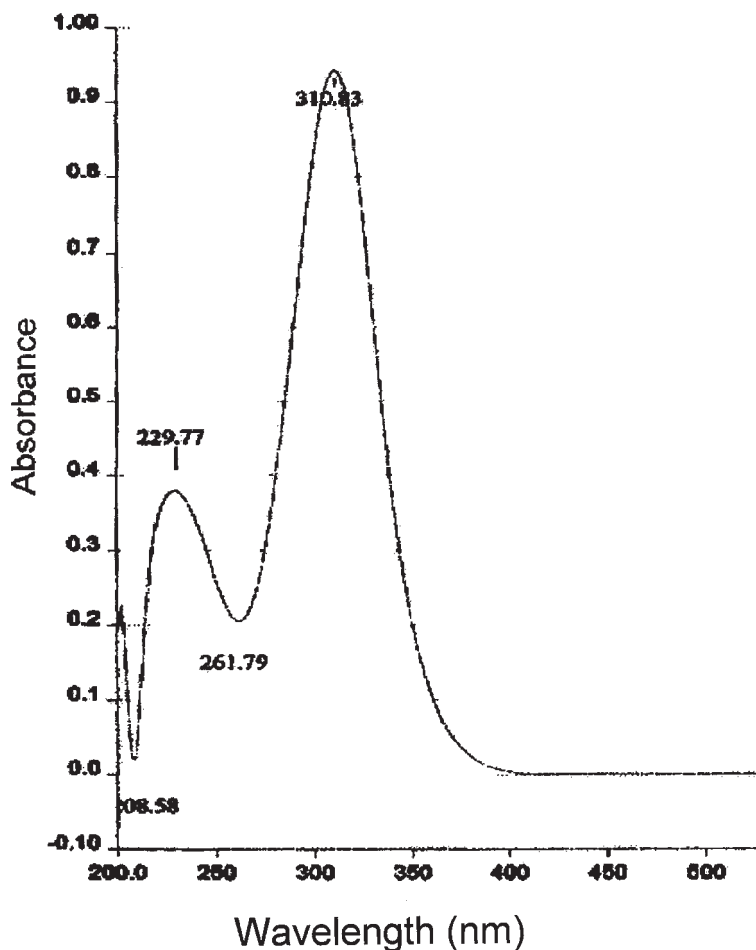


Figure 10. Ultraviolet absorption spectrum of ornidazole, 20 $\mu\text{g/mL}$ in isopropanol.

spectrometer operated at 300 MHz (tetramethylsilane was used as the internal standard) [14]. The spectra are shown in Figures 12–15, and Table 4 provides a summary of assignments for the observed resonance bands.

3.9.3.2 ^{13}C -NMR spectrum

The ^{13}C -NMR spectrum of ornidazole (Figure 16) was obtained in deuterio-chloroform at ambient temperature using tetramethylsilane

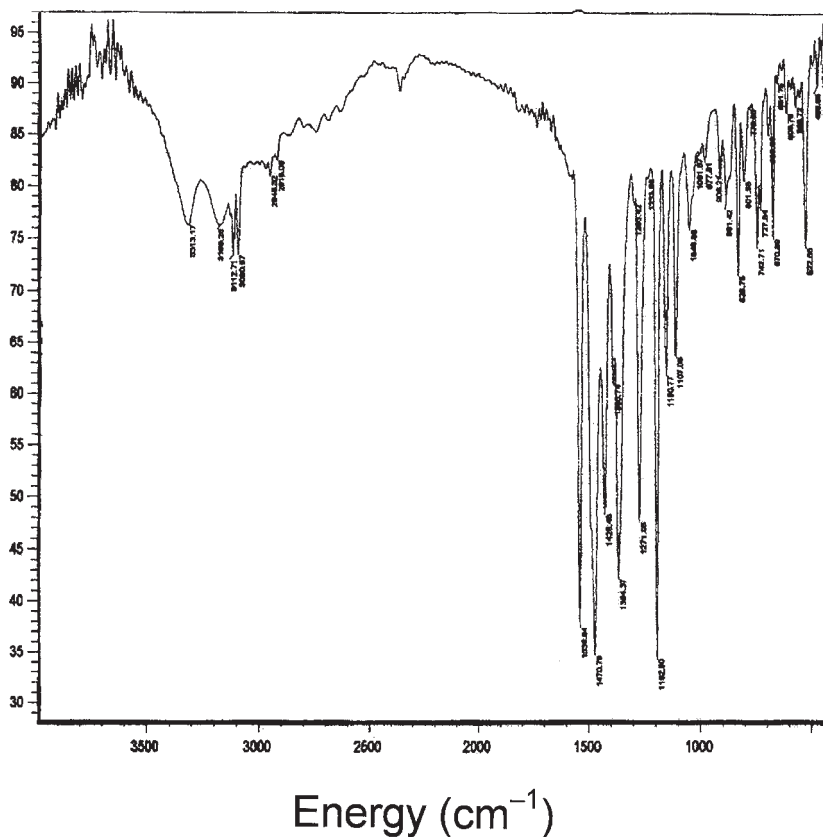


Figure 11. Infrared absorption spectrum of ornidazole, obtained in a KBr pellet.

as an internal standard [14]. The one-dimensional, DEPT 135 (Figure 17), DEPT 90 (Figure 18) COSY 45 (Figure 19), and HMQC (HETERO-COSY, Figure 20) spectra were used to develop the ¹³C chemical shift assignments that are summarized in Table 5.

3.10 Mass spectrometry

The mass spectrum of ornidazole was recorded using a VG70-250S mass spectrometer, and is shown in Figure 21 [14]. The molecular ion peak was found at $m/z = 219$ (6.63%), and the other observed characteristic peaks are shown in Table 6.

Table 3

Infrared Spectral Assignments of Ornidazole

Energy (cm^{-1})	Assignments
3174.10	O–H stretching mode
3113.5 and 3089	C–H stretching mode
1536.99	Asymmetric NO_2 stretching mode
1361 and 1269.5	Symmetric NO_2 stretching mode
1149	C–O stretching mode
828	C–N, NO_2 stretching mode

4. METHODS OF ANALYSIS

4.1 Identification

4.1.1 Infrared spectrum

The infrared spectrum of ornidazole, obtained in a potassium bromide pellet, can be used for identification of the drug substance. The compound will exhibit peaks at 3174.1, 1536.9, 1361, and 1269.5 cm^{-1} .

4.1.2 Ultraviolet absorption

A 20 $\mu\text{g/mL}$ solution of ornidazole dissolved in Isopropanol will exhibit absorption maxima at 230 and 311 nm.

4.1.3 High-performance liquid chromatography

The retention time of the ornidazole peak in the HPLC procedure is same as that of authentic ornidazole reference standard.

4.2 Titrimetric analysis

An analytical method for the quantitative determination of ornidazole in the presence of some impurities or degradation products was presented

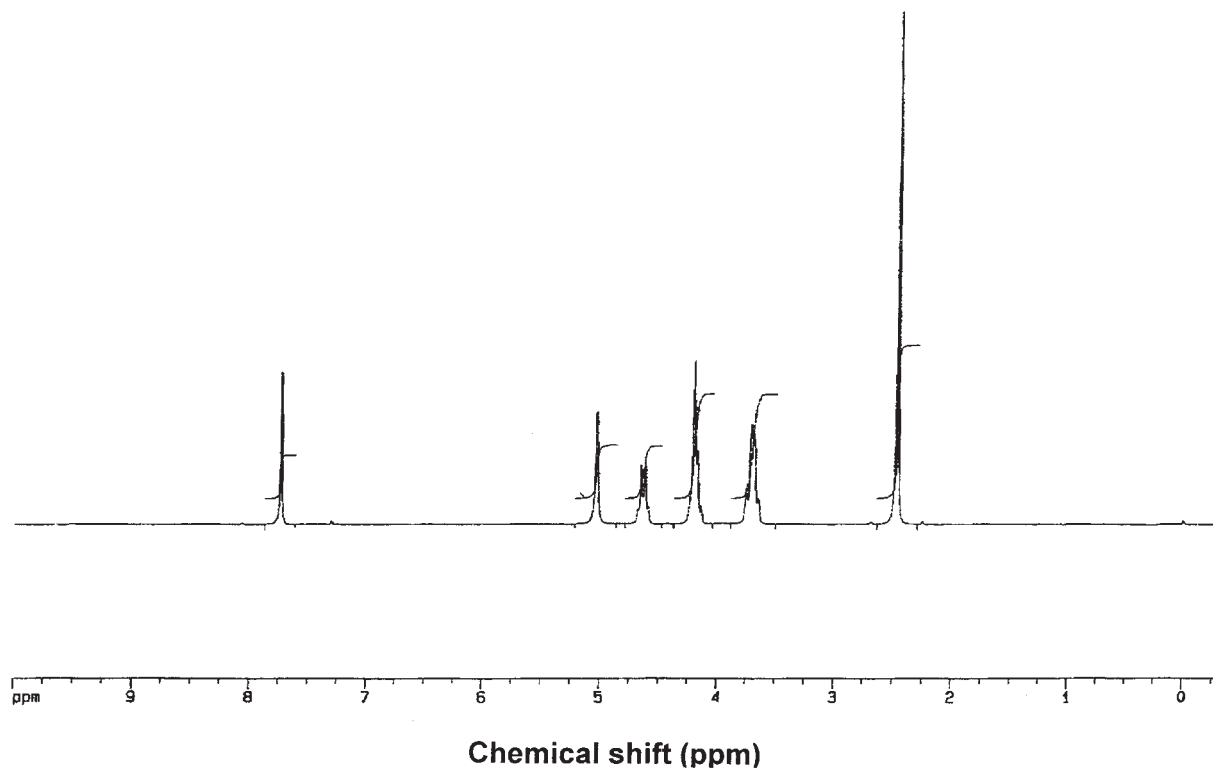


Figure 12. ^1H -NMR spectrum of ornidazole in CDCl_3 .

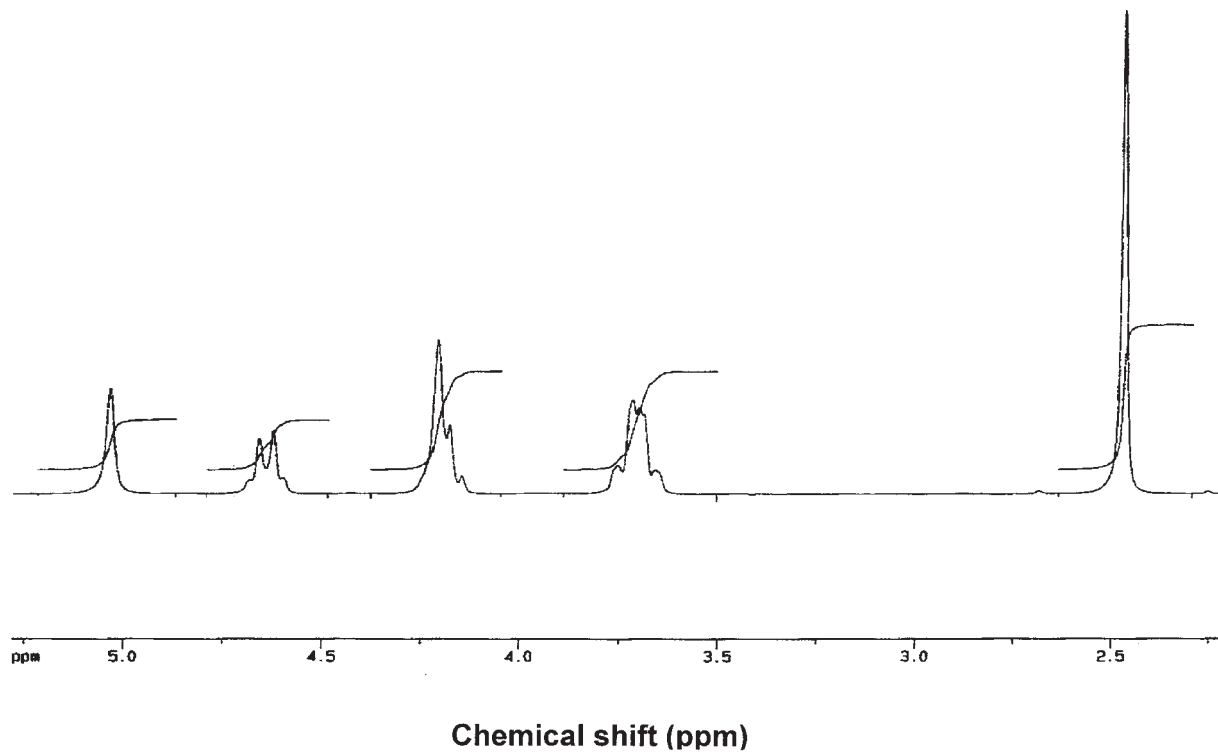


Figure 13. Expanded ^1H -NMR spectrum of ornidazole in CDCl_3 .

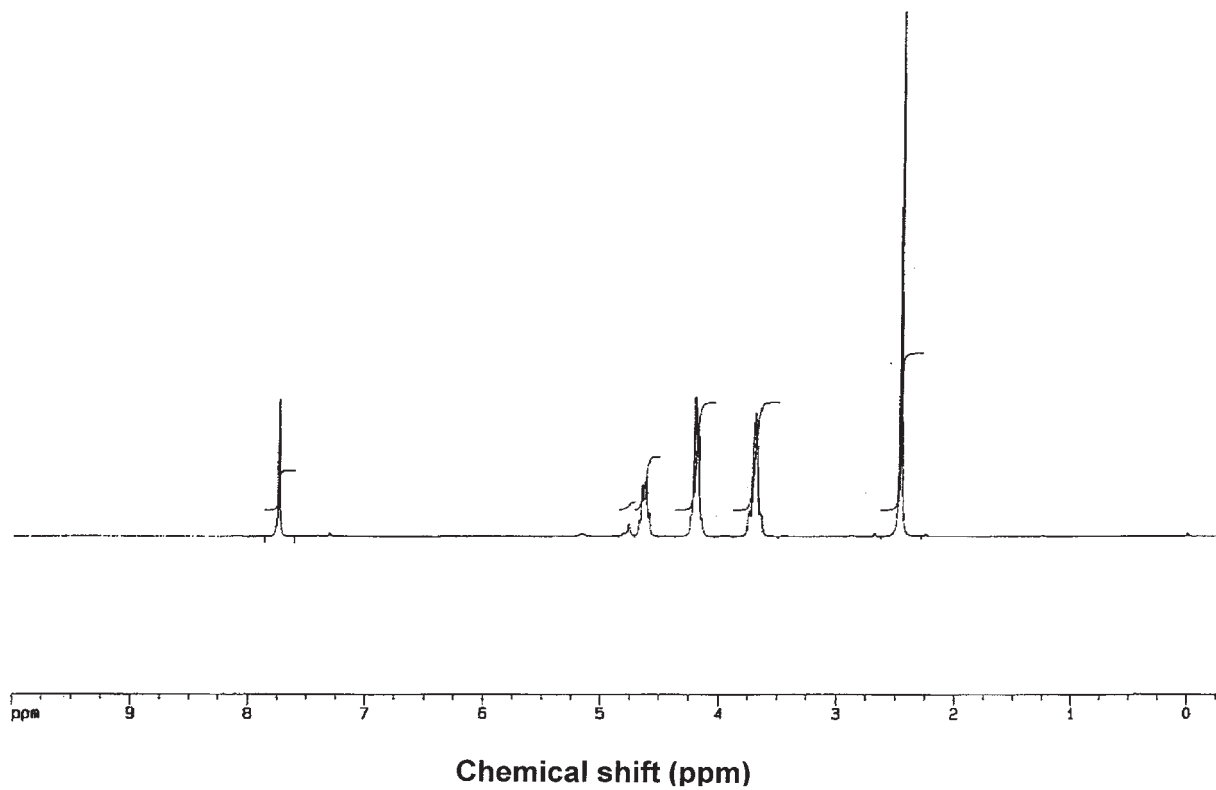


Figure 14. ^1H -NMR spectrum of ornidazole in deuterium oxide.

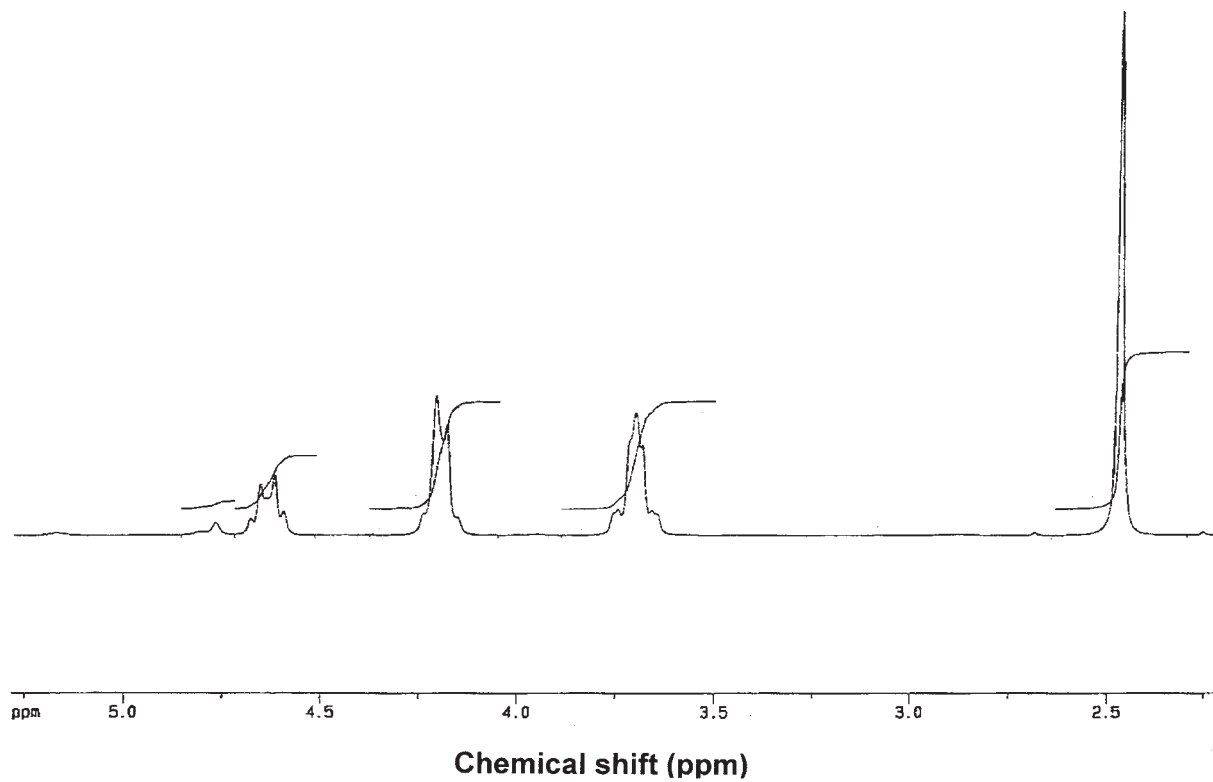
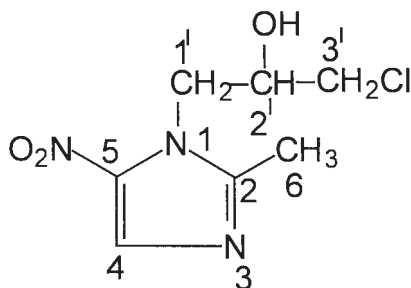


Figure 15. Expanded D₂O exchange spectrum of ornidazole.

Table 4

Assignments for the Resonance Bands Observed in the ^1H -NMR Spectrum of Ornidazole



Chemical shift (ppm)	Number of protons	Multiplicity	Assignment
2.47	3	Singlet	2-CH ₃
3.65–3.75	2	Multiplet	3'-CH ₂ Cl
4.14–4.21	2	Triplet	1'-CH ₂ N
4.60–4.68	1	Multiplet	2'- <u>CHOH</u>
5.04	1	Singlet	2'-CH <u>OH</u>
7.79	1	Singlet	4

by Visan *et al.* [34]. Ornidazole was quantitatively determined by potentiometric titration, using 0.1N HClO₄ as a titrant, and impurities were evaluated separately using densitometry.

4.3 Electrochemical analysis

Several electrochemical methods for the analysis of ornidazole have been reported [19–24]. The most studied among these methods are based on polarography [25–29] and voltammetry [30–32].

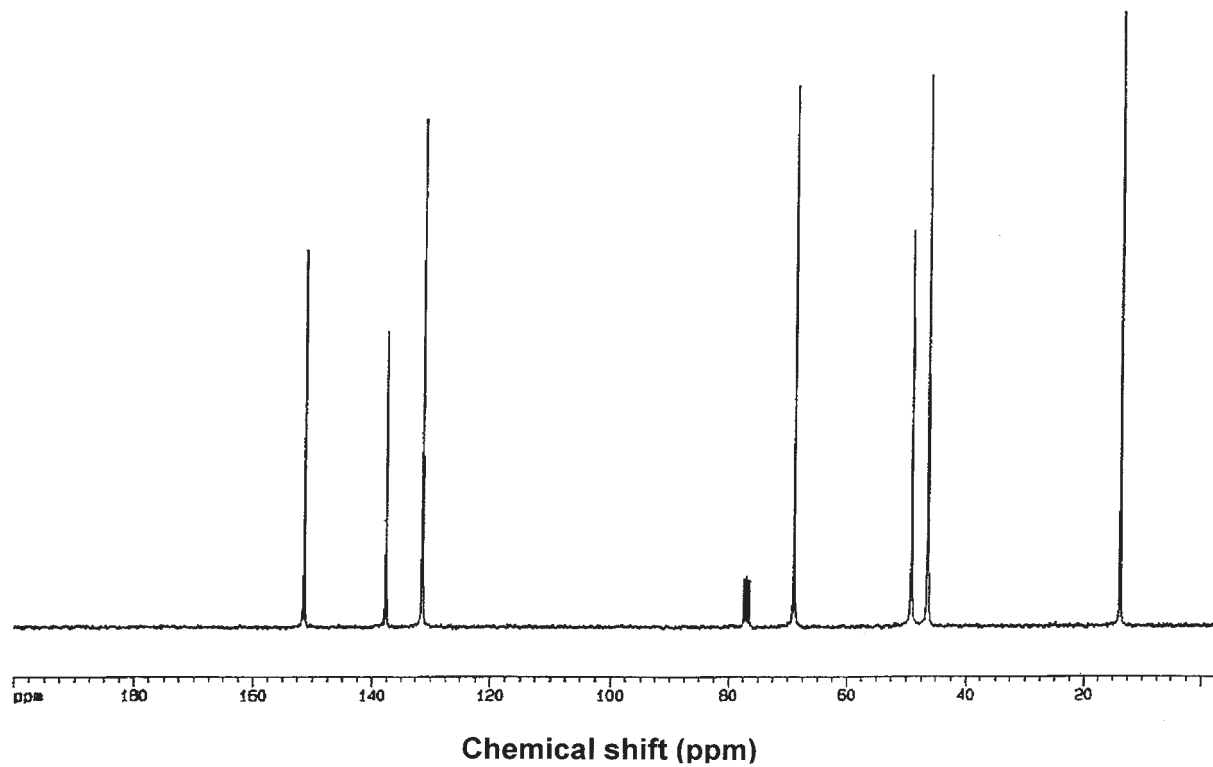


Figure 16. ^{13}C -NMR spectrum of ornidazole in CDCl_3 .

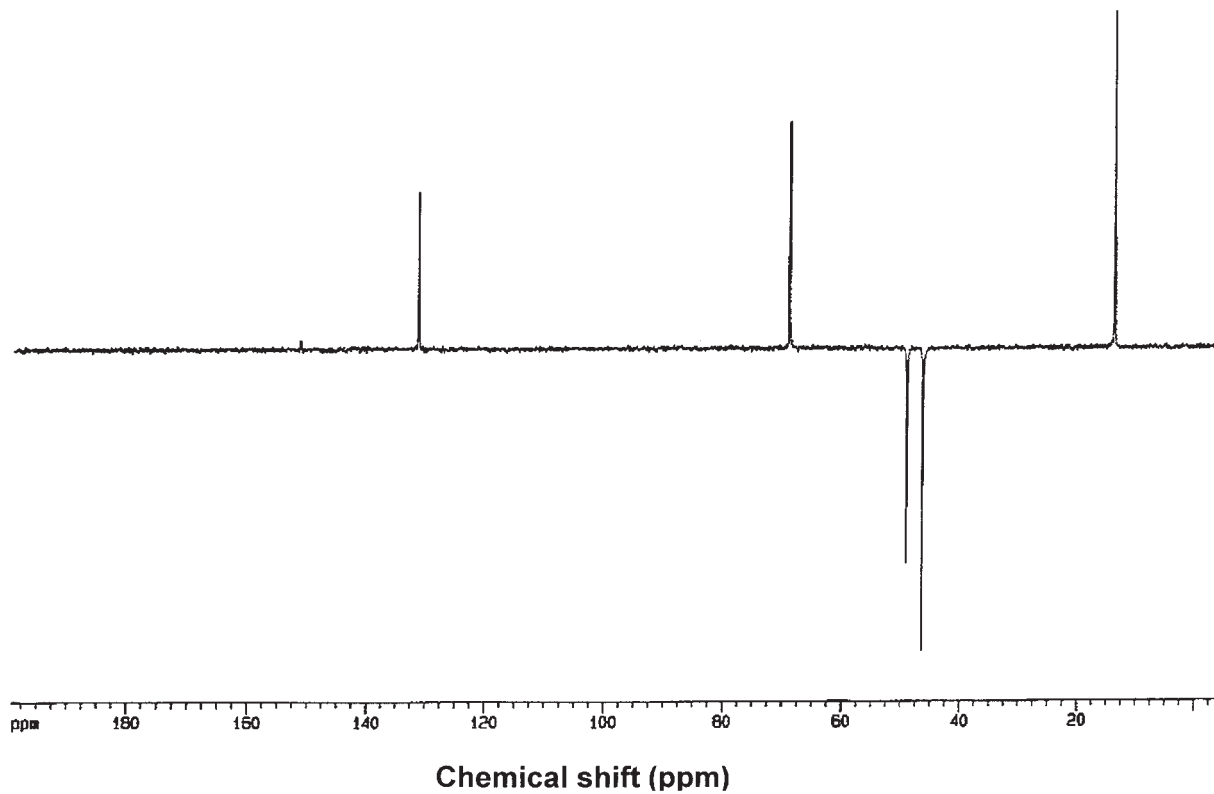


Figure 17. DEPT 135 ^{13}C -NMR spectrum of ornidazole.

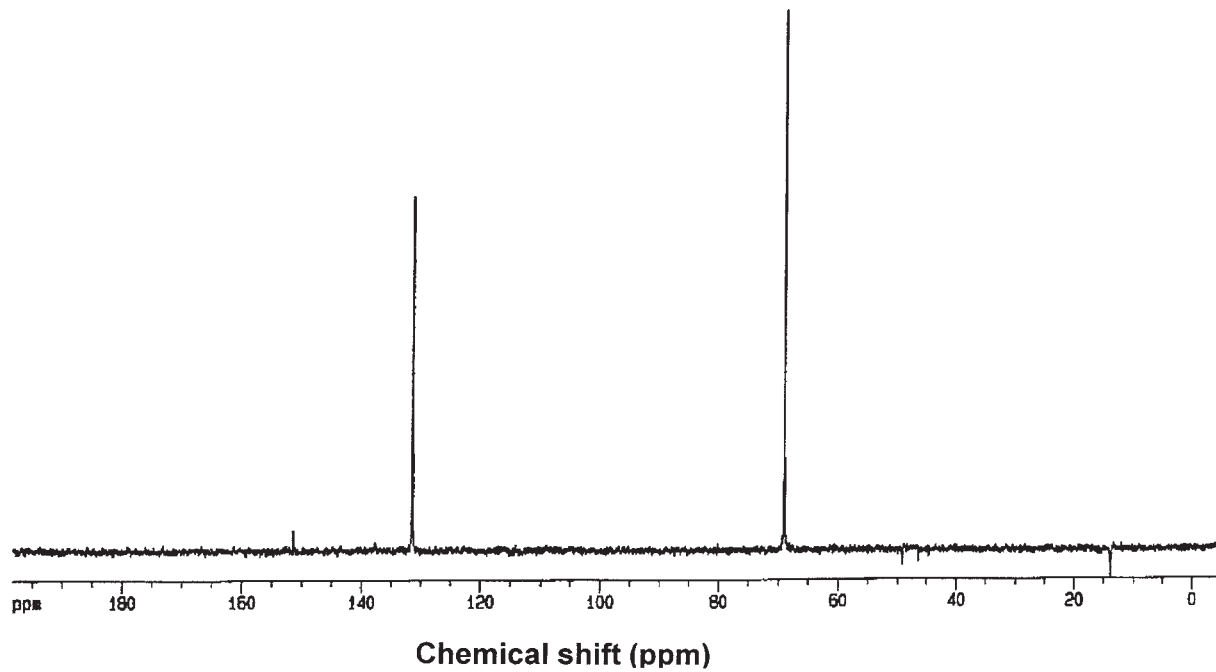


Figure 18. DEPT 90 ^{13}C -NMR spectrum of ornidazole.

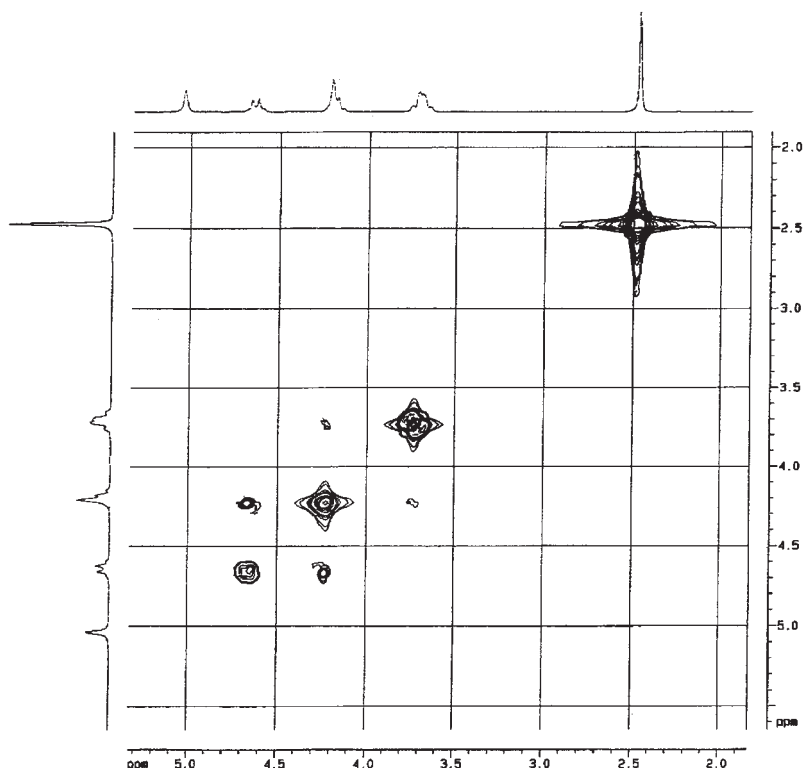


Figure 19. HOMOCOSY NMR spectrum of ornidazole.

4.3.1 Polarography

The electrochemical reduction of ornidazole was studied by Sankar *et al.* [25]. A single polarographic wave (0.43 V vs. SCE in citrate buffer at pH = 6.0) was observed in all the supporting electrolytes. The reduction was diffusion controlled, and the methods used were D.C. polarography and differential pulse polarography. A noninvasive polarographic method was used for dissolution studies of ornidazole tablets, using a dropping Hg electrode with the modified Levy beaker method [27]. The polarographic sensor probe was placed directly into the dissolution flask, thereby eliminating the transfer lines and pumps typically required with the invasive (sampling) mode of analysis. An excellent correlation was observed with UV spectrophotometric data.

A sensitive differential pulse polarographic assay for the determination of ornidazole in plasma was reported by Brooks *et al.* [28]. The plasma

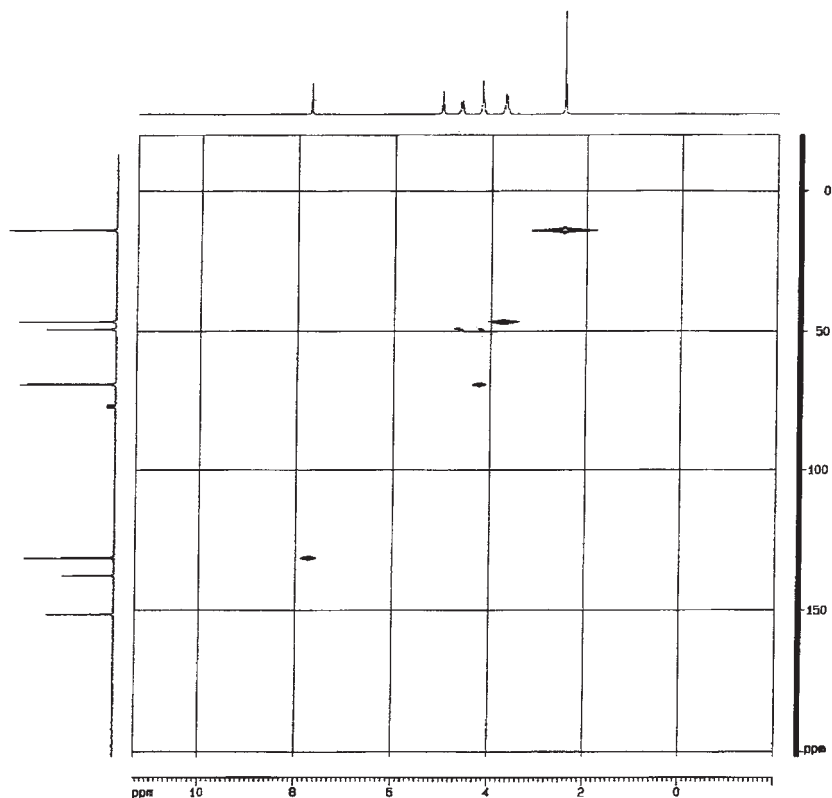


Figure 20. HETEROCOSY NMR spectrum of ornidazole.

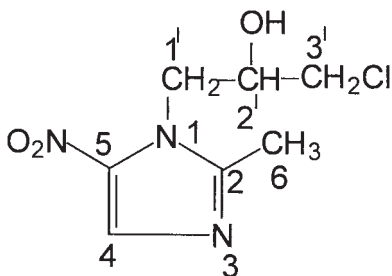
samples were extracted with ethyl acetate and then buffered to pH 7.0 ± 0.2 . The residual extract was dissolved in 0.1N NaOH and analyzed by differential pulse polarography, making use of reduction of the nitro group at approximately -0.600 V versus the saturated calomel electrode (SCE). The assay was applied to the determination of ornidazole in blood and in urine of dogs after an oral dose of 10 mg/kg.

4.3.2 Voltammetry

Ornidazole was determined in tablets and in injection solutions by linear-sweep voltammetry (Hg dropping electrode), in solutions buffered at pH 5.5 [30]. The method compared favorably with the spectrophotometric determination of ornidazole.

Table 5

Assignments for the Resonance Bands Observed in the ^{13}C -NMR Spectrum of Ornidazole



Chemical shift (ppm)	Carbon number
14.51	6
46.935	3
49.66	1
69.98	2
132.480	4
138.267	5
151.842	2

Another voltammetric analysis method was developed by Barety *et al.*, who described the electrochemical behavior of ornidazole in dimethyl sulfoxide (DMSO) [32].

4.4 Spectroscopic analysis

4.4.1 Spectrophotometry

A direct determination method of ornidazole was reported by Reddy *et al.* [35]. The absorbance of ornidazole dissolved in 0.1N HCl was found to

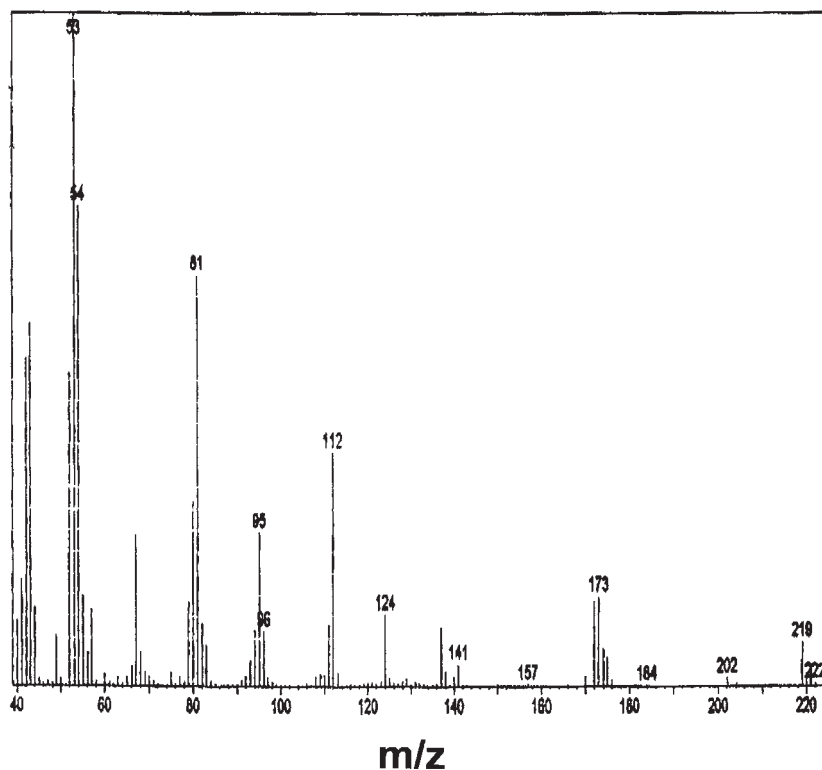


Figure 21. Mass spectrum of ornidazole.

obey Beer's law over the concentration range of 5–30 $\mu\text{g/mL}$, and the recovery was close to 100%.

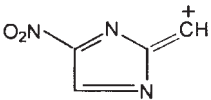
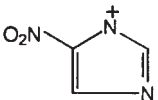
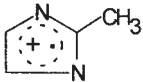
Another method reported the simultaneous determination of azomycin and ornidazole in mixture by first-order derivative spectrophotometry [36]. The method involves absorption of azomycin and ornidazole in a medium containing Britton–Robinson buffer at pH 4. The method depends upon the undissociated form of azomycin and dissociated form of ornidazole, and was applied to the simultaneous determination of both analytes in eggs and poultry feed.

4.4.2 Colorimetry

Various authors have described a number of colorimetric analysis methods for ornidazole, either alone or in combinations with other drugs. Most of the methods are based on the formation of colored condensation

Table 6

Assignments for the Peaks Observed in the Mass Spectrum of Ornidazole

<i>m/z</i>	Intensity (%)	Assignment
202	1.23	$M^+ - OH$
184	0.16	$M^+ - Cl$
173	13.37	$M^+ - NO_2$
124	10.69	
112	34.71	
95	22.70	$\begin{array}{c} + \\ \\ OH \\ \\ CH_3CHCH_2Cl + 1 \end{array}$
81	61.14	
53	100.00	$[C_4H_5]^+$

products with aromatic aldehydes, or upon formation of ion-pair complexes with dyes [33, 35, 37–40].

Reddy *et al.* described the method for determination of ornidazole in bulk and in dosage forms [35]. They used the reaction of reduced ornidazole with 3-methyl-2-benzothiazolinone hydrazone in the presence of $FeCl_3$ to give a green complex, which showed an absorbance maximum at 645 nm. Zuhri *et al.* used bromothymol blue to form a colored complex of ornidazole, and the absorbance of this complex was measured at 446 nm [37]. The proposed method was successfully applied for determination of ornidazole in commercial dosage forms.

p-dimethylaminobenzaldehyde and *p*-dimethyl-aminocinnamaldehyde have been used to prepare condensation products of ornidazole, exhibiting absorbance maxima at 480 and 460 nm, respectively [38]. Both complexes were found to obey Beer's law over the concentration ranges employed for this method. Another method given by Salman *et al.* makes use of an amine group produced by the reduction of the nitro group, which is then coupled with *p*-dimethylaminobenzaldehyde [39]. This method was used to assay both injection solutions and tablet dosage forms.

In another method, the quantitative formation of the diazonium salt of ornidazole by coupling with *N*-(1-naphthyl)ethylenediamine was used to produce a colored derivative [40]. In this work, two different procedures were provided, and both derivatized compounds were stable, and exhibited absorption at 530 and 500 nm, respectively.

4.4.3 Nuclear magnetic resonance

An accurate, rapid, precise, and reproducible NMR assay for ornidazole in bulk and in tablets has been reported [33]. The method is based on the integrated intensities of the 2-methyl protons of ornidazole relative to the integrated intensities of the methyl protons of an internal standard (acetanilide).

4.5 Chromatographic methods of analysis

4.5.1 Thin-layer chromatography

Several TLC methods have been developed to detect ornidazole, and the defining characteristics of these methods can be summarized as follows:

Eluent	R _f	Analysis	Reference
CH ₃ COOCH ₃ :CHCl ₃ : HCOOH [25:25:1]	0.49	UV absorbance	7
CH ₃ COOCH ₃ : CHCl ₃ :NH ₃ [25:25:1]	0.61	UV absorbance	7
CH ₃ COOCH ₃ :CHCl ₃ : HCOOH [80:20:2]	0.63	UV absorbance	7
CHCl ₃ : MeOH [97 : 3]	0.23	UV absorbance	18

A rapid, sensitive, and cost effective high-performance TLC assay has been developed for measurement of ornidazole in human plasma in support of bioavailability and bio-equivalence studies [46]. The method includes a single-stage extraction procedure without the use of an internal standard. Known amounts of extract and ornidazole (20 ng/ μ L as external standard) were spotted on a precoated silica gel Merck 60 F₂₅₄, 20 \times 10 cm, by a Camag Automatic TLC Sampler III. Quantification was achieved using a Camag TLC Scanner with CATS evaluation software. The authors have also discussed the cost, time, and validation comparison between HPTLC and HPLC methods.

4.5.2 Gas chromatography

A gas chromatographic method for ornidazole has been reported, which made use of 3% OV-1 on Chromosorb W-HP as the stationary phase [41].

Bhatia *et al.* described a sensitive and selective electron capture gas chromatography method for the determination of ornidazole in blood [42]. The hydroxyl function in the *N*-1 substitution was converted to its respective trimethylsilyl derivative before chromatography on an OV-11 column. Blood levels as low as 50 ng/mL of ornidazole were measured using this method.

4.5.3 High-performance liquid chromatography

Several HPLC methods for the determination of ornidazole and/or its degradation products/metabolites in various dosage forms [17, 41, 43–45] and in biological matrices [15, 46–52] have been reported.

4.5.3.1 HPLC determination in pharmaceutical products

Various authors have reported different HPLC methods for the determination of ornidazole in its bulk form, as well as in various dosage forms [17, 41, 43–45]. One of the recent methods published by Bakshi *et al.* [45] described a stability indicating method based on reversed-phase HPLC, and reports on the degradation of ornidazole under different stress conditions (hydrolysis, oxidation, and photolysis). The system consisted of a 600 E pump, a 996 photo-diode array (PDA) detector, a 717 auto injector, and a degasser module. The chromatographic separations were carried on a 10 μ m supelcosil LC-18-DB column (250 \times 4.6 mm i.d.). Separations were achieved using isocratic elution, and initial studies were carried out using H₂O–MeOH as the mobile phase. Good separations were achieved by varying the ratio of methanol and acetonitrile in the mobile phase (flow rate of 1 mL/min).

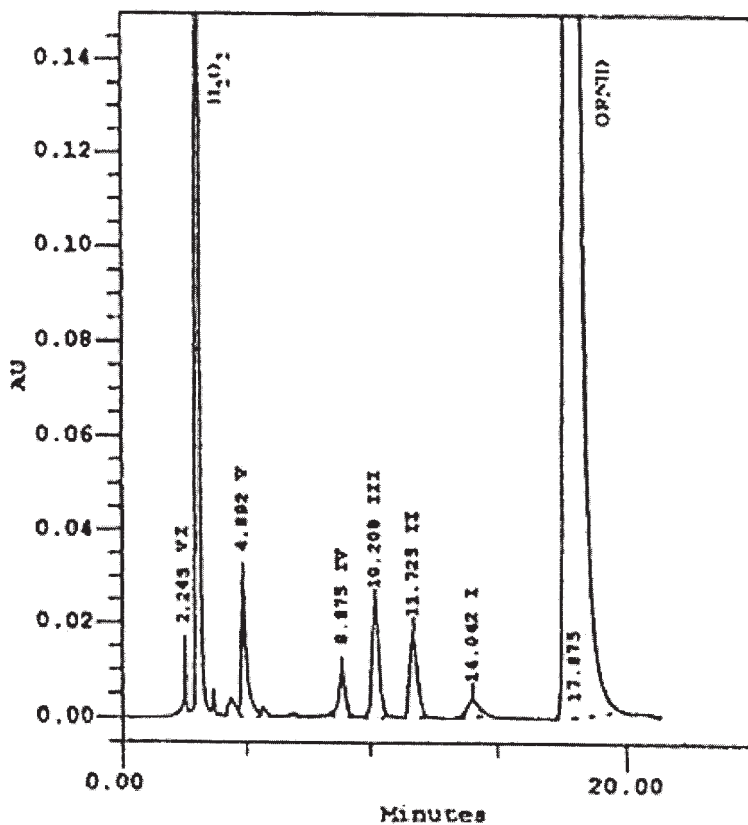


Figure 22. Chromatogram showing the HPLC separation of ornidazole and its degradation products. I and IV represent oxidative degradation products, V and VI represent the degradation product in phosphate buffer (pH 8), III represents the photolytic degradation product in 0.1 M HCl.

The analyzing wavelength in most cases was 310 nm, but in selective cases where drug decrease was noted without appearance of any degradant peak in the chromatogram, PDA analysis was performed to study the behavior at other wavelengths. Figure 22 shows the chromatogram illustrating the separation of ornidazole and other degradation products when using this method.

A few HPLC studies have been reported regarding the separation of the enantiomers of ornidazole [63, 64].

4.5.3.2 HPLC determination in biological matrices

High-Performance Liquid Chromatography methods have been used to determine ornidazole in a number of publications, and the important parameters of the various literature methods are listed in [Table 7](#).

4.5.4 Capillary electrophoresis

Various methods have been reported for the separation of racemic ornidazole using capillary zone electrophoresis in the presence of different chiral solvating agents (CSA). These include the use of permethyl- α - and γ -cyclodextrins [53, 54], α -, β -, and γ -cyclodextrins [55–58], and hydroxypropyl α -, β -, and γ -cyclodextrins [59–61].

The enantiomeric separation of the analyte has been correlated with the interaction strengths of ornidazole with the CSA. Hence the concentration of CSA is a crucial parameter for optimized separation of enantiomers. Permethylated CSA agents led to a higher rate of successful enantiomer separation relative to the native α -cyclodextrins.

α -, β -, and γ -cyclodextrins, and derivatized cyclodextrins (hydroxypropyl- and sulfobutyl ether- β -cyclodextrins) were also used as a chiral buffer modifiers for the resolutions [62]. It was found that empirical factors, such as type, concentration, and pH of the run buffer affected the separation of enantiomers.

5. STABILITY

5.1 Solution-phase stability

The decomposition of ornidazole was studied by Valdes-Santurio *et al.* as a function of pH and temperature [17]. Degradation products were isolated and identified, and their structures are shown in [Figure 23](#). The study results indicated that the drug was stable in acidic media below pH 6. At higher pH values, however, ornidazole (**I**) rapidly hydrolyzed to an epoxide via an intramolecular nucleophilic attack, and a subsequent opening of the epoxide (**II**) to yield a diol (**III**).

Contradictory to this report, Bakshi *et al.* reported that the drug is unstable in almost all conditions, such as in alkaline media, under acidic conditions, under oxidative stress, and in acidic media in the presence of light [45]. These authors successfully achieved the separation of drug and the degradation products under various conditions. Ornidazole decomposes in alkaline conditions first to an epoxide, which is converted

Table 7

HPLC Methods for Determination of Ornidazole in Biological Matrices

S.No.	Column	Mobile phase	Flow rate (mL/min)	Detection (by UV)	Reference
1	Waters μ Bondapak C18 (300 \times 3.9 mm i.d.) Packed with silica gel (10 μ m) with a C18 chemically bonded nonpolar stationary phase	Methanol : Water 50 : 50	1	313 nm	15
2	LiChrospher 100 column RP18 endcapped, particle size 5 μ m, column dia 4 mm	Methanol : Water (25 : 75)	1	318 nm	46
3	Nucleosil 5C18 column	Methanol : 0.067M Phosphate buffer pH 6, 80 : 20 for ornidazole 17 : 83 for metabolites	–	312 nm	47

(continued)

Table 7 (continued)

S.No.	Column	Mobile phase	Flow rate (mL/min)	Detection (by UV)	Reference
4	MOS-Hypersil RP-8 column	Methanol : 0.01 M KH_2PO_4 (3 : 7)	–	318 nm	48
5	Zorbax C8	MeCN : H_2O : D/4 reagent (30 : 70 : 1)	–	317 nm	49
6	μ Bondapack C18 reversed-phase column	Water : ethanol (1 : 9)	2	318 nm	50
7	Lichrosorb RP 8	Ethanol : water (1 : 9)	–	317 nm	51
8	Lichrosorb RP 18.5 μm Length 12.5	Ethanol : water 20 : 80	1	318 nm	52

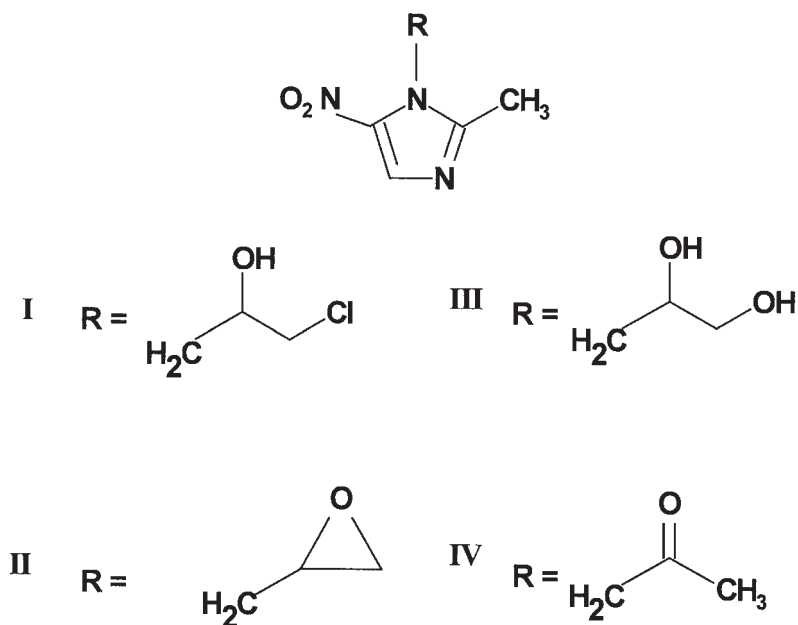


Figure 23. Structures of ornidazole and its degradation products.

further to diol. The drug was found to degrade under oxidative stress at room temperature, being decomposed to an extent of 8% in 3% H_2O_2 in 8 h. The degradation amount increased to 53% over the same time period when using 30% H_2O_2 . The drug substance degrades under oxidative conditions to yield nonchromophoric products. In addition, a mild degradation was also observed under neutral and photolytic conditions.

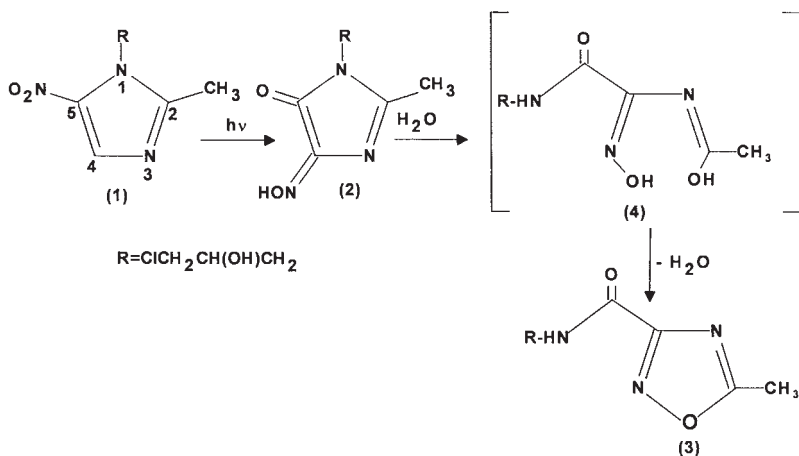
Alberola *et al.* studied the stability of ornidazole (10 mg/mL in 0.9% sodium chloride) in polyvinyl chloride bags stored at ambient, refrigeration, and freezing temperature for 30 days [66]. Over 90% of the initial drug concentration remained in all samples throughout the study period.

Rodriguez *et al.* studied the stability of 10 mg/mL solutions of ornidazole (in 5% dextrose and in 0.9% sodium chloride) in plastic bags stored at 5° and 25°C with/without light, and in the presence or absence of 250 mg of gentamycin for up to 30 days [67]. They observed that the drug was stable for at least 15 days in all solutions and under all storage conditions.

5.2 Photolytic stability

Originally prepared, colorless aqueous solutions of ornidazole became slightly yellow when exposed to daylight. This observation led Pfoertner *et al.* to study the photochemical reactions of dissolved ornidazole [65].

In a first reaction step, the photo-rearrangement of ornidazole (**1**) yields 1-(3-chloro-2-hydroxypropyl)-2-methyl-2-imidazoline-4,5-dione-4-oxime (**2**). Upon hydrolysis and subsequent elimination of water from a proposed intermediate (**4**), the resulting compound leads to *N*-(3-chloro-2-hydroxypropyl)-5-methyl-1, 2, 4-oxadiazole-3-carboxamide (**3**).



Barbara *et al.* conducted a photodegradation kinetic study in aqueous solution [68]. They found that the process was a first-order reaction, characterized by a complex mechanism. The photostability of ornidazole was found to depend on the electrophilicity of the substituent on C₅. A kinetic study of photodegradation of ornidazole and other nitroimidazole derivatives in the solid state was carried out by the same authors [69]. The kinetics of photodegradation was determined by “alkali-halide matrix” technique, which enabled the conclusion to be made that the solid-state decomposition proceeds according to a first-order kinetics.

In another study, ornidazole degradation was studied by HPLC and electron paramagnetic resonance methods [70]. Radicals, produced by radiolysis of ornidazole, were found to be stable when compared to the stability of radicals produced from two drugs. The decay kinetics of radical anions from ornidazole and other 5-nitroimidazoles were studied

after pulsed electron radiolysis [71], where the authors reported second-order kinetics for the decay.

Tablets containing ornidazole were kept at 35 and 60°C, both in the dark and under light for 90 days [72]. The tablets kept only at high temperature were not discolored during the study period, while tablets exposed to light underwent a yellowing reaction.

6. DRUG METABOLISM AND PHARMACOKINETICS

6.1 Absorption, distribution, and excretion

Ornidazole is readily absorbed from the gastrointestinal tract and vaginal mucosa. A peak plasma concentration of about 30 µg/mL has been achieved within 2 h of a single oral dose of 1.5 g, which falls to about 9 µg/mL after 24 h and 2.5 µg/mL after 48 h [2, 168–172]. After repeated oral doses of 500 mg every 12 h, steady state peak and trough concentrations were found to be 14 and 6 µg/mL, respectively. Peak plasma concentrations of about 5 µg/mL have been reported 12 h after the insertion of a 500-mg vaginal pessary.

The plasma elimination half-life of ornidazole is 14.1 ± 0.05 h, the mean residence time is 19.4 ± 0.6 h and the mean plasma clearance is 50.6 ± 2.1 mL/min. [52]. Less than 15% of the substance is bound to plasma proteins. It is widely distributed in body tissues and fluids, including cerebrospinal fluid [171, 173, 174]. The plasma, epiploic fat drug concentrations, fat penetration of ornidazole, and ceftriaxone given for antimicrobial prophylaxis were studied in 11 patients. Ornidazole (500 mg dose) was administered intravenously after the induction of anesthesia [175]. Ornidazole concentrations ranged between 8.7 and 4.9 µg/mL in plasma, and 4.6 and 2.5 µg/g in fat samples. Rates of penetration into the omentum remained between 50 and 70% for ornidazole.

The pharmacokinetics of ornidazole have been evaluated in 12 neonates or infants (aged 1–42 weeks) after intravenous infusion of 20 mg/kg over 20 min [176]. The distribution phase was short ($t_{1/2} = 0.31$ h) and was followed by an elimination phase ($t_{1/2} = 14.67$ h). The mean apparent volume of distribution was 0.96 L/kg. Total plasma clearance observed was between 0.4 and 1.4 mL/min·kg. The plasma concentration 24 h after the infusion was 7.32 mg/L, which was above the minimum inhibitory concentration for clinically significant anaerobic bacteria.

Helmbrecht *et al.* observed blood acetaldehyde concentrations following the administration of alcohol, finding these to be similar to concentrations observed after the combined administration of alcohol and ornidazole [177]. The study was conducted in experimental animals and in volunteers.

The elimination of ornidazole is impaired in patients having cirrhosis of the liver. A 500-mg single intravenous dose was administered to 10 patients with severe liver cirrhosis, and the pharmacokinetics compared with those of 10 healthy volunteers [52]. The mean half-life in patients was doubled to 21.9 ± 2.9 h. This finding suggests the need for dose adjustment in liver patients, which has been further confirmed by studies of patients with other forms of liver diseases [178, 179].

In the case of patients having advanced chronic renal failure, the half-life of intravenously administered ornidazole was not prolonged. The half-life was halved in patients on continuous ambulatory peritoneal dialysis. This finding suggests that modification of the usual dose in such patients is not required, and additionally, ornidazole should be administered after the dialysis session rather than before [180]. In another study, it was observed that the total body clearance of ornidazole was unaffected in chronic renal failure, and these authors recommended an additional dose in such patients before hemodialysis to compensate for drug removal during that procedure [181].

Schwartz *et al.* compared the pharmacokinetic characteristics of ornidazole and metronidazole in man [168]. Both drugs were labeled with ^{14}C in the imidazole ring at position 2, and a crossover study was conducted in four volunteers (dosing at 750 mg). It was found that the mean peak plasma concentrations were 10.9 $\mu\text{g/mL}$ for ornidazole and 12.3 $\mu\text{g/mL}$ for metronidazole, with these being attained in 2–4 h and 30–60 min after administration, respectively. The volume of distribution was same for both drugs. Their binding to plasma was 14.4 h for ornidazole and 8.4 h for metronidazole. The mean radioactivity recovered from urine and feces during the first 5 days was 85% of the dose for ornidazole and 91% for metronidazole, the major proportion in each case being in the urine. The radioactivity found in feces was 22.1% of the dose for ornidazole.

To enhance the antimicrobial spectrum of the quinolones against anaerobic and gram-positive bacteria, 500 mg ornidazole was co-administered with fleroxacin [182]. It was found that the addition of ornidazole did not effect the pharmacokinetics of quinolones.

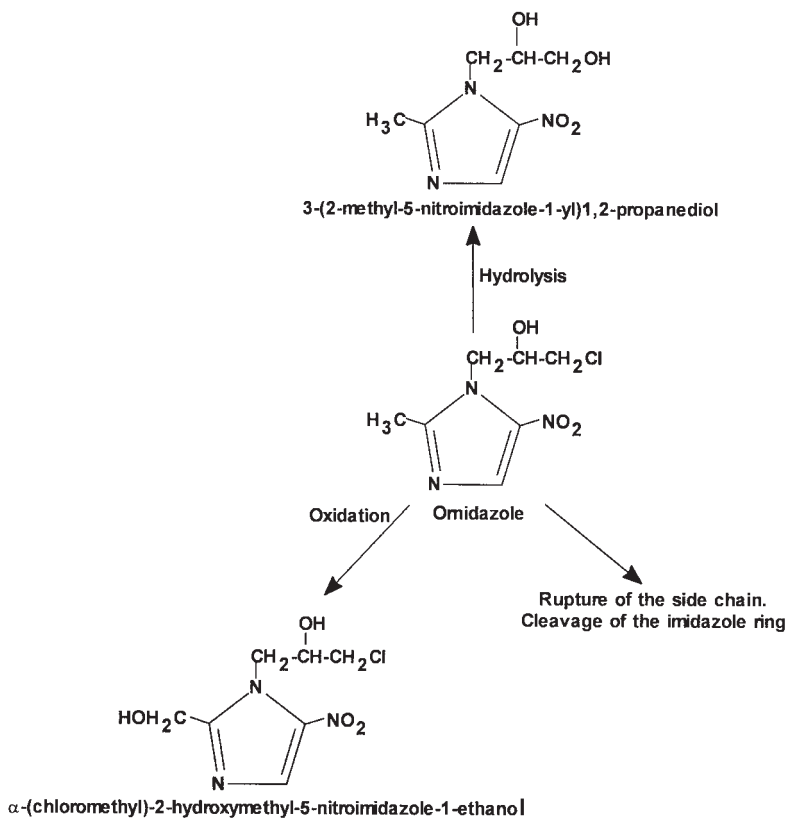


Figure 24. Metabolism of ornidazole.

6.2 Metabolism

Ornidazole is metabolized in the liver and excreted in urine (mainly as conjugates and metabolites), and to a lesser extent in the feces [183]. The major route of elimination entails biotransformations through the liver, and through biliary excretion to some extent. The known major pathways of metabolites are shown in Figure 24. Ornidazole and hydroxylated metabolites are eliminated in both free form, and in the form of conjugates [52, 183].

7. TOXICITY

The oral LD₅₀ values in rats and mice are 1780 and 1420 mg/kg, respectively [140]. Another report showed a LD₅₀ (mg/kg) in mice of

greater than 2000 for oral administration and greater than 2000 for i.p. administration [1, 6].

In humans, ornidazole is well-tolerated, with a mild and transient side effect profile. The most frequently encountered side effect of ornidazole is dizziness, alone or in combination with other adverse effects. The other side effects occurring to a less extent are nausea, pyrosis, intestinal spasms, and metallic taste. Vertigo, fatigue, and other discomforts such as loose stools, insomnia, skin rash, and headache have also been reported [2].

In recent years, there has been a considerable interest in the study of the mutagenic activity of nitroimidazoles. Various studies have been conducted to evaluate *in vitro* [184] and *in vivo* [15, 22, 185–187] mutagenic activity of nitroimidazoles. As reported by Chin *et al.*, most 5-nitroimidazoles had a 1-2 order of magnitude greater mutagenicity towards *Salmonella typhimurium* TA 100 (base-pair substitution sensitive) than toward TA 98 (frame-shift sensitive) [188]. The spectrum of observed mutagenic efficiencies for the drugs could be correlated to some extent with the electron affinity of these compounds.

Another study conducted by Voogd *et al.* showed that the nitroimidazoles without a nitro group were not mutagenic [189]. A relation between the chemical structure and mutagenic action was deduced for nitroimidazoles. After administration of ornidazole, the mutagenicity of human blood and urine was determined using the Ames test in *Salmonella typhimurium* TA 98 and TA 100. The mutagenic activity in blood was detectable for 6 h, and in urine for 72 h, after administration of 1 g ornidazole [190]. The same effect was observed in rats, when their urine was tested for mutagenicity after drug administration [191].

Cantelli-Forti *et al.* studied the mutagenicity of bile after drug administration, and found that the metabolites present in bile are more mutagenic than those of the parent drug [192]. Another study revealed that ornidazole is a potent mutagenic agent even without microsomal enzyme activation, and that it also induced frame-shift mutation in the TA 98 strain [193]. However, there are no reports regarding its mutagenic activity in patients.

When ornidazole was used as an antiprotozoal agent in dogs, it evoked convulsions after several days of treatment. The histopathological studies

showed a marked degeneration of cerebellar purkinje cells. This effect was not observed in mice, rats, guinea pigs, or rabbits [194].

Reproduction studies with ornidazole were performed by McClain *et al.* [4]. Different doses of ornidazole (0, 25, 100, and 400 mg/kg/day) were administered to male rats 61 days prior to mating, and for 2 weeks to female rats prior to mating and throughout gestation and lactation. In high doses, a decrease in pregnancy rate was observed without altered mating performance. Crossover matings between high-dose-treated and control male rats showed that male fertility was affected, and the effect was reversible after cessation of treatment. There was no effect on the fertility of female rats. Additional studies by these authors revealed that high dosing (400 mg/kg/day) produces infertility in male rats by inhibiting epididymal sperm motility in terms of decreased sperm velocity. These effects are rapidly reversible after the cessation of treatment [195].

These results were further confirmed by Toth *et al.* [196]. There was no significant change in motility in animals receiving ornidazole at 200 mg/kg/day when with controls reported by Oberlaender *et al.* [197]. It was suggested that the antifertility action is due to direct action of an ornidazole metabolite on the epididymal spermatozoa. Further studies conducted by Yeung *et al.* [198] revealed that antifertility action occurs via damage to spermatozoa in the upper regions of the female tract, possibility reflecting in capacitation as a result of reduced energy production and due to a disturbed glycolytic pathway [199]. ³⁶Cl-ornidazole was administered to male rats [200] and its conversion to *R,S*-chlorohydrin or ultimately to the glycolytic inhibitor (*S*)-3-chloroacetaldehyde [199] further confirmed the studies conducted by Oberlaender *et al.*

In another study, structural analogs of ornidazole were fed to determine which part of ornidazole molecule is responsible for its antifertility action [201]. The study results revealed that only ornidazole and its acetate were effective antifertility agents. Additional studies were conducted by various authors to confirm the mechanism of action of antifertility action of ornidazole [202–205].

8. PHARMACOLOGY

Ornidazole, similar in activity to metronidazole, was first introduced in 1974 for the treatment of *Trichomonas vaginalis*. The drug has antiprotozoal and antibacterial properties against anaerobic bacteria

[2, 73–75]. Like metronidazole, it is used in the management of susceptible protozoal anaerobic infections. Ornidazole has a longer half-life (12–14 h) relative to that of metronidazole (6–8 h), giving it a therapeutic advantage [4]. Ornidazole reduces the dosage frequency and duration of therapy in many of the relevant clinical infections.

Nitroimidazole drugs require reductive activation to exert antimicrobial activity [26, 76, 77]. The antimicrobial activity of the nitroimidazoles has been proposed to be due to the reduction of the nitro group to a more reactive amine that attacks microbial DNA, inhibiting further synthesis and causing degradation of existing DNA [4, 78–83].

Ornidazole has shown a marked antibacterial and antiprotozoal activity under *in vitro* conditions [84–92], and also in laboratory animals [93–96]. The activity of ornidazole has been confirmed by various clinical studies in humans suffering from intestinal and liver amoebiasis [97–99], intestinal lamblia^s [100] and vaginal trichomoniasis [101]. The antibacterial spectrum of ornidazole includes bacteria such as the *Peptostreptococcus* species, *Clostridium difficile*, the *Clostridium* species, *Bacteroides fragilis*, the *Prevotella* species, the *Porphyromonas* species, the *Fusobacterium* species, *Actinomycetes*, the *Propionibacterium* species, and the *Eubacterium* species. The drug is highly effective against various protozoa, namely *Trichomonas vaginalis*, *Entamoeba histolytica*, and *Giardia intestinalis*. Various laboratory and clinical studies listed in Table 8 shows the activity of ornidazole against various bacteria and protozoan.

The minimum inhibitory concentration reported for ornidazole against *Bacteroides* strains is 4–16 mg/L [161]. Ornidazole is effective in the treatment of severe hepatic and intestinal amoebiasis, giardiasis, trichomoniasis of uro-genital tract, and bacterial vaginosis [162]. It is also effectively used in the treatment and prophylaxis of susceptible anaerobic infections in dental gastrointestinal surgery [163]. Ornidazole is an effective and safe drug for the treatment of active Crohn's disease [164–167].

9. PHARMACEUTICS

Ornidazole can be orally administered by tablets after food intake, by vaginal pessary, or through an intravenous route. When given intravenously, solutions of ornidazole should be diluted to 5 mg/mL or less, with 100 or 200 mL being infused over 15–30 min.

Table 8

Literature Studies Indicating the Activity of Ornidazole Against Various Bacteria and Protozoans

Organism	References
<i>Bacteroides fragilis</i>	85, 102–116
<i>Clostridium perfringens</i>	85, 103, 106, 107, 109, 114, 116–119
<i>Clostridium difficile</i>	92, 122
<i>Peptostreptococcus</i> species	112, 120
<i>Peptococcus</i> species	120
<i>Fusobacterium</i> species	121
<i>Propionibacterium</i>	122
Other anaerobic bacteria	84, 89, 111, 122–129
<i>Trichomonas vaginalis</i>	21, 91, 130–142
<i>Entamoeba histolytica</i>	6, 87, 88, 137, 140, 143–146
<i>Trichomonas gallinae</i>	93
<i>Giardiasis intestinalis</i>	147–153
<i>Fungi</i>	86, 90, 154–155
<i>Actinomycetes</i>	156
<i>Camplobacter</i> species	157
<i>Helicobater pylori</i>	158–160

For the treatment of amoebiasis, 0.5 g of ornidazole is given orally twice daily for 5–10 days. Children are given 25 mg/kg body weight daily as a single dose for 5–10 days. Patients with amoebic dysentery may be given 1.5 g as a single daily dose for 3 days, with the children's dose being 40 mg/kg daily. In severe amoebic dysentery and amoebic liver abscess, ornidazole may be given by intravenous infusion in a dose of 0.5–1 g initially, followed by 0.5 g every 12 h for 3–6 days. In these circumstances, the children's dose is 20–30 mg/kg daily.

For the treatment of giardiasis, 1 or 1.5 g of ornidazole is given orally as a single daily dose for 1 or 2 days. The children's dose is 30 or 40 mg/kg daily.

For the treatment of trichomoniasis, a single dose of 1.5 g orally, or 1 g orally in conjunction with 0.5 g vaginally, is given. 5-day courses of ornidazole 0.5 g twice daily orally are also used. Sexual partners should be treated concomitantly. The children's dose is 25 mg/kg as a single oral dose.

For the treatment of anaerobic bacterial infections, ornidazole is given by intravenous infusion, in an initial dose of 0.5–1 g, followed by 1 g daily as a single dose or in two divided doses for 5–10 days. Oral therapy using 0.5 g every 12 h should be substituted as soon as possible. Children may be given 10 mg/kg every 12 h for 5–10 days [2].

For the prevention of postoperative anaerobic bacterial infections, 1 g is given by intravenous infusion about 30 min before surgery [95].

A 10 volunteer crossover study was conducted to compare two ornidazole dosage schedules. Each subject received two 0.5 g doses every 12 h, and 1 g daily, at one-week intervals. The pharmacokinetic data indicated that ornidazole could be administered once a day [206].

The use of ornidazole in pregnant women was studied by Bourget *et al.* [207]. One gram of ornidazole was administered once daily to five pregnant women suffering with either chorioamnionitis or pyelonephritis. Local and systemic tolerability of ornidazole was excellent, and patients showed complete remission without premature delivery. There was no accumulation of ornidazole, and all pharmacokinetic parameters were same as seen in healthy subjects. Children born to trial patients showed normal initial development, and their growth was normal. Therefore, the dosage regimen of ornidazole requires no adjustment during pregnancy.

Ornidazole has been formulated into various pharmaceutical forms. They include tablets, intravenous infusion fluids [208, 209], infusion concentrates for IV administration after dilution, suspensions, pessaries, suppositories [210, 211], and hard gelatin capsules [211].

The *in vitro* evaluation of ornidazole suppositories was performed by Matusova *et al.* [211]. Penetration of ornidazole through different filtration barriers or membranes into a gel with silver was evaluated. Suppositories made of Cocoa butter, *Adeps neutralis*, macrogol base, and hard gelatin capsules containing 0.5 g ornidazole were compared. The release and penetration was fastest from hard gelatin capsules and *Adeps neutralis*.

A world-wide patent describes a novel composition containing targeted vesicular for treatment of *H. pylori* infections and for protection of the cells [212]. Another patent discloses an antiprotozoal composition, which is taken orally and has a gastric juice-resistant coating [213]. The formulation acts topically directly on the intestinal site of inflammation. The dosage form is indicated for topical treatment of inflammatory intestinal illnesses.

Sanso *et al.* developed a double capsule where an internal capsule is placed inside an external one [214]. The dosage form is preferably used in triple or quadruple therapies against *H. pylori* infections. The external capsule contains bismuth subcitrate and ornidazole, and the internal capsule contains tetracycline or omeprazole.

Two another patents deal with locally administrable, biodegradable, and sustained-release pharmaceutical compositions of ornidazole for periodontitis [215] and skin injuries [216].

10. REFERENCES

1. S. Budavari, ed., *The Merck Index*, 13th edn., Merck & Co., White House Station, N.J., p. 1229 (2001).
2. *Martindale: The Complete Drug Reference*, 33rd edn., The Pharmaceutical Press, London, p. 599 (2002).
3. J. Elks and C.R. Ganellin ed., *Dictionary of Drugs*, Chapman and Hall, U.K., p. 905 (1990).
4. R.M. McClain and J.C. Downing, *Toxicol. Appl. Pharmacol.*, **92**, 480 (1988).

5. M. Hoffer (Hoffmann-La-Roche), **Neth. Pat. Appl. NL 6606853** (1966); Chem. Abs., **68**, 21933 (1968).
6. M. Hoffer and E. Grunberg, *J. Med. Chem.*, **17**, 1019 (1974).
7. J. Suwinski, A. Rajca, J. Watras, and M. Widel, *Acta. Pol. Pharm.*, **37**, 59 (1980).
8. J. Balak and M. Polievka, **Czech Pat. CS 245808** (1987); Chem. Abs., **110**, 135238 (1989).
9. J. Balak, M. Polievka, and J. Skodova, **Czech Pat. CS 243559** (1987); Chem. Abs., **110**, 57661 (1989).
10. M. Simko, F. Bachraty, E. Zlatinsky, L. David, and A. Rybar, **Czech Pat. CS 237849** (1987); Chem. Abs., **109**, 6511 (1988).
11. J. Jakubcova, L. David, A. Rybar, R. Frimm, and A. Martvon, **Czech Pat. CS 211414** (1984); Chem. Abs., **101**, 151850 (1984).
12. V. Massonneau and M. Mulhauser, **Eur. Pat. Appl. EP 399901** (1990); Chem. Abs., **114**, 122371 (1991).
13. R. Skupin, T.G. Cooper, R. Frohlich, J. Prigge, and G. Haufe, *Tetrahedron Asymmetry*, **8**, 2453 (1997).
14. Database, Panacea Biotech Ltd., Lalru, India.
15. G.C. Forti, M.C. Guerra, A.M. Barbaro, P. Hrelia, G.L. Biagi, and P.A. Borea, *J. Med. Chem.*, **29**, 555 (1986).
16. H.S. Shin, H. Song, E. Kim, and K.B. Chung, *Bull. Korean Chem. Soc.*, **16**, 912 (1995).
17. J.R. Valdes-Santurio, J.A. Martinez Perez, B. Lopez Pelaez, and C. Martinez Manchado, *S.T.P. Pharma Sci.*, **5**, 391 (1995).
18. K. Nagarajan, V. Sudarsanam, P.C. Parthasarathy, V.P. Arya, and S.J. Shenoy, *Ind. J. Chem.*, **21B**, 1006 (1982).
19. S.A.Oezkan, Z. Senturk, and I. Biryol, *Int. J. Pharm.*, **157**, 137 (1997).
20. J.H. Tocher and D.I. Edwards, *Free Radical Res. Commun.*, **4**, 269 (1988).
21. N. Yarlett, T.E. Gorrell, R. Marczak, and M. Muller, *Mol. Biochem. Parasitol.*, **14**, 29 (1985).
22. G. Aicardi, G. Cantelli-Forti, M.C. Guerra, A.M. Barbaro, and G.L. Biagi, *Dev. Oncol.*, **15**, 300 (1983).
23. G. Aicardi, G. Cantelli-Forti, M.C. Guerra, A.M. Barbaro, and G.L. Biagi, *Fortschr. Onkol.*, **10**, 300 (1983).
24. R.J. Knox, D.I. Edwards, and R.C. Knight, *Int. J. Radiat. Oncol. Biol. Phys.*, **10**, 1315 (1984).
25. P.S. Sankar and S.J. Reddy, *Indian J. Environ. Prot.*, **9**, 589 (1989).
26. P.J. Declerck and C.J. De Ranter, *J. Chem. Soc., Faraday Trans. 1*, **83**, 257 (1987).

27. M.R. Hackman and M.A. Brooks, *J. Pharm. Sci.*, **67**, 842 (1978).
28. M.A. Brooks, L.D'Arconte, and J.A.F. De Silva, *J. Pharm. Sci.*, **65**, 112 (1976).
29. J.M. Lopez Fonseca, M.C. Gomez Rivera, and J.C. Garcia Monteagudo, *Anal. Lett.*, **26**, 109 (1993).
30. M. Warowna, Z. Fijalek, A. Dziekanska, and A. Korzeniewska, *Acta Pol. Pharm.*, **48**, 17 (1991).
31. J.H. Tocher and D.I. Edwards, *Free Radical Res. Commun.*, **5**, 327 (1989).
32. D. Barety, B. Resibois, G. Vergoten, and Y. Moschetto, *J. Electroanal. Chem. Interfacial Electrochem.*, **162**, 335 (1984).
33. M.M.A. Hassan, A.I. Jado, and B.E.D.M. El-Shazly, *Spectrosc. Lett.*, **22**, 111 (1989).
34. V. Visan, M.S. Ionescu, M. Dragos, D. Belu, and V. Cosofret, *Rev. Chim. (Bucharest)*, **40**, 728 (1989).
35. M.N. Reddy, G.V.H. Raju, K.N.V. Satyanarayana, K.V.K. Rao, and D.G. Sankar, *J. Inst. Chem. (India)*, **72**, 157 (2000).
36. M.I. Toral, C. Soto, P. Jaque, A.E. Tapia, and P. Richter, *Bol. Soc. Chil. Quim.*, **43**, 349 (1998).
37. A.Z.A. Zuhri, W. Voelter, S. Al-Khalil, and I. Salahat, *Sci. Pharm.*, **68**, 109 (2000).
38. S. Manjunath, K.U.M. Ravi, and S.A. Raju, *Asian J. Chem.*, **12**, 797 (2000).
39. A. Salman and C. Suemer, *Sci. Pharm.*, **64**, 145 (1996).
40. V.V. Padhye, S.J. Kachhwaha, and S.R. Dhaneshwar, *East. Pharm.*, **42**, 121 (1999).
41. T. Daldrup, F. Susanto, and P. Michalke, *Fresenius'Z Anal. Chem.*, **308**, 413 (1981).
42. S.C. Bhatia and V.D. Shanbhag, *J. Chromatogr.*, **305**, 325 (1984).
43. Y.R. Ku, M.J. Tsai, and K.C. Wen, *Yaowu Shipin Fenxi*, **4**, 141 (1996).
44. T. Daldrup, P. Michalke, and W. Boehme, *Chromatogr. Newsl.*, **10**, 1 (1982).
45. M. Bakshi, B. Singh, A. Singh, and S. Singh, *J. Pharm. Biomed. Anal.*, **26**, 891 (2001).
46. www.camag.ch/pdf_dat/a-72_1e.pdf (Internet file).
47. P. Heizmann, R. Geschke, and K.P. Zinapold, *J. Chromatogr.*, **534**, 233 (1990).
48. K. Rona and B. Gachalyi, *J. Chromatogr.*, **420**, 228 (1987).

49. A. Groppi, P. Papa, M. Montagna, and G. Carosi, *J. Chromatogr.*, **380**, 437 (1986).
50. H. Merdjan, C. Bonnat, E. Singlas, and B. Diquet, *J. Chromatogr.*, **273**, 475 (1983).
51. J.N. Colin, B. Diquet, E. Singlas, and A. Thuillier, *Feuill. Biol.*, **22**, 127 (1981).
52. A.M. Taburet, F. Delion, P. Attali, J.J. Thebault, and E. Singlas, *Clin. Pharmacol. Ther.*, **40**, 359 (1986).
53. X.F. Zhu, B. Lin, A. Jakob, S. Wuerthner, and B. Koppenhoefer, *Electrophoresis*, **20**, 1878 (1999).
54. B. Koppenhoefer, A. Jakob, X. Zhu, and B. Lin, *J. High Resolut. Chromatogr.*, **23**, 413 (2000).
55. B. Koppenhoefer, U. Epperlein, A. Jakob, S. Wuerthner, Z. Xiaofeng, and B. Lin, *Chirality*, **10**, 548 (1998).
56. B. Lin, X. Zhu, S. Wuerthner, U. Epperlein, and B. Koppenhoefer, *Talanta*, **46**, 743 (1998).
57. B. Proksa, M. Koos, and B. Steiner, *Chem. Pap.*, **51**, 276 (1997).
58. B. Lin, X. Zhu, B. Koppenhoefer, and U. Epperlein, *LC-GC*, **15**, 44 (1997).
59. B. Koppenhoefer, U. Epperlein, R. Schlunk, X. Zhu, and B. Lin, *J. Chromatogr. A*, **793**, 153 (1998).
60. B. Lin, X.F. Zhu, U. Epperlein, M. Schwierskott, R. Schlunk, and B. Koppenhoefer, *J. High Resolut. Chromatogr.*, **21**, 215 (1998).
61. B. Koppenhoefer, U. Epperlein, X. Zhu, and B. Lin, *Electrophoresis*, **18**, 924 (1997).
62. B. Chankvetadze, G. Endresz, and G. Blaschke, *J. Chromatogr. A*, **700**, 43 (1995).
63. H. Dittmann and W.A. Konig, *J. High Resolut. Chromatogr.*, **23**, 583 (2000).
64. B. Chankvetadze, L. Chankvetadze, S. Sidamonidze, E. Yashima, and Y. Okamoto, *J. Pharm. Biomed. Anal.*, **14**, 1295 (1996).
65. K.H. Pfoertner and J.J. Daly, *Helv. Chim. Acta*, **70**, 171 (1987).
66. C.G.E. Alberola, B.G. Castillo, C.D. Giron, and A.B. Morell, *Farmacia e Clinica*, **11**, 766 (1994).
67. J.M. Rodriguez-Sasiain, M. Prieto, F. Errecalde, N. Jaio, and M.J. Martinez-Bengochea, *Eur. J. Hosp. Pharm.*, **4**, 17 (1994).
68. B. Marciniec and A. Bugaj, *Acta Pol. Pharm.*, **52**, 197 (1995).
69. B. Marciniec, A. Bugaj, and W. Kedziora, *Pharmazie*, **52**, 220 (1997).

70. J.P. Basly, J.L. Duroux, M. Bernard, and B. Penicaut, *J. Chim. Phys. Phys.-Chim. Biol.*, **93**, 1 (1996).
71. P. Wardman, *Life Chem. Rep.*, **3**, 22 (1985).
72. J. Godovic, J. Kucera, and M. Chalabala, *Cesk. Farm.*, **30**, 156 (1981).
73. D.J. Edwards, *Antibiot. Chemother.*, **7**, 404 (1997).
74. E. Winkelmann and W. Raether, *Arzneim.-Forsch.*, **36**, 234 (1986).
75. Y. Wen and R. Zhang, *Yiyao Gongye*, **16**, 324 (1985).
76. P.J. Declerck and C.J. De Ranter, *Analisis*, **15**, 148 (1987).
77. M.V.M. Lafleur, E.J. Pluijmackers-Westmijze, and H. Loman, *Int. J. Radiat. Oncol. Biol. Phys.*, **12**, 1211 (1986).
78. C.W. Plant and D.I. Edwards, *J. Antimicrob. Chemother.*, **2**, 203 (1976).
79. A. Zahoor, M.V.M. Lafleur, R.C. Knight, H. Loman, and D.I. Edwards, *Biochem. Pharmacol.*, **36**, 3299 (1987).
80. R.C. Knight, I.M. Skolimowski, and D.I. Edwards, *Biochem. Pharmacol.*, **27**, 2089 (1978).
81. D.I. Edwards, *J. Antimicrob. Chemother.*, **3**, 43 (1977).
82. D.I. Edwards, M. Dye, and H. Carne, *J. Gen. Microbiol.*, **76**, 135 (1973).
83. D.I. Edwards, R.J. Knox, M.I. Skolimowski, and R.C. Knight, Avail; K.H. Spitzzy and K. Karrer, **Proc. Int. Congr. Chemother.**, **13th**, **2**, 88/105-88/107, Verlag H. Egermann, Vienna (1983).
84. B. Kargul and T. Kadir, *Chemotherapy*, **47**, 203 (2001).
85. S.K. Ray, P. Parimoo, I. Nandi, R. Venkidesh, M.V.S. Murthy, S. Srisunder, V. Anand, K. Rajesh, and N. Rangaraj, *Arzneim.-Forsch.*, **48**, 286 (1998).
86. A.E. Cury and M.P.M. Hirschfeld, *Mycoses*, **40**, 187 (1997).
87. R. Cedillo-Rivera, A. Tapia-Contreras, J. Torres, and O. Munoz, *Arch. Med. Res.*, **28**, 295 (1997).
88. B.D. Mata-Cardenas, J. Vargas-Villarreal, M.T. Gonzalez-Garza, and S. Said-Fernandez, *Pharm. Sci.*, **2**, 513 (1996).
89. K. Nagarajan, R. Gowrishankar, V.P. Arya, T. George, M.D. Nair, S.J. Shenoy, and V. Sudarsanam, *Indian J. Exp. Biol.*, **30**, 193 (1992).
90. R. Lacroix, F. Reynouard, J. Lacroix, and C. Combescot, *Ann. Pharm. Fr.*, **46**, 205 (1988).
91. V.S. Latter and M.A. Walters, *Acta Univ. Carol. Biol.*, **30**, 553 (1988).
92. J. Wuest and U. Hardegger, *Zentralbl. Bakteriol. Mikrobiol. Hyg.*, **267**, 383 (1988).

93. E. Munoz, J. Castella, and J.F. Gutierrez, *Vet. Parasitol.*, **78**, 239 (1998).
94. R. Kadlubowski and P. Wasiewicz, *Wiad. Parazytol.*, **31**, 69 (1985).
95. R. Richle, H.J. Scholer, P. Angehm, M. Fernex, H. Hummler, F. Jeunet, K. Scharer, M. Schupbach, and D.E. Schwartz., *Arzneim.-Forsch.*, **28**, 612 (1978).
96. M. Fernex, F. Jeunet, and R. Richle, **Proc. Int. Congr. Chemother.**, **8th**, **1**, 978, volume date 1973 (1974).
97. C. Kee-Mok, C. Hai-Young, and S. Chin-Thack, *Yonsei Rep. Trop. Med.*, **3**, 123 (1972).
98. S.J. Powell and R. Elsdon-Dew, *Am. J. Trop. Med. Hyg.*, **21**, 518 (1972).
99. A. Ruas, M.H.C. Ramalho, J. Correia Do Valle, and J.R. Ataide, *Cent. Afr. J. Med.*, **19**, 128 (1973).
100. H.R. Wolfensberger, **Proc. Int. Congr. Trop. Med. and Malaria**, **9th**, **Athens** (1973).
101. T.H. Lean and D. Vengadasalam, *Br. J. Vener. Dis.*, **49**, 69 (1973).
102. M.A. Attisso, G. Dusart, M. Simeon de Buochberg, and M. Zuccarelli, *Pathol. Biol.*, **35**, 813 (1987).
103. M.A. Attisso, M. Simeon de Buochberg, G. Dusart, H. Maillols, and M. T. Chateau, *Pharm. Hosp. Fr.*, **77**, 629 (1986).
104. L. Jokipii and A.M.M. Jokipii, *Antimicrob. Agents Chemother.*, **28**, 561 (1985).
105. H. Hof, B. Eisenbarth, A. Denzler, O. Zak, and E. Schweizer, *J. Antimicrob. Chemother.*, **16**, 205 (1985).
106. H. Werner, K. Kuchenbecker, and R. Hammann, *Immun. Infekt.*, **11**, 143 (1983).
107. V. Hingst, E. Von Garrel, and H.G. Sonntag, *Fortschr. Antimikrob. Antineoplastischen. Chemother.*, **2**, 553 (1983).
108. A. Avlami, V. Matsakas, H. Giamarellou, and A. Sahin, *Chemioterapia*, **2**, (5 suppl. **Mediterr. Congr. Chemother, Proc.**, **3rd**, **1982**), 71 (1983).
109. H.M. Bianchini, J. Smayevsky, P. Martini, and A. Roncoroni, *Rev. Argent. Microbiol.*, **13**, 97 (1981).
110. A.V. Reynolds, *J. Antimicrob. Chemother.*, **8**, 91 (1981).
111. C. Romond, C. Lepage, H. Beerens, and A. Miannay, *Rev. Inst. Pasteur Lyon*, **14**, 229 (1981).
112. B. Olsson-Liljequist, and C.E. Nord, *Scand. J. Infect. Dis.*, **26**, 42 (1981).
113. A.V. Reynolds, *J. Pharm. Pharmacol.*, **31**, 29P (1979).

114. A. Palmu, O.V. Renkonen, and V. Aromaa, *J. Infect. Dis.*, **139**, 586 (1979).
115. L. Jokipii and A.M.M. Jokipii, *J. Antimicrob. Chemother.*, **3**, 571 (1977).
116. H. Giamarellou, M. Volanaki, A. Avlami, K. Tsatsiadis, E. Petrochilos, and G.K. Daikos, *Chemotherapy*, **28**, 502 (1982).
117. T.I. Sergeeva, E.P. Zemlyanitskaya, B.S. Ataeva, and L.V. Bol'shakov, *Antibiot. Khimioter.*, **35**, 49 (1990).
118. H. Gnarpe and A. Lundback, *Curr. Chemother.*, **Proc. Int. Congr. Chemother.**, **10th, 1**, 718, Volume date 1977, Am. Soc. Microbiol., Washington D.C. (1978).
119. J.E. Garcia Sanchez, A.C. Gomez Garcia, J. Prieto Prieto, and M.C. Saenz Gonzalez, *Curr. Chemother.*, **Proc. Int. Congr. Chemother.**, **10th, 1**, 289, Volume date 1977, Am. Soc. Microbiol., Washington D.C. (1978).
120. E.J.C. Goldstein, V.L. Sutteer, and S.M. Finegold, *Antimicrob. Agents Chemother.*, **14**, 609 (1978).
121. J.A. Garcia Rodriguez, J.E. Garcia Sanchez, M.C. Saenz Gonzalez, and J. Prieto Prieto, *Pharmatherapeutica*, **1**, 573 (1977).
122. J. Wust, *Antimicrob. Agents Chemother.*, **11**, 631 (1977).
123. A. Dublanchet and R. Durieux, *Ann. Microbiol. (Paris)*, **131 A**, 45 (1980).
124. C. Blomquist and H. Gnarpe, *Drugs Exp. Clin. Res.*, **5**, 5 (1979).
125. R. Erkkola and H. Jarvinen, *Ann. Chir. Gynaecol. Suppl.*, **202**, 94 (1987).
126. M. Wenzel, M. Heinrich, and C. Schmidt, *Pharmatherapeutica*, **4**, 351 (1985).
127. R. Hoel, A. Salveson, S. Reinertsen, C. Neess, and I. Matheson, *Scand. J. Infect. Dis.*, **14**, 135 (1982).
128. L. von Konow and C.E. Nord., *J. Antimicrob. Chemother.*, **11**, 207 (1983).
129. H. Giamarellou, M. Gelnoff-Volanski, M. Avlami, A. Kanellackapoulou, and G.K. Daikos, *J. Antimicrob. Chemother.*, **7**, 569 (1981).
130. T. Meri, T.S. Jokiranta, L. Suhonen, and S. Meri, *J. Clin. Microbiol.*, **38**, 763 (2000).
131. D. Lloyd, N. Yarlett, and N.C. Yarlett, *Biochem. Pharmacol.*, **35**, 61 (1986).
132. A. Mattana, C. Juliano, V. Picci, F. Franconi, and P. Cappuccinelli, *Microbiologica*, **16**, 359 (1993).

133. F. Reynouard, J. Lacroix, R. Lacroix, and C. Combescot, *Bull. Soc. Fr. Parasitol.*, **4**, 7 (1986).
134. N. Yarlett, N.C. Yarlett, and D. Lloyd, *Biochem. Pharmacol.*, **35**, 1703 (1986).
135. A. Kurnatowska, A. Kurnatowska, and E. Horwatt, *Wiad. Parazytol.*, **31**, 169 (1985).
136. A.Kurnatowska, D. Bialasiewicz, and E. Domagalina, *Wiad. Parazytol.*, **31**, 175 (1985).
137. W. Raether and H. Seidenath, *Ann. Trop. Med. Parasitol.*, **77**, 13 (1983).
138. J.G. Meingassner, *Experientia*, **33**, 1160 (1977).
139. J.G. Meingassner and H. Mieth, *Arzneim.-Forsch.*, **27**, 638 (1977).
140. E. Grunberg, R. Cleeland, H.N. Prince, and E.H. Titsworth, *Proc. Soc. Exp. Biol. Med.*, **133**, 490 (1970).
141. F. Saracoglu, K. Gol, I. Sahin, B. Turkkani, C. Atalay, and C. Oztopcu, *Int. J. Gynecol. Obstet.*, **62**, 59 (1998).
142. J.G.E.M. Linder, F.H.F. Plantema, N.M. de Vos, and A.A. Hoogkamp-Korstanje, *Chemotherapy*, **25**, 243 (1979).
143. T. Chintana, P. Sucharit, V. Mahakittikun, C. Siripanth, and W. Suphadtanaphongs, *Southeast Asian J. Trop. Med. Public Health*, **17**, 591 (1986).
144. K. Nagarajan, V.P. Arya, T. George, M.D. Nair, V. Sudarsanam, D.K. Ray, and V.B. Shrivastava, *Indian J. Chem.*, **23B**, 342 (1984).
145. D.K. Ray, V.B. Shrivastava, J.S. Tendulkar, A.K. Dutta, K.K. Bhopale, D.K. Chatterjee, and K. Nagarajan, *Ann. Trop. Med. Parasitol.*, **77**, 287 (1983).
146. J. Savel, *Ann. Pharm. Fr.*, **34**, 249 (1976).
147. P.F.L. Boreham, R.E. Phillips, and R.W. Shepherd, *J. Antimicrob. Chemother.*, **16**, 589 (1985).
148. P.F.L. Boreham, R.E. Phillips, and R.W. Shepherd, *J. Antimicrob. Chemother.*, **18**, 393 (1986).
149. B.U. Bulut, S.B. Gulnar, and D. Aysev, *Scand. J. Infect. Dis.*, **28**, 493 (1996).
150. R. Kuzmicki and J. Jeske, *Wiad. Parazytol.*, **40**, 65 (1994).
151. B. Oren, E. Schgurensky, M. Ephros, I. Tamir, and R. Raz, *Eur. J. Clin. Microbiol. Infect. Dis.*, **10**, 963 (1991).
152. A. Degremont, D. Sturchler, E. Wolfensberger, and B. Osterwalder, *Schweiz. Med. Wochenschr.*, **111**, 2039 (1981).
153. H.P.T. Werkman and J.H.E.T. Meuwissen, *Lancet*, **2**, 1373 (1979).

154. J.S. Ryu, D.Y. Min, M.C. Kim, N.S. Kim, and M.H. Shin, *J. Microbiol. Biotechnol.*, **11**, 124 (2001).
155. R. Piccolomini, A. Arpini, L. Cellini, and M. Pagano, *Boll. Ist Sieroter. Milan*, **62**, 257 (1983).
156. I. M. Madinier, T.B. Fosse, C. Hitzig, Y. Charbit, and L.R. Hannoun, *J. Periodontol.*, **70**, 888 (1999).
157. H. Hof and V. Sticht-Groh, *Infection* (Munich), **12**, 36 (1984).
158. F.S. Lehmann, J. Drewe, L. Terracciano, and C. Beglinger, *Aliment. Pharmacol. Ther.*, **14**, 305 (2000).
159. A. Uygun, Y. Ates, A. Erdil, A. Kadayifci, C. Cetin, M. Gulsen, N. Karaeren, and K. Dagalp, *Clin. Ther.*, **21**, 1539 (1999).
160. M. Tzivras, A. Archimandritis, V. Balatsos, V. Delis, S. Souyioultzis, N. Skandalis, E. Kanellopoulou, Z. Manika, and P. Davaris, *Eur. J. Gastroenterol. Hepatol.*, **9**, 1185 (1997).
161. A. Dublanchet, J. Caillon, J.P. Emond, H. Chardon, and H.B. Drugeon, *Eur. J. Clin. Microbiol.*, **5**, 346 (1986).
162. H. Andrews, *New Ethicals*, **2**, 21 (1999).
163. *IJCP's Medinews*, ed. K.K. Aggarwal, IJCP Publication (P) Ltd., New Delhi, June, 16–30, 21 (2000).
164. J.K. Triantafillidis, D. Nicolakis, A. Emmanoullidis, A. Antoniou, K. Papatheodorou, and P. Cheracakis, *Ital. J. Gastroenterol.*, **28**, 10 (1996).
165. J.K. Triantafillidis, A. Antoniou, A. Emmanoulidis, D. Nicolakis, C. Barbatzas, and P. Cheracakis, *Ital. J. Gastroenterol. Hepatol.*, **30**, 446 (1998).
166. G. Adams, D. Naughton, and I. Stratford, **PCT Intl. Appl. WO 9912548** (1999); *Chem. Abs.*, **130**, 232488 (1999).
167. G. Adams, D. Naughton, and I. Stratford, **PCT Intl. Appl. WO 9912547** (1999); *Chem. Abs.*, **130**, 232487 (1999).
168. D.E. Schwartz and F. Jeunet, *Chemotherapy*, **22**, 19 (1976).
169. I. Matheson, K.H. Johannessen, and B. Bjorkvoll, *Br. J. Vener. Dis.*, **53**, 236 (1977).
170. L. Guyot, C.M. Gelec, J. Moreau, O. Varoquaux, and M. Pays, *Therapie*, **42**, 201 (1987).
171. C. Martin, B. Bruguerolle, M.N. Mallet, M. Condomines, B. Sastre, and F. Gouin, *Antimicrob. Agents Chemother.*, **34**, 1921 (1990).
172. K.C. Lamp, C.D. Freeman, N.E. Klutman, and M.K. Lacy, *Clin. Pharmacokinetics*, **36**, 353 (1999).
173. M. Armengaud, J.C. Auvergnat, P. Belgaric, V.T. Tran, N. Picot, and D.E. Schwartz, *Curr. Chemother.*, **Proc. Int. Congr. Chemother.**, **10th**, **1**, 723, Volume date 1977 (1978).

174. A.M.M. Jokipii and L. Jokipii, *Infection (Munich)*, **8**, 101 (1980).
175. A. Steib, B. Jacobberger, M. Von Bandel, F. Beck, and J.C. Otteni, *Antimicrob. Agents Chemother.*, **37**, 1873 (1993).
176. A. Turcant, J.C. Granry, P. Allain, and M. Cavellat, *Eur. J. Clin. Pharmacol.*, **32**, 111 (1987).
177. J. Helmbrecht and H. Schweitzer, *Blutalkohol*, **18**, 29 (1981).
178. P. Bourget, P. Attali, F. Delion, E. Singlas, and A.M. Taburet, *J. Pharm. Clin.*, **7**, 25 (1988).
179. A.M. Taburet, P. Attali, P. Bourget, J.P. Etienne, and E. Singlas, *Clin. Pharmacol. Ther.*, **45**, 373 (1989).
180. H. Merdjan, A. Baumelou, B. Diquet, O. Chick, and E. Singlas, *Br. J. Clin. Pharmacol.*, **19**, 211 (1985).
181. A. Baumelou, A. Bentchikou, R. Brouard, E. Singlas, and M. Legrain, *J. Pharm. Clin.*, **5**, 73 (1986).
182. M. Boeckh, H. Lode, K.M. Deppermann, S. Grineisen, F. Shokry, R. Held, K. Wernicke, P. Koeppe, and J. Wagner, *Antimicrob. Agents Chemother.*, **34**, 2407 (1990).
183. D.E. Schwartz, J.C. Jordan, W. Vetter, and G. Oesterheld, *Xenobiotica*, **9**, 571 (1979).
184. C.E. Voogd, J.J. Van der Stel, and J.J.J.A.A. Jacobs, *Mutat. Res.*, **48**, 155 (1977).
185. G.L. Biagi, G. Cantelli-Forti, A.M. Barbaro, M.C. Guerra, P. Hrelia, and P.A. Borea, *J. Med. Chem.*, **30**, 420 (1987).
186. G.L. Biagi, A.M. Barbaro, M.C. Guerra, G. Cantelli-Forti, G. Aicardi, and P.A. Borea, *Teratog. Carcinog. Mutagen.*, **3**, 429 (1983).
187. G. Cantelli-Forti, G. Aicardi, M.C. Guerra, A.M. Barbaro, and G.L. Biagi, *Teratog. Carcinog. Mutagen.*, **3**, 51 (1983).
188. J.B. Chin, D.M.K. Sheinin, and A.M. Rauth, *Mutat. Res.*, **58**, 1 (1978).
189. C.E. Voogd, J.J. Van der Stel, and J.J.J.A.A. Jacobs, *Mutat. Res.*, **66**, 207 (1979).
190. M. Cerna, L. Dobias, V. Hajek, P. Rossner, and R.J. Sram, *Cesk. Farm.*, **39**, 127 (1990).
191. G. Cantelli-Forti, M.C. Guerra, P. Hrelia, A.M. Barbaro, and G.L. Biagi, *Drugs Exp. Clin. Res.*, **10**, 325 (1984).
192. G. Cantelli-Forti, M.C. Guerra, M. Scotti, P. Hrelia, M. Paolini, and G.L. Biagi, *Arch. Toxicol.*, **13**, 333 (1989).

193. W.H. Byeon, H.H. Hyun, and S.Y. Lee, *Misaengmul Hakhoe Chi*, **14**, 151 (1976).
194. K. Schaerer, *Verh. Deut. Ges. Pathol.*, **56**, 407 (1972).
195. R.M. McClain and J.C. Downing, *Toxicol. Appl. Pharmacol.*, **92**, 488 (1988).
196. G.P. Toth, S.R. Wang, H. McCarthy, D.R. Tocco, and M.K. Smith, *Reprod. Toxicol.*, **6**, 507 (1992).
197. G. Oberlaender, C.H. Yeung, and T.G. Cooper, *J. Reprod. Fertil.*, **100**, 551 (1994).
198. C.H. Yeung, G. Oberlaender, and T.G. Cooper, *J. Reprod. Fertil.*, **103**, 257 (1995).
199. G. Oberlaender, C.H. Yeung, and T.G. Cooper, *J. Reprod. Fertil.*, **106**, 231 (1996).
200. A.R. Jones and T.G. Cooper, *Xenobiotica*, **27**, 711 (1997).
201. T.G. Cooper, C.H. Yeung, R. Skupin, and G. Haufe, *J. Androl.*, **18**, 431 (1997).
202. W. Bone, C.H. Yeung, R. Skupin, G. Haufe, and T.G. Cooper, *Int. J. Androl.*, **20**, 347 (1997).
203. W. Bone and T.G. Cooper, *Int. J. Androl.*, **23**, 284 (2000).
204. W. Bone, N.G. Jones, G. Kamp, C.H. Yeung, and T.G. Cooper, *J. Reprod. Fertil.*, **118**, 127 (2000).
205. A. Wagenfeld, C.H. Yeung, S. Shivaji, V.R. Sundareswaran, H. Ariga, and T.G. Cooper, *J. Androl.*, **21**, 954 (2000).
206. F. Delion, J.J. Thebault, and E. Singlas, *J. Pharm. Clin.*, **4**, 301 (1985).
207. P. Bourget, N. Dechelette, H. Fernandez, and V.Q. Desmaris, *J. Antimicrob. Chemother.*, **35**, 691 (1995).
208. M.B. Fawzi, **Brit. UK Pat. Appl. GB 2000025** (1979), *Chem. Abs.*, **91**, 181447 (1979).
209. F. Dietlin, D. Fredj, and B. Dinnequin, **Fr. Demande FR 2624736** (1989); *Chem. Abs.*, **112**, 125222 (1990).
210. M. Asikoglu, L. Kirilmaz, O. Cagliyan, and P. Unak, *Acta Pharm. Turc.*, **41**, 1 (1999).
211. D. Matusova, *Cesko-Slov. Farm.*, **42**, 279 (1993).
212. A. Singh and R. Jain (Panacea Biotec Ltd., New Delhi), **PCT Int. Appl. WO 2000042987** (2000); *Chem. Abs.*, **133**, 125302 (2000).
213. M. Kist and N. Otterbeck, **Ger. Pat. DE 19850445** (2000); *Chem. Abs.*, **132**, 313708 (2000).

- 214. G. Sanso, **PCT Intl. Appl. WO 9930693** (1999); Chem. Abs., **131**, 49489 (1999).
- 215. J.Y. Lee, M.Y. Seo, I.J. Choi, J.H. Kim, and C.M. Pai, **PCT Int. Appl. WO 9744016** (1997), Chem. Abs. **128**, 53237 (1998).
- 216. M. Dittrich, P. Jilek, L. Hajkova, V. Fanta, J. Dolczalova, M. Vackova, V. Buchta, M. Hartmanova, J. Mraz, and Z. Hajzman, **Czech Pat. CZ 282292** (1997); Chem. Abs., **128**, 132410 (1998).

Sertraline (*L*)-Lactate: Comprehensive Profile

Michael D. Likar,¹ Jon Bordner,² Diane M. Rescek³ and
Thomas R. Sharp¹

¹*Analytical Research and Development*

²*Chemical Research and Development*

³*Exploratory Medicinal Sciences*

Pfizer Inc.

Pfizer Global Research and Development

Groton, CT 06340

USA

CONTENTS

1.	Description	187
1.1	Nomenclature	187
1.1.1	Systematic chemical name.	187
1.1.2	Nonproprietary names	187
1.2	Formulae.	187
1.2.1	Empirical formula, molecular weight, CAS number	187
1.2.2	Structural formula	187
1.3	Elemental analysis	188
1.4	Appearance	188
1.5	Uses and applications	188
2.	Methods of Preparation	188
3.	Physical Properties	189
3.1	Ionization constants	189
3.2	Solubility characteristics	190
3.3	Hygroscopicity.	190
3.4	Particle morphology	191
3.5	Crystallographic properties	191
3.5.1	Single crystal structure	191
3.5.2	X-ray powder diffraction pattern.	203
3.6	Thermal methods of analysis.	212
3.6.1	Melting behavior	212
3.6.2	Differential scanning calorimetry.	212
3.6.3	Thermogravimetric analysis	213
3.7	Spectroscopy	213
3.7.1	UV–VIS spectroscopy	213
3.7.2	Vibrational spectroscopy	214
3.7.3	Nuclear magnetic resonance spectrometry	214
3.8	Mass spectrometry	220
4.	Methods of Analysis	224
4.1	Identification	224
4.2	Titrimetric analysis.	229
4.3	Quantitation of lactic acid.	230
4.4	Thin-layer chromatography.	230
4.5	High-performance liquid chromatography	230
5.	Stability	231
5.1	Forced degradation studies	231
5.2	Solid-state stability.	231
6.	Acknowledgments	233
7.	References	233

1. DESCRIPTION

1.1 Nomenclature

1.1.1 Systematic chemical name

(1*S*-*cis*)-4-(3,4-dichlorophenyl)-1,2,3,4-tetrahydro-*N*-methyl-1-naphthalenamine (*S*)-2-hydroxypropanoate

1.1.2 Nonproprietary names

Sertraline (*L*)-lactate

Sertraline (*L*)-(+)-lactate

1.2 Formulae

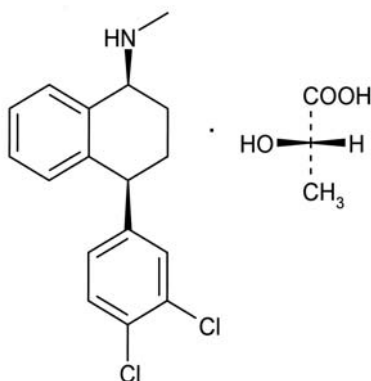
1.2.1 Empirical formula, molecular weight, CAS number

The empirical formulas and molecular weights of sertraline, sertraline hydrochloride, and sertraline (*L*)-lactate are as follows:

	Empirical formula	Molecular weight
Sertraline	$C_{17}H_{17}NCl_2$	306.23
Sertraline Hydrochloride	$C_{17}H_{17}NCl_2 \cdot HCl$	342.69
Sertraline (<i>L</i>)-Lactate	$C_{17}H_{17}NCl_2 \cdot C_3H_6O_3$	396.31

CAS numbers: 79617-96-2 (Sertraline) and 79559-97-0 (Sertraline hydrochloride).

1.2.2 Structural formula



1.3 Elemental analysis

The calculated elemental composition of sertraline (*L*)-lactate is as follows:

carbon:	60.61%
hydrogen:	5.85%
oxygen:	12.11%
nitrogen:	3.53%
chlorine:	17.89%

1.4 Appearance

Sertraline (*L*)-lactate is a white to off-white crystalline powder.

1.5 Uses and applications

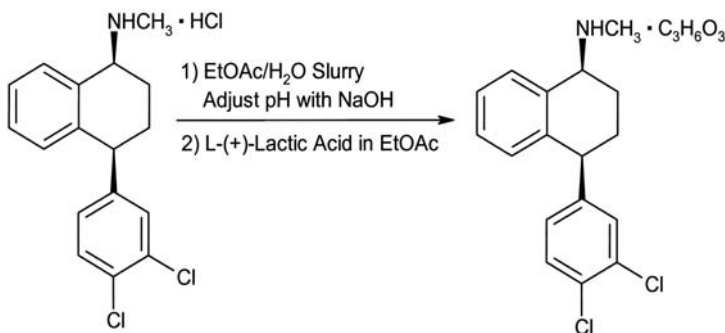
Sertraline is a selective serotonin reuptake inhibitor (SSRI) used to treat depression, obsessive-compulsive disorder, panic disorder, and posttraumatic stress disorder [1, 2]. ZOLOFT® (sertraline hydrochloride) tablets and oral concentrate are available for oral administration. The tablets contain sertraline hydrochloride in amounts equivalent to 25, 50, and 100 mg of sertraline. The oral concentrate contains 20 mg/mL of sertraline. ZOLOFT is administered once daily at doses between 25 and 200 mg.

Sertraline (*L*)-lactate is a physically and chemically stable salt of sertraline that is more soluble in water than the free base or hydrochloride salt. These properties of sertraline (*L*)-lactate make it well suited for use in pharmaceutical dosage forms such as sustained-release tablets [3, 4].

2. METHODS OF PREPARATION

Sertraline (*L*)-lactate can be prepared from sertraline hydrochloride, sertraline mandelate, or sertraline free base [4], the syntheses of which have been previously published [2].

Sertraline (*L*)-lactate can be prepared from sertraline hydrochloride as illustrated in the following scheme:



First, sertraline hydrochloride is slurried in a mixture of water and ethyl acetate. To this slurry, a dilute aqueous solution of sodium hydroxide is added to neutralize the hydrochloride salt and thereby produce the free base of sertraline. The pH of the mixture is maintained between 6.5 and 9.5. Concurrently, the free base of sertraline is extracted into the organic phase. The organic phase is then separated from the aqueous solution and washed with water to remove any remaining chloride ions. The temperature of the organic solution is increased to approximately 40°C and a molar excess (*e.g.*, 5%) of *L*-(+)-lactic acid is added while stirring the mixture. Sertraline (*L*)-lactate precipitates as a crystalline solid. The product may be granulated at 25–30°C for several hours. The crystals are then collected by filtration, washed with ethyl acetate, and dried at elevated temperature (30–60°C) and reduced pressure for 24–48 h. Milling may be used to reduce the particle size of the drug substance.

3. PHYSICAL PROPERTIES

3.1 Ionization constants

The pK_a of sertraline, as determined by the potentiometric titration of sertraline (*L*)-lactate in a 1 : 1 v/v solvent mixture of ethanol and water, was found to be 8.6. This pK_a is essentially the same as that measured for sertraline hydrochloride (pK_a = 8.5) [2].

3.2 Solubility characteristics

The equilibrium solubility of sertraline (*L*)-lactate in water and other solvents was determined by preparing saturated solutions. These solutions were subsequently filtered, diluted, and assayed by reversed-phase high-performance liquid chromatography (HPLC).

The solubility of sertraline (*L*)-lactate in water at 25°C is approximately 125 mg/mL [3, 4], which is significantly higher than that of sertraline hydrochloride (3.8 mg/mL) [2]. The pH of a saturated solution of sertraline (*L*)-lactate was approximately 5.1.

The aqueous solubility of sertraline (*L*)-lactate, however, is highly dependent on the presence of other dissolved compounds (such as chloride ions, organic acids, calcium salts, *etc.*) and pH [3]. Sertraline free base will precipitate when its salts are subjected to basic conditions.

The solubility of sertraline (*L*)-lactate in a number of non-aqueous solvents at ambient temperature is as follows:

Solvent	Solubility (mg/mL)
Methylene chloride	118
Methanol	40
Isopropyl alcohol	19
Ethyl acetate	4.7
Acetonitrile	3.0
Hexane	< 0.03

These results indicate that sertraline (*L*)-lactate is soluble in methylene chloride and methanol, and practically insoluble in hexane.

3.3 Hygroscopicity

The hygroscopicity of sertraline (*L*)-lactate was studied using a controlled relative-humidity microbalance (VTI Corporation). The moisture

isotherms at 25°C were collected over the relative humidity range of 10–98%. As shown in Figure 1, the hysteresis between the adsorption curve and the subsequent desorption curve is insignificant. The drug substance adsorbs less than 0.1% water at relative humidities up to approximately 85%. Based on these results, sertraline (L)-lactate is considered nonhygroscopic.

3.4 Particle morphology

The particle morphology of sertraline (L)-lactate was studied using optical microscopy and scanning electron microscopy. The particles exhibited birefringence. As shown in Figure 2, aggregates of microcrystalline particles were observed. Although crystallization conditions can affect particle size, crystallization of sertraline (L)-lactate from ethyl acetate consistently produces one crystal form.

3.5 Crystallographic properties

3.5.1 Single crystal structure

Crystallographic quality crystals were obtained from ethyl acetate. A representative crystal was surveyed, and a 1 Å data set (maximum

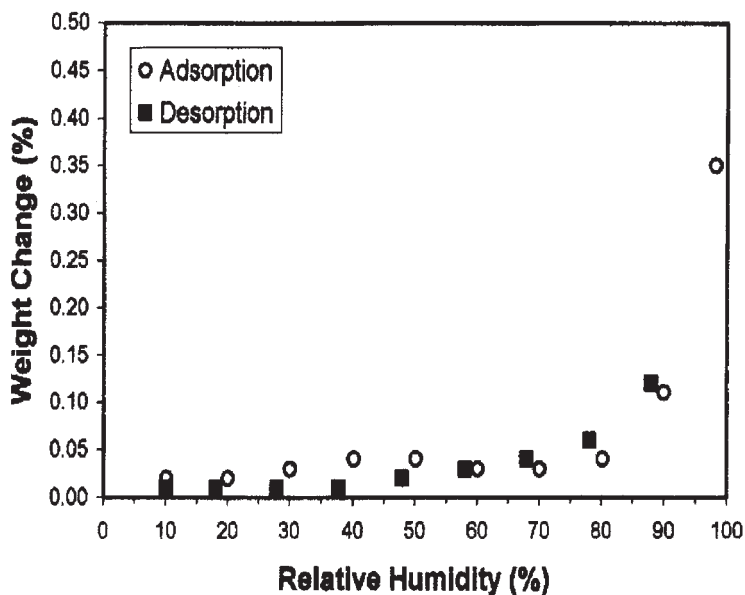


Figure 1. Moisture isotherms of sertraline (L)-lactate.



Figure 2. Scanning electron photomicrograph of sertraline (*L*)-lactate, obtained at a magnification of 100 \times .

$\sin \theta/\lambda = 0.5$) was collected using a Siemens R3RA/v diffractometer. Atomic scattering factors were taken from the International Tables for X-ray Crystallography [5]. All crystallographic calculations were facilitated by the SHELXTL system [6]. All diffractometer data were collected at room temperature. Pertinent crystal, data collection, and refinement information are summarized in Table 1. The numbers in parentheses are estimated standard deviations.

Table 1

Crystal Data and Structure Refinement for Sertraline (*L*)-Lactate

Empirical formula	$\text{C}_{17}\text{H}_{18}\text{NCl}_2^+\text{C}_3\text{H}_5\text{O}_3^-$
Formula weight	396.31
Temperature	293(2) K
Wavelength	1.54178 Å
Crystal system	Monoclinic
Space group	P2(1)
Unit cell dimensions	$a = 8.660(5)$ Å
	$b = 24.429(12)$ Å
	$c = 9.382(3)$ Å
	$\alpha = 90^\circ$
	$\beta = 91.94(3)^\circ$
	$\gamma = 90^\circ$
Volume	$1983.7(16)$ Å ³
Molecules/unit cell	4
Calculated density	1.327 g/cm ³
Absorption coefficient	3.101 mm ⁻¹
F(000)	832
Crystal size	$0.11 \times 0.07 \times 0.07$ mm ³

(continued)

Table 1 (continued)

Reflections collected	2273
Independent reflections	2103[R(int) = 0.0339]
Refinement method	Full-matrix least-squares on F^2
Data/restraints/parameters	2103/0/474
Goodness-of-fit on F^2	0.967
Final R indices [$I > 2\sigma(I)$]	$R1 = 0.0545$, $wR2 = 0.1288$
Absolute structure parameter	0.01 (4)
Largest difference peak and hole	0.201 and -0.261 eA^{-3}

A trial structure was obtained using the direct method, which was found to refine in a routine manner. Hydrogen positions were calculated wherever possible. The methyl hydrogens and hydrogens on nitrogen were located by difference Fourier techniques and then idealized. The hydrogens on oxygen were located by difference Fourier techniques and allowed to refine. The hydrogen parameters were added to the structure factor calculations but were not refined. The shifts calculated in the final cycles of least squares refinement were all less than 0.1 of the corresponding standard deviations. The final R -index was 5.45%. A final difference Fourier revealed no missing or misplaced electron density.

The refined structure in [Figure 3](#) was plotted using the SHELXTL plotting package. The absolute configuration was determined by the method of Ibers and Hamilton [7, 8]. The X-ray absolute configuration was in agreement with an (*S*)-lactate configuration. Coordinates, anisotropic temperature factors, distances, and angles are given in [Tables 2–6](#). The X-ray analysis confirms the structure of sertraline (*L*)-lactate.

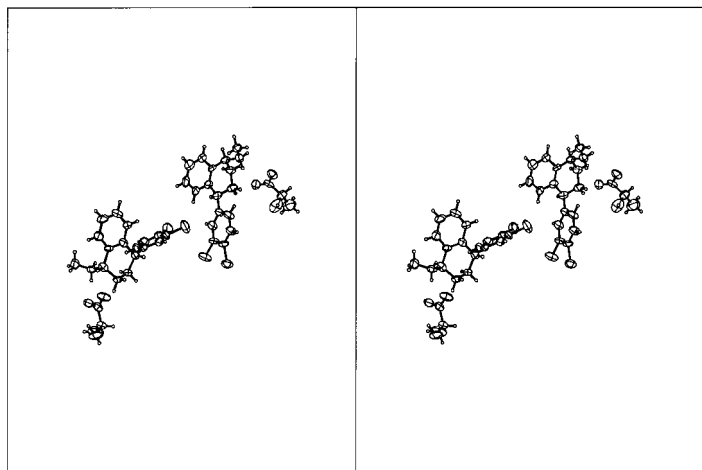
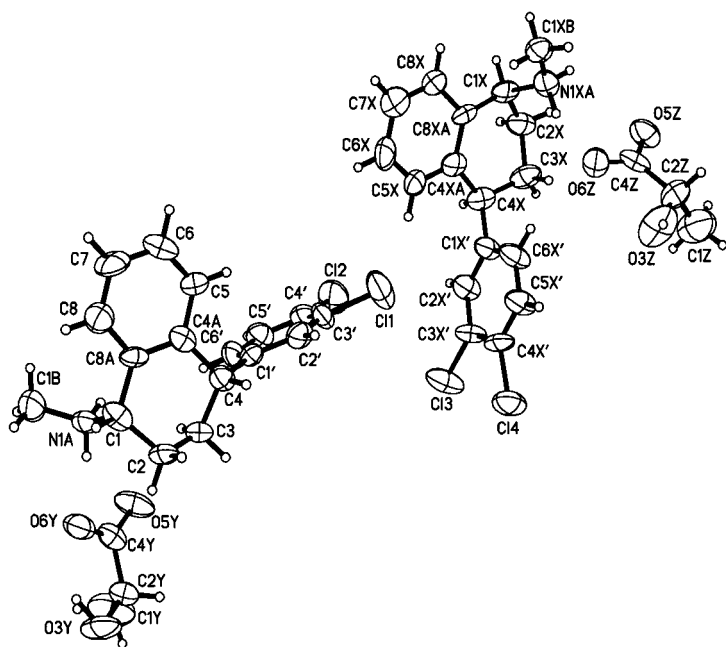


Figure 3. Structure derived for sertraline (*L*)-lactate from a single crystal X-ray analysis. A stereoscopic view of the molecular conformation is shown below.

Table 2

Atomic Coordinates ($\times 10^4$) and Equivalent Isotropic Displacement Parameters ($\text{\AA}^2 \times 10^3$) for Sertraline (*L*)-Lactate

	<i>x</i>	<i>y</i>	<i>z</i>	<i>U</i> (eq)		<i>x</i>	<i>y</i>	<i>z</i>	<i>U</i> (eq)
C(1)	−4183(15)	4373(5)	7863(11)	49(3)	C(4XA)	703(14)	6584(5)	−3160(12)	48(3)
N(1A)	−4127(11)	3769(5)	7470(9)	49(3)	C(5X)	−48(17)	6300(6)	−2105(13)	58(4)
C(1B)	−5562(16)	3456(7)	7618(14)	72(4)	C(6X)	−1591(19)	6298(5)	−2002(16)	67(4)
C(2)	−2558(14)	4577(6)	8225(11)	54(3)	C(7X)	−2501(17)	6605(7)	−2959(17)	79(4)
C(3)	−1665(14)	4611(6)	6888(12)	55(3)	C(8X)	−1804(16)	6889(6)	−4027(14)	61(4)
C(4)	−2324(13)	5029(5)	5832(11)	47(3)	C(8XA)	−188(13)	6896(5)	−4111(11)	45(3)
C(4A)	−4075(13)	4979(5)	5663(11)	43(3)	C(1X')	3232(15)	6544(6)	−1788(12)	54(3)
C(5)	−4881(16)	5268(6)	4578(12)	54(3)	C(2X')	3953(15)	6082(5)	−1250(12)	57(4)
C(6)	−6418(18)	5253(6)	4430(14)	67(4)	C(3X')	4646(14)	6086(6)	98(12)	53(3)
C(7)	−7291(15)	4981(6)	5426(16)	70(4)	Cl(3)	5554(5)	5501(2)	742(4)	86(1)

C(8)	−6565(16)	4707(6)	6501(14)	58(4)
C(8A)	−4953(14)	4695(5)	6661(11)	41(3)
C(1′)	−1530(13)	5020(5)	4408(11)	45(3)
C(2′)	−1021(14)	5518(6)	3799(13)	56(3)
C(3′)	−303(15)	5492(5)	2503(13)	53(3)
Cl(1)	241(6)	6116(2)	1755(4)	92(2)
C(4′)	−13(15)	5017(6)	1815(12)	57(3)
Cl(2)	972(5)	4996	260(3)	82(1)
C(5′)	−492(15)	4541(6)	2425(13)	55(3)

C(4X′)	4723(15)	6565(7)	877(12)	58(4)
C1(4)	5698(5)	6600(2)	2531(3)	79(1)
C(5X′)	3974(17)	7025(5)	354(13)	65(4)
C(6X′)	3280(17)	7006(5)	−983(12)	65(4)
C(1Y)	1330(20)	2577(7)	9572(17)	110(6)
C(2Y)	550(14)	3117(6)	9848(13)	56(4)
O(3Y)	103(13)	3152(5)	11262(9)	91(4)
C(4Y)	−785(18)	3215(5)	8797(13)	52(3)
O(5Y)	−482(12)	3257(5)	7514(9)	86(3)

(continued)

Table 2 (Continued)

	x	y	z	$U(\text{eq})$			x	y	z	$U(\text{eq})$
C(6')	-1227(15)	4534(5)	3693(13)	54(3)		O(6Y)	-2089(13)	3238(4)	9294(9)	68(3)
C(1X)	509(15)	7221(6)	-5299(12)	50(3)		C(1Z)	6328(19)	8751(9)	-2625(18)	112(6)
N(1XA)	645(13)	7825(5)	-4928(10)	56(3)		C(2Z)	4662(16)	8842(7)	-2426(14)	67(4)
C(1XB)	-808(15)	8110(5)	-4597(13)	60(4)		O(3Z)	4354(17)	8756(6)	-998(11)	106(6)
C(2X)	2120(16)	7019(6)	-5602(13)	69(4)		C(4Z)	3600(17)	8478(6)	-3355(13)	53(3)
C(3X)	3139(15)	6940(6)	-4273(11)	64(4)		O(5Z)	3796(11)	8494(4)	-4678(8)	68(3)
C(4X)	2443(14)	6525(5)	-3250(11)	50(3)		O(6Z)	2598(11)	8204(4)	-2781(8)	62(2)

$U(\text{eq})$ is defined as one-third of the trace of the orthogonalized U_{ij} tensor.

Table 3

Bond Lengths (Å) for Sertraline (*L*)-Lactate

C(1)–N(1A)	1.521(14)	C(3X)–C(4X)	1.534(17)
C(1)–C(2)	1.521(17)	C(4X)–C(1X')	1.512(15)
C(1)–C(8A)	1.510(15)	C(4X)–C(4XA)	1.519(16)
N(1A)–C(1B)	1.470(15)	C(4XA)–C(8XA)	1.388(16)
C(2)–C(3)	1.498(15)	C(4XA)–C(5X)	1.388(17)
C(3)–C(4)	1.521(16)	C(5X)–C(6X)	1.343(18)
C(4)–C(4A)	1.525(15)	C(6X)–C(7X)	1.393(19)
C(4)–C(1')	1.523(15)	C(7X)–C(8X)	1.375(18)
C(4A)–C(5)	1.405(15)	C(8X)–C(8XA)	1.404(16)
C(4A)–C(8A)	1.409(15)	C(1X')–C(6X')	1.358(17)
C(5)–C(6)	1.334(17)	C(1X')–C(2X')	1.375(17)
C(6)–C(7)	1.391(19)	C(2X')–C(3X')	1.382(16)
C(7)–C(8)	1.349(18)	C(3X')–C(4X')	1.381(18)
C(8)–C(8A)	1.400(16)	C(3X')–Cl(3)	1.730(12)
C(1')–C(6')	1.394(16)	C(4X')–C(5X')	1.379(17)
C(1')–C(2')	1.420(17)	C(4X')–Cl(4)	1.744(11)
C(2')–C(3')	1.386(17)	C(5X')–C(6X')	1.373(16)
C(3')–C(4')	1.355(17)	C(1Y)–C(2Y)	1.507(18)
C(3')–Cl(1)	1.750(12)	C(2Y)–O(3Y)	1.397(14)

(continued)

Table 3 (continued)

C(4')–C(5')	1.367(17)	C(2Y)–C(4Y)	1.514(17)
C(4')–Cl(2)	1.716(13)	C(4Y)–O(5Y)	1.245(14)
C(5')–C(6')	1.368(15)	C(4Y)–O(6Y)	1.238(14)
C(1X)–C(8XA)	1.511(16)	C(1Z)–C(2Z)	1.478(19)
C(1X)–N(1XA)	1.521(16)	C(2Z)–O(3Z)	1.391(18)
C(1X)–C(2X)	1.516(17)	C(2Z)–C(4Z)	1.530(18)
N(1XA)–C(1XB)	1.479(15)	C(4Z)–O(6Z)	1.234(15)
C(2X)–C(3X)	1.515(15)	C(4Z)–O(5Z)	1.258(13)

Table 4

Bond Angles (°) for Sertraline (*L*)-Lactate

N(1A)–C(1)–C(2)	109.5(10)	C(3X)–C(2X)– C(1X)	113.7(11)
N(1A)–C(1)–C(8A)	109.9(9)	C(2X)–C(3X)– C(4X)	111.6(11)
C(2)–C(1)–C(8A)	112.2(10)	C(1X')–C(4X)– C(4XA)	111.4(10)
C(1B)–N(1A)–C(1)	116.6(10)	C(1X')–C(4X)– C(3X)	111.9(10)

(continued)

Table 4 (continued)

C(3)–C(2)–C(1)	109.3(9)	C(4XA)–C(4X)– C(3X)	112.6(10)
C(2)–C(3)–C(4)	113.0(10)	C(8XA)– C(4XA)–C(5X)	117.9(12)
C(4A)–C(4)–C(1')	112.6(9)	C(8XA)– C(4XA)–C(4X)	123.2(12)
C(4A)–C(4)–C(3)	111.3(10)	C(5X)–C(4XA)– C(4X)	118.8(11)
C(1')–C(4)–C(3)	113.0(10)	C(6X)–C(5X)– C(4XA)	123.0(13)
C(5)–C(4A)–C(8A)	117.6(11)	C(5X)–C(6X)– C(7X)	119.6(14)
C(5)–C(4A)–C(4)	120.2(11)	C(6X)–C(7X)– C(8X)	119.3(14)
C(8A)–C(4A)–C(4)	121.9(10)	C(7X)–C(8X)– C(8XA)	120.6(12)
C(6)–C(5)–C(4A)	122.1(12)	C(4XA)– C(8XA)–C(8X)	119.4(12)
C(5)–C(6)–C(7)	120.4(12)	C(4XA)– C(8XA)–C(1X)	122.4(11)
C(8)–C(7)–C(6)	119.3(13)	C(8X)–C(8XA)– (C1X)	118.1(11)
C(7)–C(8)–C(8A)	122.0(13)	C(6X')–C(1X')– C(2X')	118.2(10)

(continued)

Table 4 (continued)

C(8)–C(8A)–C(4A)	118.5(10)	C(6X')–C(1X')–C(4X)	122.3(11)
C(8)–C(8A)–C(1)	120.3(11)	C(2X')–C(1X')–C(4X)	119.5(12)
C(4A)–C(8A)–C(1)	121.2(11)	C(1X')–C(2X')–C(3X')	120.6(12)
C(6')–C(1')–C(2')	118.1(10)	C(2X')–C(3X')–C(4X')	120.0(11)
C(6')–C(1')–C(4)	122.2(11)	C(2X')–C(3X')–C1(3)	119.5(10)
C(2')–C(1')–C(4)	119.7(11)	C(4X')–C(3X')–C1(3)	120.2(9)
C(3')–C(2')–C(1')	117.9(11)	C(5X')–C(4X')–C(3X')	119.3(9)
C(4')–C(3')–C(2')	123.6(11)	C(5X')–C(4X')–C1(4)	119.0(11)
C(4')–C(3')–Cl(1)	119.9(10)	C(3X')–C(4X')–C1(4)	121.7(10)
C(2')–C(3')–Cl(1)	116.5(10)	C(6X')–C(5X')–C(4X')	118.8(11)
C(3')–C(4')–C(5')	117.8(11)	C(1X')–C(6X')–C(5X')	122.8(12)
C(3')–C(4')–Cl(2)	122.4(10)	O(3Y)–C(2Y)–C(1Y)	110.8(11)

(continued)

Table 4 (continued)

C(5')–C(4')–Cl(2)	119.8(11)	O(3Y)–C(2Y)–C(4Y)	112.3(11)
C(4')–C(5')–C(6')	122.0(12)	C(1Y)–C(2Y)–C(4Y)	111.2(11)
C(5')–C(6')–C(1')	120.6(11)	O(5Y)–C(4Y)–O(6Y)	125.9(13)
C(8XA)–C(1X)–N(1XA)	111.8(9)	O(5Y)–C(4Y)–C(2Y)	117.5(13)
C(8XA)–C(1X)–C(2X)	111.1(10)	O(6Y)–C(4Y)–C(2Y)	116.6(11)
N(1XA)–C(1X)–C(2X)	107.1(11)	O(3Z)–C(2Z)–C(1Z)	108.5(12)
C(1XB)–N(1XA)–C(1X)	116.4(10)	O(3Z)–C(2Z)–C(4Z)	109.2(12)
C(1Z)–C(2Z)–C(4Z)	114.3(13)	O(6Z)–C(4Z)–C(2Z)	119.0(11)
O(6Z)–C(4Z)–O(5Z)	124.5(13)	O(5Z)–C(4Z)–C(2Z)	116.5(13)

3.5.2 X-ray powder diffraction pattern

The XRPD pattern of sertraline (*L*)-lactate shown in [Figure 4](#) was obtained using a Siemens Diffractometer 5000. The crystallographic parameters derived from this pattern are given in [Table 7](#).

An XRPD pattern for sertraline (*L*)-lactate was calculated using the unit cell parameters of the solved single crystal structure. As shown in

Table 5

Anisotropic Displacement Parameters ($\text{\AA}^2 \times 10^3$) for Sertraline (*L*)-Lactate

	U_{11}	U_{22}	U_{33}	U_{23}	U_{13}	U_{12}
C(1)	75(10)	44(8)	27(6)	−6(6)	9(6)	8(7)
N(1A)	54(7)	62(7)	30(5)	4(5)	−5(5)	4(6)
C(1B)	83(11)	75(10)	57(9)	8(8)	−7(8)	−25(9)
C(2)	61(9)	66(9)	34(7)	3(6)	−20(6)	−5(7)
C(3)	52(8)	63(9)	48(7)	15(7)	−19(6)	1(7)
C(4)	62(9)	42(7)	37(7)	−1(6)	−5(6)	−6(7)
C(4A)	58(9)	32(7)	38(7)	−3(6)	2(6)	7(7)
C(5)	40(8)	62(9)	59(8)	12(7)	−12(7)	6(7)
C(6)	83(12)	64(9)	52(8)	19(7)	−9(8)	18(9)
C(7)	44(8)	68(9)	97(11)	7(10)	−24(9)	22(8)

	U_{11}	U_{22}	U_{33}	U_{23}	U_{13}	U_{12}
C(4XA)	62(9)	38(7)	43(7)	−18(7)	−15(7)	0(7)
C(5X)	61(11)	58(9)	53(8)	5(7)	−15(7)	−25(8)
C(6X)	74(12)	45(9)	82(10)	−6(8)	0(9)	−25(9)
C(7X)	62(10)	78(11)	95(11)	11(11)	−7(9)	−4(9)
C(8X)	59(10)	58(9)	64(9)	3(8)	−19(7)	−12(8)
C(8XA)	36(8)	57(8)	43(7)	−5(7)	−16(6)	−1(7)
C(1X')	66(9)	50(9)	44(7)	7(7)	−9(6)	8(7)
C(2X')	85(10)	43(8)	43(7)	−7(7)	−5(7)	9(7)
C(3X')	57(9)	68(10)	32(7)	4(7)	−9(6)	23(7)
C1(3)	125(3)	74(3)	59(2)	12(2)	−12(2)	44(2)

	U_{11}	U_{22}	U_{33}	U_{23}	U_{13}	U_{12}
C(8)	57(10)	52(9)	65(9)	2(7)	1(7)	5(7)
C(8A)	56(9)	30(6)	35(7)	-8(6)	-19(6)	7(6)
C(1')	52(8)	43(8)	40(7)	0(7)	-17(6)	-14(7)
C(2')	67(9)	42(8)	58(9)	-9(7)	-19(7)	-7(7)
C(3')	85(10)	37(8)	37(8)	9(7)	-10(7)	-18(7)
Cl(1)	163(4)	58(2)	56(2)	9(2)	3(2)	-35(3)
C(4')	72(10)	58(9)	41(7)	-2(9)	-14(6)	-7(9)
Cl(2)	103(3)	97(3)	47(2)	-2(2)	14(2)	-14(3)
C(5')	72(10)	52(9)	41(8)	-7(7)	-8(7)	-2(7)

	U_{11}	U_{22}	U_{33}	U_{23}	U_{13}	U_{12}
C(4X')	58(9)	84(11)	32(7)	5(8)	-21(6)	4(8)
C1(4)	110(3)	79(3)	46(2)	1(2)	-25(2)	5(2)
C(5X')	111(12)	43(9)	40(8)	-9(6)	-21(8)	8(8)
C(6X')	109(12)	39(8)	45(8)	1(6)	-15(8)	22(8)
C(1Y)	130(15)	110(15)	90(11)	0(11)	-10(11)	69(13)
C(2Y)	61(9)	57(9)	51(8)	10(7)	-9(7)	9(7)
O(3Y)	78(7)	160(11)	33(5)	-8(6)	-16(5)	7(7)
C(4Y)	79(11)	44(8)	34(8)	4(6)	3(8)	8(8)
O(5Y)	118(8)	112(8)	27(5)	6(5)	-4(5)	25(7)

(continued)

Table 5 (continued)

C(6')	77(10)	36(8)	47(8)	2(6)	−9(7)	−15(7)	O(6Y)	87(8)	65(6)	51(6)	14(5)	−16(5)	1(6)
C(1X)	60(9)	59(8)	29(7)	−13(6)	−15(6)	3(7)	C(1Z)	97(15)	152(18)	85(12)	4(12)	−15(10)	−7(13)
N(1XA)	83(9)	59(7)	27(5)	0(5)	−8(5)	−12(7)	C(2Z)	67(11)	76(10)	57(9)	−13(8)	−13(8)	−8(8)
C(1XB)	71(10)	56(9)	53(8)	−4(7)	−22(7)	−4(8)	O(3Z)	121(11)	168(16)	30(6)	−30(7)	10(6)	−45(11)
C(2X)	69(10)	84(11)	53(8)	16(8)	−15(7)	3(9)	C(4Z)	72(10)	51(8)	37(8)	13(7)	0(7)	27(8)
C(3X)	59(9)	99(12)	34(7)	−7(8)	−9(6)	1(8)	O(5Z)	103(7)	69(6)	31(5)	6(4)	−1(4)	2(5)
C(4X)	53(9)	52(8)	45(7)	−20(7)	−10(6)	16(7)	O(6Z)	81(6)	76(6)	29(4)	2(4)	0(5)	−22(6)

The anisotropic displacement factor exponent takes the following form: $-2\pi^2[h^2a^{*2}U_{11}+\cdots+2hk\,a^*\,b^*\,U_{12}]$.

Table 6

Hydrogen Coordinates ($\times 10^4$) and Isotropic Displacement Parameters ($\text{\AA}^2 \times 10^3$) for Sertraline (L)-Lactate

	<i>x</i>	<i>y</i>	<i>z</i>	<i>U</i> (eq)		<i>x</i>	<i>y</i>	<i>z</i>	<i>U</i> (eq)
H(1)	−4804	4412	8711	80	H(1XZ)	−1511	8091	−5409	80
H(1AA)	−3843	3743	6558	80	H(2XA)	2039	6673	−6108	80
H(1AB)	−3382	3609	8017	80	H(2XB)	2610	7280	−6222	80
H(1BA)	−5391	3081	7359	80	H(3XA)	3273	7288	−3789	80
H(1BB)	−6359	3609	7003	80	H(3XB)	4150	6813	−4544	80
H(1BC)	−5875	3473	8589	80	H(4X)	2637	6160	−3641	80
H(2A)	−2605	4935	8668	80	H(5X)	544	6103	−1438	80
H(2B)	−2046	4328	8894	80	H(6X)	−2050	6093	−1296	80
H(3A)	−1661	4254	6435	80	H(7X)	−3567	6617	−2876	80
H(3B)	−602	4707	7136	80	H(8X)	−2409	7078	−4700	80
H(4)	−2116	5391	6252	80	H(2X')	3974	5766	−1799	80

(continued)

Table 6 (continued)

H(5)	−4326	5476	3943	80
H(6)	−6909	5425	3655	80
H(7)	−8365	4988	5351	80
H(8)	−7153	4521	7155	80
H(2')	−1164	5851	4256	80
H(5')	−311	4211	1964	80
H(6')	−1527	4202	4081	80
H(1X)	−148	7181	−6165	80
H(1XA)	1304	7859	−4171	80
H(1XB)	1070	7999	−5665	80
H(1XX)	−590	8486	−4373	80
H(1XY)	−1265	7936	−3796	80

H(5X')	3938	7343	898	80
H(6X')	2825	7322	−1353	80
H(1YA)	1614	2560	8594	80
H(1YB)	624	2284	9762	80
H(1YC)	2232	2543	10183	80
H(2Y)	1314	3406	9702	80
H(3YA)	−1090(160)	3170(50)	11130(130)	80
H(1ZA)	6557	8808	−3608	80
H(1ZB)	6593	8383	−2356	80
H(1ZC)	6917	9003	−2040	80
H(2Z)	4427	9225	−2657	80
H(3ZA)	4100(200)	8950(80)	−720(190)	80

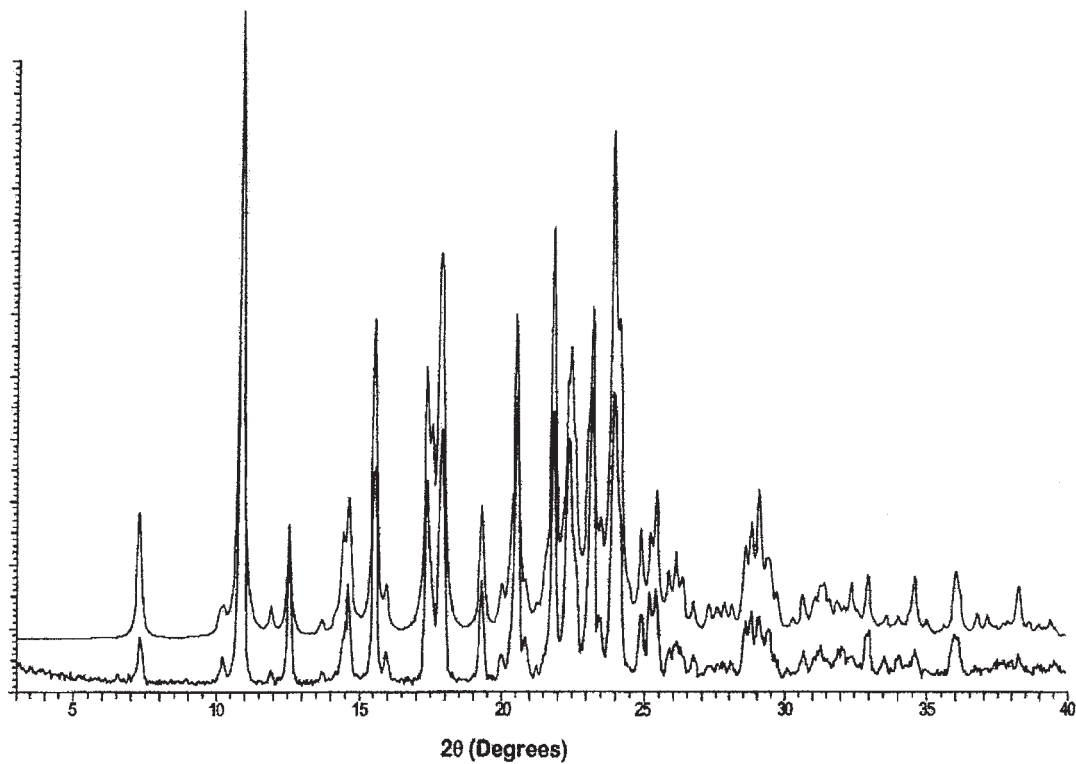


Figure 4. Calculated (top) and experimental (bottom) X-ray powder diffraction patterns of sertraline (L)-lactate.

Table 7

Crystallographic Parameters Derived from the XRPD
Pattern of Sertraline (*L*)-Lactate

Scattering angle (°2 θ)	<i>d</i> -Spacing (Å)	Relative intensity (%)
7.257	12.1720	8.6
10.199	8.6662	5.6
10.853	8.1452	100.0
11.846	7.4646	3.2
12.535	7.0559	22.1
14.593	6.0650	17.6
15.528	5.7019	37.5
15.877	5.5773	6.3
17.331	5.1126	35.0
17.829	4.9709	43.8
19.267	4.6030	18.1
20.005	4.4348	5.8
20.511	4.3266	50.3
20.814	4.2643	8.6
21.831	4.0679	47.0
22.375	3.9701	42.2

(continued)

Table 7 (continued)

Scattering angle (°2 θ)	<i>d</i> -Spacing (Å)	Relative intensity (%)
23.183	3.8335	50.9
23.474	3.7866	12.4
23.943	3.7136	50.1
24.160	3.6807	29.9
24.892	3.5740	12.5
25.213	3.5292	16.1
25.434	3.4992	16.7
25.864	3.4419	6.8
26.694	3.3367	5.7
28.557	3.1231	11.3
29.046	3.0716	12.1
29.362	3.0394	10.0
30.680	2.9117	6.4
32.057	2.7897	7.1
33.004	2.7118	9.7
35.983	2.4938	9.2

Figure 4, the calculated pattern compares favorably with that of the sertraline (*L*)-lactate reference standard.

3.6 Thermal methods of analysis

3.6.1 Melting behavior

The melting point of sertraline (*L*)-lactate was determined with the aid of a capillary melting-point apparatus (heating rate of 1°C/min). The compound was observed to undergo a complete melt at approximately 150.5°C.

3.6.2 Differential scanning calorimetry

The DSC thermogram in Figure 5 was collected using a Perkin–Elmer DSC-4 thermal analyzer. The sample was heated at a rate of 20°C/min under a nitrogen atmosphere. The thermogram shows a melting

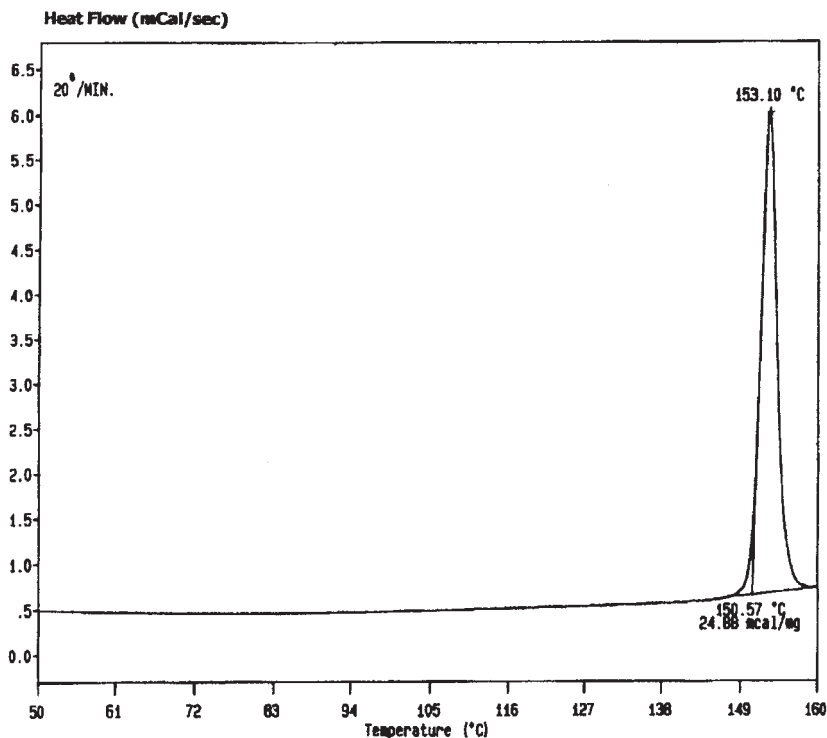


Figure 5. Differential scanning calorimetry thermogram of sertraline (*L*)-lactate.

endotherm, characterized by an onset temperature of 150.6°C and a peak maximum of 153.1°C. Integration of the melting endotherm yielded a molar heat of fusion equal to 41.3 kJ/mol.

3.6.3 Thermogravimetric analysis

Thermogravimetric analysis was performed using a Perkin–Elmer TGS-2 thermal analyzer, with the sample heated at a rate of 20°C/min in a nitrogen atmosphere. As shown in Figure 6, heating a sample of sertraline (L)-lactate from approximately 30–150°C resulted in a weight loss of less than 0.3%. Significant weight loss, which is attributed to sample decomposition, is observed above the melting point.

3.7 Spectroscopy

3.7.1 UV–VIS spectroscopy

The UV absorption spectrum of sertraline (L)-lactate was obtained in methanol, methanolic-0.1 N HCl, and methanolic-0.01 N NaOH. The spectra obtained in all three solvent systems exhibited absorption maxima

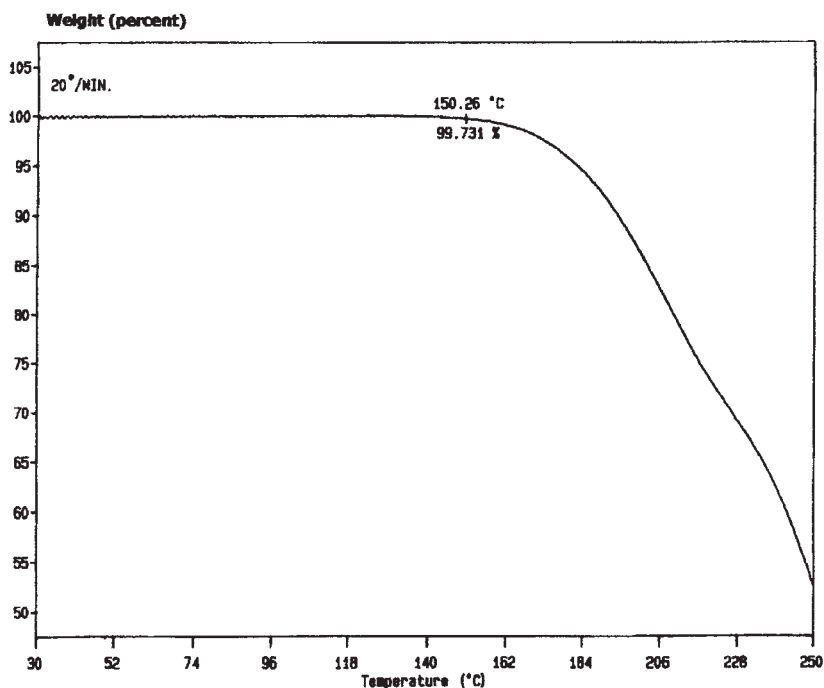


Figure 6. Thermogravimetric analysis of sertraline (L)-lactate.

(λ_{\max}) at 266, 274, and 282 nm, which are consistent with those reported for sertraline hydrochloride [2]. The spectrum of the drug substance dissolved in methanol is presented in Figure 7(a).

As shown in Figure 7(b), sertraline (*L*)-lactate was found to obey Beer's Law at all three wavelengths. The molar absorptivity ($M^{-1} \text{ cm}^{-1}$) of sertraline (*L*)-lactate at each wavelength maximum is as follows:

Solvent	$\lambda = 266 \text{ nm}$	$\lambda = 274 \text{ nm}$	$\lambda = 282 \text{ nm}$
Methanol	855	943	547
0.1 N HCl/ Methanol	876	975	541
0.01 N NaOH/ Methanol	643	724	541

3.7.2 Vibrational spectroscopy

The infrared absorption spectrum of sertraline (*L*)-lactate, which is shown in Figure 8, was collected in a KBr matrix using diffuse reflectance infrared Fourier transform (DRIFT) spectroscopy. A Nicolet Magna-IR 550 Series II spectrophotometer was used to collect this spectrum.

The frequencies of the absorption bands, and assignments for their origins, are provided in Table 8. The spectrum is consistent with the structure of the drug substance.

3.7.3 Nuclear magnetic resonance spectrometry

The 500 MHz ^1H -NMR and 125 MHz ^{13}C -NMR spectra of sertraline (*L*)-lactate dissolved in 99.5% deuterated methylene chloride were obtained using a Bruker DMX-500 spectrometer equipped with a 5 mm z-gradient inverse broadband probe. All chemical shifts were measured relative to external tetramethylsilane (TMS).

The ^1H -NMR and ^{13}C -NMR spectra are shown in Figures 9 and 10, respectively. The COSY, HMQC, and long-range HMQC (optimized for 6 Hz) spectra are shown in Figures 11–13. Assignments for the observed resonance bands are collected in Table 9, including an atomic numbering

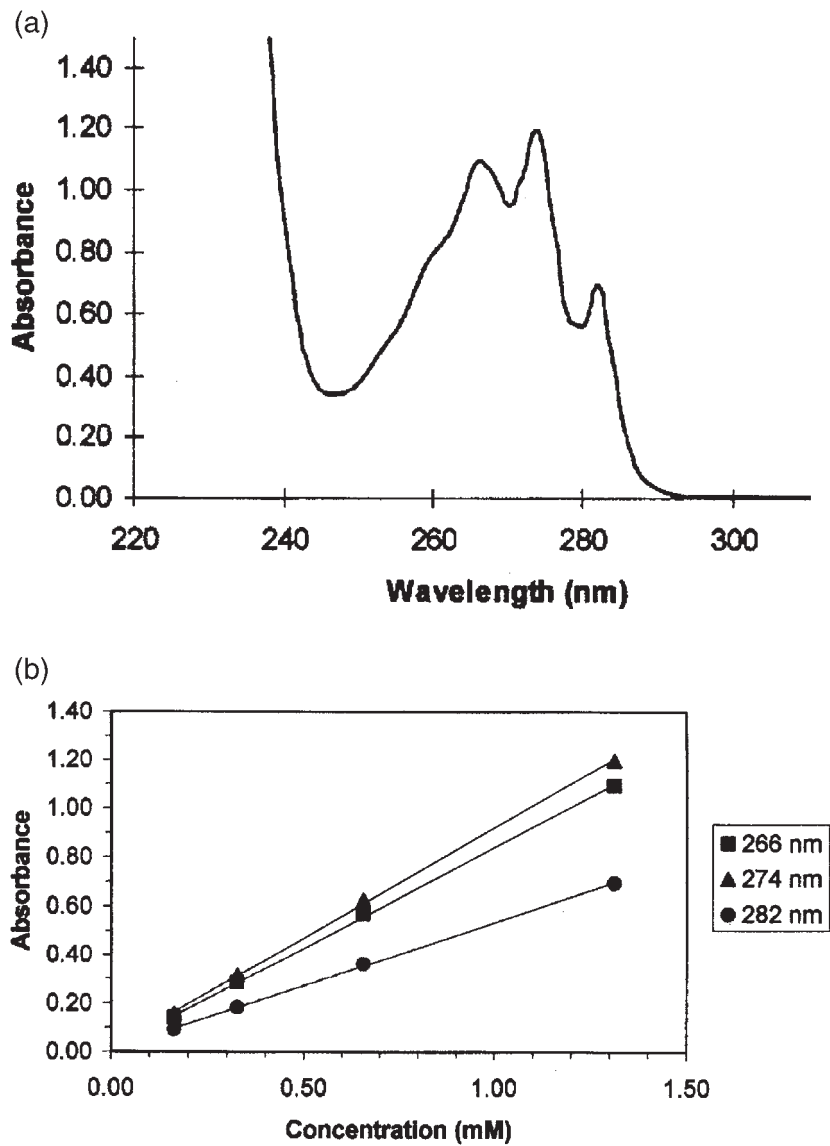


Figure 7. (a) Ultraviolet absorption spectrum of sertraline (*L*)-lactate dissolved in methanol. (b) Beer's law relationship at the various peak maxima.

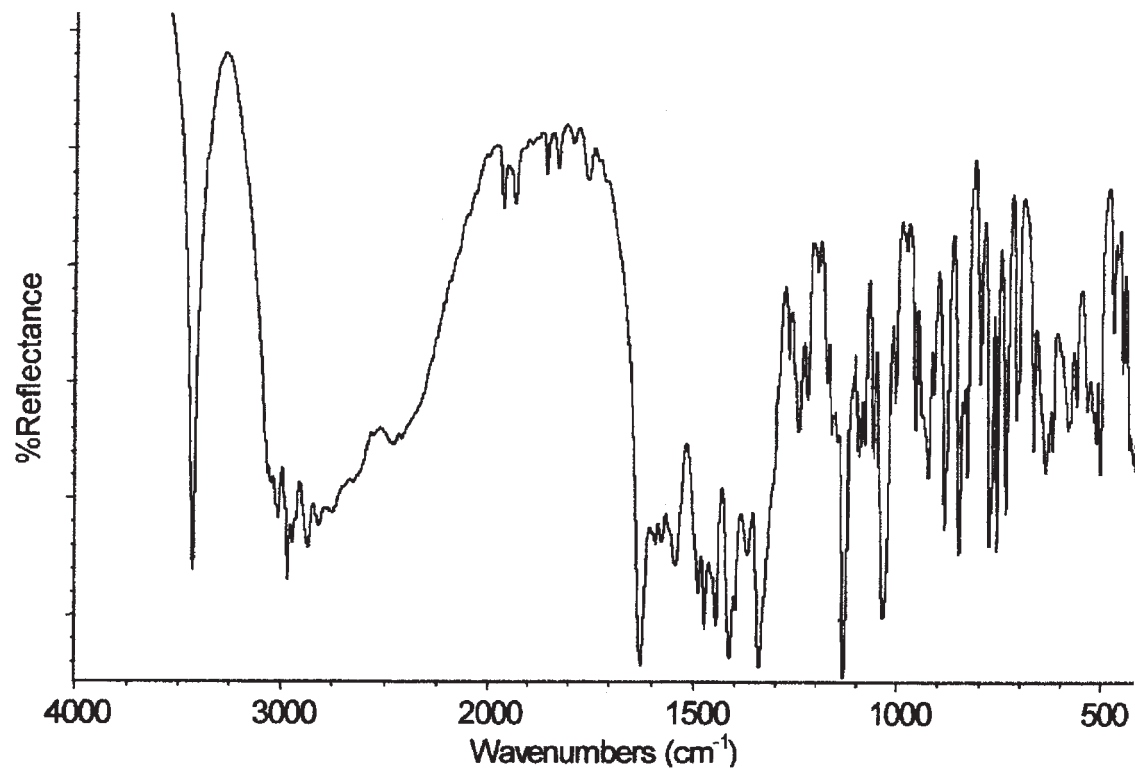


Figure 8. Infrared absorption spectrum of sertraline (*L*)-lactate.

Table 8

Infrared Absorption Bands of Sertraline (*L*)-Lactate

Frequency (cm^{-1})	Assignment
3436(s)	O–H stretching vibration
3100–2300 (m)	Aromatic C–H stretching vibrations Aliphatic C–H stretching vibrations NH_2^+ stretching vibrations
1627(s)	Asymmetric CO_2^- stretching vibration
1593 (w) 1578 (w) 1545 (m)	NH_2^+ bending vibrations Aromatic C=C ring stretching vibrations
1489 (m) 1474 (m) 1457 (m) 1446 (m)	Aromatic C=C ring stretching vibrations Asymmetric CH_3 bending vibration CH_2 scissoring vibrations
1414 (s)	Symmetric CO_2^- stretching vibration
1370 (m)	Symmetric CH_3 bending vibration
1341 (s)	O–H bending vibration
1132 (s) 1034 (s)	C–O stretching vibration C–N stretching vibration Aromatic C–Cl stretching vibrations
884 (m) 850 (m) 776 (m) 759 (m) 737 (m)	C–C–O symmetric stretching vibration Aromatic C–H out-of-plane bending vibrations NH_2^+ rocking vibrations

Intensities: s = strong; m = medium; w = weak.

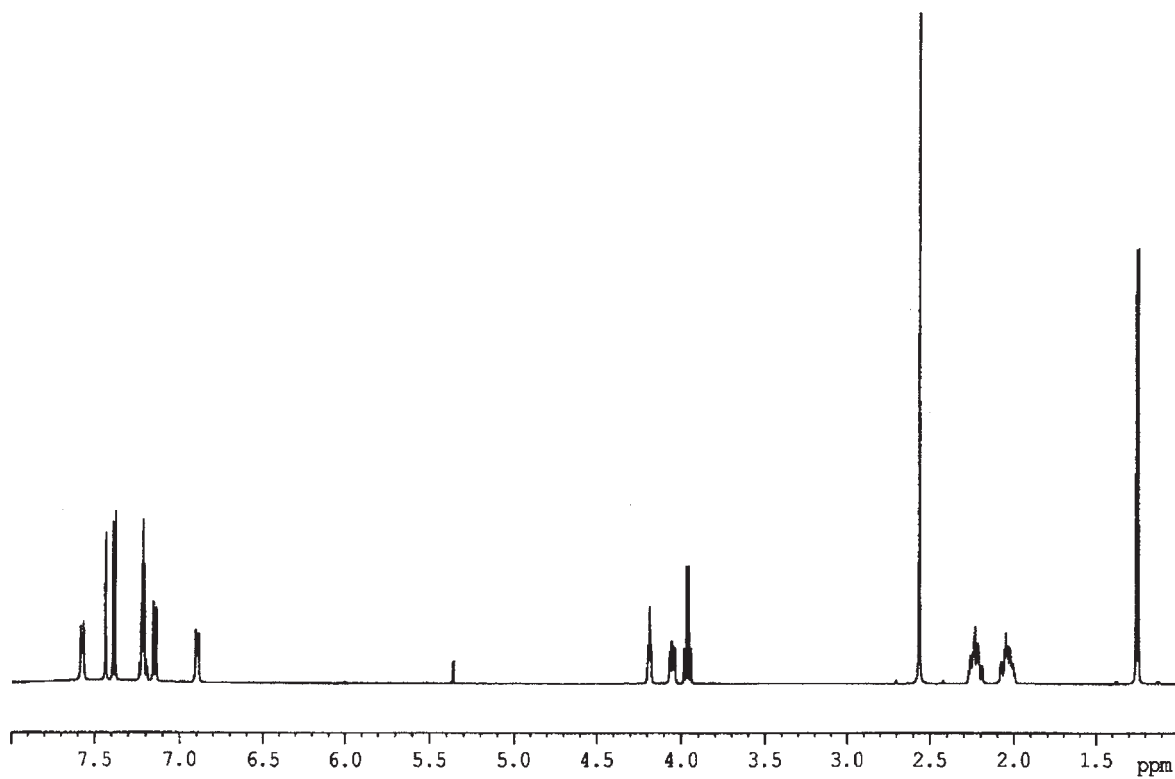


Figure 9. ^1H -NMR spectrum of sertraline (*L*)-lactate.

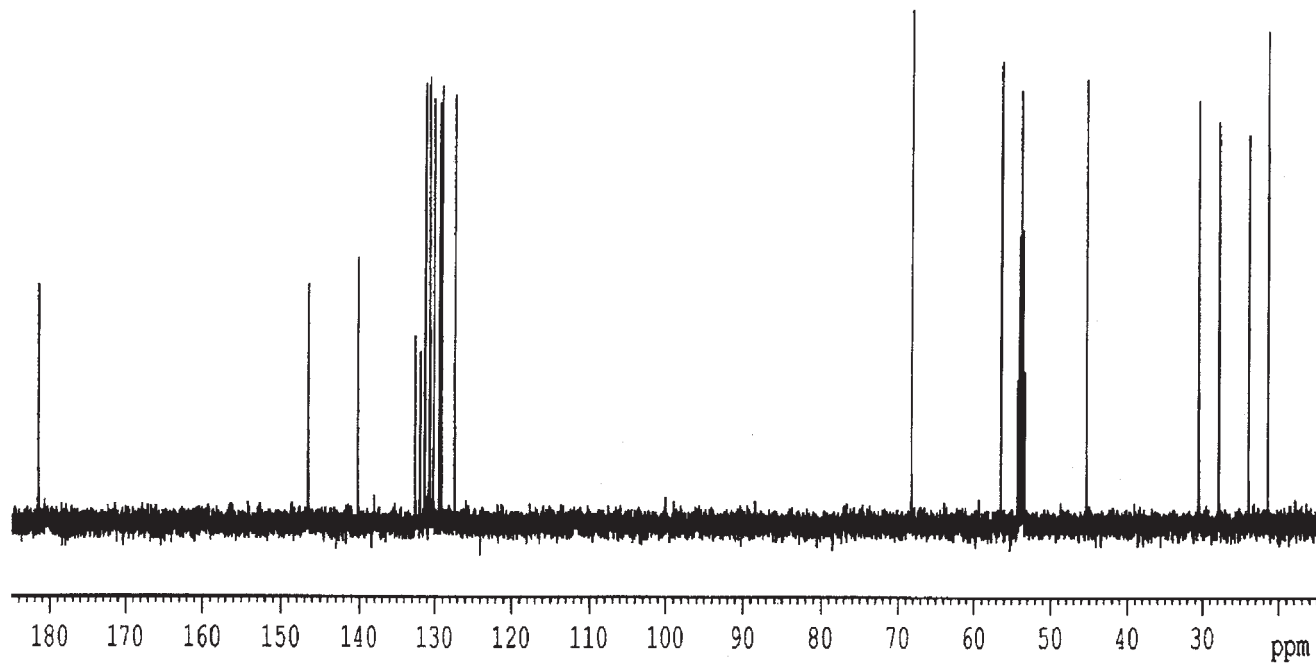


Figure 10. ^{13}C -NMR spectrum of sertraline (*L*)-lactate.

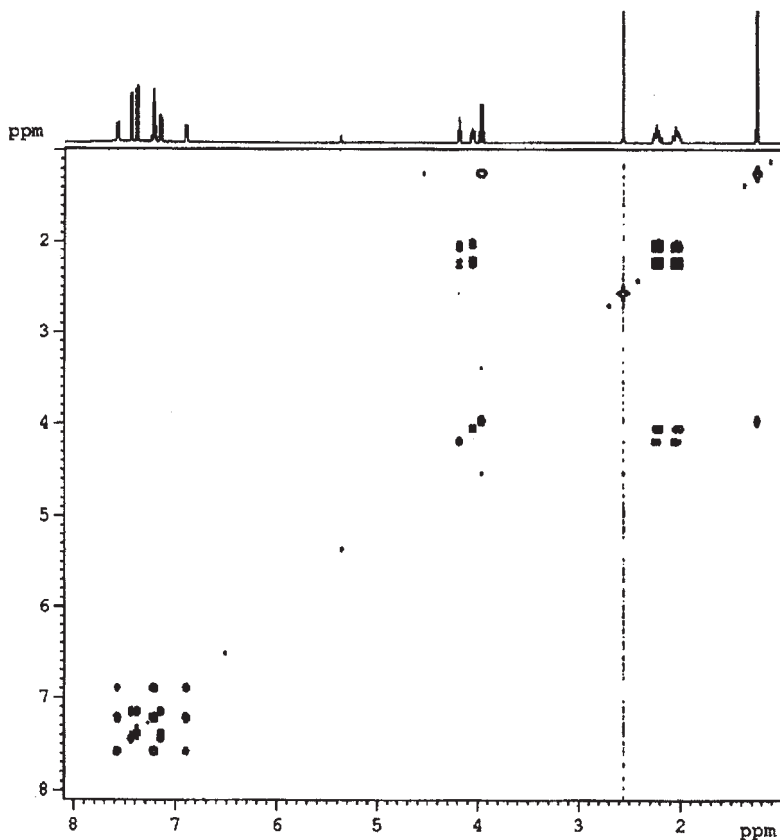
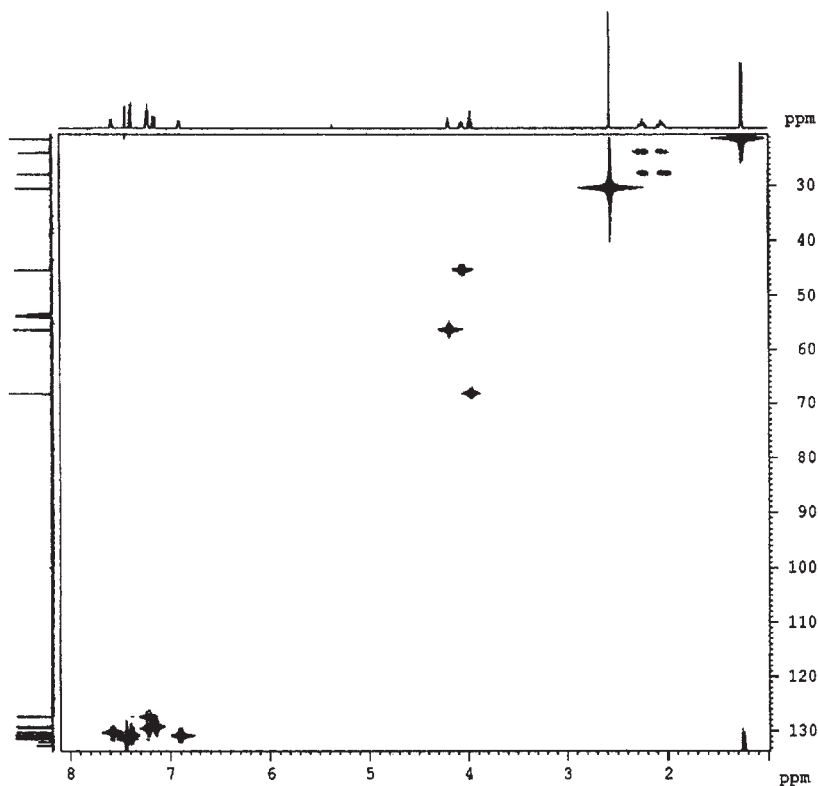


Figure 11. COSY spectrum of sertraline (*L*)-lactate.

scheme. The spectra are consistent with the structure of sertraline (*L*)-lactate.

3.8 Mass spectrometry

Sertraline (*L*)-lactate was characterized by electron impact (EI) and fast atom bombardment (FAB) mass spectrometry. The prominent features in the spectra of the lactate salt also appear in the spectra of the previously characterized hydrochloride salt [2, 9], and are consistent with losses from the proposed structure. The prominent chlorine isotope patterns associated with the observed fragment ions supports the peak assignments.

Figure 12. HMQC spectrum of sertraline (*L*)-lactate.

The EI mass spectrum is shown in [Figure 14](#) and the proposed EI-induced fragmentation scheme is shown in [Figure 15](#). The molecular ion is not observed by EI for sertraline. Rather, radical loss of H^\bullet results in an abundant $[\text{M}-\text{H}]^+$ at a mass to charge ratio (m/z) of 304. This behavior is characteristic of sertraline and a number of secondary amine analogs, even at low ionization energies. Neutral loss of methylamine immediately after ionization accounts for the ion at m/z 274. The m/z 159 species corresponds to the dichlorotropylium ion, $\text{C}_7\text{H}_5\text{Cl}_2^+$, originating from the pendant dichlorobenzene ring and one carbon of the tetrahydronaphthalene ring. These observations were made by direct insertion probe distillation. Sertraline free base is gas chromatographable. EI GC-MS experiments yield similar results.

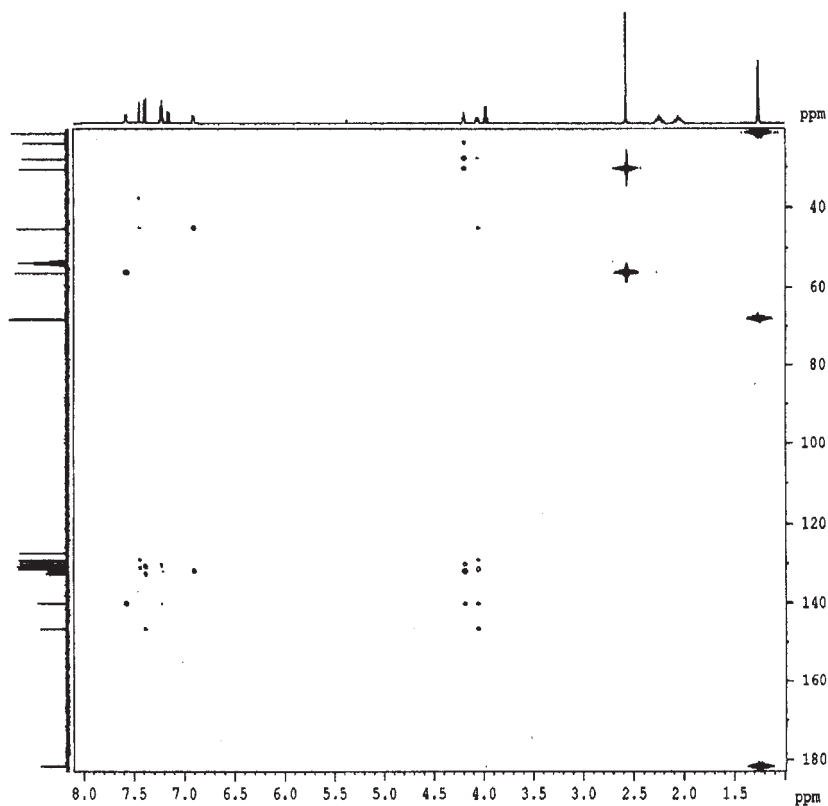
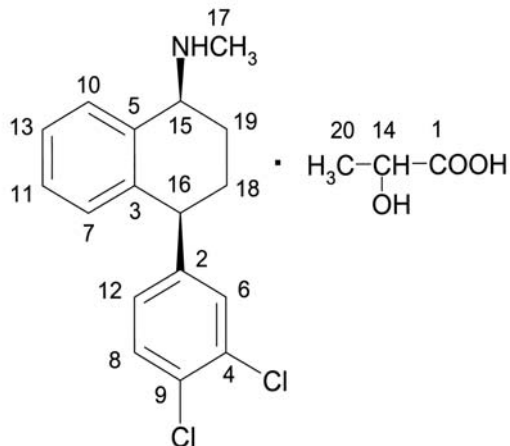


Figure 13. Long-range HMQC spectrum of sertraline (*L*)-lactate.

The FAB mass spectrum is shown in Figure 16 and the proposed FAB-induced fragmentation scheme is shown in Figure 17. The protonated molecular ion $[M+H]^+$ is apparent at a m/z of 306. The ion at m/z 275 originates by neutral loss of methylamine from the protonated molecular ion. The m/z 159 species corresponds to the dichlorotropylium ion.

Sertraline behaves well under atmospheric pressure ionization conditions, producing an abundant $[M+H]^+$ ion. Some salt adduct formation is apparent for the various salt forms. MS-MS collision-induced decomposition of the $[M+H]^+$ ion is consistent with previously assigned fragmentations.

Table 9

¹H-NMR and ¹³C-NMR Assignments for Sertraline (*L*)-Lactate


Assignment	¹³ C (δ, ppm)	Number of protons	¹ H (δ, ppm)	Multiplicity	<i>J</i> (Hz)
1	181.58	0	—	—	—
2	146.59	0	—	—	—
3	140.20	0	—	—	—
4	132.62	0	—	—	—
5	131.97	0	—	—	—
6	131.34	1	7.43	d	2.1
7	130.78	1	6.89	m	—
8	130.74	1	7.38	d	8.5
9	130.68	0	—	—	—

(continued)

Table 9 (continued)

Assign- ment	$^{13}\text{C}(\delta, \text{ppm})$	Number of protons	$^1\text{H}(\delta, \text{ppm})$	Multi- plicity	$J(\text{Hz})$
10	130.22	1	7.57	m	—
11	129.45	1	7.21	dt	7.3, 2.1
12	129.14	1	7.14	dd	8.5, 2.1
13	127.42	1	7.22	dt	7.3, 2.1
14	68.24	1	3.96	q	6.8
15	56.43	1	4.18	t	4.7
16	45.39	1	4.05	dd	9.0, 4.0
17	30.56	3	2.56	s	—
18	27.88	2	2.22, 2.02	m	—
19	23.92	2	2.24, 2.04	m	—
20	21.45	3	1.25	d	6.8

Multiplicity: s = singlet; d = doublet; t = triplet; q = quartet; dd = doublet of doublets; dt = doublet of triplets; m = multiplet.

4. METHODS OF ANALYSIS

4.1 Identification

The identity of a sample of sertraline (*L*)-lactate is established through the use of infrared spectroscopy, reversed-phase HPLC, and thin-layer chromatography (TLC). The infrared spectrum, HPLC retention time,

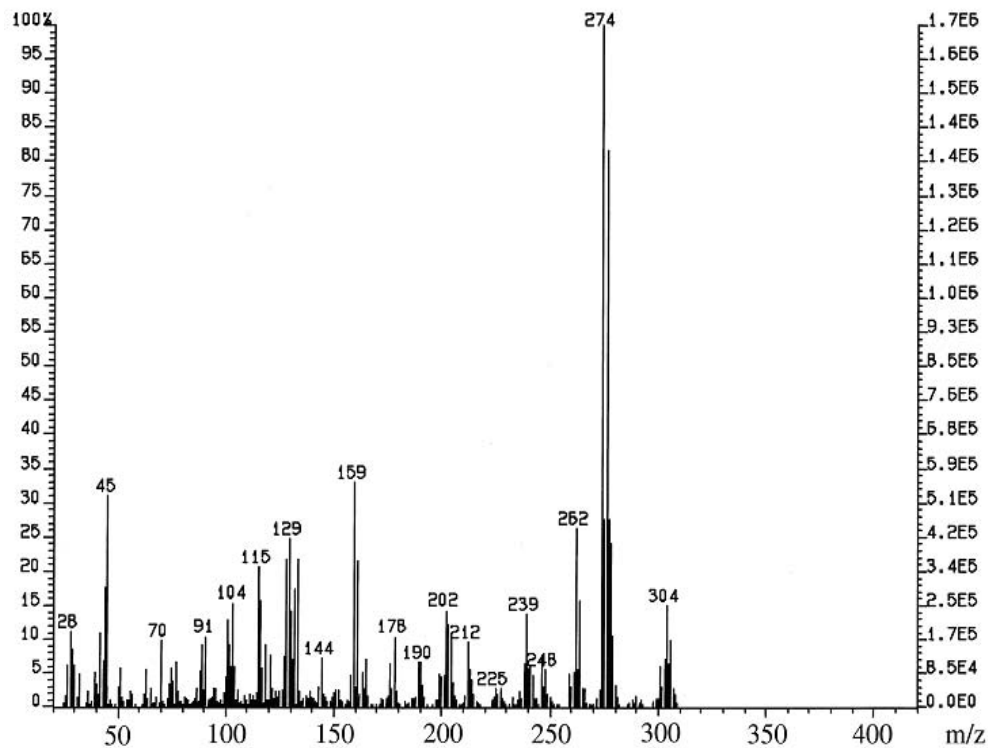
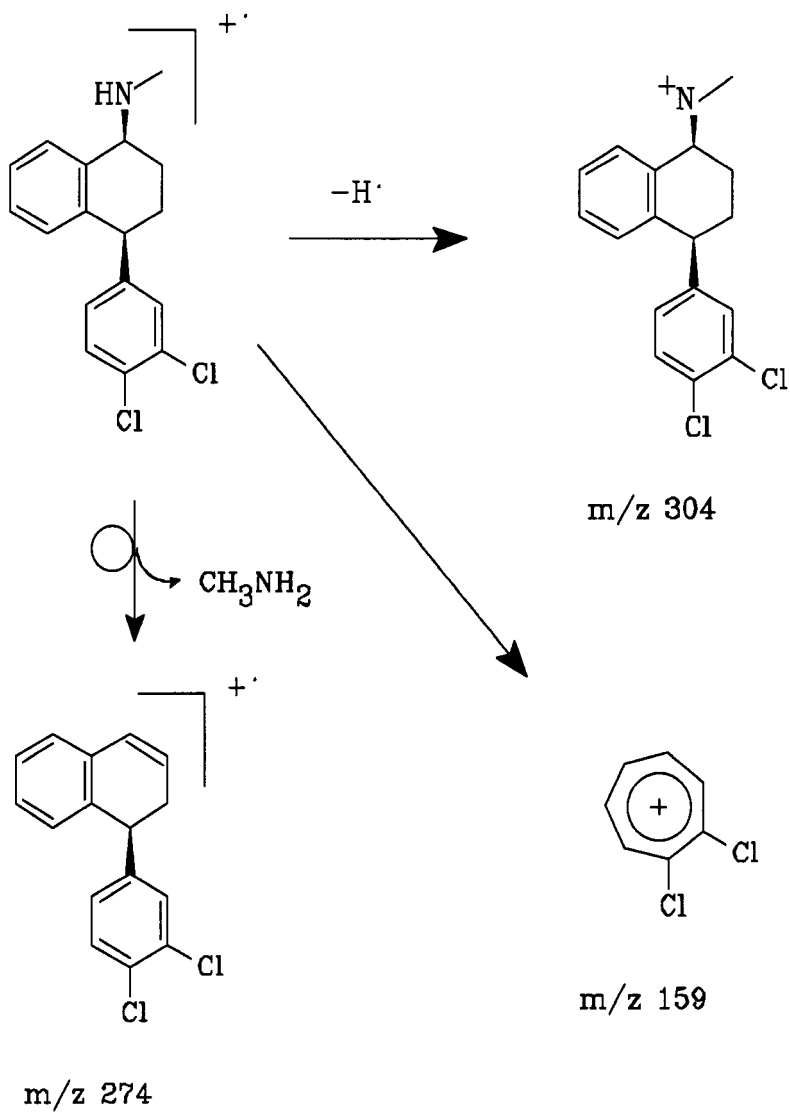


Figure 14. Electron-impact (EI) mass spectrum of sertraline (L)-lactate.

Figure 15. Proposed EI-induced fragmentation of sertraline (*L*)-lactate.

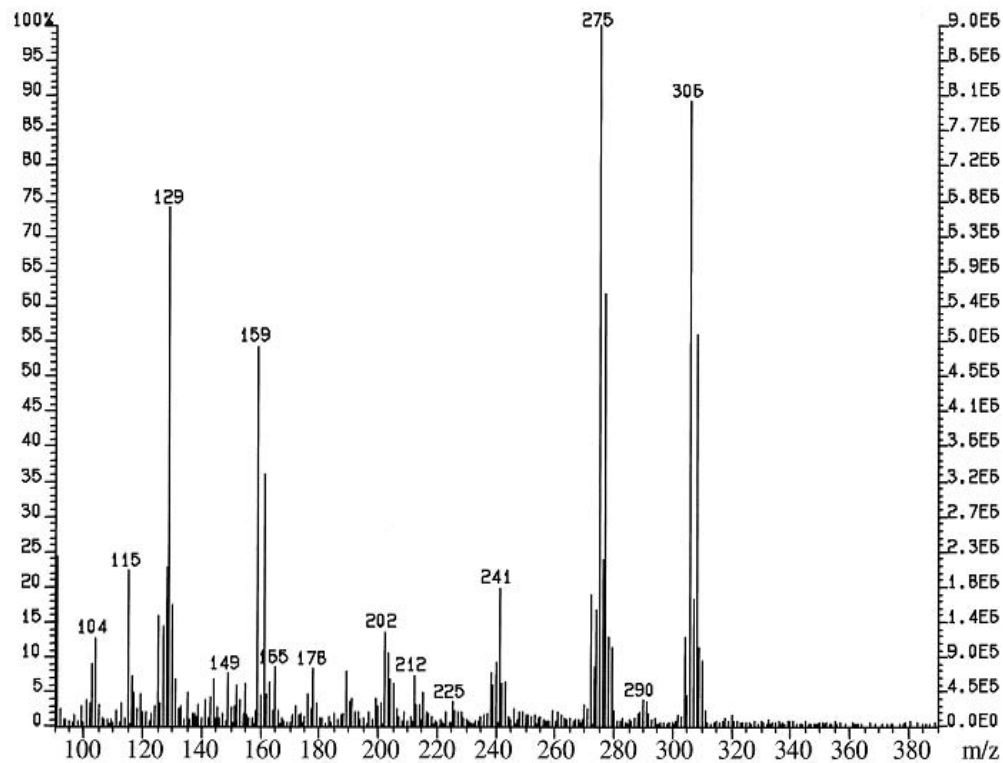


Figure 16. Fast-Atom Bombardment (FAB) mass spectrum of sertraline (L)-lactate.

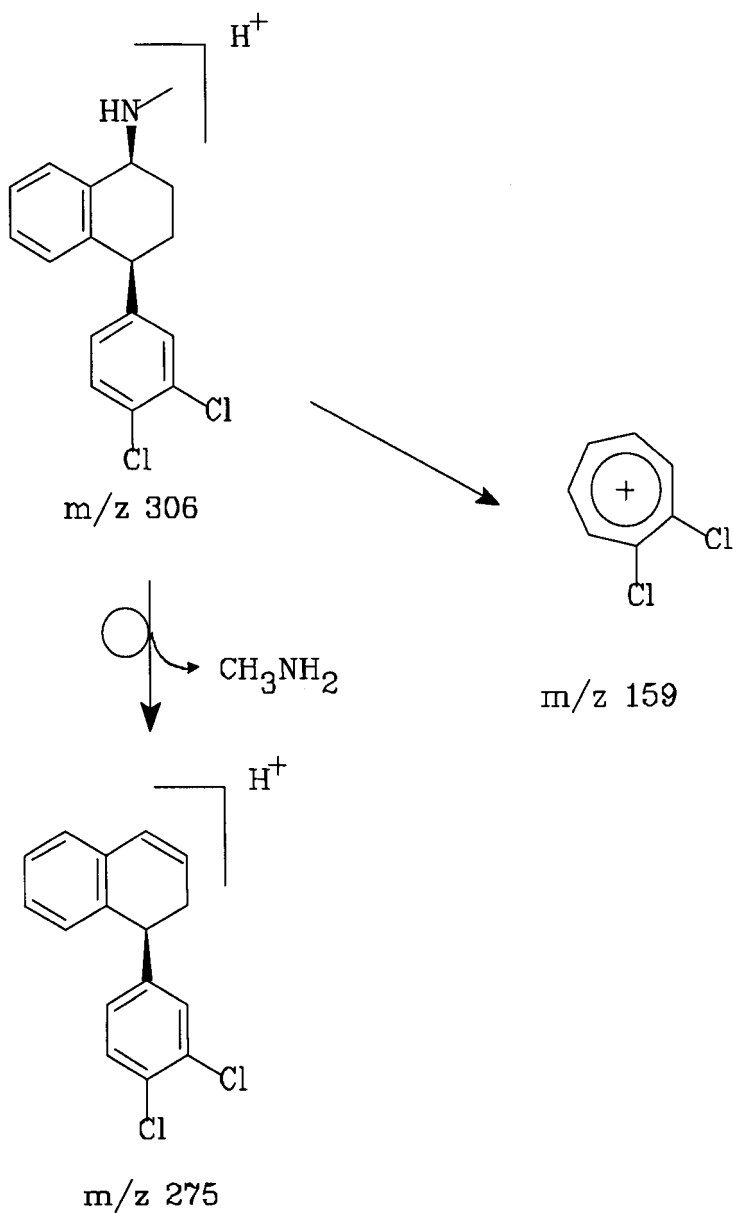


Figure 17. Proposed FAB-induced fragmentation of sertraline (*L*)-lactate.

and TLC R_F value of the sample must match those of the authentic reference standard. The crystal form of the sample is verified by infrared spectroscopy and X-ray powder diffraction.

4.2 Titrimetric analysis

Potentiometric titration is used to assay samples of sertraline (*L*)-lactate. As shown in Figure 18, a titration curve with a single inflection point is obtained when the drug substance is dissolved in a 1:1 v/v solvent mixture of ethanol and water, and titrated with 0.5 N NaOH.

When 94.46 mg of the reference standard lot was assayed by this method, a neutralization equivalent (molecular weight) of 395.6 was calculated.

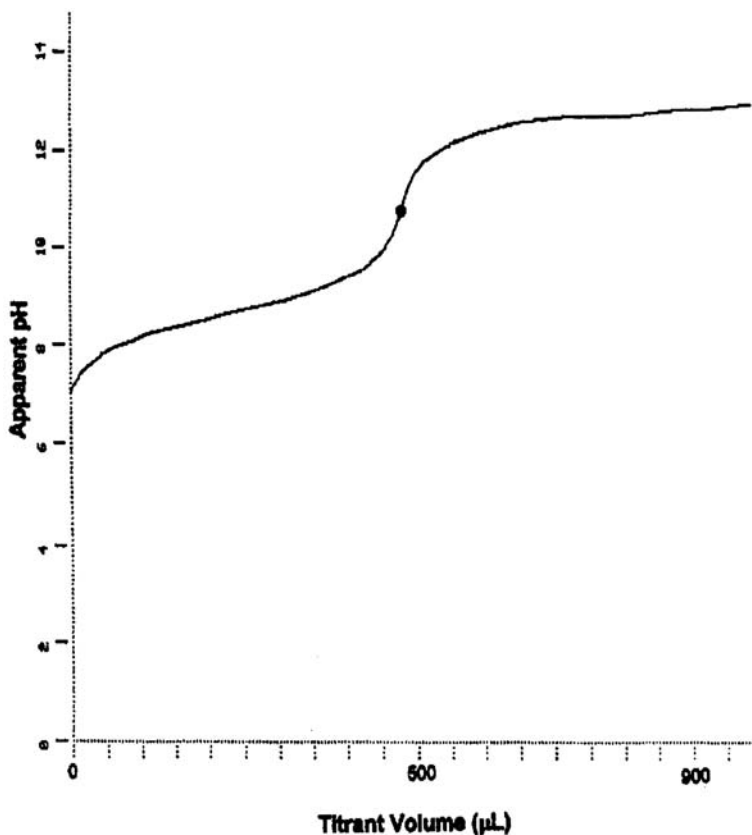


Figure 18. Potentiometric titration curve of sertraline (*L*)-lactate.

This molecular weight, which is 99.8% of the theoretical value, is consistent with the stoichiometry of sertraline (*L*)-lactate.

4.3 Quantitation of lactic acid

Reversed-phase HPLC with UV detection at 210 nm is used to determine the amount of lactic acid in a sample of the drug substance. A Zorbax[®]-NH₂ column (250 × 4.6 mm) maintained at 30°C is used in this method. The mobile phase is a 980:20:2 v/v/v mixture of acetonitrile, water, and concentrated phosphoric acid (85%), eluted at a flow rate of 1.0 mL/min. This method separates lactic acid from sertraline and drug-related impurities.

When the sertraline lactate reference standard was analyzed by this method, it was found to contain 22.5% lactic acid, or 99.1% of the theoretical amount.

4.4 Thin-layer chromatography

Thin-layer chromatography is used to establish the identity of sertraline (*L*)-lactate, and to estimate the levels of potential process-related impurities and degradation products in the drug substance. The chromatographic systems and detection methods used are the same as those reported for sertraline hydrochloride [2].

4.5 High-performance liquid chromatography

The identity, assay (potency), and purity of sertraline (*L*)-lactate is determined using an isocratic reversed-phase HPLC method. The method uses an Inertsil C-18 column (150 × 4.6 mm), and UV detection at 230 nm. The mobile phase is a 270:230:500 v/v/v mixture of tetrahydrofuran, methanol, and buffer (25 mM TEA phosphate) adjusted to an apparent pH of 8.0 with triethylamine (TEA). The flow rate is 1.0 mL/min and the column temperature is maintained at 40°C. This method separates sertraline from lactic acid, its potential process-related impurities, and its degradation products.

The identity and enantiomeric purity of the drug substance is determined using a second isocratic reversed-phase HPLC method. This method uses a 250 × 4.6 mm acetylated Cyclobond I column and UV detection at 230 nm. The mobile phase is a 350:650:10:1 v/v/v/v mixture of methanol, water, acetic acid, and TEA, and the flow rate is 1.0 mL/min.

5. STABILITY

5.1 Forced degradation studies

Degradation studies were performed on sertraline (*L*)-lactate under strongly acidic, strongly alkaline, and oxidative conditions to identify the potential degradation products of the drug substance. Suspensions of the drug substance in 0.1 N HCl and 0.1 N NaOH were prepared and refluxed for 24 h. A solution of sertraline (*L*)-lactate in 3% hydrogen peroxide was stirred at ambient temperature for 24 h. All solids and solutions were analyzed by reversed-phase HPLC, and analysis of the samples permitted the following observations and conclusions to be drawn:

- Sertraline (*L*)-lactate is stable under strongly acidic conditions. The suspension was filtered after 24 h and the filtered solids were dried prior to analysis. No degradation products were found in either the solids or the filtered solution.
- Sertraline (*L*)-lactate is also stable when exposed to strongly alkaline conditions. Refluxing in base resulted in the separation of organic and aqueous layers. No significant degradation (less than 0.3% total) was observed when the organic layer was analyzed. No degradation products were found in the aqueous solution.
- Under oxidative conditions, the total degradation of sertraline (*L*)-lactate was less than 1.7%. The primary degradants formed under these conditions were not observed during accelerated or long-term stability studies of the drug substance.

It was concluded from this work that sertraline (*L*)-lactate is a very stable compound.

5.2 Solid-state stability

The stability of sertraline (*L*)-lactate was studied over a period of 36 months according to the following protocol:

Storage condition	Container	Time Period	
		Weeks	Months
50°C/20%RH	A, B	3, 6	3
40°C/75%RH	A, B, C	3, 6	3, 6

Storage condition	Container	Time Period	
		Weeks	Months
30°C/60%RH	A, B	–	3, 6, 36
25°C/60%RH	A, B	–	3, 6, 36
5°C	A, B	3, 6	3, 6, 36

For this work, approximately 1 g of drug substance was placed into the following container systems:

- (A) 15 cc amber glass bottle with metal screw cap.
- (B) 2.5'' × 4.0'' × 0.004'' clear low-density polyethylene bag that is closed with a twist-tie and placed inside a cardboard mailing tube with metal ends and metal screw caps.
- (C) 15 cc amber glass bottle with gauze covering the mouth of the bottle.

Container B most closely simulates the container/closure system recommended for storage of the bulk drug substance.

The photostability of sertraline (*L*)-lactate was evaluated by spreading samples of the drug substance in polystyrene Petri dishes covered with quartz plates. These samples were exposed to either UV light (spectral distribution from 320 to 400 nm, with a maximum energy emission between 350 and 370 nm, for a total minimum exposure of 200 watt-hours per square meter) or fluorescent light (spectral distribution from 450 to 650 nm, for a total minimum exposure of 1.2 million lux-hours).

The stability samples were evaluated for appearance, potency and purity by HPLC, and water content by Karl Fischer titrimetry. The infrared absorption spectrum of each sample was also recorded.

The following conclusions were drawn from this study:

- No significant changes in the appearance of the drug substance were observed for any of the stability samples.

- No significant changes in potency were observed. After 36 months storage, the assay values of the stability samples ranged from 99.0% to 100.5% of initial.
- No significant degradation was observed in any of the stability samples. Total degradant levels increased by 0.2% or less during this study.
- The water content of the samples remained below 0.1%.
- The infrared absorption spectra conformed to that of the reference standard of sertraline (L)-lactate.

These studies demonstrate that sertraline (L)-lactate is stable for at least 36 months when stored at or below 30°C.

6. ACKNOWLEDGMENTS

The authors acknowledge and thank all of the Pfizer colleagues who have contributed to the development and characterization of sertraline (L)-lactate. In particular, we would like to thank L.R. Brostrom, D.L. Decosta, P.D. Hammen, G.J. Horan, C.M.V. Moore, J.D. Ringling, M.C. Schafer, R.M. Shanker, M.P. Snyder, C.A. Solanto, M.L. Teague, M. Treadway, and J.B. Zung.

7. REFERENCES

1. "ZOLOFT® (sertraline hydrochloride) Tablets and Oral Concentrate", *Physicians' Desk Reference*, 56th edn., Medical Economics Company, Inc., Montvale, NJ, p. 2751 (2002).
2. B.M. Johnson and P-T.L. Chang, "Sertraline Hydrochloride", in: *Analytical Profiles of Drug Substances and Excipients*, H.G. Brittain, (ed.), Volume 24, Academic Press, New York, pp. 443–486 (1996).
3. D.T. Friesen, S.M. Herbig, R.M. Shanker, and B.J. West, **PCT Int. Appl. WO 99 01120**; *Chem. Abs.* **130**, 115031 (1999).
4. M.T. am Ende, W.J. Curatolo, H.L. Friedman, R.M. Shanker, S.M. Herbig, D.T. Friesen, and B.J. West, **PCT Int. Appl. WO 99 01121**; *Chem. Abs.* **130**, 115032 (1999).
5. *International Tables for X-ray Crystallography*, J.A. Ibers and W.C. Hamilton, (eds.), Volume IV, Kynoch Press, Birmingham, pp. 55, 99, and 149 (1974).

6. **SHELXTL**, Version 5.1, Bruker AXS (1997).
7. J. Ibers and W.C. Hamilton, *Acta Cryst.*, **17**, 781 (1964).
8. W.C. Hamilton, *Acta Cryst.*, **18**, 502 (1965).
9. T.R. Sharp, G.J. Horan, and S.V.O. Day, “Mass Spectrometry of Sertraline and Related Compounds”, presented at the 41st Annual Conference on Mass Spectrometry and Allied Topics, May 31–June 4, 1993, San Francisco, California.

Profiles of Excipients

Propylparaben:

Physical Characteristics

Marcellino Rudyanto¹, Masataka Ihara², Kiyosei Takasu²,
Masahiro Yoshida², Hadi Poerwono¹, I Ketut Sudiana³,
Gunawan Indrayanto¹ and Harry G. Brittain⁴

¹*Faculty of Pharmacy, Airlangga University
Jalan Dharmawangsa Dalam, Surabaya 60286
Indonesia*

²*Graduate School of Pharmaceutical Sciences, Tohoku University
Aobayama, Sendai 980-8578, Japan*

³*Faculty of Medicine, Airlangga University
Jalan Prof. Dr. Moestopo 47, Surabaya 60131
Indonesia*

⁴*Center for Pharmaceutical Physics
10 Charles Road, Milford, NJ 08848
USA*

CONTENTS

1.	General Information	239
1.1	Nomenclature	239
1.1.1	Systematic chemical name	239
1.1.2	Nonproprietary names	239
1.1.3	Proprietary names	239
1.2	Formulae	239
1.2.1	Empirical formula, molecular weight, CAS number	239
1.2.2	Structural formula	239
1.3	Elemental analysis	239
1.4	Appearance	240
2.	Physical Characteristics of Propylparaben	240
2.1	Ionization constants	240
2.2	Partition coefficient	240
2.3	Solubility characteristics	240
2.4	Particle morphology	242
2.5	Crystallographic properties	242
2.5.1	Single crystal structure	242
2.5.2	X-ray powder diffraction pattern	244
2.6	Hygroscopicity	245
2.7	Thermal methods of analysis	246
2.7.1	Melting behavior	246
2.7.2	Differential scanning calorimetry	246
2.8	Spectroscopy	250
2.8.1	Ultraviolet absorption spectroscopy	250
2.8.2	Vibrational spectroscopy	250
2.8.3	Nuclear magnetic resonance	251
2.8.3.1	^1H -NMR spectrum	251
2.8.3.2	^{13}C -NMR spectrum	258
2.9	Mass spectrometry	258
3.	Stability of Propylparaben	258
3.1	Solid-state stability	258
3.2	Solution-phase stability	261
3.3	Stability in biological fluids	264
4.	Incompatibilities with Functional Groups	267
5.	Acknowledgments	268
6.	References	268

1. GENERAL INFORMATION

1.1 Nomenclature

1.1.1 *Systematic chemical name*
 Propyl 4-hydroxybenzoate

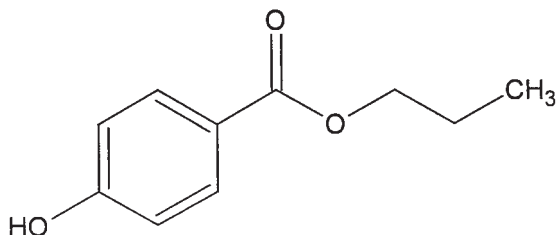
1.1.2 *Nonproprietary names [1-4]*
 Propylparaben; 4-hydroxybenzoic acid propyl ester; propyl *p*-hydroxybenzoate; propagin; propylis oxybenzoas; propylis parahydroxybenzoas

1.1.3 *Proprietary names [1-4]*
 Chemocide PK, E 216, Nipasol M, Propyl Chemosept, Propyl Parasept, Solbrol P, Tegosept P

1.2 Formulae

1.2.1 *Empirical formula, molecular weight, CAS number*
 Empirical Formula: $C_{10}H_{12}O_3$
 Molecular Weight: 180.20
 CAS Number: 94-13-3

1.2.2 *Structural formula*



1.3 Elemental analysis

The calculated elemental composition of propylparaben is as follows:

carbon:	66.65%
hydrogen:	6.71%
oxygen:	26.64%

1.4 Appearance

Propylparaben occurs as odorless, tasteless, colorless crystals, or a white crystalline powder [1–4].

2. PHYSICAL CHARACTERISTICS OF PROPYLPARABEN

2.1 Ionization constants

The reported dissociation constant (pKa) of propylparaben is 8.4 at 22°C [4]. This value agrees very well with the pKa value of 8.23 ± 0.15 that was calculated using PhysChem Version 6.0 (Advanced Chemistry Development, Toronto, Canada).

2.2 Partition coefficient

Partition coefficients for propylparaben in vegetable oils and water, as determined by Wan *et al.*, are shown in Table 1 [10]. It has been reported that the empirically determined partition coefficient values may vary considerably, and are affected by the purity of the oil used for the determination [4]. Table 2 summarizes the partition coefficient of propylparaben in various o/w emulsions [11].

Using ACD PhysChem Version 6.0, the partition coefficient of propylparaben was calculated to be 2.93 ± 0.22 . The pH dependence of the distribution coefficient was also calculated, and this is illustrated in Figure 1. The neutral form of the compound is seen to be quite hydrophobic, but once neutralization of the *p*-hydroxy group takes place, propylparaben becomes considerably more hydrophilic.

2.3 Solubility characteristics

Propylparaben has been reported to be very slightly soluble in water, but freely soluble in alcohol and ether [1, 3]. The solubilities of propylparaben in various solvents are shown in Table 3 [5, 6], and the solubilities of propylparaben in water at 25°C as a single component and in mixtures with other parabens are shown in Table 4 [7, 8]. It is important to note that when measured together with methyl, ethyl, and butyl parabens, the solubility of propylparaben decreases by approximately 50%. The aqueous solubility of propylparaben can be increased significantly by using 2-hydroxypropyl- β -cyclodextrin as a solubilizing agent [9].

Table 1

Partition Coefficient of Propylparaben in Vegetable Oil and Water

Solvent	Oil : water partition coefficient
Corn oil	58.0
Mineral oil	0.3
Peanut oil	51.8
Soybean oil	65.9
Mineral oil–corn oil (1 : 4)	36.1
Mineral oil–corn oil (2 : 3)	25.4
Mineral oil–corn oil (3 : 2)	12.2
Mineral oil–corn oil (4 : 1)	5.6
Mineral oil–soya oil (1 : 4)	45.0
Mineral oil–soya oil (2 : 3)	31.2
Mineral oil–soya oil (3 : 2)	17.9
Mineral oil–soya oil (4 : 1)	7.7

The pH dependence of the aqueous solubility of propylparaben was calculated using PhysChem Version 6.0 (Advanced Chemistry Development, Toronto, Canada), and is illustrated in [Figure 2](#). As would be anticipated from the distribution coefficient results, the hydrophobic neutral form of propylparaben is predicted to exhibit low aqueous solubility, but the compound is predicted to become considerably more soluble once neutralization of the *p*-hydroxy group takes place to yield a hydrophilic compound.

Table 2

Partition Coefficient of Propylparaben in O/W Emulsions

Components of emulsion	Composition (g) per 100 g emulsion				
Miglyol	10.0	10.0	10.0	10.0	10.0
Olive oil	10.0	10.0	10.0	10.0	10.0
Butylated hydroxyl toluene	0.2	0.2	0.2	0.2	0.2
Stearylamine	–	–	–	0.025	0.3
Egg phospholipid	1.2	1.2	1.2	1.2	1.2
Phosphatidylglycerol	0.05	0.03	–	–	–
Glycerol	2.4	2.4	2.4	2.4	2.4
Propylparaben	0.12	0.12	0.12	0.12	0.12
Partition coefficient	29.2	30.0	34.4	46.2	295.9

2.4 Particle morphology

Crystals of propylparaben are translucent and colorless, belonging to the monoclinic system [7]. Photomicrographs of crystalline propylparaben, obtained using optical microscopy, are shown in Figure 3. The crystals exhibit modest first-order birefringence, which can be transformed into pale yellow through the use of a red quarter-wave plate. The morphology of propylparaben was also characterized using Crystal Observation Technique and Scanning Electron Microscopy (model JSM-T100), and is shown in Figure 4.

2.5 Crystallographic properties

2.5.1 Single crystal structure

The single crystal structure of propylparaben has been solved by Giordano and coworkers, and the defining unit cell parameters are summarized in Table 5 [7]. The unit cell contains two crystallographically independent

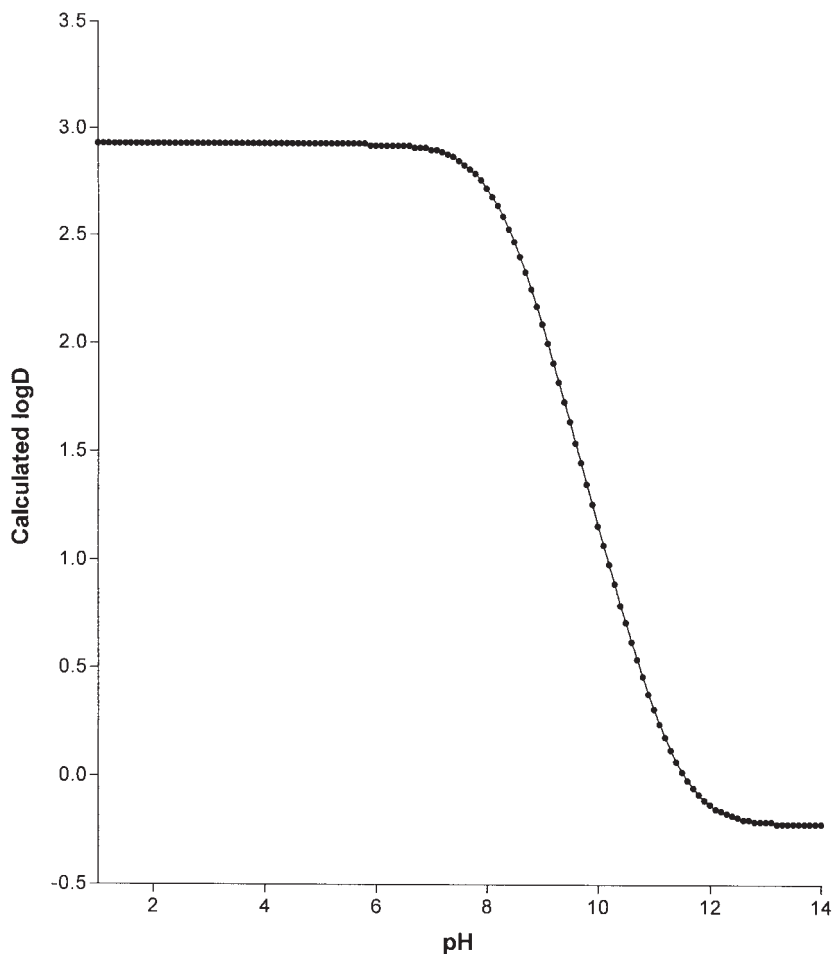


Figure 1. pH dependence of the distribution of propylparaben, calculated using PhysChem Version 6.0 (Advanced Chemistry Development, Toronto, Canada).

molecules that form into separate, but structurally analogous, infinite chains, utilizing head-to-tail hydrogen bonding between hydroxyl group (donor) and carbonyl group (acceptor). Within a given chain, successive molecules are related by a two-fold screw axis parallel to the array. As illustrated in [Figure 5](#), the symmetry-independent molecules are nearly coplanar, so that the resulting crystal structure is characterized by a distinctive layered motif.

Table 3

Solubility of Propylparaben in Various Solvents

Solvent	Solubility at 25°C, unless otherwise stated	Reference
Acetone	1 in 0.9	6
Benzene	1 in 33	6
Carbon tetrachloride	1 in 125	6
Ethanol	1 in 1.1	5
Ethanol (50%)	1 in 5.6	5
Ether	1 in 2	6
Glycerin	1 in 250	5
Methanol	1 in 0.8	6
Mineral oil	1 in 3330	5
Peanut oil	1 in 70	5
Propylene glycol	1 in 3.9	5
Propylene glycol (50%)	1 in 110	5
Water	1 in 4350 at 15°C	5
	1 in 2500	5
	1 in 225 at 80°C	5

2.5.2 X-ray powder diffraction pattern

X-ray powder diffraction (XRPD) patterns were obtained using a Rigaku MiniFlex powder diffraction system, equipped with a horizontal goniometer in the $\theta/2\theta$ mode. The X-ray source was nickel-filtered K- α emission

Table 4

Solubility of Propylparaben in Water at 25°C as Single Component, and in Mixtures with other Parabens

Paraben components in the mixture	Solubility (mM)	Reference
Propyl (single component)	2.18	7
	2.02	8
Propyl + Methyl	2.20	7
Propyl + Ethyl	1.11	7
Propyl + Butyl	2.09	7
Propyl + Methyl + Ethyl	1.11	7
Propyl + Ethyl + Butyl	1.09	7
Propyl + Methyl + Butyl	2.11	7
Propyl + Methyl + Ethyl + Butyl	1.10	7
	1.12	8

of copper (1.54056 \AA). Samples were packed into an aluminum holder using a back-fill procedure, and were scanned over the range of $50\text{--}6^\circ 2\theta$, at a scan rate of $0.5^\circ 2\theta/\text{min}$. Calibration of each powder pattern was effected using the characteristic scattering peaks of aluminum at 44.738 and $38.472^\circ 2\theta$. The powder pattern thus obtained is shown in Figure 6, while a summary of scattering angles, d -spacings, and relative intensities is given in Table 6.

2.6 Hygroscopicity

Propylparaben is not reported to be hygroscopic. The water content of a commercial sample of propylparaben (sourced from Ueno Fine Chemicals Industry, Ltd., Lot No. BH2311) was determined by the Karl Fisher titration method to be 0.24%.

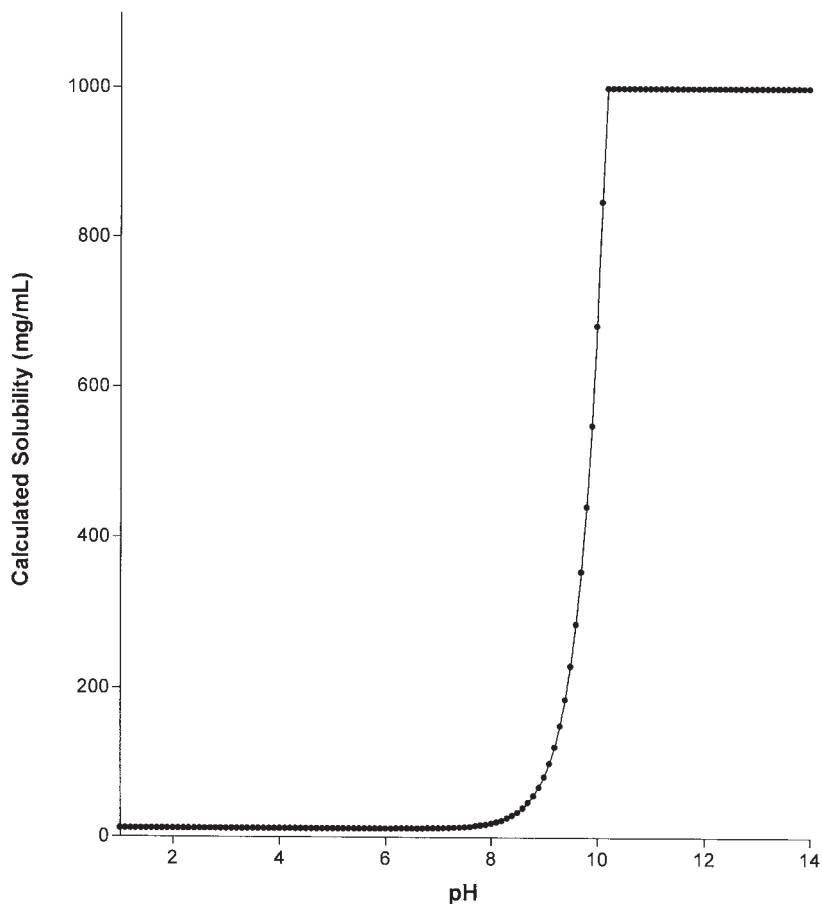


Figure 2. pH dependence of the aqueous solubility of propylparaben, calculated using PhysChem Version 6.0 (Advanced Chemistry Development, Toronto, Canada).

2.7 Thermal methods of analysis

2.7.1 Melting behavior

The melting point of propylparaben is reported to be 95–99°C [1–4].

2.7.2 Differential scanning calorimetry

Measurements of differential scanning calorimetry (DSC) were obtained on a TA Instruments 2910 thermal analysis system. The sample was

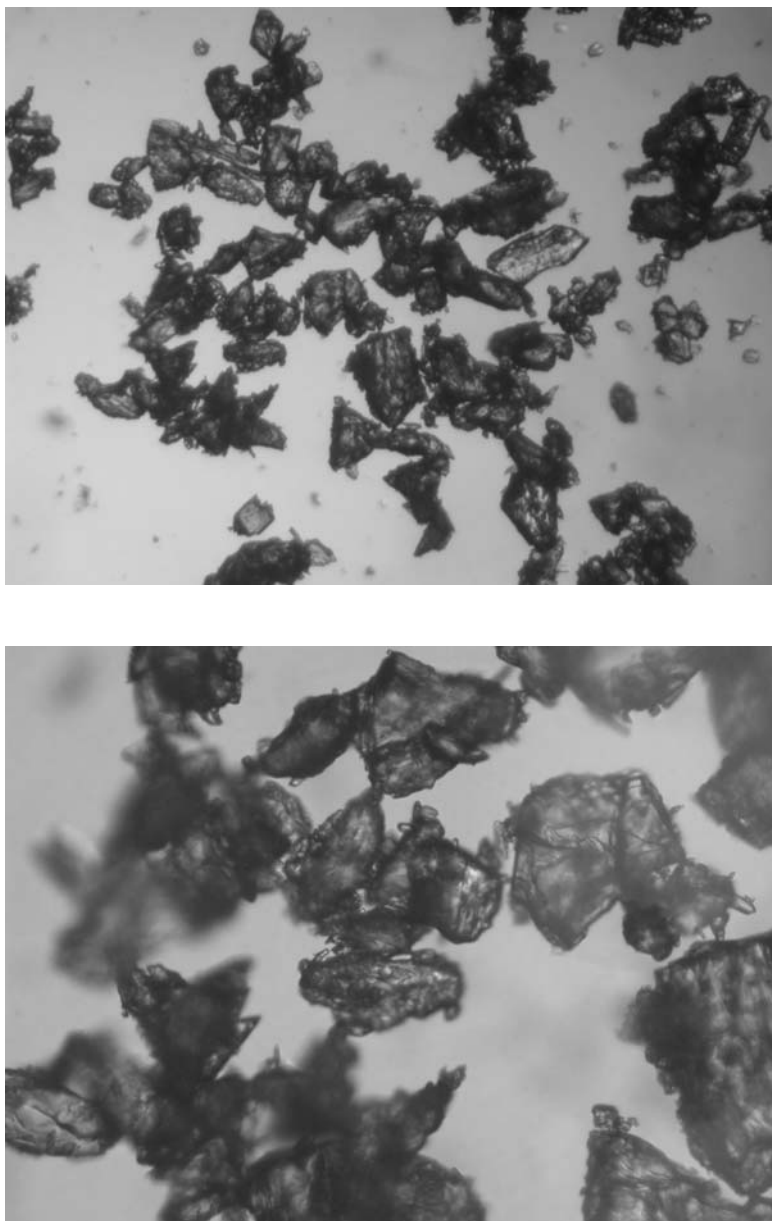


Figure 3. Morphology of propylparaben, obtained using optical microscopy at magnifications of 40 \times (upper) and 100 \times (lower).

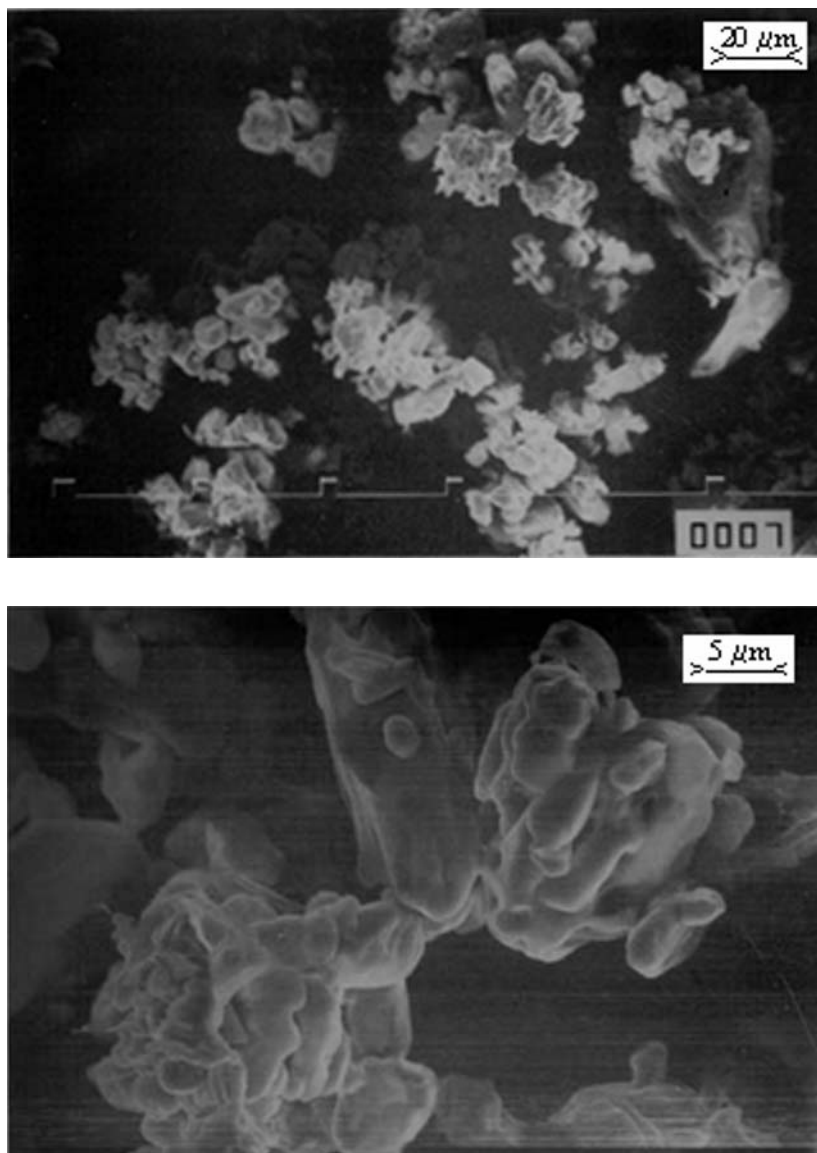


Figure 4. Morphology of propylparaben, obtained using scanning electron microscopy at magnifications of 200× (upper) and 700× (lower).

Table 5

Unit Cell Parameters Defining the Crystal Structure of Propylparaben [7]

System	Monoclinic
Space group	$P2_1/c$
a	12.0435(2) Å
b	13.8292(3) Å
c	11.7847(3) Å
β	108.63(1)°
Cell volume	1860.0 Å ³
Density, calculated	1.287 g/cm ³
Density, measured	1.29(1) g/cm ³
Number of molecules in the unit cell (Z)	8
R factor (on F)	0.090

accurately weighed into an aluminum DSC pan, and covered with an aluminum lid that was crimped in place. The sample was then heated over the range of 25–150°C, at a heating rate of 10°C/min.

The resulting thermogram is shown in [Figure 7](#), which consisted of a single endothermic event attributed to the melting process. The onset temperature was found to be 94.1°C, and the endothermic event exhibited a peak maximum at 97.8°C. Integration of the melting endotherm yielded a value of 137.5 J/g for the enthalpy of fusion. The events observed in the DSC study are consistent with the reported melting point values.

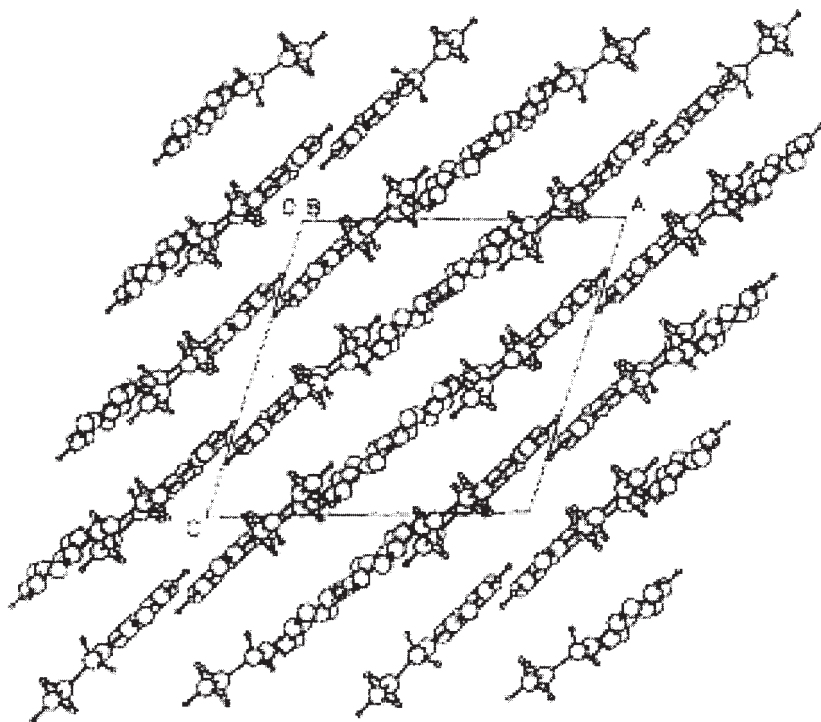


Figure 5. The [010] projection of propylparaben crystal structure showing the characteristic molecular layers situated midway between the (202) planes [7].

2.8 Spectroscopy

2.8.1 Ultraviolet absorption spectroscopy

The UV absorption spectrum of propylparaben in methanol was obtained at a concentration 1.0×10^{-4} M, using a Beckman DU-600 spectrophotometer. The resulting spectrum is shown in Figure 8, consisting of a single absorption band exhibiting a maximum at 256.5 nm (assigned to the $\Pi \rightarrow \Pi^*$ electronic transition localized on the phenyl ring). The molar absorptivity of this transition was calculated to be 1.43×10^4 .

2.8.2 Vibrational spectroscopy

The infrared absorption spectrum of propylparaben was obtained from the Integrated Spectral Data Base System for Organic Compounds

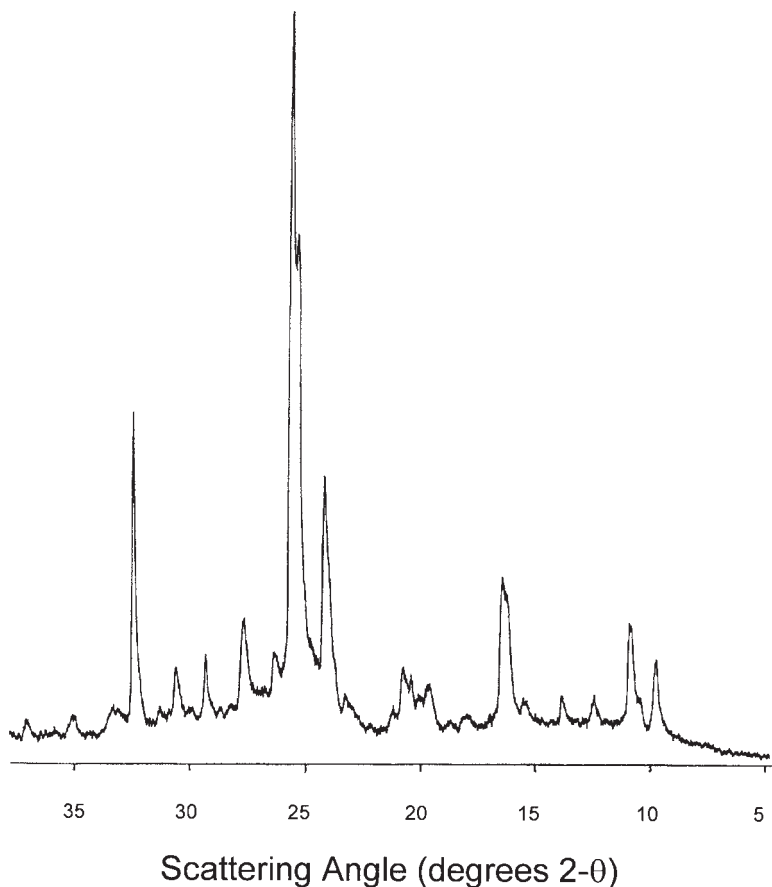


Figure 6. X-ray powder diffraction pattern of propylparaben.

(National Institute of Advanced Industrial Science and Technology, Japan), and are shown in [Figures 9 and 10](#) [12]. Assignments for some of the absorption bands are provided in [Table 7](#).

The Raman spectrum of propylparaben is shown in [Figure 11](#), and the same assignments given in [Table 7](#) apply to this spectrum as well.

2.8.3 Nuclear magnetic resonance

2.8.3.1 ^1H -NMR spectrum

The 300 MHz ^1H -NMR spectrum of propylparaben in CDCl_3 was obtained using Varian Gemini-2000 spectrometer, and is shown in

Table 6

Crystallographic Data from the X-Ray Powder Diffraction Pattern of Propylparaben

Scattering angle (°2θ)	d-Spacing (Å)	Relative intensity (%)
9.887	8.9385	10.0
10.414	8.4879	4.0
10.865	8.1365	14.0
12.368	7.1504	3.7
13.797	6.4131	4.0
15.376	5.7579	4.0
16.353	5.4159	21.3
17.857	4.9630	2.0
18.609	4.7642	1.3
19.586	4.5286	6.3
19.962	4.4441	7.3
20.338	4.3628	8.7
20.714	4.2845	10.0
21.165	4.1942	4.0
22.143	4.0112	1.3
23.195	3.8315	4.7

(continued)

Table 6 (continued)

Scattering angle (°2 θ)	<i>d</i> -Spacing (Å)	Relative intensity (%)
24.023	3.7014	35.3
25.030	3.5547	68.7
25.125	3.5415	100.0
26.278	3.3886	9.3
27.556	3.2342	13.3
28.158	3.1665	2.0
28.609	3.1176	1.3
29.211	3.0547	9.3
29.887	2.9871	2.0
30.489	2.9295	7.3
31.241	2.8607	2.7
32.248	2.7736	44.7
33.045	2.7085	6.0
33.271	2.6907	6.7
35.000	2.5616	6.7
37.105	2.4209	6.0

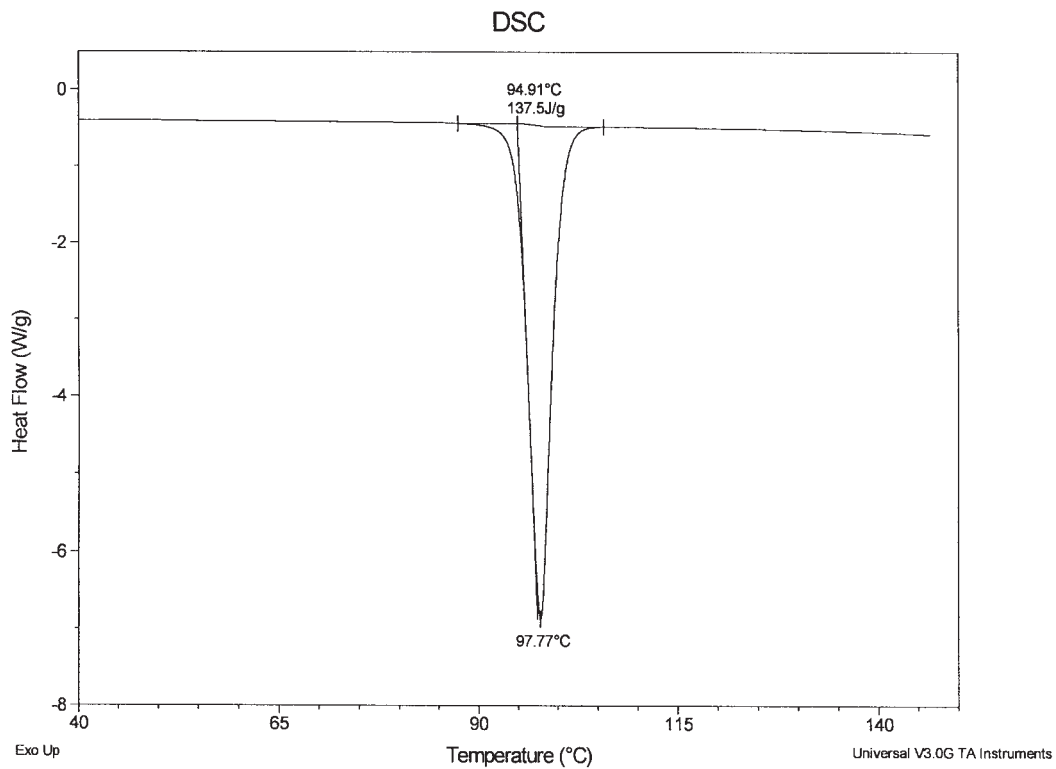


Figure 7. Differential scanning calorimetry thermogram of propylparaben.

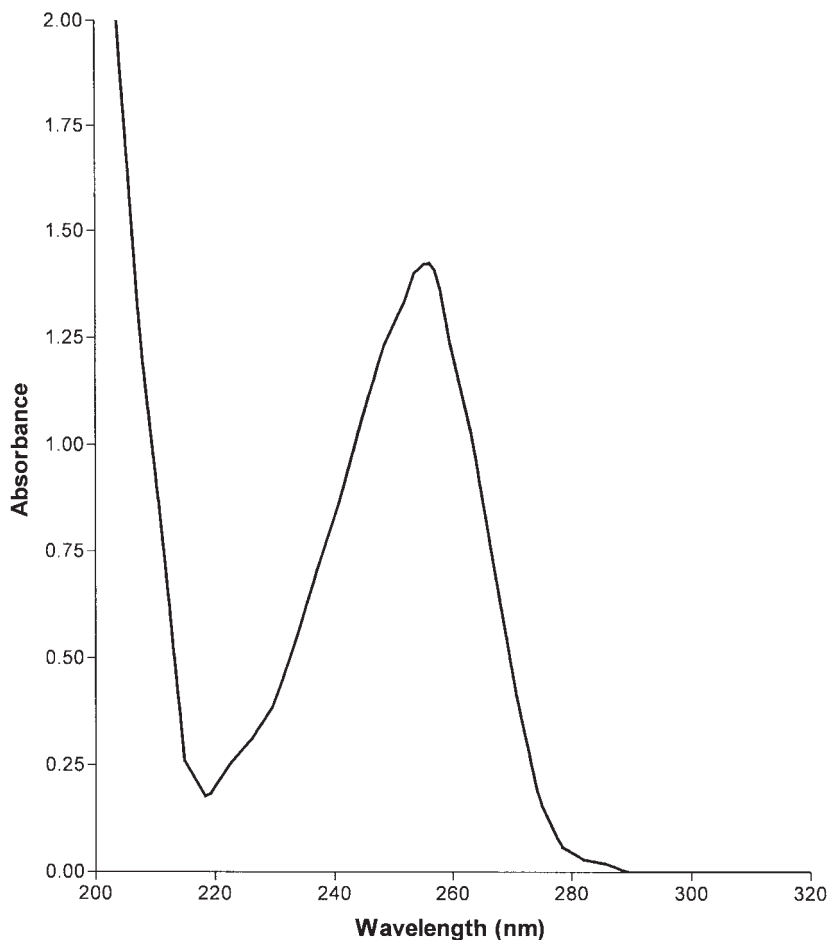


Figure 8. Ultraviolet absorption spectrum of propylparaben, obtained in methanolic solution.

Figure 12. All chemical shifts are reported in units of ppm relative to the tetramethylsilane (TMS) internal standard, and assignments for the observed bands are given in [Table 8](#).

The 90 MHz ^1H -NMR spectrum of propylparaben, obtained from the Integrated Spectral Data Base System for Organic Compounds (The National Institute of Advanced Industrial Science and Technology, Japan) is shown in [Figure 13](#) [12].

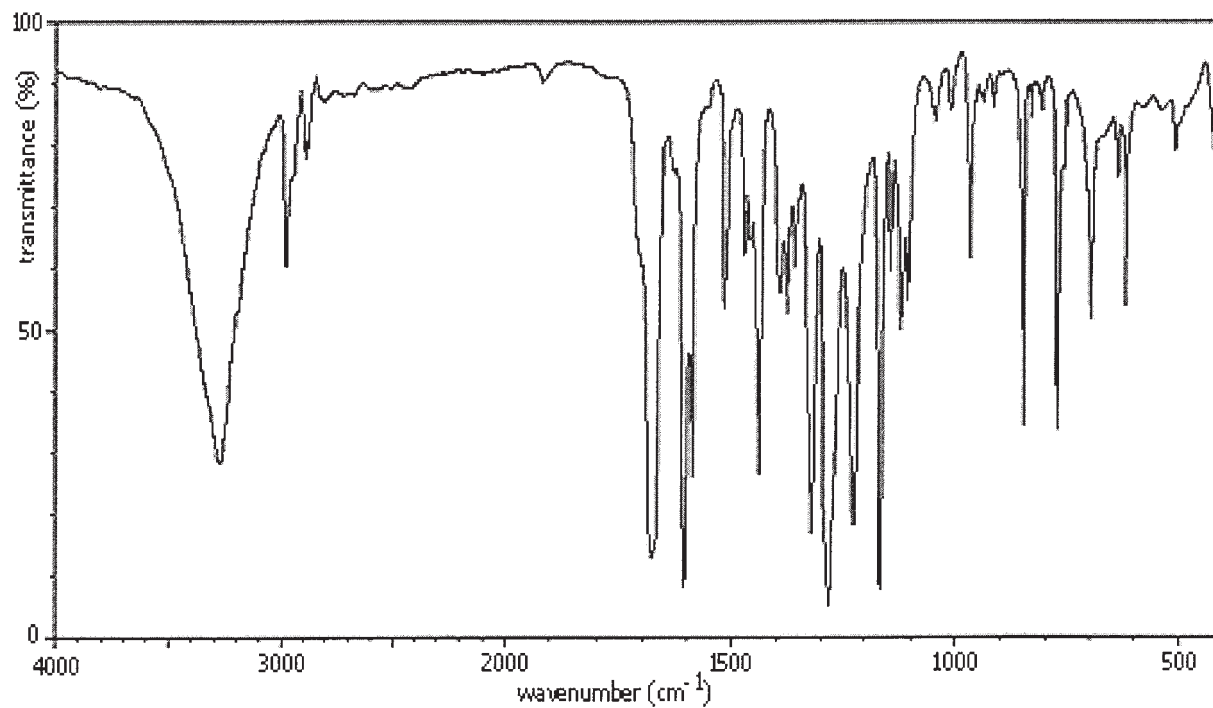


Figure 9. Infrared absorption spectrum of propylparaben (KBr pellet). [Obtained from the Integrated Spectral Data Base System for Organic Compounds, The National Institute of Advanced Industrial Science and Technology, Japan].

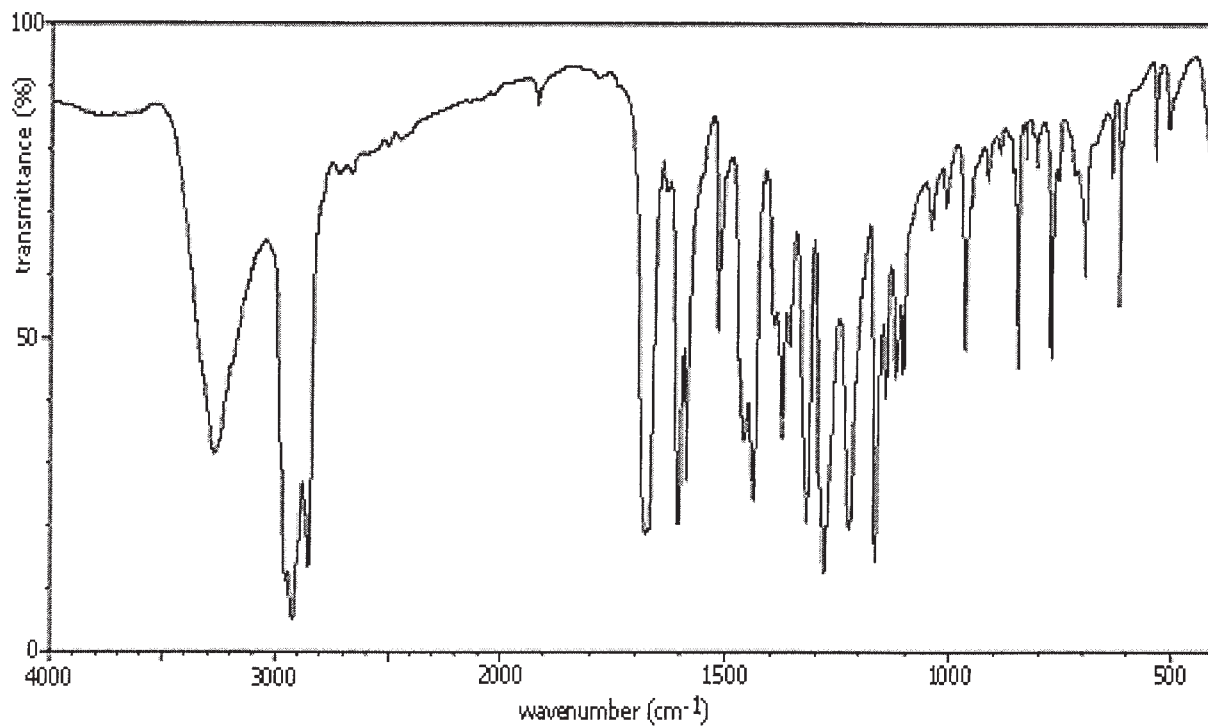


Figure 10. Infrared absorption spectrum of propylparaben (Nujol mull). [Obtained from the Integrated Spectral Data Base System for Organic Compounds, The National Institute of Advanced Industrial Science and Technology, Japan].

Table 7

Assignments for Some of the Transitions Observed in the Infrared Absorption Spectrum of Propylparaben

Energy		Band assignment
KBr Pellet	Nujol Mull	
3276	3268	OH stretching
1678	1677	C=O stretching

2.8.3.2 ^{13}C -NMR spectrum

The 75 MHz broadband decoupled ^{13}C -NMR spectrum of propylparaben was obtained in CDCl_3 using a Varian Gemini-2000 spectrometer, and the resulting spectrum is shown in Figure 14. Chemical shifts of the resonance lines were measured relative to TMS, and assignments for the observed peaks are found in Table 9.

The 23 MHz ^{13}C -NMR spectrum of propylparaben, obtained from the Integrated Spectral Data Base System for Organic Compounds (The National Institute of Advanced Industrial Science and Technology, Japan) is shown in Figure 15 [12].

2.9 Mass spectrometry

The mass spectrum of propylparaben was recorded using a JEOL JMS-DX-303 spectrometer, operated in the electron impact mode. The resulting mass spectrum is shown in Figure 16, and assignments for the major observed fragments are found in Table 10.

3. STABILITY OF PROPYLPARABEN

3.1 Solid-state stability

Propylparaben is known to be stable in contact with air [6], but the bulk substance should still be stored in a cool, dry place in a well-closed container [4].

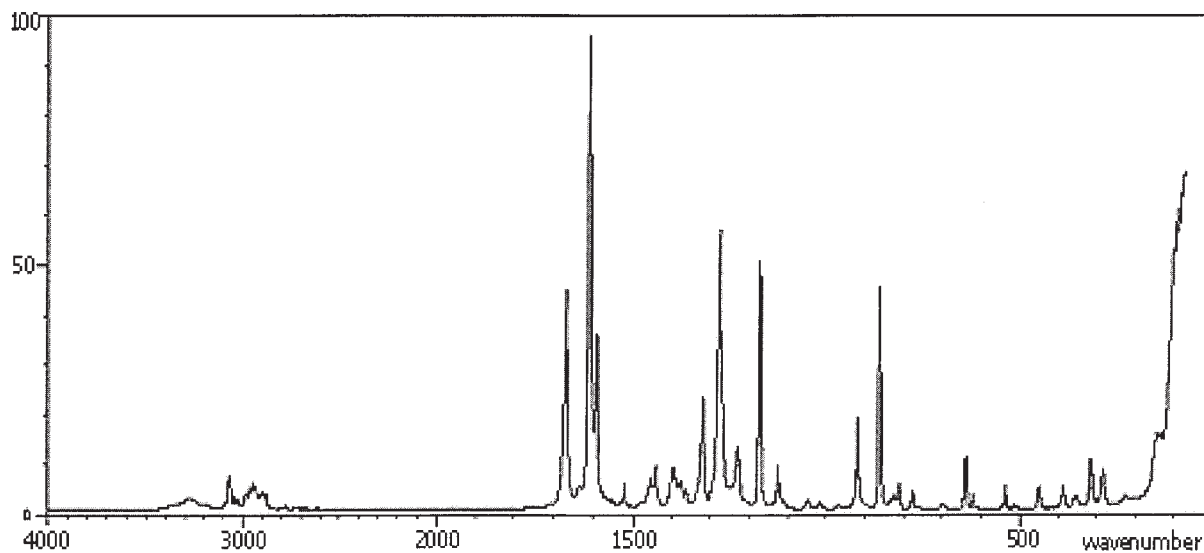


Figure 11. Raman spectrum of propylparaben. [Obtained from the Integrated Spectral Data Base System for Organic Compounds, The National Institute of Advanced Industrial Science and Technology, Japan].

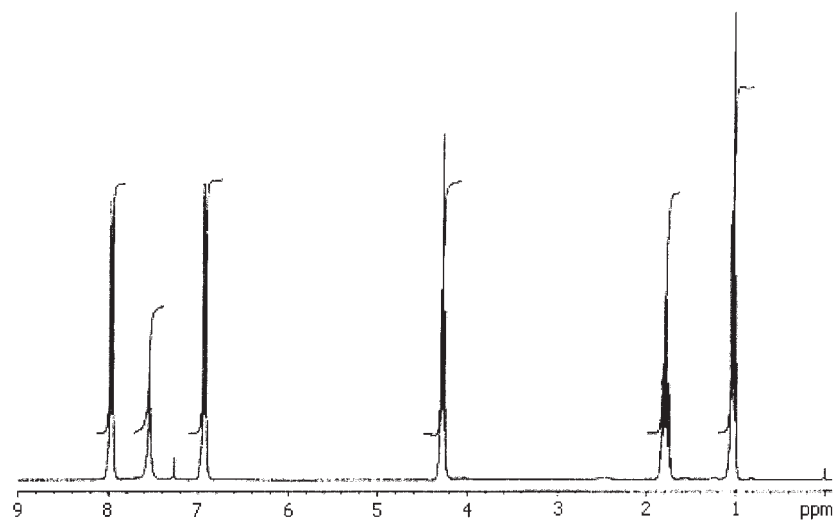
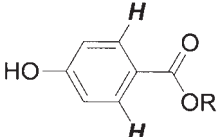
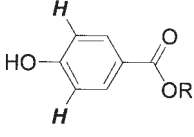


Figure 12. 300 MHz proton nuclear magnetic resonance spectrum of propylparaben.

Table 8

Assignments for the Resonance Bands in the ^1H -NMR Spectrum of Propylparaben

Chemical shifts (ppm)	Number of proton	Proton
7.95	2	
7.31	1	<i>HO</i> —
6.91	2	
4.27	2	$-\text{OCH}_2\text{CH}_2\text{CH}_3$
1.78	2	$-\text{OCH}_2\text{CH}_2\text{CH}_3$
1.02	3	$-\text{OCH}_2\text{CH}_2\text{CH}_3$

3.2 Solution-phase stability

The literature regarding the solution-phase stability of propylparaben is not consistent. According to Aalto, propylparaben is resistant to hydrolysis in cold or hot water [6]. Aqueous solutions buffered at pH 3 and 6 showed no evidence of hydrolysis after heating for 2 h at 100°C and 30 min at 120°C. At pH 8, these heating periods hydrolyzed about 6% of propylparaben. In solutions at pH 3, 7, and 8, no hydrolysis was noted after six weeks at 25°C [6].

Kamada *et al.* reported the degradation of propylparaben in acidic media between 40 and 100°C [13], but Blaug and Grant found no detectable hydrolysis of propylparaben below pH 6.41 [14]. Sunderland and Watts observed hydrolysis of the paraben at pH values in the range of

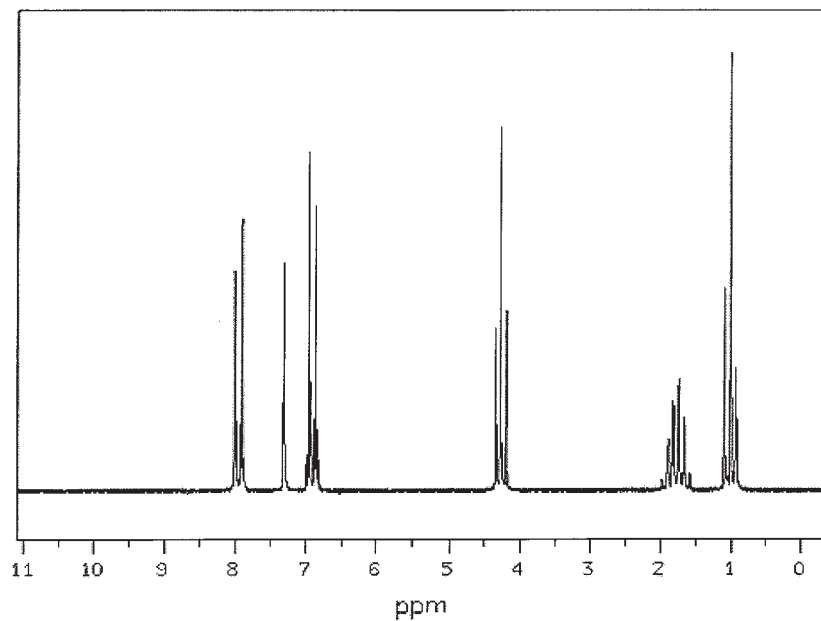


Figure 13. 90 MHz proton nuclear magnetic resonance spectrum of propylparaben. [Obtained from the Integrated Spectral Data Base System for Organic Compounds, The National Institute of Advanced Industrial Science and Technology, Japan].

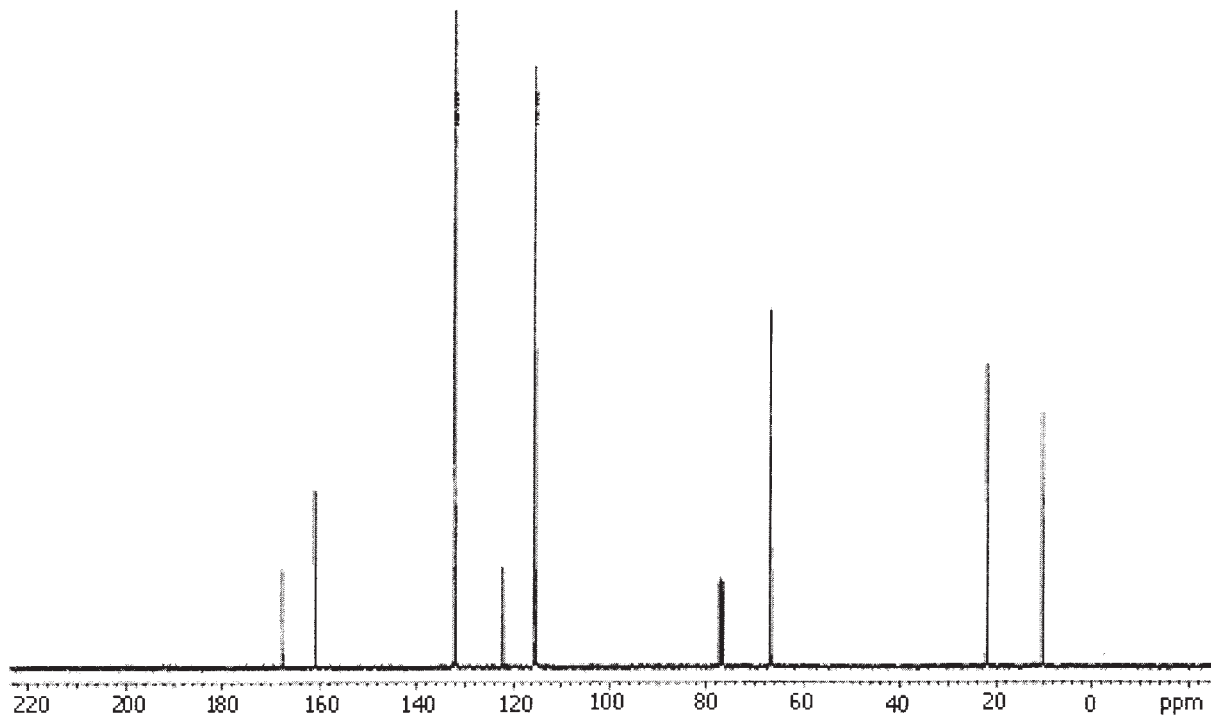
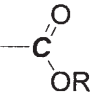
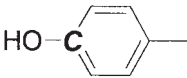
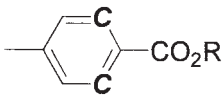
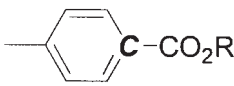
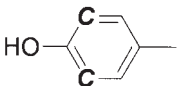


Figure 14. 75 MHz carbon nuclear magnetic resonance spectrum of propylparaben.

Table 9

Assignments for the Resonance Bands in the ^{13}C -NMR Spectrum of Propylparaben

Chemical shifts (ppm)	Carbon
167.94	
161.13	
132.04	
121.95	
115.51	
66.90	$-\text{OCH}_2\text{CH}_2\text{CH}_3$
22.14	$-\text{OCH}_2\text{CH}_2\text{CH}_3$
10.50	$-\text{OCH}_2\text{CH}_2\text{CH}_3$

1.26–10.59, showing that the hydrolysis can be catalyzed by either H^+ or OH^- ions [15].

3.3 Stability in biological fluids

Propylparaben, along with its metabolites, was found in blood and urine after its oral and intravenous administration [16].

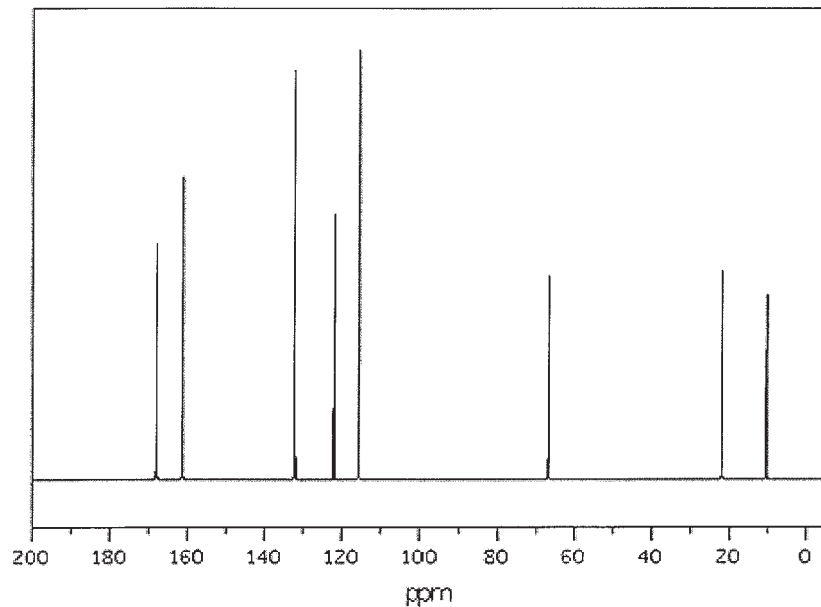


Figure 15. 25 MHz carbon nuclear magnetic resonance spectrum of propylparaben. [Obtained from the Integrated Spectral Data Base System for Organic Compounds, The National Institute of Advanced Industrial Science and Technology, Japan].

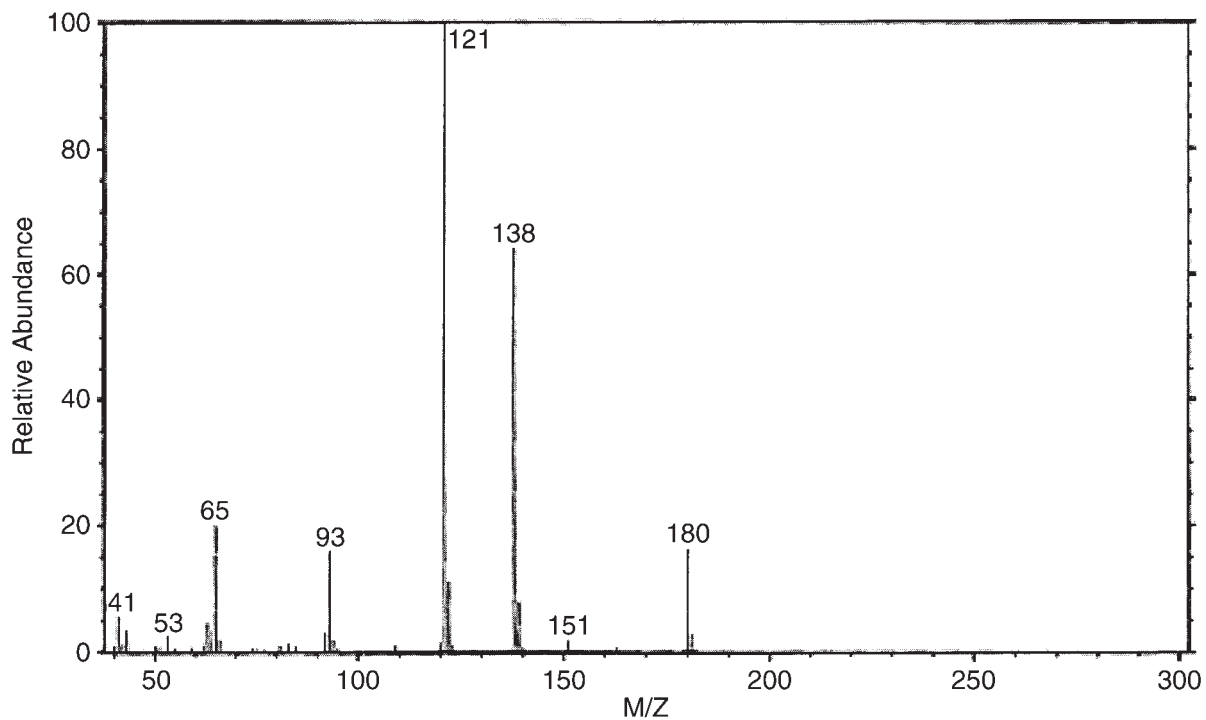


Figure 16. Mass spectrum of propylparaben.

Table 10

Assignments for the Major Fragment Ions in the Mass Spectrum of Propylparaben

<i>m/z</i> ratio	Relative intensity (%)	Fragment assignment
180	16.3	$\left[\text{HO}-\text{C}_6\text{H}_4-\text{C}(=\text{O})\text{OC}_3\text{H}_7 \right]^+ \quad (\text{M}^+)$
138	64.2	$\left[\text{HO}-\text{C}_6\text{H}_4-\text{C}(=\text{O})\text{OH} \right]^+$
121	100.0	$\left[\text{HO}-\text{C}_6\text{H}_4-\text{C}=\text{O} \right]^+$
93	15.9	$\left[\text{O}-\text{C}_6\text{H}_5 \right]^+$
65	20.3	$[\text{C}_5\text{H}_5]^+$

4. INCOMPATIBILITIES WITH FUNCTIONAL GROUPS

Propylparaben has been found to be absorbed by magnesium trisilicate [17]. The degree of adsorption was strongly influenced by pH, and the amount of propylparaben adsorbed decreased with increasing pH.

It has also been reported that propylparaben is bound by Tween 80 (polyoxyethylene 20 sorbitan monooleate). At a concentration of 5% Tween 80, only 4.5% of the total propylparaben was present as unbound and capable of acting as a preservative [18].

Absorption of propylparaben by plastics has been reported, with the amount absorbed dependent upon the type of plastic and the vehicle [19].

Propylparaben was found to undergo a transesterification reaction with polyols, which accelerated its degradation [20].

Propylparaben is discolored in the presence of iron, and is subjected to hydrolysis by weak alkalis and strong acids [4].

5. ACKNOWLEDGMENTS

The authors wish to thank Dr. Irminda Kris Murwani (Humboldt University, Berlin) and Mr. Junaidi Khotib (Hoshi University, Tokyo) for their assistance in literature searching, and Mr. Abdul Rahman (Airlangga University, Surabaya) for taking some of the photomicrographs.

6. REFERENCES

1. *The Merck Index*, 12th edn., Merck Research Laboratories, Division of Merck & Co., Inc., Whitehouse Station, NJ., p. 8045 (1996).
2. *Martindale: The Complete Drug Reference*, 32nd edn., K. Parfitt, ed., Pharmaceutical Press, Taunton, Massachusetts, p. 1117 (1999).
3. *British Pharmacopoeia 2000*, Volume 1, The Stationery Office, Norwich, UK, pp. 1304–1305 (2000).
4. *Handbook of Pharmaceutical Excipients*, 3rd edn., A.H. Kibbe, ed., American Pharmaceutical Association and Pharmaceutical Press, Washington and London, pp. 450–453 (2000).
5. T.E. Haag and D.F. Loncrini, “Esters of para-hydroxybenzoic acid”, in *Cosmetic and Drug Preservation*, J.J. Kabara, ed., Marcel Dekker, New York, pp. 63–77 (1984).
6. T.R. Aalto, M.C. Firman, and N.E. Rigler, *J. Am. Pharm. Assoc.*, **42**, 449–457 (1953).
7. F. Giordano, R. Bettini, C. Donini, A. Gazzaniga, M.R. Caira, G.G.Z. Zhang, and D.J.W. Grant, *J. Pharm. Sci.*, **88**, 1210–1216 (1999).
8. C. McDonald, L. Palmer, and M. Boddy, *Drug Development and Industrial Pharmacy*, **22**, 1025–1029 (1996).

9. H. Matsuda, K. Ito, Y. Sato, D. Yoshizawa, M. Tanaka, A. Taki, H. Sumiyoshi, T. Utsuki, F. Hirayama, and K. Uekama, *Chem. Pharm. Bull.*, **41**, 1448–1452 (1993).
10. L.S.C. Wan, T.R.R. Kurup, and L.W. Chan, *Pharm. Acta Helv.*, **61**, 308–313 (1986).
11. N. Pongcharoenkiat, G. Narshimhan, R.T. Lyons, and S.L. Hem, *J. Pharm. Sci.*, **91**, 559–570 (2002).
12. **Integrated Spectral Data Base System for Organic Compounds**, The National Institute of Advanced Industrial Science and Technology, Japan (<http://www.aist.go.jp/RIODB/SDBS/> access date: March 20, 2003).
13. A. Kamada, N. Yata, K. Kubo, and M. Arakawa, *Chem. Pharm. Bull.*, **21**, 2073–2076 (1973).
14. S.M. Blaug and D.E. Grant, *J. Soc. Cosmet. Chem.*, **25**, 495–506 (1974).
15. V.B. Sunderland and D.W. Watts, *Int. J. Pharm.*, **19**, 1–15 (1984).
16. P.S. Jones, D. Thigpen, J.L. Morrison, and A.P. Richardson, *J. Am. Pharm. Assoc.*, **45**, 268–273 (1956).
17. M.C. Allwood, *Int. J. Pharm.*, **11**, 101–107 (1982).
18. N.K. Patel and H.B. Kostenbauder, *J. Am. Pharm. Assoc.*, **47**, 289–293 (1958).
19. K. Kakemi, H. Sezaki, E. Arakawa, K. Kimura, and K. Ikeda, *Chem. Pharm. Bull.*, **19**, 2523–2529 (1971).
20. B. Runesson and K. Gustavii, *Acta Pharm. Suec.*, **23**, 151–162 (1986).

Related Methodology Review Articles

X-Ray Diffraction of Pharmaceutical Materials

Harry G. Brittain

*Center for Pharmaceutical Physics
10 Charles Road
Milford, NJ 08848, USA*

CONTENTS

1.	Introduction	274
1.1	Historical background	275
1.2	Description of crystalline solids	276
1.3	Solid-state symmetry	280
1.4	Diffraction of electromagnetic radiation by crystalline solids	281
2.	Single-Crystal X-Ray Diffraction	283
2.1	Case study: theophylline anhydrate and monohydrate	284
2.2	Crystallographic studies of polymorphism	287
3.	X-Ray Powder Diffraction	301
3.1	Determination of phase identity	302
3.2	Degree of crystallinity	305
3.3	Phase composition of mixtures	309
3.4	Thermodiffraction	312
3.5	XRPD as a stability-indicating assay method	314
4.	Summary	315
5.	References	316

1. INTRODUCTION

The effect exerted by the crystallographic structure of a compound on both its chemical and physical properties is profound, and is only now becoming fully appreciated by workers in the pharmaceutical field. Numerous examples now exist where stabilization was brought about by subtle manipulation of the crystal state, or where instability arose as a consequence of a solid-state reaction.

All properly designed investigations into the solid state of a pharmaceutical compound begin with an understanding of the structural aspects involved, and it is generally accepted that the primary tool for the study of solid-state crystallography is that of x-ray diffraction. To properly comprehend the power of this technique, we will first examine the processes associated with the ability of a crystalline solid to act as a diffraction grating for the electromagnetic radiation termed 'x-rays'. In latter sections, we will separately discuss the practice of x-ray diffraction as applied to the characterization of single crystals and to the study of powdered crystalline solids.

1.1 Historical background

X-ray crystallography has its origins in studies performed to discover the nature of the radiation emitted by cathode ray tubes, known at the time as “Roentgen rays” or “x-radiation”. It was not clear at the end of the 19th century whether these rays were corpuscular or electromagnetic in nature. Since it was known that they moved in straight lines, cast sharp shadows, were capable of crossing a vacuum, acted on a photographic plate, excited substance to fluoresce, and could ionize gases, it appeared that they had the characteristics of light. But at the same time, the fact that mirrors, prisms, and lenses that operated on ordinary light had no effect on these rays, they could not be diffracted by ordinary gratings, and neither birefringence or polarization could be induced in such beams by passage through biaxial crystals, suggesting a corpuscular nature.

The nature of x-radiation ultimately became understood through studies of their diffraction, although the experimental techniques differed from those of classical diffraction studies. The existence of optical diffraction effects had been known since the 17th century, when it was shown that shadows of objects are larger than they ought to be if light traveled past the bodies in straight lines undetected by the bodies themselves. During the 19th century, the complete theory of the diffraction grating was worked out, where it was established that in order to produce diffraction spectra from an ordinary grating, the spacings of the lines on the grating had to be of the same size and magnitude as the wavelength of the incident light. Laue argued that if x-rays consisted of electromagnetic radiation having a very short wavelength, it should be possible to diffract the rays once a grating having sufficiently small spacings could be found.

The theory of crystals developed by Bravais [1] suggested that the atoms in a solid were in regular array, and estimates of atomic size showed that the distances between the sheets of atoms were probably about the same as the existing estimates for the wavelengths of the x-radiation. Laue suggested the experiment of passing an x-ray beam rays through a thin slice of crystalline zinc blende, since this material had an understood structure. Friedrich and Knipping tried the experiment, and found a pattern of regularly placed diffracted spots arranged round the central un-deflected x-ray beam, thus showing that the rays were diffracted in a regular manner by the atoms of the crystal [2]. In 1913, Bragg reported the first x-ray diffraction determination of a crystal structure, deducing the structures of KCl, NaCl, KBr, and KI [3]. Eventually the complicated explanation advanced by Laue to explain the phenomenon was simplified

by Bragg, who introduced the concept of “reflexion”, as he originally termed diffraction [4].

Bragg established that the diffraction angles were governed by the spacings between atomic planes within a crystal. He also reported that the intensities of diffracted rays were determined by the types of atoms present in the solid, and their arrangement within a crystalline material. Atoms with higher atomic numbers contain larger numbers of electrons, and consequently scatter x-rays more strongly than atoms characterized by lower atomic numbers. This difference in scattering power leads to marked differences in the intensities of diffracted rays, and such data provides information on the distribution of atoms within the crystalline solid. In a later section we will examine the x-ray diffraction phenomenon in more detail, but prior to that, a short discussion of crystallography is necessary.

1.2 Description of crystalline solids

Since a number of extensive discussions of crystallography are available [5–9], it is necessary to provide only the briefest outline of the nature of crystalline solids. An ideal crystal is constructed by an infinite regular spatial repetition of identical structural units. For the organic molecules of pharmaceutical interest, the simplest structural unit will contain one or more molecules. The structure of crystals is ordinarily explained in terms of a periodic *lattice*, or a three-dimensional grid of lines connecting points in a given structure. For organic molecules, a group of atoms is attached to a lattice point. It is important to note that the points in a lattice may be connected in various ways to form infinite number of different lattice structures. The crystal structure is formed only when a fundamental unit is attached identically to each lattice point, and extended along each crystal axis through translational repetition.

To illustrate the relation between a crystal lattice and crystal planes, [Figure 1](#) shows three different families of planes that have been drawn through a common lattice type. The lattice is seen to be the trapezoidal grid in the background, and the different crystal planes are depicted as dashed lines. Acceptable planes are those that pass through the points of lattice intersections. It is relatively easy to see that for a given lattice type, there are only a finite number of planes that can be drawn. Whether all of these can be identified in a particular crystal will depend greatly upon the nature of the system, and the intermolecular interactions among the molecules incorporated in the structure.

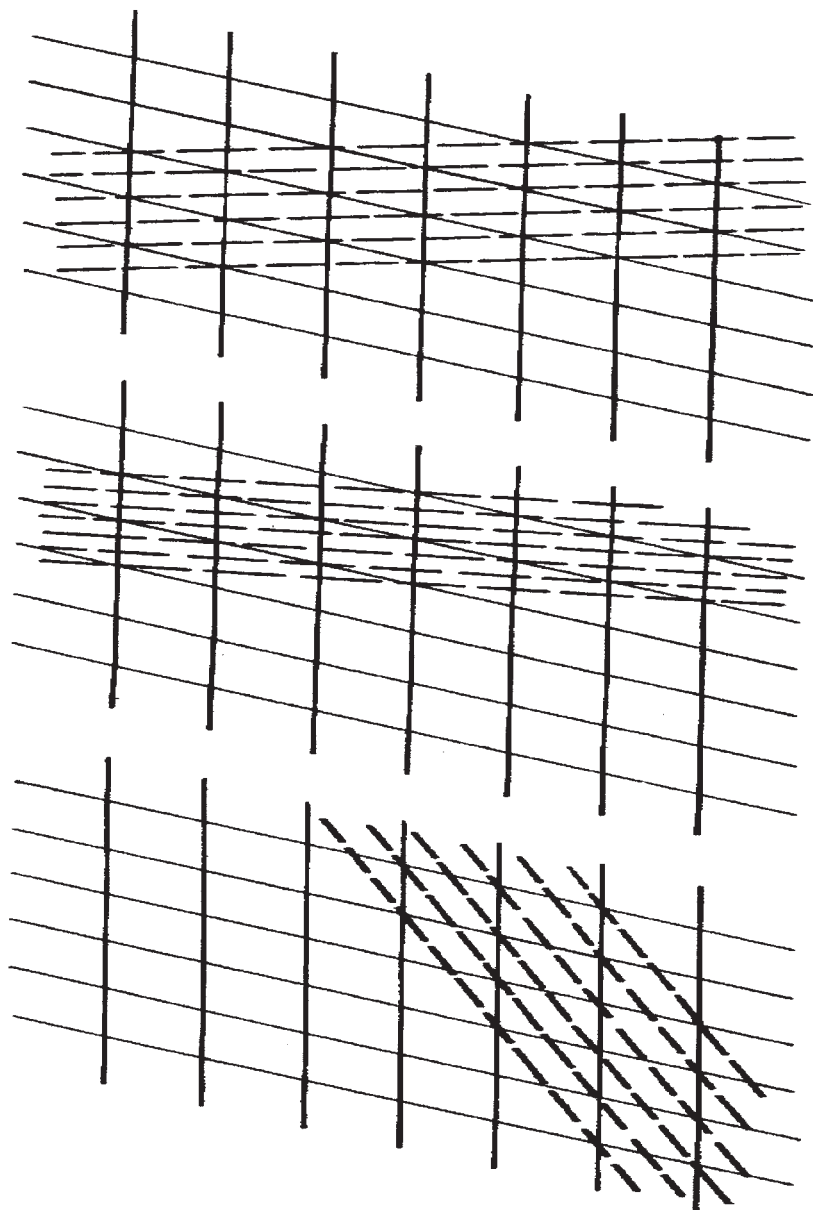


Figure 1. Families of planes passing through lattice points.

The points on a lattice are defined by three fundamental translation vectors, **a**, **b**, and **c**, such that the atomic arrangement looks the same in every respect when viewed from any point **r** as it does when viewed at point **r'**:

$$\mathbf{r}' = \mathbf{r} + n_1\mathbf{a} + n_2\mathbf{b} + n_3\mathbf{c} \quad (1)$$

where n_1 , n_2 , and n_3 are arbitrary integers. The lattice and translation vectors are said to be *primitive* if any two points from which an identical atomic arrangement is obtained through the satisfaction of equation (1) with a suitable choice of the n_1 , n_2 , and n_3 integers. It is common practice to use the primitive translation vectors to define the axes of the crystal, although other non-primitive crystal axes can be used for the sake of convenience. A lattice translation operation is defined as the displacement within a lattice, with the vector describing the operation being given by:

$$\mathbf{T} = n_1\mathbf{a} + n_2\mathbf{b} + n_3\mathbf{c} \quad (2)$$

The crystal axes, **a**, **b**, and **c**, form three adjacent edges of a parallelepiped. The smallest parallelepiped built upon the three unit translations is known as the *unit cell*. Although the unit cell is an imaginary construct, it has an actual shape and definite volume. The crystal structure is generated through the periodic repetition, by the three unit translations, of matter contained within the volume of the unit cell. A unit cell does not necessarily have a definite absolute origin or position, but does have the definite orientation and shape defined by the translation vectors. A cell will fill all space under the action of suitable crystal translation operations, and will occupy the minimum volume permissible.

The unit cell is defined by the lengths (a , b , and c) of the crystal axes, and by the angles (α , β , and γ) between these. The usual convention is that α defines the angle between the b - and c -axes, β defines the angle between the a - and c -axes, and γ defines the angle between the a - and b -axes. There are seven fundamental types of primitive unit cell (whose characteristics are provided in Table 1), and these unit cell characteristics define the seven *crystal classes*. If the size of the unit cell is known (*i.e.*, α , β , γ , a , b , and c have been determined), then the unit cell volume (V) may be used to calculate the density (ρ) of the crystal:

$$\rho = ZM/VA \quad (3)$$

Table 1

The Seven Crystal Classes, Defined From Their
Fundamental Unit Cells

System	Relationship between cell edges	Relationship between cell angles
Cubic	$a = b = c$	$\alpha = \beta = \gamma = 90^\circ$
Tetragonal	$a = b \neq c$	$\alpha = \beta = \gamma = 90^\circ$
Orthorhombic	$a \neq b \neq c$	$\alpha = \beta = \gamma = 90^\circ$
Monoclinic	$a \neq b \neq c$	$\alpha = \gamma = 90^\circ \quad \beta \neq 90^\circ$
Triclinic	$a \neq b \neq c$	$\alpha \neq \beta \neq \gamma \neq 90^\circ$
Hexagonal	$a = b \neq c$	$\alpha = \beta = 90^\circ \quad \gamma = 120^\circ$
Trigonal	$a = b = c$	$\alpha = \beta = 90^\circ \quad \gamma \neq 90^\circ$

where M is the molecular weight of the substance in the crystal, A is Avogadro's number, and Z is the number of molecular units in the unit cell. When ρ is measured for a crystal (generally by flotation) for which the elemental composition of the molecule involved is known, then Z may be calculated. The value of Z is of great importance because it can provide molecular symmetry information from a consideration of the symmetry properties of the lattice.

As illustrated in [Figure 1](#), the points of a lattice can be considered as lying in various sets of parallel planes. These, of course, are not limited to lying along a single Cartesian direction, but can instead be situated along any combination of axis directions permitted by the structure of the lattice. Consider a given set of parallel planes, which cuts across the a -, b -, and c -axes at different points along each axis. If the a -axis is divided into h units, the b -axis into k units, and c -axis into l units, then $h \ k \ l$ are the *Miller indices* of that set of planes, and the set of planes is identified by its Miller indices as $(h \ k \ l)$. If a set of planes happens to be parallel to one axis, then its corresponding Miller index is zero.

For instance, a plane that lies completely in the ab -plane is denoted as the (001) plane, a plane that lies completely in the ac -plane is denoted as the (010) plane, a plane that lies completely in the bc -plane is denoted as the (100) plane, and the plane that equally intersects the a -, b -, and c -axes is denoted as the (111) plane. The values of h , k , and l are independent quantities, and are defined only by their spatial arrangements within the unit cell.

1.3 Solid-state symmetry

Crystal lattices can be depicted not only by the lattice translation defined in Equation (2), but also by the performance of various point symmetry operations. A *symmetry operation* is defined as an operation that moves the system into a new configuration that is equivalent to and indistinguishable from the original one. A *symmetry element* is a point, line, or plane with respect to which a symmetry operation is performed. The complete ensemble of symmetry operations that define the spatial properties of a molecule or its crystal are referred to as its *group*. In addition to the fundamental symmetry operations associated with molecular species that define the *point group* of the molecule, there are additional symmetry operations necessary to define the *space group* of its crystal. These will only be briefly outlined here, but additional information on molecular symmetry [10] and solid-state symmetry [11] is available.

Considering molecular symmetry first, the simplest operation is the *identity*, which leaves the system unchanged and hence in an orientation identical with that of the original. The second symmetry operation is that of *reflection* through a plane, and is denoted by the symbol σ . The effect of reflection is to change the sign of the coordinates perpendicular to the plane, while leaving unchanged the coordinates parallel to the plane. The third symmetry operation is that of *inversion* through a point, and is denoted by the symbol i . In Cartesian coordinates, the effect of inversion is to change the sign of all three coordinates that define a lattice point in space. The fourth type of symmetry operation is the *proper rotation*, which represents the simple rotation about an axis which passes through a lattice point. Only rotations by angles of 2π (360°), $2\pi/2$ (180°), $2\pi/3$ (120°), $2\pi/4$ (90°), and $2\pi/6$ (60°) radians are permissible, these being denoted as onefold (symbol C_1), twofold (symbol C_2), threefold (symbol C_3), fourfold (symbol C_4), and sixfold (symbol C_6) proper rotation axes. The final type of symmetry operation is the *improper rotation*, which represents the combination of a proper rotation axis followed by the performance of a reflection operation. Once again, only improper

rotations by angles of 2π (360°), $2\pi/2$ (180°), $2\pi/3$ (120°), $2\pi/4$ (90°), and $2\pi/6$ (60°) radians are permissible, and are denoted as onefold (symbol S_1), twofold (symbol S_2), threefold (symbol S_3), fourfold (symbol S_4), and sixfold (symbol S_6) proper rotation axes.

There are two additional symmetry operators required in the definition of space groups. These operators involve translational motion, for now we are moving molecules into one another along three dimensions. One of these is referred to as the *screw axis*, and the other is the *glide plane*. The screw operation rotates the contents of the cell by 180° , and then translates everything along its axis by one-half the length of the parallel unit cell edge. The glide operation reflects everything in a plane, and then translates by one-half of the unit cell along one direction in the same plane.

The symmetry of a crystal is ultimately summed up in its crystallographic *space group*, which is the entire set of symmetry operations that define the periodic structure of the crystal. Bravais showed that when the full range of lattice symmetry operations was taken into account, one could define a maximum of 230 distinct varieties of crystal symmetry, or space groups. The space groups are further classified as being either symmorphic or nonsymmorphic. A symmorphic space group is one which is entirely specified by symmetry operations acting at a common point, and which do not involve one of the glide or screw translations. The symmorphic space groups are obtained by combining the 32 point groups with the 14 Bravais lattices, yielding a total of 73 space groups out of the total of 230. The nonsymmorphic space groups are specified by at least one operation that involves a nonprimitive translation, and one finds that there are a total of 157 nonsymmorphic space groups.

1.4 Diffraction of electromagnetic radiation by crystalline solids

Laue explained the reflection of x-rays by crystals using a model where every atom of the crystal bathed in the beam of x-rays represents a secondary radiating source in which the wavelength and phase remain unchanged. Then, for a three-dimensional regular array, these secondary waves interfere with one another in such a way that, except for certain calculable directions, destructive interference occurs. In the special directions, however, there is constructive interference and strong scattered X-ray beams can be observed.

Bragg provided a much simpler treatment of the scattering phenomenon. He assumed that the atoms of a crystal are regularly arranged in space,

and that they can be regarded as lying in parallel sheets separated by a definite and defined distance. Then he showed that scattering centers arranged in a plane act like a mirror to x-rays incident on them, so that constructive interference would occur for the direction of specular reflection. As shown in Figure 1, an infinite number of sets of parallel planes can be passed through the points of a space-lattice. If we now consider one set of planes, defined by a Miller index of $(h\ k\ l)$, each plane of this set produces a specular reflectance of the incident beam. If the incident x-rays are monochromatic (having wavelength equal to λ), then for an arbitrary glancing angle of θ , the reflections from successive planes are out of phase with one another. This yields destructive interference in the scattered beams. However, by varying θ , a set of values for θ can be found so that the path difference between x-rays reflected by successive planes will be an integral number (n) of wavelengths, and then constructive interference will occur.

Bragg's model is illustrated in Figure 2, where the horizontal lines represent two successive planes of the set. The spacing of these planes

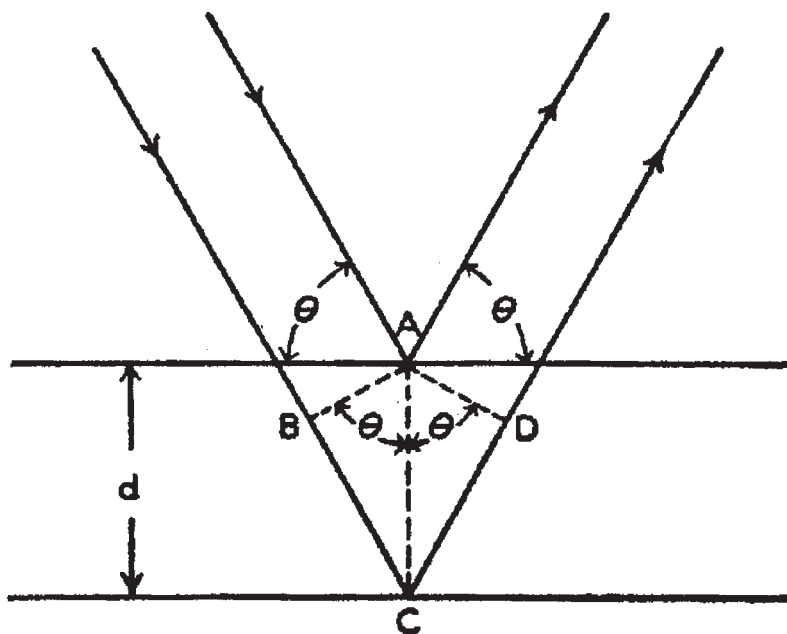


Figure 2. Diffraction of electromagnetic radiation by planes of atoms in a crystalline solid.

(denoted as d) is the perpendicular distance between them. The path difference is $\{(BC)+(CD)\}$, and for constructive interference this pathlength must equal $(n\lambda)$. But since $\{(BC)+(CD)\}$ must equal to $(2d \sin \theta)$, one deduces an expression universally known as Bragg's law:

$$2d \sin \theta = n\lambda \quad (4)$$

Unlike the case of diffraction of light by a ruled grating, the diffraction of x-rays by a crystalline solid leads to observation of constructive interference (*i.e.*, reflection) that occurs only at the critical Bragg angles. When reflection does occur, it is stated that the plane in question is reflecting in the n th order, or that one observes n th order diffraction for that particular crystal plane. Therefore one will observe an x-ray scattering response for every plane defined by a unique Miller index of $(h\ k\ l)$.

Consider a crystal, characterized by some unit cell that contains Z atoms per unit cell. Taking each of the Z atoms in succession as origin of a lattice, one can envision the crystal as composed of Z identical interpenetrating lattices, with their displacements relative to each other being decided by the distribution of the Z atoms within the unit cell. All these lattices will be characterized by identical Bragg angles, but the reflections from the Z -independent lattices will interfere with one another. This interference will determine the intensity of the reflection for that plane, but the Bragg angle will be independent of the atomic distribution within the cell, and will depend only on the details of the external cell geometry.

The analysis of x-ray diffraction data is divided into three parts. The first of these is the geometrical analysis, where one measures the exact spatial distribution of x-ray reflections and uses these to compute the size and shape of a unit cell. The second phase entails a study of the intensities of the various reflections, using this information to determine the atomic distribution within the unit cell. Finally, one looks at the x-ray diagram to deduce qualitative information about the quality of the crystal or the degree of order within the solid. This latter analysis may permit the adoption of certain assumptions that may aid in the solving of the crystalline structure.

2. SINGLE-CRYSTAL X-RAY DIFFRACTION

Since this review will focus more on applications of x-ray diffraction rather on theoretical aspects, the actual methodology used to deconvolute

scattering data into structural information will not be addressed. It is sufficient to note that the analysis of x-ray diffraction data consists of two main aspects. The first of these is a geometrical analysis, where the size and shape of a unit cell is computed from the exact spatial distribution of x-ray reflections. The second examination yields the atomic distribution within the unit cell from a study of the intensities of the various reflections. Throughout the process, one uses the x-ray diagram in order to deduce qualitative information about the quality of the crystal or the degree of order within the solid. Readers interested in learning more details of the process should consult any one of a number of standard texts for additional information [6–8, 12–15].

At the end of the process, one obtains a large amount of information regarding the solid-state structure of a compound. Its three-dimensional structure and molecular conformation become known, as do the patterns of molecular packings that enable the assembly of the crystal. In addition, one obtains complete summaries of bond angles and bond lengths for the molecular conformation in the crystal, as well as detailed atomic coordinates for all the atoms present in the solid. One generally finds crystallography papers divided as being either inorganic [16] or organic [17] in focus, but studies of the crystallography of organic compounds is of most interest to the pharmaceutical community. After all, drugs are merely organic compounds that have a pharmacological function.

From the analysis of the x-ray diffraction of a single crystal, one obtains information on the three-dimensional conformation of the compound, a complete summary of the bond angles and bond lengths of the compound in question, and detailed information regarding how the molecules assemble to yield the complete crystal.

2.1 Case study: theophylline anhydrate and monohydrate

The type of structural information that can be obtained from the study of the x-ray diffraction of single crystals will be illustrated through an exposition of studies conducted on the anhydrate and hydrate phases of theophylline (3,7-dihydro-1,3-dimethyl-1*H*-purine-2,6-dione). The structure of this compound and a suitable atomic numbering system, are given in [Figure 3](#).

As discussed above, one obtains a large amount of structural information upon completion of the data analysis, which will be illustrated using

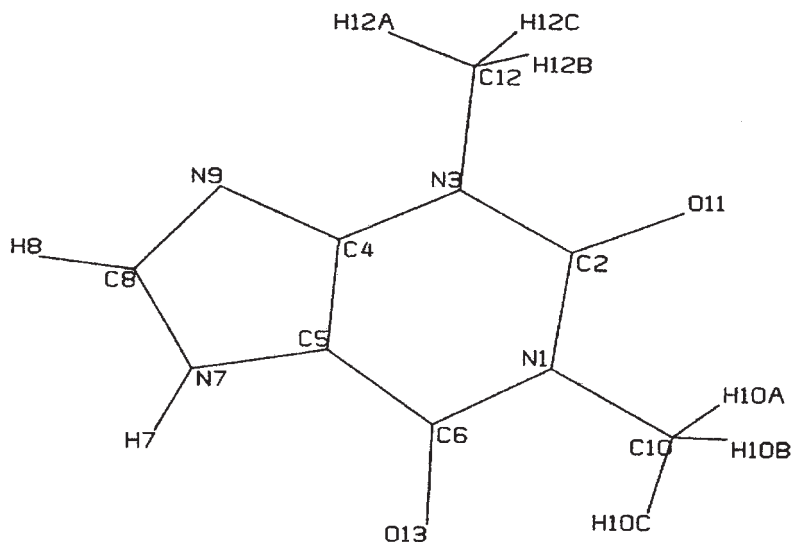


Figure 3. Molecular structure and suitable atomic numbering system for theophylline.

the example of theophylline monohydrate [20] (Table 2). Table 3 contains a summary of intramolecular distances involving the nonhydrogen atoms in the structure, while Table 4 shows the intramolecular distances involving hydrogen atoms. Table 5 contains a summary of bond angles involving the nonhydrogen atoms, and Table 6 contains the bond angles involving hydrogen atoms.

The compilation of bond length and angle information, all of which must agree with known chemical principles, enables one to deduce the molecular conformation of the molecule in question. Such illustrations are usually provided in the form of ORTEP drawings, where atomic sizes are depicted in the form of ellipsoids at the 50% probability level. The molecular conformation of theophylline in the anhydrate and monohydrate phase is shown in Figure 4. As would be expected from a rigid and planar molecule, these conformations do not differ significantly.

Of far greater use to structural scientists are the visualizations that illustrate how the various molecules assemble to constitute the unit cell, and the relationships of the molecules in them. This process is illustrated in Figures 5–7 for our study of theophylline monohydrate, which first

Table 2

Crystallographic Parameters Defining the Unit Cells
of Theophylline Anhydrate and Theophylline
Monohydrate phase

	Anhydrate [18]	Monohydrate [19]
Crystal class	Orthorhombic	Monoclinic
Space group	$Pna2_1$	$P2_1/n$
Unit cell lengths	$a = 24.612 \text{ \AA}$ $b = 3.8302 \text{ \AA}$ $c = 8.5010 \text{ \AA}$	$a = 4.468 \text{ \AA}$ $b = 15.355 \text{ \AA}$ $c = 13.121 \text{ \AA}$
Unit cell angles	$\alpha = 90^\circ$ $\beta = 90^\circ$ $\gamma = 90^\circ$	$\alpha = 90^\circ$ $\beta = 97.792^\circ$ $\gamma = 90^\circ$
Molecules in unit cell	4	4
Cell volume	801.38 \AA^3	891.9 \AA^3
Density	1.493 g/cm^3	1.476 g/mL

shows the details of the unit cell and proceed on to provide additional information about the molecular packing motifs in the crystal. As one progresses through the depictions of [Figures 5–7](#), the role of the water molecules in the structure becomes clear. Theophylline molecules are effectively bound into dimeric units by the bridging water molecules, which ultimately form an infinite chain of water molecules hydrogen-bonded to layers of theophylline molecules [19].

The molecular packing in the monohydrate phase is fundamentally different than that of the anhydrate phase, as shown in [Figure 8](#) [18]. Here, the theophylline molecules form hydrogen-bonded networks composed of one N–H \cdots N hydrogen bond and two bifurcated C–H \cdots O hydrogen bonds.

Table 3

Intramolecular Distances in Theophylline Monohydrate
Involving Nonhydrogen Atoms [20]

Atom (1)	Atom (2)	Distance (Å)*
O ₁₁	C ₂	1.219 (8)
O ₁₃	C ₆	1.233 (8)
N ₁	C ₂	1.420 (9)
N ₁	C ₆	1.399 (8)
N ₁	C ₁₀	1.486 (8)
N ₃	C ₂	1.379 (8)
N ₃	C ₄	1.375 (8)
N ₃	C ₁₂	1.469 (8)
N ₇	C ₅	1.407 (8)
N ₇	C ₈	1.331 (9)
N ₉	C ₄	1.365 (8)
N ₉	C ₈	1.345 (9)
C ₄	C ₅	1.350 (9)
C ₅	C ₆	1.421 (9)

* The estimated error in the last digit is given in parentheses.

2.2 Crystallographic studies of polymorphism

It is now accepted that the majority of organic compounds are capable of being crystallized in different crystal forms [21–23]. One defines *polymorphism* as signifying the situation where a given compound

Table 4

Intramolecular Distances in Theophylline Monohydrate
Involving Hydrogen Atoms [20]

Atom (1)	Atom (2)	Distance (Å)
O ₁₄	H _{14A}	0.833
O ₁₄	H _{14B}	0.985
N ₇	H ₇	0.877
C ₈	H ₈	0.986
C ₁₀	H _{10A}	0.926
C ₁₀	H _{10B}	0.967
C ₁₀	H _{10C}	0.950
C ₁₂	H _{12A}	0.954
C ₁₂	H _{12B}	0.973
C ₁₂	H _{12C}	0.932

crystallizes in more than one structure, and where the two crystals would yield exactly the same elemental analysis. *Solvatomorphism* is defined as the situation where a given compound crystallizes in more than one structure, and where the two crystals yield differing elemental analyses owing to the inclusion of solvent molecules in the crystal structure. Theophylline, discussed above in detail, is a solvatomorphic system.

When considering the structures of organic molecules, one finds that different modifications can arise in two main distinguishable ways. Should the molecule be constrained to exist as a rigid grouping of atoms, these may be stacked in different motifs to occupy the points of different lattices. This type of polymorphism is then attributable to packing phenomena, and so is termed packing polymorphism. On the other hand, if the molecule in question is not rigidly constructed and can exist in distinct

Table 5

Intramolecular Bond Angles in Theophylline Monohydrate
Involving Nonhydrogen Atoms [20]

Atom (1)	Atom (2)	Atom (3)	Bond angle (°)*
C ₂	N ₁	C ₆	127.6 (6)
C ₂	N ₁	C ₁₀	115.4 (6)
C ₆	N ₁	C ₁₀	116.9 (6)
C ₂	N ₃	C ₄	119.6 (6)
C ₂	N ₃	C ₁₂	118.6 (6)
C ₄	N ₃	C ₁₂	121.7 (6)
C ₅	N ₇	C ₈	105.9 (6)
C ₄	N ₉	C ₈	102.2 (6)
O ₁₁	C ₂	N ₁	121.2 (7)
O ₁₁	C ₂	N ₃	122.7 (7)
N ₁	C ₂	N ₃	116.1 (7)
N ₃	C ₄	N ₉	125.1 (6)
N ₃	C ₄	C ₅	121.6 (6)
N ₉	C ₄	C ₅	113.4 (7)
N ₇	C ₅	C ₄	104.5 (6)
N ₇	C ₅	C ₆	130.6 (7)

(continued)

Table 5 (continued)

Atom (1)	Atom (2)	Atom (3)	Bond angle (°)*
C ₄	C ₅	C ₆	124.9 (7)
O ₁₃	C ₆	N ₁	121.7 (7)
O ₁₃	C ₆	C ₅	128.1 (6)
N ₁	C ₆	C ₅	110.2 (7)
N ₇	C ₈	N ₉	114.1 (6)

*The estimated error in the last digit is given in parentheses.

conformational states, then it can happen that each of these conformationally distinct modifications may crystallize in its own lattice structure. This latter behavior has been termed conformational polymorphism [24].

During the very first series of studies using single-crystal X-ray crystallography to determine the structures of organic molecules, Robertson reported the structure of resorcinol (1,3-dihydroxybenzene) [25]. This crystalline material corresponded to that ordinarily obtained at room temperature, and was later termed the α -form. Shortly thereafter, it was found that the α -form underwent a transformation into a denser crystalline modification (denoted as the β -form) when heated at about 74°C, and that the structure of this newer form was completely different [26]. The salient crystallographic properties of these two forms are summarized in Table 7, and the crystal structures of the α - and β -forms (viewed down the c -axis, or (001) crystal plane) are shown in Figure 9.

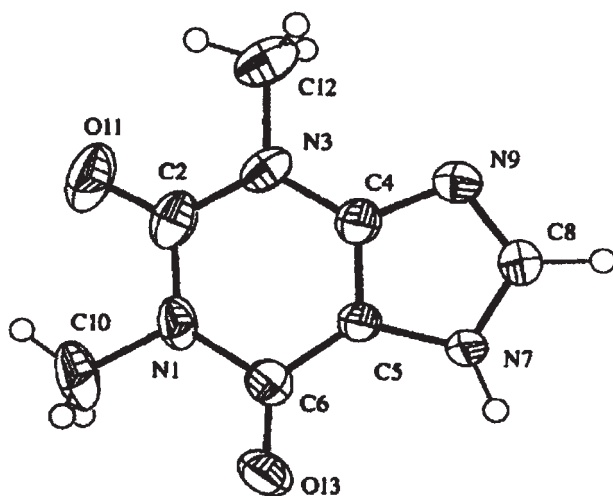
By its nature, resorcinol is locked into a single conformation, and it is immediately evident from a comparison of the structures in Figure 9 that each form is characterized by a different motif of hydrogen bonding. In particular, the α -form features a relative open architecture that is maintained by a spiraling array of hydrogen bonding that ascends

Table 6

Intramolecular Bond Angles in Theophylline Monohydrate
Involving Hydrogen Atoms [20]

Atom (1)	Atom (2)	Atom (3)	Bond angle (°)
H _{14A}	O ₁₄	H _{10B}	104.53
C ₅	N ₇	H ₇	125.5
C ₈	N ₇	H ₇	129.5
N ₇	C ₈	H ₈	123.4
N ₉	C ₈	H ₈	122.4
N ₁	C ₁₀	H _{10A}	109.95
N ₁	C ₁₀	H _{10B}	107.73
N ₁	C ₁₀	H _{10C}	109.25
H _{10A}	C ₁₀	H _{10B}	110.10
H _{10A}	C ₁₀	H _{10C}	111.65
H _{10B}	C ₁₀	H _{10C}	108.07
N ₃	C ₁₂	H _{12A}	109.58
N ₃	C ₁₂	H _{12B}	108.63
N ₃	C ₁₂	H _{12C}	111.62
H _{12A}	C ₁₂	H _{12B}	107.20
H _{12A}	C ₁₂	H _{12C}	110.67
H _{12B}	C ₁₂	H _{12C}	109.02

Anhydrate phase



Monohydrate phase

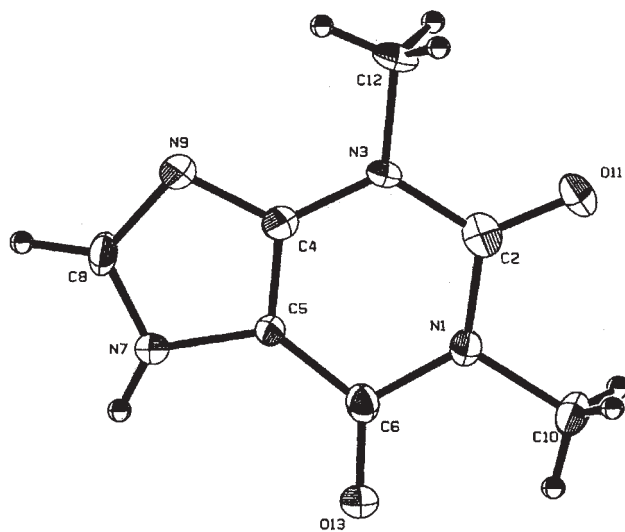


Figure 4. Conformation of the theophylline molecule in the anhydrate phase [18], [used with permission] and in the monohydrate phase [20].

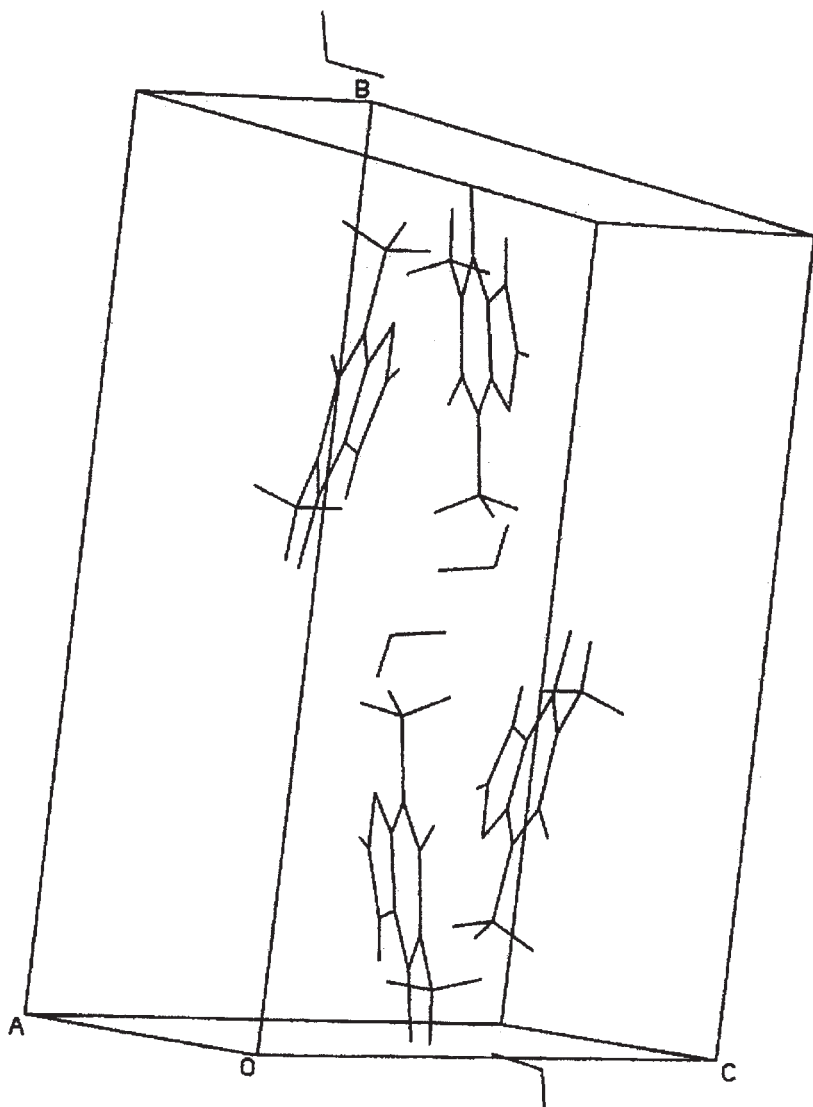


Figure 5. Composition of the unit cell of the theophylline monohydrate crystal phase [20].

through the various planes of the crystal. In the view illustrated (defined by the *ab*-plane), the apparent closed tetrameric grouping of hydroxyl groups is actually a slice through the ascending spiral. The effect of the thermally-induced phase transformation is to collapse the open

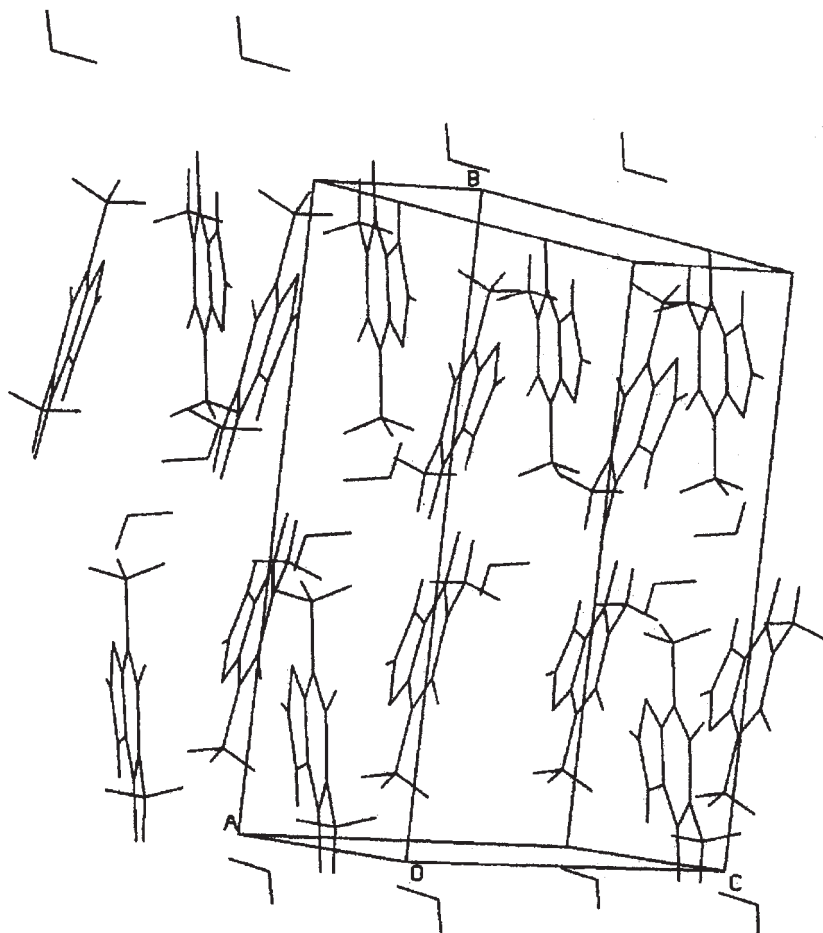


Figure 6. Addition of two unit cells in the theophylline monohydrate crystal phase [20].

arrangement of the α -form by a more compact and parallel arrangement of the molecules in the β -form. This structural change causes an increase in crystal density on passing from the α -form (1.278 g/cm^3) to the β -form (1.327 g/cm^3). In fact, the molecular packing existing in the β -form was described as being more typical of hydrocarbons than of a hydroxylic compound [26].

Probucol (4,4'-[(1-methylethylidene)bis(thio)]-bis-[2,6-bis(1,1-dimethylethyl)phenol]) is a cholesterol-lowering drug that has been reported to

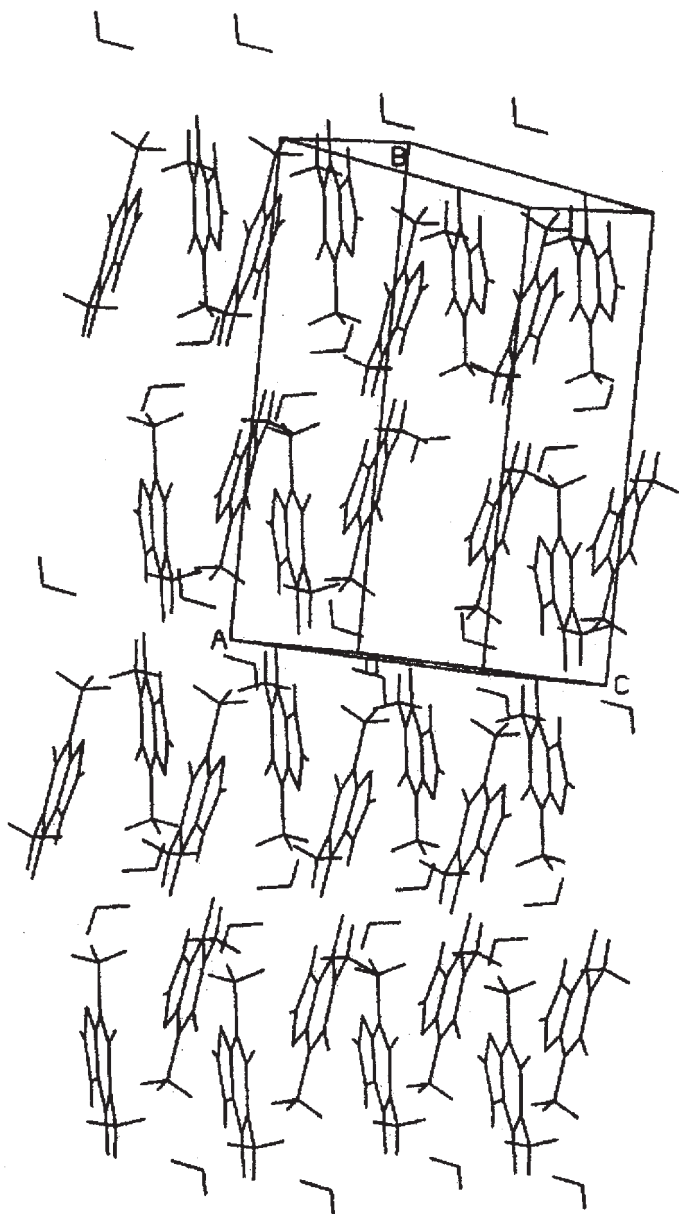


Figure 7. Molecular packing in the theophylline monohydrate crystal phase [20].

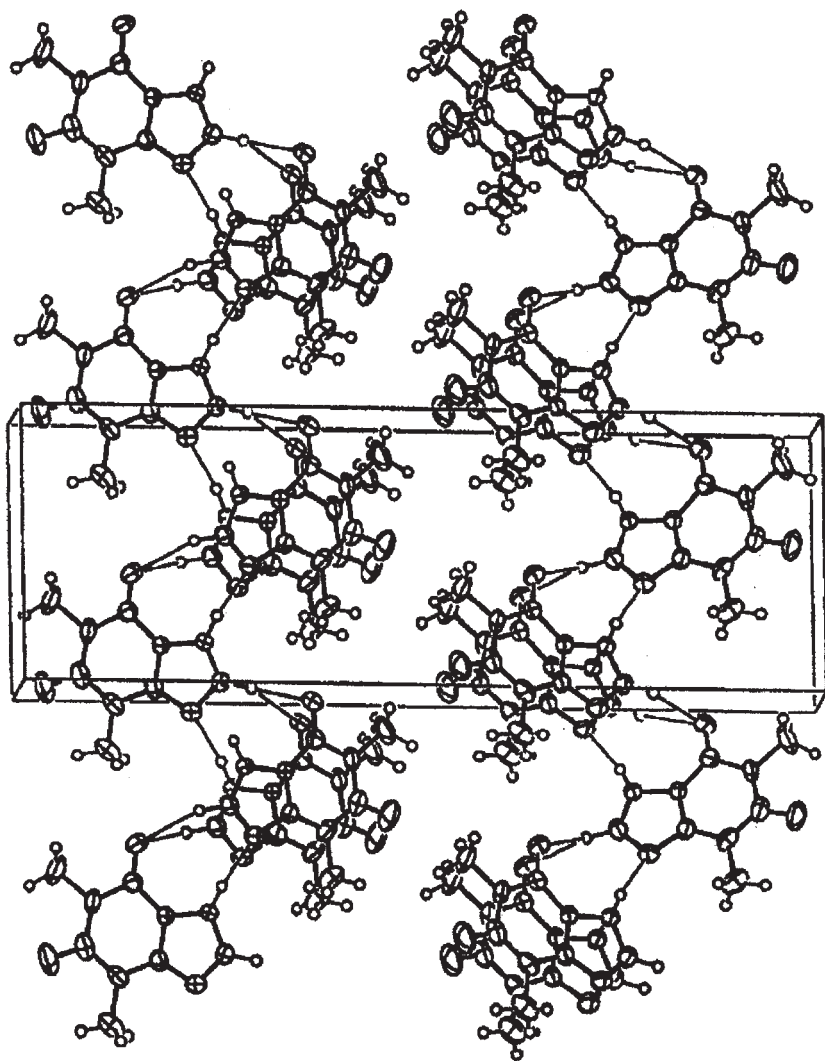


Figure 8. Molecular packing in the theophylline anhydrate crystal phase [18, used with permission].

exist in two forms [27]. Form II has been found to exhibit a lower melting point onset relative to Form I, and samples of Form II spontaneously transform to Form I upon long-term storage. The structures of these two polymorphic forms have been reported, and a summary of the

Table 7

Crystallographic Properties of the Two Polymorphs of Resorcinol [24, 25]

	α -Form	β -Form
Crystal class:	Orthorhombic	Orthorhombic
Space group:	<i>Pna</i>	<i>Pna</i>
Unit cell lengths:	$a = 10.53 \text{ \AA}$ $b = 9.53 \text{ \AA}$ $c = 5.66 \text{ \AA}$	$a = 7.91 \text{ \AA}$ $b = 12.57 \text{ \AA}$ $c = 5.50 \text{ \AA}$
Unit cell angles:	$\alpha = 90^\circ$ $\beta = 90^\circ$ $\gamma = 90^\circ$	$\alpha = 90^\circ$ $\beta = 90^\circ$ $\gamma = 90^\circ$
Molecules in unit cell:	4	4
Cell volume:	567.0 \AA^3	546.9 \AA^3
Density:	1.278 g/mL	1.327 g/mL

crystallographic data obtained in this work is provided in [Table 8](#). In addition, detailed views of the crystal structures are given in [Figure 10](#).

The conformations of the probucol molecule in the two forms were found to be quite different. In Form II, the C—S—C—S—C chain is extended, and the molecular symmetry approximates C_{2v} . This molecular symmetry is lost in the structure of Form I, where now the torsional angles around the two C—S bonds deviate significantly from 180° . Steric crowding of the phenolic groups by the *t*-butyl groups was evident from deviations from trigonal geometry at two phenolic carbons in both forms. Using a computational model, the authors found that the energy of Form II was 26.4 kJ/mole higher than the energy of Form I, indicating the less symmetrical conformer to be more stable. The crystal density of Form I was found to be approximately 5% higher than that of Form II,

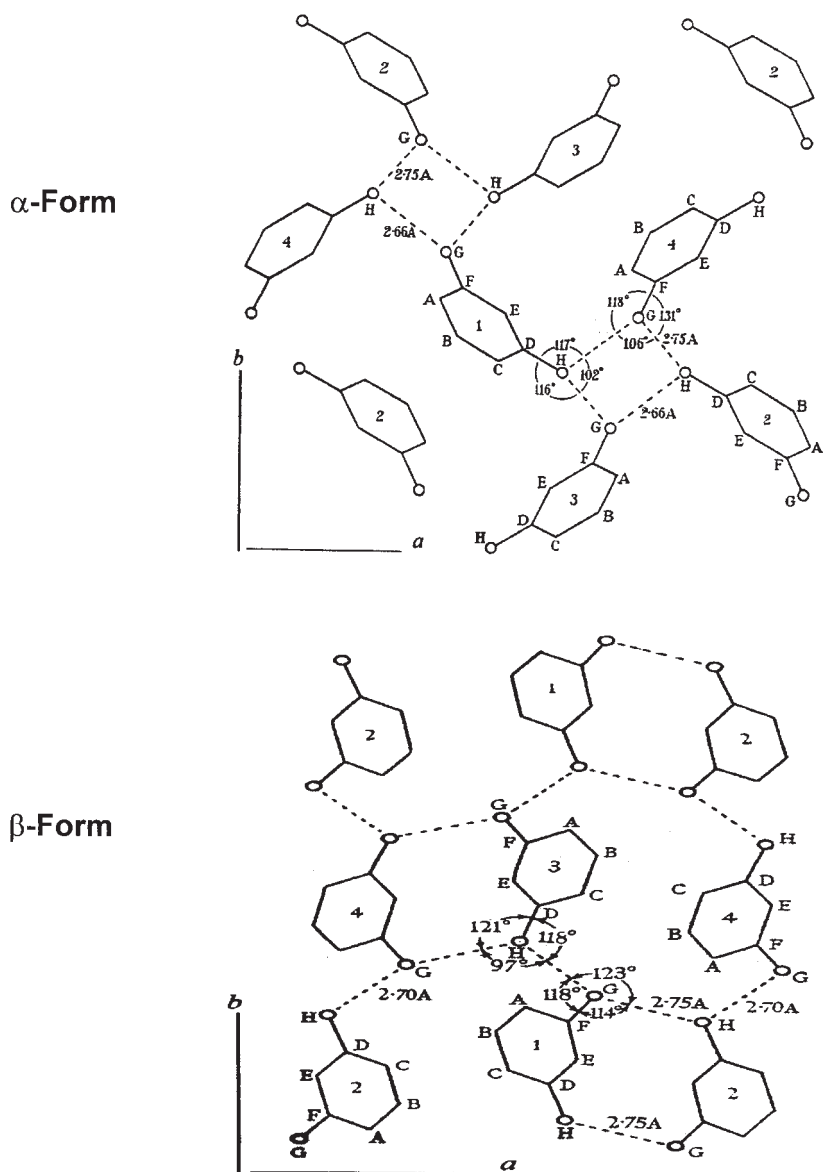


Figure 9. Crystal structures of the α - and β -forms of resorcinol, as viewed down the c -axis (001 plane). The figure is adapted from data given in [24] and [25].

Table 8

Crystallographic Properties of the Two Polymorphs
of Probucol [27]

	Form I	Form II
Crystal class	Monoclinic	Monoclinic
Space group	$P2_1/c$	$P2_1/n$
Unit cell lengths	$a = 16.972 \text{ \AA}$ $b = 10.534 \text{ \AA}$ $c = 19.03 \text{ \AA}$	$a = 11.226 \text{ \AA}$ $b = 15.981 \text{ \AA}$ $c = 18.800 \text{ \AA}$
Unit cell angles	$\alpha = 90^\circ$ $\beta = 113.66^\circ$ $\gamma = 90^\circ$	$\alpha = 90^\circ$ $\beta = 104.04^\circ$ $\gamma = 90^\circ$
Molecules in unit cell	4	4
Cell volume	3116.0 \AA^3	3272.0 \AA^3
Density	1.102 g/mL	1.049 g/mL

indicating that the conformational state of the probucol molecules in Form I yielded more efficient space filling.

Owing to the presence of the functional groups present in drug substance molecules that promote their efficacious action, the crystallization possibilities for such materials can be wide-ranging. Conformationally rigid molecules may associate into various fundamental units through alterations in their hydrogen-bonding interactions, and the packing of these different unit cells yields nonequivalent crystal structures. When a drug molecule is also capable of folding into multiple conformational states, the packing of these can yield a further variation in unit cell types and the generation of new crystal structures. Often, the lattice interactions and intimate details of the crystal packing may lead to a stabilization of a metastable conformation that may nevertheless be quite stable in the solid state. Finally, when additional lattice stabilization can be obtained through the use of bridging water or solvate molecules,

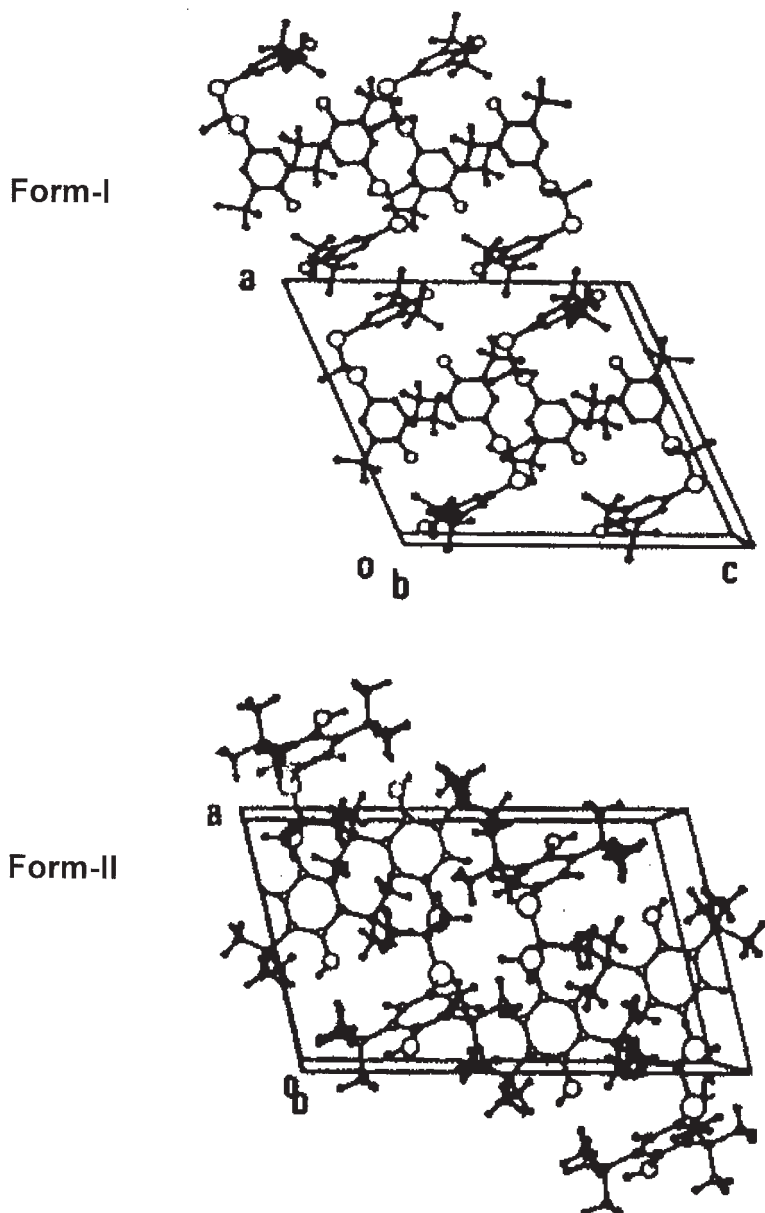


Figure 10. Crystal structures of the α - and β -forms of resorcinol, as viewed down the c -axis (001 plane). The figure is adapted from data given in [24] and [25].

then polymorphism can be further complicated by the existence of solvatomorphism.

3. X-RAY POWDER DIFFRACTION

Although single-crystal x-ray diffraction undoubtedly represents the most powerful method for the characterization of crystalline materials, it does suffer from the drawback of requiring the existence of a suitable single crystal. Very early in the history of x-ray diffraction studies, it was recognized that the scattering of x-ray radiation by powdered crystalline solids could be used to obtain structural information, leading to the practice of x-ray powder diffraction (XRPD).

The XRPD technique has become exceedingly important to pharmaceutical scientists, since it represents the easiest and fastest method to obtain fundamental information on the structure of a crystalline substance in its ordinarily obtained form. Since the majority of drug substances are obtained as crystalline powders, the powder pattern of these substances is often used as a readily obtainable fingerprint for determination of its structural type. In fact, it is only by pure coincidence that two compounds might form crystals for which the ensemble of molecular planes happened to be identical in all space. One such example is provided by the respective trihydrate phases of ampicillin and amoxicillin [28], but such instances are uncommon.

As previously discussed, Bragg [4] explained the diffraction of x-rays by crystals using a model where the atoms of a crystal are regularly arranged in space, in which they were regarded as lying in parallel sheets separated by a definite and defined distance. He then showed that scattering centers arranged in a plane act like a mirror to x-rays incident on them, so that constructive interference would occur for the direction of specular reflection. Within a given family of planes, defined by a Miller index of (*h k l*) and each plane being separated by the distance *d*, each plane produces a specular reflectance of the incident beam. If the incident x-rays are monochromatic (having wavelength equal to λ), then for an arbitrary glancing angle of θ , the reflections from successive planes are out of phase with one another. This yields destructive interference in the scattered beams. However, by varying θ , a set of values for θ can be found so that the path difference between x-rays reflected by successive planes will be an integral number (*n*) of wavelengths, and then constructive interference will occur. The mathematical relationship governing the mechanics of diffraction was discussed earlier as Bragg's law.

Unlike the case of diffraction of light by a ruled grating, the diffraction of X-rays by a crystalline solid leads to observation of constructive interference (*i.e.*, reflection) that occurs only at the critical Bragg angles. When reflection does occur, it is stated that the plane in question is reflecting in the n th order, or that one observes n th order diffraction for that particular crystal plane. Therefore, one will observe an x-ray scattering response for every plane defined by a unique Miller index of ($h\ k\ l$).

To measure a powder pattern, a randomly oriented powdered sample is prepared so as to expose all possible planes of a crystalline powder. The scattering angle, θ , is measured for each family of crystal planes by slowly rotating the sample and measuring the angle of diffracted x-rays with respect to the angle of the incident beam. Alternatively, the angle between sample and source can be kept fixed, while moving the detector to determine the angles of the scattered radiation. Knowing the wavelength of the incident beam, the spacing between the planes (identified as the d -spacings) is calculated using Bragg's Law.

Typical applications of x-ray powder diffraction methodology include the evaluation of polymorphism and solvatomorphism, the study of phase transitions, and evaluation of degrees of crystallinity. More recently, advances have been made in the use of powder diffraction as a means to obtain solved crystal structures. A very useful complement to ordinary powder x-ray diffraction is variable temperature x-ray diffraction. In this method, the sample is contained on a stage that can be heated to any desired temperature. The method is extremely useful for the study of thermally-induced phenomena, and can be a vital complement to thermal methods of analysis.

3.1 Determination of phase identity

The United States Pharmacopeia contains a general chapter on x-ray diffraction [29], which sets the criterion that identity is established if the scattering angles in the powder patterns of the sample and reference standard agree to within the calibrated precision of the diffractometer. It is noted that it is generally sufficient that the scattering angles of the ten strongest reflections obtained for an analyte agree to within either ± 0.10 or $\pm 0.20^\circ 2\theta$, which ever is more appropriate for the diffractometer used. Older versions of the general test contained an additional criterion for relative intensities of the scattering peaks, but it has been noted that relative intensities may vary considerably from that of the reference

standard making it impossible to enforce a criterion based on the relative intensities of corresponding scattering peaks.

It is usually convenient to identify the angles of the 10 most intense scattering peaks in a powder pattern, and to then list the accepted tolerance ranges of these based on the diffractometer used for the determinations. Such a representation has been developed for data obtained for racemic mandelic acid, and for its separated (*S*)-enantiomer, using a diffractometer system whose precision was known to be $\pm 0.15^\circ 2\theta$ [30]. The criteria are shown in Table 9, the form of which enables the ready identification of a mandelic acid sample as being either racemic or enantiomerically pure. It should be noted that the powder pattern of the separated (*R*)-enantiomer would necessarily have to be identical to that of the separated (*S*)-enantiomer.

Useful tabulations of the XRPD patterns of a number of compounds have been published by Koundourellis and coworkers, including twelve diuretics [31], twelve vasodilators [32], and 12 other commonly used drug substances [33]. These compilations contain listings of scattering angles, *d*-spacings, and relative intensities suitable for the development of acceptance criteria.

Without a doubt, one of the most important uses of XRPD in pharmaceuticals is derived from application as the primary determinant of polymorphic or solvatomorphic identity [34]. Since these effects are due to purely crystallographic phenomena, it is self-evident that x-ray diffraction techniques would represent the primary method of determination. Owing to its ease of data acquisition, XRPD is particularly useful as a screening technique for batch characterization, following the same general criteria already described. It is prudent, however, to confirm the results of an XRPD study through the use of a confirmatory technique, such as polarizing light microscopy, differential scanning calorimetry, solid-state vibrational spectroscopy, or solid-state nuclear magnetic resonance.

The literature abounds with countless examples that illustrate how powder diffraction has been used to distinguish between the members of a polymorphic system. It is absolutely safe to state that one could not publish the results of a phase characterization study without the inclusion of XRPD data. For example, Figure 11 shows the clearly distinguishable XRPD powder patterns of two anhydrous forms of a new chemical entity. These are easily distinguishable on the overall basis of their powder patterns, and one could place the identification on a more

Table 9

XRPD Identity Test Criteria for Mandelic Acid

Lower limit of acceptability for scattering peak ($^{\circ}2\theta$)	Accepted angle for scattering peak ($^{\circ}2\theta$)	Upper limit of acceptability for scattering peak ($^{\circ}2\theta$)
Racemic Phase		
11.271	11.421	11.571
16.264	16.414	16.564
18.607	18.757	18.907
21.715	21.865	22.015
22.173	22.323	22.473
23.345	23.495	23.645
25.352	25.502	25.652
27.879	28.029	28.179
33.177	33.327	33.477
41.857	42.007	42.157
Enantiomerically Pure (<i>S</i>)-Phase		
6.381	6.531	6.681
6.686	6.836	6.986
7.298	7.448	7.598
8.011	8.161	8.311

(continued)

Table 9 (continued)

Lower limit of acceptability for scattering peak ($^{\circ}2\theta$)	Accepted angle for scattering peak ($^{\circ}2\theta$)	Upper limit of acceptability for scattering peak ($^{\circ}2\theta$)
Enantiomerically Pure (<i>S</i>)-Phase		
20.798	20.948	21.098
23.345	23.495	23.645
24.109	24.259	24.409
26.605	26.755	26.905
30.018	30.168	30.318
36.284	36.434	36.584

quantitative basis through the development of criteria similar to those developed for the mandelic acid system.

X-ray powder diffraction can be similarly used to differentiate between the members of a solvatomorphic system. For instance, [Figure 12](#) shows the powder patterns obtained for the anhydrate and monohydrate phases of lactose. The existence of structural similarities in the two forms are suggested in that the main scattering peaks of each form are clustered near $20^{\circ}2\theta$, but the two solvatomorphs are easily differentiated from an inspection of the patterns. The differentiation could also be rendered more quantitative through the development of a table similar to that developed for the mandelic acid system.

3.2 Degree of crystallinity

When reference samples of the pure amorphous and pure crystalline phases of a substance are available, calibration samples of known degrees of crystallinity can be prepared by the mixing of these. Establishment of a

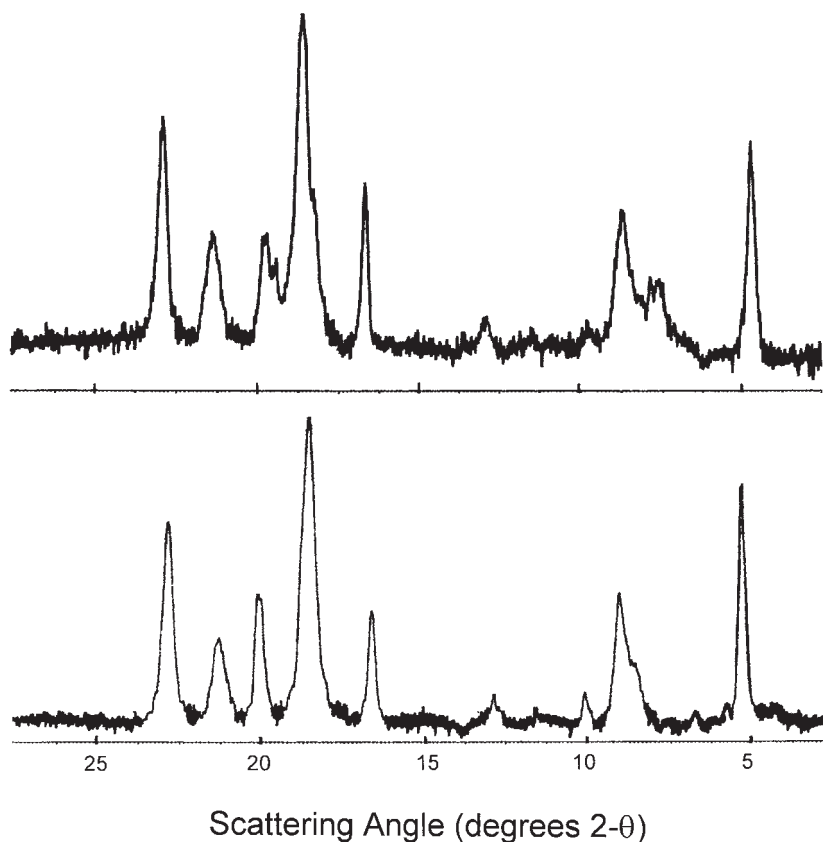
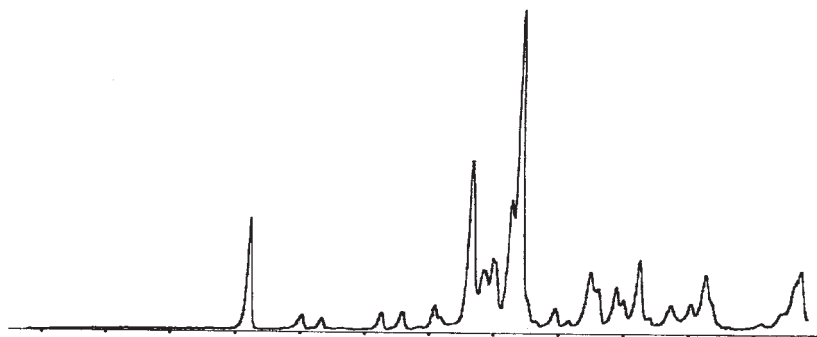


Figure 11. X-ray powder diffraction patterns of the two anhydrous forms of a new chemical entity.

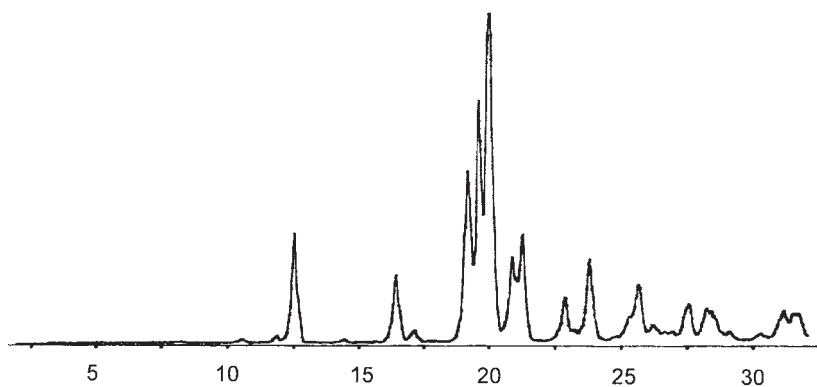
calibration curve (XRPD response vs. degree of crystallinity) permits the evaluation of unknown samples to be performed.

In a classic study that illustrates the principles of the method, a XRPD procedure was described for the estimation of the degree of crystallinity in digoxin samples [35]. Crystalline product was obtained commercially, and the amorphous phase was obtained through ball-milling of this substance. Calibration mixtures were prepared as a variety of blends prepared from the 100% crystalline and 0% crystalline materials, and acceptable linearity and precision was obtained in the calibration curve of XRPD intensity versus actual crystallinity. [Figure 13](#) shows the

Anhydrate Phase



Monohydrate Phase



Scattering Angle (degrees 2-θ)

Figure 12. X-ray powder diffraction patterns of the anhydrate and monohydrate phases of lactose.

powder pattern of an approximately 40% crystalline material, illustrating how these workers separated out the scattering contributions from the amorphous and crystalline phases.

Other studies have used quantitative XRPD to evaluate the degree of crystallinity in bulk drug substances, such as calcium gluceptate [36], imipenem [37], cefditoren pivoxil [38], and a Lumaxis analog [39].

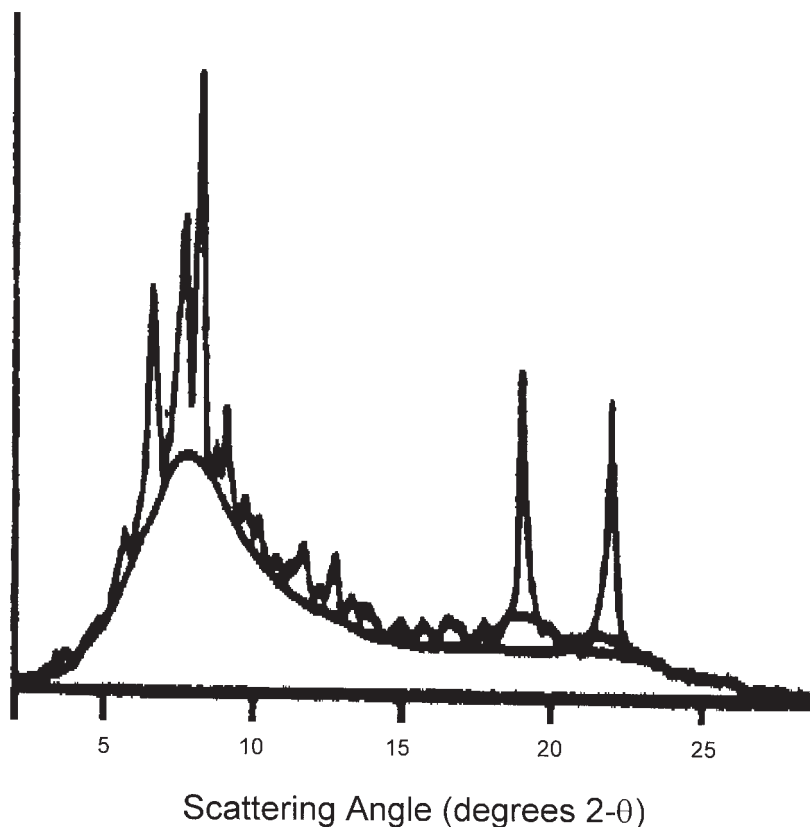


Figure 13. X-ray powder diffraction pattern of digoxin, whose degree of crystallinity was reduced to 40% by ball-milling. The figure was adapted from data contained in [32].

When the excipient matrix in a formulation is largely amorphous, similar XRPD methods can be used to determine the amount of crystalline drug substance present in a drug product. The principles were established in a study that included a number of solid dose forms [40], and also in another study involving a determination of the amount of crystalline acetaminophen in some solid dispersions [41]. The same principles have been used to characterize the crystalline content within lyophilized solids [42], where the matrix is again an amorphous material.

3.3 Phase composition of mixtures

Once the characteristic XRPD patterns of one or more analytes have been established, it is usually possible to develop quantitative methods of analysis. The methodology is based on the premise that each component will contribute to the overall scattering by an amount that is proportional to its weight fraction in a mixture, and that the powder pattern of each analyte contains one or more peaks whose scattering angle is unique to that analyte. Quantitative analysis requires the use of reference standards that contribute known scattering peaks at appropriate scattering intensities. This can be achieved through the use of metal sample holders where, some of the metal scattering peaks are used as external standards. The author has had great success in this regard using aluminum sample holders, using the scattering peaks at 38.472° and $44.738^\circ 2\theta$ to calibrate both intensity and scanning rate. Others have used internal standards, mixing materials such as elemental silicon or lithium fluoride into the sample matrix.

Although simple intensity correction techniques can be used to develop very adequate XRPD methods of quantitative analysis, the introduction of more sophisticated data acquisition and handling techniques can greatly improve the quality of the developed method. For instance, improvement of the powder pattern quality through use of the Rietveld method has been used to evaluate mixtures of two anhydrous polymorphs of carbamazepine and the dihydrate solvatomorph [43]. The method of whole pattern analysis developed by Rietveld [44] has found widespread use in crystal structure refinement and in the quantitative analysis of complex mixtures. Using this approach, the detection of analyte species was possible even when their concentration was less than 1% in the sample matrix. It was reported that good quantitation of analytes could be obtained in complex mixtures even without the requirement of calibration curves.

The use of parallel beam optics as a means for determining the polymorphic composition in powder compacts has been discussed [45]. In this study, compressed mixtures of known polymorphic composition were analyzed in transmission mode, and the data processed using profile-fitting software. The advantage of using the transmission, rather than reflectance, is that the results were not sensitive to the geometrical details of the compact surfaces and that spurious effects associated with preferential orientation were minimized.

The effects of preferred orientation in XRPD analysis can be highly significant, and are most often encountered when working with systems characterized by plate-like or tabular crystal morphologies. As discussed earlier, a viable XRPD sample is one that presents equal numbers of all scattering planes to the incident x-ray beam. Any orientation effect that minimizes the degree of scattering from certain crystal planes will strongly affect the observed intensities, and this will in turn strongly affect the quantitation. The three polymorphs of mannitol each are obtained as needles, and thus represented a good system for evaluating the effect of preferential orientation on quantitative XRPD [46]. Through the use of small particle sizes and sample rotation, the preferential orientation effects were held to a minimum, and allowed discrimination of the polymorphs at around the 1% level.

As a first example, consider ranitidine hydrochloride, which is known to crystallize in two anhydrous polymorphs. The XRPD patterns of the two forms are shown in Figure 14, where it is evident that the two structures are significantly different [47]. For a variety of reasons, most workers are extremely interested in determining the quantity of Form II in a bulk Form I sample, and it is clear from the figure that the scattering peaks around 20° and $23.5^\circ 2\theta$ would be particularly useful for this purpose. The analysis of Form-II in bulk Form-I represents an extremely favorable situation, since the most intense scattering peaks of the analyte are observed at scattering angles where the host matrix happens not to yield diffraction. In our preliminary studies, it was estimated that a limit of detection of 0.25% w/w Form-II in bulk Form-I could be achieved. On the other hand, if there was a reason to determine the level of Form I in a bulk Form II sample, then the scattering peaks around 9° and $25^\circ 2\theta$ would suffice. For this latter instance, a preliminary estimate limit of detection of 0.50% w/w Form-I in bulk Form-II was deduced [47].

The complications associated with preferential orientation effects were addressed in detail during studies of a benzoic acid/benzil system [48]. The use of various sample packing methods was considered (vacuum free-fall, front-faced packing *vs.* rear-faced packing, *etc.*), but the best reduction in the effect was achieved by using materials having small particle sizes that were produced by milling. Through the use of sieving and milling, excellent linearity in diffraction peak area as a function of analyte concentration was attained. The authors deduced a protocol for

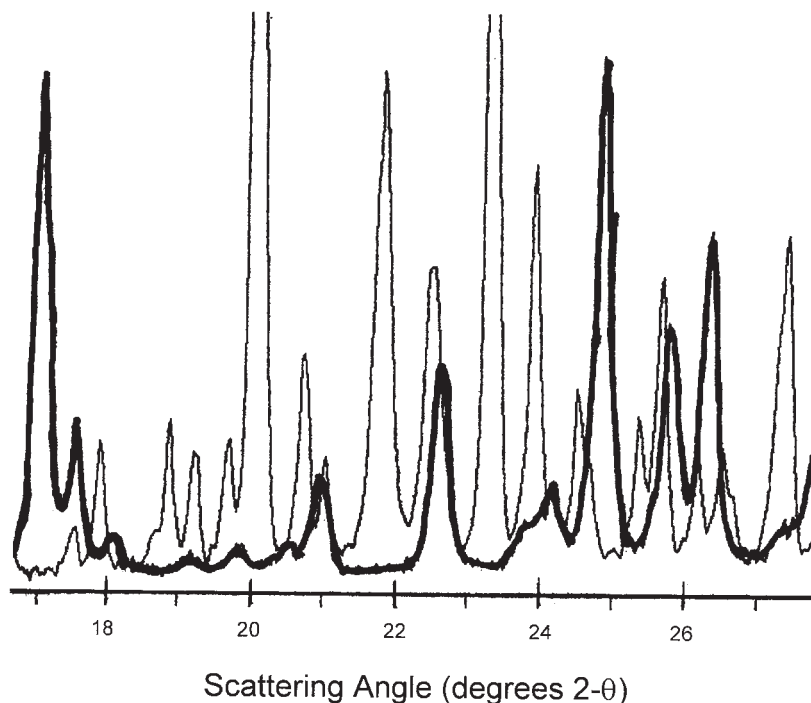


Figure 14. X-ray powder diffraction patterns of ranitidine hydrochloride, Form-I (thick trace) and Form-II (thin trace) [47].

development of a quantitative XRPD method that consisted of six main steps:

1. Calculation of the mass absorption coefficient of the drug substance
2. Selection of appropriate diffraction peaks for quantification
3. Evaluation of the loading technique for adequate sample size
4. Determination of whether preferred orientation effects can be eliminated through control of the sample particle size
5. Determination of appropriate milling conditions to obtain reproducibility in peak areas
6. Generation of calibration curves from physical mixtures

After completion of these steps, one then should have a quantitative XRPD method that is suitable for analysis of real samples.

Another example of a well-designed method for the quantitative XRPD determination of polymorphs was developed for the phase analysis of prazosin hydrochloride [49]. As an example of a XRPD method for the determination of solvatomorphs, during the quantitation of cefepine dihydrochloride dihydrate in bulk samples of cefepine dihydrochloride monohydrate, a limit of detection of 0.75% w/w and a limit of quantitation of 2.5% w/w were associated with a working range of 2.5–15% w/w [50].

Quantitative XRPD methods have also been developed for the determination of drug substances in excipient matrices. For instance, it was found that approximately 2% of selegilin hydrochloride can be observed reliably in the presence of crystalline mannitol or amorphous modified starch [51]. The effects of temperature on the polymorphic transformation of chlorpropamide forms A and C during tableting were investigated using XRPD [52]. Even though form A was the stable phase and form C was metastable, the results suggested that the two forms were mutually transformed. It was found that the crystalline forms were converted to a noncrystalline solid by the mechanical energy, and that resulting noncrystalline were transformed into either form A or form C depending on the nature of the compression process.

Since the separated enantiomers of a dissymmetric compound must crystallize in a different space group than does the racemic mixture, it should not be unanticipated that quantitative XRPD would be useful in the determination of enantiomeric composition. For instance, the differing XRPD characteristics of (*S*)-(+)-ibuprofen relative to the (*RS*)-racemate have been exploited to develop a sound method for the determination of the enantiomeric purity of ibuprofen samples [53].

3.4 Thermodiffraction

The performance of XRPD on a hot stage enables one to obtain powder patterns at elevated temperatures, and permits one to deduce structural assignments for thermally-induced phase transitions. Determination of the origin of thermal events taking place during the conduct of differential thermal analysis or differential scanning calorimetry is not always straight-forward, and the use of supplementary XRPD technology can be extremely valuable. By conducting XRPD studies on a heatable stage, one can bring the system to positions where a DSC thermogram indicates the existence of an interesting point of thermal equilibrium.

One of the uses for thermodiffraction that immediately comes to mind concerns the desolvation of solvatomorphs. For instance, after the dehydration of a hydrate phase, one may obtain either a crystalline anhydrate phase or an amorphous phase. The XRPD pattern of a dehydrated hydrate will clearly indicate the difference. In addition, should one encounter an equivalence in powder patterns between the hydrate phase and its dehydrated form, this would indicate the existence of channel-type water (as opposed to genuine lattice water) [54].

A XRPD system equipped with a heatable sample holder has been described, which permitted highly defined heating up to 250°C [55]. The system was used to study the phase transformation of phenanthrene and the dehydration of caffeine hydrate. An analysis scheme was developed for the data that permitted one to extract activation parameters for these solid-state reactions from a single nonisothermal study run at a constant heating rate.

In another study, thermodiffraction was used to study phase transformations in mannitol and paracetamol, as well as the desolvation of lactose monohydrate and the dioxane solvatomorph of paracetamol [56]. The authors noted that in order to obtain the best data, the heating cycle must be sufficiently slow to permit the thermally-induced reactions to reach completion. At the same time, the use of overly long cycle times can yield sample decomposition. In addition, the sample conditions are bound to differ relative to the conditions used for a differential scanning calorimetry analysis, so one should expect some differences in thermal profiles when comparing data from analogous studies.

The commercially available form of Aspartame is hemihydrate Form II, which transforms into hemihydrate Form I when milled, and a 2.5-hydrate species is also known [57, 58]. XRPD has been used to study the desolvation and ultimate decomposition of the various hydrates. When heated to 150°C, both hemihydrate forms dehydrate into the same anhydrous phase, which then cyclizes to 3-(carboxymethyl)-6-benzyl-2,5-dioxopiperazine if heated to 200°C. The 2.5-hydrate was shown to dehydrate to hemihydrate Form II when heated to 70°C, and this product was then shown to undergo the same decomposition sequence as directly crystallized hemihydrate Form II. Various XRPD patterns obtained during the heating sequence of the 2.5-hydrate are shown in Figure 15.

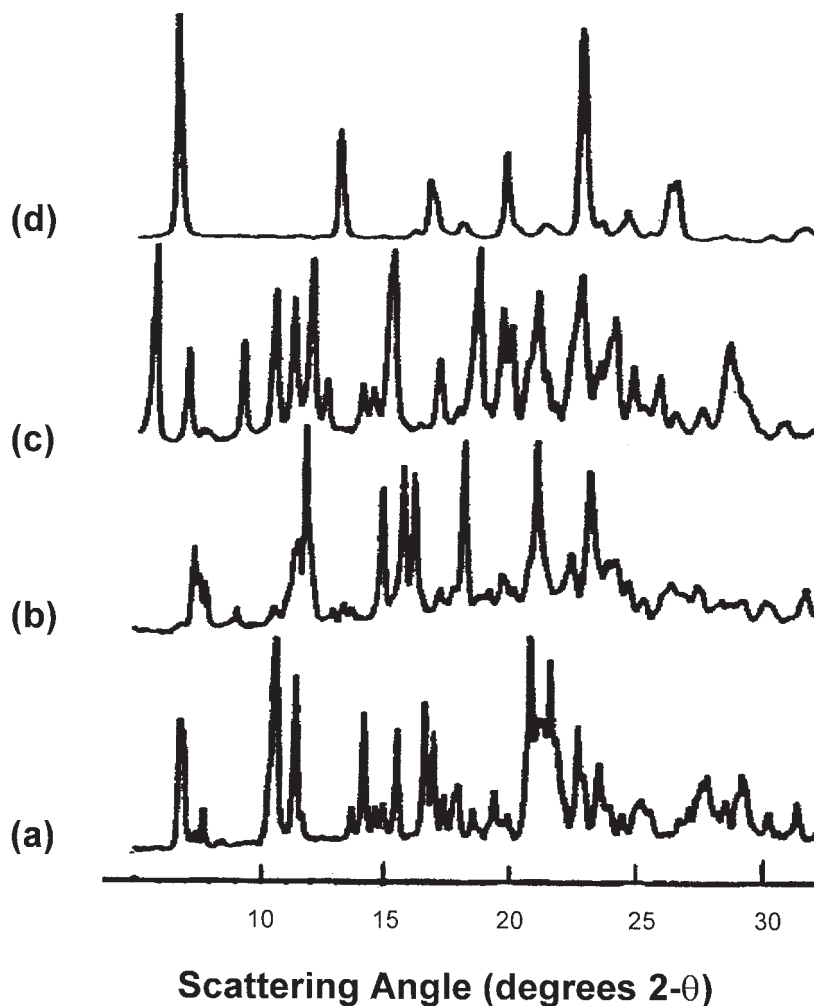


Figure 15. X-ray powder diffraction patterns of aspartame (a) 2.5-hydrate, (b) hemihydrate, (c) anhydrate, and (d) dioxopiperazine degradant. The data were adapted from [13].

3.5 XRPD as a stability-indicating assay method

When the phase identity, or degree of crystallinity (or lack thereof), of a drug substance is important to its performance in a drug product, XRPD can serve as a vital stability-indicating assay method. There is no doubt

that XRPD can be validated to the status of any other stability-indicating assay, and that one can use the usual criteria of method validation to establish the performance parameters of the method. This aspect would be especially important when either a metastable or an amorphous form of the drug substance has been chosen for development. One may conduct such work either on samples that have been stored at various conditions and pulled at designated time points, or on substances that are maintained isothermally and the XRPD periodically measured.

For example, amorphous clarithromycin was prepared by grind and spray drying processes, and XRPD was used to follow changes in crystallinity upon exposure to elevated temperature and relative humidity [59]. Exposure of either substance to a 40°C/82% RH environment for seven days led to formation of the crystalline form, but the spray-dried material yielded more crystalline product than did the ground material. This finding, when supported with thermal analysis studies, led to the conclusion that the amorphous substances produced by the different processing methods were not equivalent.

4. SUMMARY

Although the diffraction of x-rays by crystalline solids was originally used to deduce the nature of the electromagnetic radiation, such diffraction has now become a commonly applied tool for the structural characterization of single-crystals and polycrystalline powders. Owing to the presence of the functional groups present in drug substance molecules that promote their efficacious action, the crystallization possibilities for such materials can be wide-ranging, leading to possibilities for polymorphism and solvatomorphism.

Conformationally rigid molecules may associate into various fundamental units through alterations in their hydrogen-bonding interactions, and the packing of these different unit cells yields nonequivalent crystal structures. When a drug molecule is also capable of folding into multiple conformational states, the packing of these can yield a further variation in unit cell types and the generation of new crystal structures. Often, the lattice interactions and intimate details of the crystal packing may lead to a stabilization of a metastable conformation that may nevertheless be quite stable in the solid state. Finally, when additional lattice stabilization can be obtained through the use of bridging water or solvate molecules, then polymorphism can be further complicated by the existence of solvatomorphism.

X-ray powder diffraction represents the methodology of choice for the crystallographic characterization of drug substances produced on a routine, batch-type basis. Properly prepared samples yield powder patterns that contain a scattering peak for each crystal plane/face, and therefore constitute an identification test for a given crystalline phase. When the data are of suitable quality, XRPD can be used to deduce details of the unit cell and the crystal structure. With the generation of appropriate calibration data, XRPD can be used as a means to deduce the degree of crystallinity in a given sample, of the composition of a physically heterogeneous mixture. Since polymorphism and solvatomorphism are crystallographic occurrences, XRPD will always be the primary determinant of the existence of such phenomena. Variable temperature XRPD is a valuable tool to understand thermally-induced reactions, and to characterize materials during the conduct of stability studies.

5. REFERENCES

1. A. Bravais, *Etudes Crystallographiques*, Gautier-Villars, Paris, 1866.
2. W. Friedrich, P. Knipping, and M. Laue, *Sitzb. Kais. Akad. Wiss., Munchen*, 303–322 (1912); *Chem. Abs.*, 7, 2009–2010 (1912).
3. W.H. Bragg and W.L. Bragg, *Proc. Roy. Soc. (London)*, **A88**, 428–438 (1913).
4. W.H. Bragg and W.L. Bragg, *X-Rays and Crystal Structure*, G. Bell and Sons, London, 1918.
5. W.L. Bragg, *The Crystalline State: A General Survey*, G. Bell and Sons, London, 1955.
6. M.J. Buerger, *X-Ray Crystallography*, John Wiley and Sons, New York, 1942.
7. M.M. Woolfson, *An Introduction to X-Ray Crystallography*, Cambridge University Press, Cambridge, 1970.
8. J.P. Glusker and K.N. Trueblood, *Crystal Structure Analysis*, Oxford University Press, New York, 1972.
9. A.F. Wells, *Structural Inorganic Chemistry*, 5th edn, Clarendon Press, Oxford, 1984.
10. F.A. Cotton, *Chemical Applications of Group Theory*, 2nd edn, Wiley-Interscience, New York, 1971.
11. G. Burns and A.M. Glazer, *Space Groups for Solid State Scientists*, Academic Press, New York, 1978.

12. J.M. Bijvoet, N.H. Kolkmeier, and C.H. MacGillavry, *X-Ray Analysis of Crystals*, Butterworths, London, 1951.
13. A. Guinier, *X-Ray Crystallographic Technology*, Hilger and Watts, London, 1952.
14. B.D. Cullity, *Elements of X-Ray Diffraction*, Addison-Wesley Publishing Co., Reading, MA, 1956.
15. J.J. Rousseau, *Basic Crystallography*, John Wiley and Sons, Chichester, 1998.
16. A.F. Wells, *Structural Inorganic Chemistry*, 5th edn, Clarendon Press, Oxford, 1984.
17. A.I. Kitaigorodskii, *Organic Chemical Crystallography*, Consultants Bureau, New York, 1961.
18. Y. Ebisuzaki, P.D. Boyle, and J.A. Smith, *Acta Cryst.*, **C53**, 777–779 (1997).
19. C. Sun, D. Zhou, D.J.W. Grant, and V.G. Young, *Acta Cryst.*, **E58**, o368–o370 (2002).
20. H.G. Brittain, G. Owoo, and J.P. Jasinski, unpublished results.
21. H.G. Brittain, *Polymorphism in Pharmaceutical Solids*, Marcel Dekker, New York, 1999.
22. S.R. Byrn, R.R. Pfeiffer, and J.G. Stowell, *Solid-State Chemistry of Drugs*, 2nd edn, SSCI Inc., West Lafayette, IN, 1999.
23. J. Bernstein, *Polymorphism in Molecular Crystals*, Clarendon Press, Oxford, UK, 2002.
24. J. Bernstein, “Conformational Polymorphism”, Chapter 13 in: *Organic Solid State Chemistry*, G.R. Desiraju, (ed.), Elsevier, Amsterdam, pp. 471–518 (1987).
25. J.M. Robertson, *Proc. Royal Soc. (London)*, **A157**, 79–99 (1936).
26. J.M. Robertson and A.R. Ubbelohde, *Proc. Royal Soc. (London)*, **A167**, 122–135 (1938).
27. J.J. Gerber, M.R. Caira, and A.P. Lötter, *J. Cryst. Spect. Res.*, **23**, 863–869 (1993).
28. M.O. Boles, R.J. Girven, and P.A.C. Gane, *Acta Cryst.*, **B34**, 461–466 (1978).
29. “X-Ray Diffraction”, General test {941}, *United States Pharmacopoeia 26*, The United States Pharmacopoeial Convention, Rockville, MD, 2003, pp. 2233–2234.
30. H.G. Brittain, “Mandelic Acid”, Chapter 6 in: *Analytical Profiles of Drug Substances and Excipients*, Volume 29, H.G. Brittain, (ed.), Academic Press, San Diego, 2002, pp. 193–197.
31. J.E. Koundourellis, C.K. Markopolou, F.A. Underwood, and B. Chapman, *J. Chem. Eng. Data*, **37**, 187–191 (1992).

32. J.E. Koundourellis, E.T. Malliou, R.A.L. Sullivan, and B. Chapman, *J. Chem. Eng. Data*, **44**, 656–660 (1999).
33. J.E. Koundourellis, E.T. Malliou, R.A.L. Sullivan, and B. Chapman, *J. Chem. Eng. Data*, **45**, 1001–1006 (2000).
34. H.G. Brittain, “Methods for the Characterization of Polymorphs and Solvates”, Chapter 6 in: ***Polymorphism in Pharmaceutical Solids***, H.G. Brittain, (ed.), Marcel Dekker, New York, pp. 227–278 (1999).
35. D.B. Black and E.G. Lovering, *J. Pharm. Pharmacol.*, **29**, 684–687 (1977).
36. R. Suryanarayanan and A.G. Mitchell, *Int. J. Pharm.*, **24**, 1–17 (1985).
37. L.S. Crocker and J.A. McCauley, *J. Pharm. Sci.*, **84**, 226–227 (1995).
38. M. Ohta, Y. Tozuka, T. Oguchi, and K. Yamamoto, *Chem. Pharm. Bull.*, **47**, 1638–1640 (1999).
39. Z.G. Li, R.L. Harlow, C.M. Forris, R.E. Olson, T.M. Sielecki, J. Liu, R.D. Vickery, and M.B. Maurin, *J. Pharm. Sci.*, **89**, 1237–1242 (2000).
40. N.V. Phadnis, R.K. Cavatur, and R. Suryanarayanan, *J. Pharm. Biomed. Anal.*, **15**, 929–943 (1997).
41. M.M. de Villiers, D.E. Wurster, J.G. Van der Watt, and A. Ketkar, *Int. J. Pharm.*, **163**, 219–224 (1998).
42. S.-D. Clas, R. Faizer, R.E. O’Connor, and E.B. Vadas, *Int. J. Pharm.*, **121**, 73–79 (1995).
43. S.S. Iyengar, N.V. Phadnis, and R. Suryanarayanan, *Powder Diffraction*, **16**, 20–24 (2001).
44. H.M. Rietveld, *J. Appl. Crystallogr.*, **2**, 65–71 (1969).
45. W. Cao, S. Bates, G.E. Peck, P.L.D. Wildfong, Z. Qiu, and K.R. Morris, *J. Pharm. Biomed. Anal.*, **30**, 1111–1119 (2002).
46. S.N. Campbell Roberts, A.C. Williams, I.M. Grimsey, and S.W. Booth, *J. Pharm. Biomed. Anal.*, **28**, 1149–1159 (2002).
47. H.G. Brittain, unpublished results.
48. W.C. Kidd, P. Varlashkin, and C.Y. Li, *Powder Diffraction*, **8**, 180–187 (1993).
49. V.P. Tanninen and J. Yliruusi, *Int. J. Pharm.*, **81**, 169–177 (1992).
50. D.E. Bugay, A.W. Newman, and W.P. Findlay, *J. Pharm. Biomed. Anal.*, **15**, 49–61 (1996).
51. J. Pirttimaki, V.-P. Lehto, and E. Laine, *Drug Dev. Indust. Pharm.*, **19**, 2561–2577 (1993).

52. M. Otsuka and Y. Matsuda, *Drug Dev. Indust. Pharm.*, **19**, 2241–2269 (1993).
53. N.V. Phadnis and R. Suryanarayanan, *Pharm. Res.*, **14**, 1176–1180 (1997).
54. G.A. Stephenson, E.G. Groleau, R.L. Kleemann, W. Xu, and D.R. Rigsbee, *J. Pharm. Sci.*, **87**, 536–542 (1999).
55. M. Epple and H.K. Cammenga, *Ber. Bunsenges. Phys. Chem.*, **96**, 1774–1778 (1992).
56. P. Conflant and A.-M. Guyot-Hermann, *Eur. J. Pharm. Biopharm.*, **40**, 388–392 (1994).
57. S.S. Leung and D.J.W. Grant, *J. Pharm. Sci.*, **86**, 64–71 (1997).
58. S. Rastogi, M. Zakrzewski, and R. Suryanarayanan, *Pharm. Res.*, **18**, 267–273 (2001).
59. E. Yonemochi, S. Kitahara, S. Maeda, S. Yamamura, T. Oguchi, and K. Yamamoto, *Eur. J. Pharm. Sci.*, **7**, 331–338 (1999).

CUMULATIVE INDEX

Bold numerals refer to volume numbers.

Acebutolol, **19**, 1
Acetaminophen, **3**, 1; **14**, 551
Acetazolamide, **22**, 1
Acetohexamide, **1**, 1; **2**, 573; **21**, 1
Acyclovir, **30**, 1
Adenosine, **25**, 1
Allopurinol, **7**, 1
Amantadine, **12**, 1
Amikacin sulfate, **12**, 37
Amiloride hydrochloride, **15**, 1
Aminobenzoic acid, **22**, 33
Aminoglutethimide, **15**, 35
Aminophylline, **11**, 1
Aminosalicylic acid, **10**, 1
Amiodarone, **20**, 1
Amitriptyline hydrochloride, **3**, 127
Amobarbital, **19**, 27
Amodiaquine hydrochloride, **21**, 43
Amoxicillin, **7**, 19; **23**, 1
Amphotericin B, **6**, 1; **7**, 502
Ampicillin, **2**, 1; **4**, 518
Apomorphine hydrochloride, **20**, 121
Arginine, **27**, 1
Ascorbic acid, **11**, 45
Aspartame, **29**, 7
Aspirin, **8**, 1
Astemizole, **20**, 173
Atenolol, **13**, 1
Atropine, **14**, 325
Azathioprine, **10**, 29
Azintamide, **18**, 1

Aztreonam, **17**, 1

Bacitracin, **9**, 1
Baclofen, **14**, 527
Bendroflumethiazide, **5**, 1; **6**, 597
Benperidol, **14**, 245
Benzocaine, **12**, 73
Benzoic acid, **26**, 1
Benzyl benzoate, **10**, 55
Betamethasone dipropionate, **6**, 43
Bretylum tosylate, **9**, 71
Brinzolamide, **26**, 47
Bromazepam, **16**, 1
Bromocriptine methanesulfonate, **8**, 47
Bumetanide, **22**, 107
Bupivacaine, **19**, 59
Busulphan, **16**, 53

Caffeine, **15**, 71
Calcitriol, **8**, 83
Camphor, **13**, 27
Captopril, **11**, 79
Carbamazepine, **9**, 87
Carbenoxolone sodium, **24**, 1
Cefaclor, **9**, 107
Cefamandole nafate, **9**, 125; **10**, 729
Cefazolin, **4**, 1
Cefixime, **25**, 39
Cefotaxime, **11**, 139
Cefoxitin sodium, **11**, 169
Ceftazidime, **19**, 95

- Ceftriaxone sodium, **30**, 21
 Cefuroxime sodium, **20**, 209
 Celiprolol hydrochloride, **20**, 237
 Cephalexin, **4**, 21
 Cephalothin sodium, **1**, 319
 Cephradine, **5**, 21
 Chloral hydrate, **2**, 85
 Chlorambucil, **16**, 85
 Chloramphenicol, **4**, 47; **15**, 701
 Chlordiazepoxide, **1**, 15
 Chlordiazepoxide hydrochloride, **1**, 39; **4**, 518
 Chloropheniramine maleate, **7**, 43
 Chloroquine, **13**, 95
 Chloroquine phosphate, **5**, 61
 Chlorothiazide, **18**, 33
 Chlorpromazine, **26**, 97
 Chlorprothixene, **2**, 63
 Chlortetracycline hydrochloride, **8**, 101
 Chlorthalidone, **14**, 1
 Chlorzoxazone, **16**, 119
 Cholecalciferol, **13**, 655
 Cimetidine, **13**, 127; **17**, 797
 Cisplatin, **14**, 77; **15**, 796
 Citric Acid, **28**, 1
 Clarithromycin, **24**, 45
 Clidinium bromide, **2**, 145
 Clindamycin hydrochloride, **10**, 75
 Clioquinol, **18**, 57
 Clofazimine, **18**, 91; **21**, 75
 Clomiphene citrate, **25**, 85
 Clonazepam, **6**, 61
 Clonfibrate, **11**, 197
 Clonidine hydrochloride, **21**, 109
 Clorazepate dipotassium, **4**, 91
 Clotrimazole, **11**, 225
 Cloxacillin sodium, **4**, 113
 Clozapine, **22**, 145
 Cocaine hydrochloride, **15**, 151
 Codeine phosphate, **10**, 93
 Colchicine, **10**, 139
 Cortisone acetate, **26**, 167
 Crospovidone, **24**, 87
 Cyanocobalamin, **10**, 183
 Cyclandelate, **21**, 149
 Cyclizine, **6**, 83; **7**, 502
 Cyclobenzaprine hydrochloride, **17**, 41
 Cycloserine, **1**, 53; **18**, 567
 Cyclosporine, **16**, 145
 Cyclothiazide, **1**, 65
 Cypropheptadine, **9**, 155
 Dapsone, **5**, 87
 Dexamethasone, **2**, 163; **4**, 519
 Diatrizoic acid, **4**, 137; **5**, 556
 Diazepam, **1**, 79; **4**, 518
 Dibenzepin hydrochloride, **9**, 181
 Dibucaine, **12**, 105
 Dibucaine hydrochloride, **12**, 105
 Diclofenac sodium, **19**, 123
 Didanosine, **22**, 185
 Diethylstilbestrol, **19**, 145
 Diflunisal, **14**, 491
 Digitoxin, **3**, 149; **9**, 207
 Dihydroergotoxine
 methanesulfonate, **7**, 81
 Diloxanide furoate, **26**, 247
 Diltiazem hydrochloride, **23**, 53
 Diocetyl sodium sulfosuccinate, **2**, 199; **12**, 713
 Diosgenin, **23**, 101
 Dipiperodon, **6**, 99
 Diphenhydramine hydrochloride, **3**, 173
 Diphenoxylate hydrochloride, **7**, 149
 Dipivefrin hydrochloride, **22**, 229
 Disopyramide phosphate, **13**, 183
 Disulfiram, **4**, 168
 Dobutamine hydrochloride, **8**, 139
 Dopamine hydrochloride, **11**, 257
 Dorzolamide hydrochloride, **26**, 283; **27**, 377
 Doxorubicine, **9**, 245
 Droperidol, **7**, 171
 Echothiophate iodide, **3**, 233
 Econazole nitrate, **23**, 127
 Edetic acid (EDTA), **29**, 57

- Emetine hydrochloride, **10**, 289
Enalapril maleate, **16**, 207
Ephedrine hydrochloride, **15**, 233
Epinephrine, **7**, 193
Ergonovine maleate, **11**, 273
Ergotamine tartrate, **6**, 113
Erthromycin, **8**, 159
Erthromycin estolate, **1**, 101; **2**, 573
Estradiol, **15**, 283
Estradiol valerate, **4**, 192
Estrone, **12**, 135
Ethambutol hydrochloride, **7**, 231
Ethynodiol diacetate, **3**, 253
Etodolac, **29**, 105
Etomidate, **12**, 191
Etoposide, **18**, 121
Eugenol, **29**, 149
- Fenoprofen calcium, **6**, 161
Fenoterol hydrobromide, **27**, 33
Flavoxate hydrochloride, **28**, 77
Flecainide, **21**, 169
Fluconazole, **27**, 67
Flucytosine, **5**, 115
Fludrocortisone acetate, **3**, 281
Flufenamic acid, **11**, 313
Fluorouracil, **2**, 221; **18**, 599
Fluoxetine, **19**, 193
Fluoxymesterone, **7**, 251
Fluphenazine decanoate, **9**, 275;
10, 730
Fluphenazine enanthate, **2**, 245; **4**, 524
Fluphenazine hydrochloride, **2**, 263;
4, 519
Flurazepam hydrochloride, **3**, 307
Flutamide, **27**, 115
Fluvoxamine maleate, **24**, 165
Folic acid, **19**, 221
Furosemide, **18**, 153
- Gadoteridol, **24**, 209
Gentamicin sulfate, **9**, 295; **10**, 731
Glafenine, **21**, 197
Glibenclamide, **10**, 337
Gluthethimide, **5**, 139
- Gramicidin, **8**, 179
Griseofulvin, **8**, 219; **9**, 583
Guaifenesin, **25**, 121
Guanabenz acetate, **15**, 319
Guar gum, **24**, 243
- Halcinonide, **8**, 251
Haloperidol, **9**, 341
Halothane, **1**, 119; **2**, 573; **14**, 597
Heparin sodium, **12**, 215
Heroin, **10**, 357
Hexestrol, **11**, 347
Hexetidine, **7**, 277
Histamine, **27**, 159
Homatropine hydrobromide, **16**, 245
Hydralazine hydrochloride, **8**, 283
Hydrochlorothiazide, **10**, 405
Hydrocortisone, **12**, 277
Hydroflumethazide, **7**, 297
Hydroxyprogesterone caproate, **4**, 209
Hydroxyzine dihydrochloride, **7**, 319
Hyoscyamine, **23**, 155
- Ibuprofen, **27**, 265
Imipramine hydrochloride, **14**, 37
Imipenem, **17**, 73
Indapamide, **23**, 233
Indinavar sulfate, **26**, 319
Indomethacin, **13**, 211
Iodamide, **15**, 337
Iodipamide, **2**, 333
Iodoxamic acid, **20**, 303
Iopamidol, **17**, 115
Iopanoic acid, **14**, 181
Ipratropium bromide, **30**, 59
Iproniazid phosphate, **20**, 337
Isocarboxazid, **2**, 295
Isoniazide, **6**, 183
Isopropamide, **2**, 315; **12**, 721
Isoproterenol, **14**, 391
Isosorbide dinitrate, **4**, 225; **5**, 556
Isosuprine hydrochloride, **26**, 359
Ivermectin, **17**, 155
- Kanamycin sulfate, **6**, 259
Ketamine, **6**, 297

- Ketoprofen, **10**, 443
Ketotifen, **13**, 239
Khellin, **9**, 371
- Lactic acid, **22**, 263
Lactose, anhydrous, **20**, 369
Lansoprazole, **28**, 117
Leucovorin calcium, **8**, 315
Levallorphan tartrate, **2**, 339
Levarterenol bitartrate, **1**, 149; **2**, 573; **11**, 555
Levodopa, **5**, 189
Levothyroxine sodium, **5**, 225
Lidocaine, **14**, 207; **15**, 761
Lidocaine hydrochloride, **14**, 207; **15**, 761
Lincomycin, **23**, 275
Lisinopril, **21**, 233
Lithium carbonate, **15**, 367
Lobeline hydrochloride, **19**, 261
Lomefloxacin, **23**, 327
Lomustine, **19**, 315
Loperamide hydrochloride, **19**, 341
Lorazepam, **9**, 397
Lovastatin, **21**, 277
- Mafenide acetate, **24**, 277
Malic acid, **28**, 153
Maltodextrin, **24**, 307
Mandelic acid, **29**, 179
Maprotiline hydrochloride, **15**, 393
Mebendazole, **16**, 291
Mebeverine hydrochloride, **25**, 165
Mefloquine hydrochloride, **14**, 157
Melphalan, **13**, 265
Meperidine hydrochloride, **1**, 175
Meprobamate, **1**, 207; **4**, 520; **11**, 587
Mercaptopurine, **7**, 343
Mesalamine, **25**, 209; **27**, 379
Mestranol, **11**, 375
Metformin hydrochloride, **25**, 243
Methadone hydrochloride, **3**, 365; **4**, 520; **9**, 601
Methaqualone, **4**, 245
Methimazole, **8**, 351
- Methixen hydrochloride, **22**, 317
Methocarbamol, **23**, 377
Methotrexate, **5**, 283
Methoxamine hydrochloride, **20**, 399
Methoxsalen, **9**, 427
Methylclothiazide, **5**, 307
Methylphenidate hydrochloride, **10**, 473
Methypylon, **2**, 363
Metipranolol, **19**, 367
Metoclopramide hydrochloride, **16**, 327
Metoprolol tartrate, **12**, 325
Metronidazole, **5**, 327
Mexiletine hydrochloride, **20**, 433
Minocycline, **6**, 323
Minoxidil, **17**, 185
Mitomycin C, **16**, 361
Mitoxanthrone hydrochloride, **17**, 221
Morphine, **17**, 259
Moxalactam disodium, **13**, 305
- Nabilone, **10**, 499
Nadolol, **9**, 455; **10**, 732
Nalidixic acid, **8**, 371
Nalmefene hydrochloride, **24**, 351
Nalorphine hydrobromide, **18**, 195
Naloxone hydrochloride, **14**, 453
Naphazoline hydrochloride, **21**, 307
Naproxen, **21**, 345
Natamycin, **10**, 513; **23**, 405
Neomycin, **8**, 399
Neostigmine, **16**, 403
Nicotinamide, **20**, 475
Nifedipine, **18**, 221
Nimesulide, **28**, 197
Nitrazepam, **9**, 487
Nitrofurantoin, **5**, 345
Nitroglycerin, **9**, 519
Nizatidine, **19**, 397
Norethindrone, **4**, 268
Norfloxacin, **20**, 557
Norgestrel, **4**, 294
Nortriptyline hydrochloride, **1**, 233; **2**, 573

- Noscapine, **11**, 407
Nystatin, **6**, 341
- Ondansetron hydrochloride, **27**, 301
Ornidazole, **30**, 123
Oxamniquine, **20**, 601
Oxazepam, **3**, 441
Oxyphenbutazone, **13**, 333
Oxytocin, **10**, 563
- Pantoprazole, **29**, 213
Papaverine hydrochloride, **17**, 367
Penicillamine, **10**, 601
Penicillin-G, benzothine, **11**, 463
Penicillin-G, potassium, **15**, 427
Penicillin-V, **1**, 249; **17**, 677
Pentazocine, **13**, 361
Pentoxifylline, **25**, 295
Pergolide mesylate, **21**, 375
Phenazopyridine hydrochloride, **3**, 465
Phenelzine sulfate, **2**, 383
Phenformin hydrochloride, **4**, 319; **5**, 429
Phenobarbital, **7**, 359
Phenolphthalein, **20**, 627
Phenoxymethyl penicillin potassium, **1**, 249
Phenylbutazone, **11**, 483
Phenylephrine hydrochloride, **3**, 483
Phenylpropanolamine hydrochloride, **12**, 357; **13**, 767
Phenytoin, **13**, 417
Physostigmine salicylate, **18**, 289
Phytonadione, **17**, 449
Pilocarpine, **12**, 385
Piperazine estrone sulfate, **5**, 375
Pirenzepine dihydrochloride, **16**, 445
Piroxicam, **15**, 509
Polythiazide, **20**, 665
Polyvinyl alcohol, **24**, 397
Polyvinylpyrrolidone, **22**, 555
Povidone, **22**, 555
Povidone-iodine, **25**, 341
Pralidoxine chloride, **17**, 533
- Praziquantel, **25**, 463
Prazosin hydrochloride, **18**, 351
Prednisolone, **21**, 415
Primidone, **2**, 409; **17**, 749
Probenecid, **10**, 639
Procainamide hydrochloride, **4**, 333; **28**, 251
Procaine hydrochloride, **26**, 395
Procarbazine hydrochloride, **5**, 403
Promethazine hydrochloride, **5**, 429
Proparacaine hydrochloride, **6**, 423
Propiomazine hydrochloride, **2**, 439
Propoxyphene hydrochloride, **1**, 301; **4**, 520 ; **6**, 598
Propyl paraben, **30**, 235
Propylthiouracil, **6**, 457
Pseudoephedrine hydrochloride, **8**, 489
Pyrazinamide, **12**, 433
Pyridoxine hydrochloride, **13**, 447
Pyrimethamine, **12**, 463
- Quinidine sulfate, **12**, 483
Quinine hydrochloride, **12**, 547
- Ranitidine, **15**, 533
Reserpine, **4**, 384; **5**, 557; **13**, 737
Riboflavin, **19**, 429
Rifampin, **5**, 467
Rutin, **12**, 623
- Saccharin, **13**, 487
Salbutamol, **10**, 665
Salicylamide, **13**, 521
Salicylic acid, **23**, 427
Scopolamine hydrobromide, **19**, 477
Secobarbital sodium, **1**, 343
Sertraline hydrochloride, **24**, 443
Sertraline lactate, **30**, 185
Sildenafil citrate, **27**, 339
Silver sulfadiazine, **13**, 553
Simvastatin, **22**, 359
Sodium nitroprusside, **6**, 487; **15**, 781
Solasodine, **24**, 487
Sorbitol, **26**, 459
Sotalol, **21**, 501

- Spirolactone, **4**, 431; **29**, 261
Starch, **24**, 523
Streptomycin, **16**, 507
Strychnine, **15**, 563
Succinylcholine chloride, **10**, 691
Sulfacetamide, **23**, 477
Sulfadiazine, **11**, 523
Sulfadoxine, **17**, 571
Sulfamethazine, **7**, 401
Sulfamethoxazole, **2**, 467; **4**, 521
Sulfasalazine, **5**, 515
Sulfathiazole, **22**, 389
Sulfisoxazole, **2**, 487
Sulfoxone sodium, **19**, 553
Sulindac, **13**, 573
Sulphamerazine, **6**, 515
Sulpiride, **17**, 607

Talc, **23**, 517
Teniposide, **19**, 575
Tenoxicam, **22**, 431
Terazosin, **20**, 693
Terbutaline sulfate, **19**, 601
Terfenadine, **19**, 627
Terpin hydrate, **14**, 273
Testolactone, **5**, 533
Testosterone enanthate, **4**, 452
Tetracaine hydrochloride, **18**, 379
Tetracycline hydrochloride, **13**, 597
Theophylline, **4**, 466
Thiabendazole, **16**, 611
Thiamine hydrochloride, **18**, 413
Thiamphenicol, **22**, 461
Thiopental sodium, **21**, 535
Thioridazine, **18**, 459
Thioridazine hydrochloride, **18**, 459
Thiostrepton, **7**, 423
Thiothixene, **18**, 527
Ticlopidine hydrochloride, **21**, 573
Timolol maleate, **16**, 641
Titanium dioxide, **21**, 659
Tobramycin, **24**, 579
 α -Tocopheryl acetate, **3**, 111
Tolazamide, **22**, 489
Tolbutamide, **3**, 513; **5**, 557; **13**, 719
Tolnaftate, **23**, 549

Tranlycypromine sulfate, **25**, 501
Trazodone hydrochloride, **16**, 693
Triamcinolone, **1**, 367; **2**, 571; **4**, 521; **11**, 593
Triamcinolone acetonide, **1**, 397; **2**, 571; **4**, 521; **7**, 501; **11**, 615
Triamcinolone diacetate, **1**, 423; **11**, 651
Triamcinolone hexacetonide, **6**, 579
Triamterene, **23**, 579
Triclobisonium chloride, **2**, 507
Trifluoperazine hydrochloride, **9**, 543
Triflupromazine hydrochloride, **2**, 523; **4**, 521; **5**, 557
Trimethaphan camsylate, **3**, 545
Trimethobenzamide hydrochloride, **2**, 551
Trimethoprim, **7**, 445
Trimipramine maleate, **12**, 683
Trioxsalen, **10**, 705
Tripeleminamine hydrochloride, **14**, 107
Triprolidine hydrochloride, **8**, 509
Tropicamide, **3**, 565
Tubocurarine chloride, **7**, 477
Tybamate, **4**, 494

Valproate sodium, **8**, 529
Valproic acid, **8**, 529
Verapamil, **17**, 643
Vidarabine, **15**, 647
Vinblastine sulfate, **1**, 443; **21**, 611
Vincristine sulfate, **1**, 463; **22**, 517
Vitamin D3, **13**, 655

Warfarin, **14**, 423

X-Ray diffraction, **30**, 271
Xylometazoline hydrochloride, **14**, 135

Yohimbine, **16**, 731

Zidovudine, **20**, 729
Zileuton, **25**, 535
Zomepirac sodium, **15**, 673